Lime - Clay Modification and its Application in the Construction of Man – Made Islands

Thesis submitted by

Mehdi Salehi (BSc.)

2009

in fulfillment of the requirements
for the degree of Master of Engineering Science
School of Engineering
James Cook University

In the name of God, the beneficent, the merciful

Read in the name of thy Lord who creates,

Creates man from a clot,

Read and thy Lord is most Generous,

Who taught by the pen,

Taught man what he knew not,

Nay, man is surely in ordinate,

Because he looks upon himself as self-sufficient

Chapter 96 Quran

STATEMENT OF ACCESS

I, the undersigned, the author of this thesis, understand that James Cook University will make it available for use within the University Library and, by microfilm or other means, allow access to users in other approved libraries.

All users consulting this thesis will have to sign the following statement:

> ***In consulting this thesis, I agree not to copy or closely paraphrase it in whole or in part without the written consent of the author; and to make proper public written acknowledgement for any assistance, which I have obtained from it.***

Beyond this, I do not wish to place any restriction on access to this thesis.

_____ _____

Signatures Date

STATEMENT OF SOURCES

DECLARATION

I declare that this thesis is my own work and has not been submitted in any form for another degree or diploma at any university or other institution of tertiary education. Information derived from the published or unpublished work of others has been acknowledged in the text and a list of references is given.

_____ _____

Signature Date

ACKNOWLEDGEMENTS

I would like to express my gratitude and love to Bita and Kimia for their encouragement, patience, support and understanding. Your happiness is my meaning in life, I love you my girls.

I would also like to extend my appreciation and gratitude to my supervisor Associate Professor Nagaratnam Sivakugan for his sincere supervision and guidance throughout the course of this study.

Special thank you to Warren O'Donnel in Geotechnical Laboratory for ongoing technical assistant. Thanks Warren for guidance and for your patience. It was an honor to know and to work with you.

I deeply acknowledge Kellie Johns (Learner Advisor) for her endless help and assistance during the process of thesis writing.

I also acknowledge the financial support received by the school of Civil Engineering, James Cook University.

Special appreciation goes to Chris Park and Mal Campbell from Coffey Pty Ltd for their assistance during the time of sampling in the Port of Brisbane.

ABSTRACT

Due to the scarcity of land following rapid development in many countries, the dredged mud may be used as fill materials to develop new land in coastal zones. Several major infrastructure facilities like ports or airports are strategically situated on these artificial lands. However, soft dredged deposits are intrinsically low in strength, and very high in compressibility. As a result of these inherently undesirable engineering characteristics, an appropriate ground improvement technique has to be employed so as to meet the engineering requirements necessary for the design and construction of overhead infrastructure facilities. The placement of a surcharge preload on a soft foundation facilitated with vertical drains is the most commonplace method used worldwide. Surcharge preloading with vertical drains is used to accelerate the rate of primary consolidation settlement and reduce the magnitude of the post construction secondary compression settlement.

In this study, an attempt was made to provide insight into some factors, aimed at improving the efficiency of the preloading used in a man-made island. A series of laboratory tests was performed to evaluate the effect of clay fabric, altered due to the addition of hydrated lime into slurry, on the primary and secondary consolidation behaviour of the dredged mud samples. As a prime objective, a unique testing method was proposed to determine the threshold value of lime below which the maximum alteration in clay fabric takes place. This threshold is known as *Lime Modification Optimum* and presents the boundary between modification (i.e. ion exchange and flocculation) and solidification (i.e. formation of the pozzolanic products) phases in lime-clay reaction. It was found that, for the type of the dredged mud used in this study, 4 percent of lime (dry weight basis) should be considered as lime modification optimum.

A set of oedometer tests was conducted in both normally consolidated (NC) and artificially overconsolidated (OC) stages on both natural and lime treated samples. The

laboratory findings revealed that with an increase of lime up to 4 percent, the increase of coefficient of consolidation, c_v, was observed up to ten fold,. Observation of the test results suggested that in the compression range, the values of the compression index, C_c, increase when increasing the lime content whereas in the recompression range, the value of the recompression index, C_r, gradually decreases with increasing % lime. This finding indicated that with increasing % lime, the magnitude of primary consolidation in the NC state increases while in the OC state it decreases. The secondary compression index, C_α, in both the compression and recompression range decreases with increasing % lime. In the compression range the decreasing of C_α together with an increase of C_c, results in a gradual reduction of $\frac{C_\alpha}{C_c}$ as the amount of lime increases. It is worthwhile stating that the surcharging effort was found to be more effective in a further reduction of the secondary compression index of the natural dredged mud in comparison with lime treated dredged mud.

In this study, empirical correlations between coefficient of consolidation, void ratio and corresponding effective stress was proposed and evaluated. It was found that for the type of the dredged mud used in this study, irrespective of the percentages of added lime, the coefficient of consolidation can be obtained by knowing the state of void ratio and effective stress at any instance during consolidation.

Further analyses of the laboratory results by means of Plaxis (finite element model software) and analytical approach suggested that the pretreatment of the dredged slurry with hydrated lime prior to discharging into a containment pond during the construction of man-made islands, may contribute significantly towards the project cost saving strategy.

PUBLICATION

JOURNAL PAPER:

Salehi, M. and Sivakugan, N. (2009). **"The effects of lime-clay modification on the consolidation behavior of the dredged mud"**: *Journal of Waterway, Port, Coastal and Ocean Engineering, ASCE* (In Print).

CONTENTS

LIST OF FIGURES

LIST OF TABLES

Chapter 1
Introduction

1.1 General

There are many countries around the world encountering a shortage of land in their ports, harbors and in general, coastal zones. To meet the increasing demand of development in these countries, it is necessary to construct different types of infrastructure, such as industrial or residential complexes, recreational facilities, airports and ports on new reclaimed lands. Usually a large volume of fill materials has to be implemented as foundation material to build such large-scale facilities. The conventional technique for the backfilling and construction of reclaimed ground is to use sand fill, mainly from inland (i.e. hill cuts materials). However, with the increasing scarcity of such fill materials, particularly in coastal zones where both environmental legislation and dominant soft clay stratums hinder the project developer, utilizing materials of low engineering properties has been considered.

At the same time, dredging and maintenance of shipway channels is vital to facilitate navigation for vessels importing and exporting commodities to and from harbors. Recycling the dredged material for construction purposes in coastal areas eliminates the cost of transporting inland soil to the project site and in the meantime it contributes to the protection of the natural environment. However, the dredged mud mainly consists of silt or clay grains and together with the presence of high moisture content, results in a lack of shear strength and poor consolidation characteristics. Hence, some kind of treatment is needed to achieve adequate engineering properties for the soft ground.

To improve the engineering behaviour of the soft mud deposit that is created during the construction of man-made islands, several improvement techniques are available in

geotechnical engineering practices, one of which is surcharge preload. The placement of surcharge preload on the soft foundation with the installation of vertical drains is the most commonplace method used worldwide. The consolidation of soil under preload is the process of decreasing the volume of saturated soil by expelling the pore water. The rate of expelling the pore water is governed by the compressibility, permeability and length of the drainage path. Figure 1.1 shows that the distance between installed vertical drains has a significant role in controlling acceleration of the ground settlement.

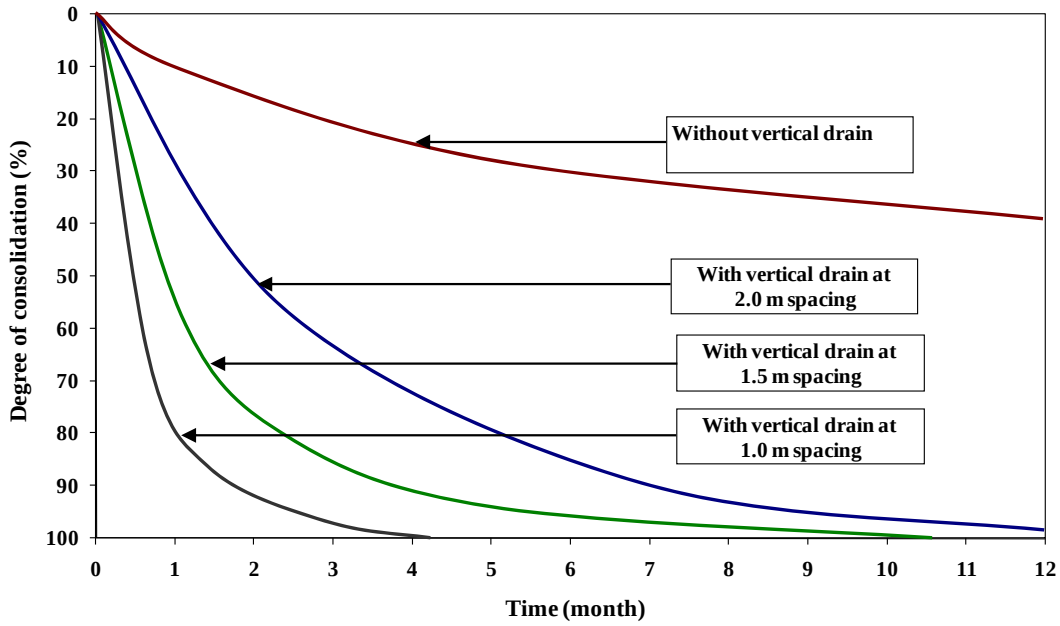

Figure 1.1 Effect of drain spacing on the consolidation rate of soft foundation (Lau et al. 2000)

Hence, to meet a tight construction schedule, the reduction of drain spacing might seem to be a viable solution to reduce the required time for preloading. However, one should note that the increase in number of installed vertical drains for the purpose of acceleration of consolidation may bring about reduction in discharge capacity of wells (due to smearing) and also contribute a significant cost towards project development which may not be desirable. Thus, increasing the rate of a soft ground settlement without reducing the drainage path necessitates the exploring of and research into other possible innovative technologies. This research tries to asses in the laboratory scale the modification effect of

lime, added to dredged mud, on the primary and secondary consolidation behaviour of the treated mud. A practical solution involving the injection of binders into the dredged mud slurry in a large industrial scale has been recently invented to enhance the geotechnical properties of the soft dredged deposits. Pneumatic Flow Mixing Method (PFMM) is a novel ground improvement technique that has been initiated and developed in Japan in recent years. In this method, which is applicable to the construction of a man-made island utilizing the dredged mud, dredged soft soil is mixed with a small amount of stabilizing agent, usually cement. The stabilizing agent is injected into a pipe by way of compressed air during the transportation of the dredged mud and is eventually gently placed on the bottom of the containment ponds for sea reclamation.

1.2 Research objectives

The main objective of this project was to develop a laboratory framework to evaluate the modification effects of lime on the consolidation behaviour of the dredged mud obtained from the Port of Brisbane. This research tried to highlight the beneficial aspects of pretreatment of the dredged mud slurry with lime, to pave the way for considering a new approach in ground improvement practices where both the chemical treatment and surcharge preloading are employed as a combined technique to enhance the engineering properties of soft dredged deposits. In attempt to reach this point, excessive laboratory tests were conducted on the ultra-fine dredged clayey sample which was collected from the selected containment pond in the Port of Brisbane. As a preliminary experimental goal, a new laboratory test method was proposed to identify the lime threshold, below which the maximum flocculation of clay particles takes place. After determination of the maximum amount of required lime content, the primary consolidation and secondary compression behaviour (with and without surcharge) of the natural and lime treated dredged mud was investigated. In addition to conventional oedometer tests, a newly designed retaining ring with a radial drainage condition was employed to investigate the anisotropy of the natural and lime treated dredged mud.

As a second objective of this research, modeling of the consolidation behaviour of the reclamation layer of the three conceptual sites under surcharge preload was carried out by the finite element modeling method (FEM) using the commercial finite element modeling software of Plaxis Version 8 (Netherland, 2008). The consolidation behaviour of the conceptual sites was analysed in unit-cell and full-scale embankment simulation, under plane strain conditions. The unit cell model analysis aimed to verify the effect of % lime on the required influence zone of the vertical drain to meet the given consolidation period. The scope of the full-scale embankment analysis was to evaluate the effect of % lime on the lateral displacement of the soft ground under embankment. The extent of the post-construction secondary compression settlement of the conceptual model for the design life of 100 years was also presented and compared for the layers with varying lime %.

It should be noted that unless otherwise stated, the laboratory data produced throughout the experimental program was employed to provide the input data for modeling practices.

1.3 Thesis organization

In chapter 1, a brief introduction is presented where the aim and scope of the present study is highlighted. The following chapter 2 aims to provide inside into the new approach in ground improvement and develops the research question. Chapter 3 discusses general theory of physico-chemical properties of clay soils together with study of the chemical reactions of the most common binders like cement and lime with clayey soil. In chapter 4, the first round of the experimental program conducted in this study is presented. In chapter 5, the history and general theories of vertical drains, surcharge preloading, and basic requirements of modeling soft ground treated with vertical drains are detailed. Chapter 6 illustrates the comprehensive laboratory test program conducted throughout this research study. In chapter 7, the consolidation behaviour of the three conceptual reclaimed layers is modeled by Plaxis. Chapter 8 presents the summary, conclusion, and recommendation for future research followed by the bibliography.

Chapter 2

New Approach in Ground Improvement

2.1 General

Dredging is the term given to digging, gathering, or pulling out material from the bottom of the sea or rivers in order to maintain waterways and navigation channels for commercial and recreational vessels. Due to the scarcity of land following rapid development in many countries the dredged sediment obtained from the process of dredging may then be used as fill materials to develop new land in coastal zones. Several major infrastructure facilities like ports or airports are then strategically situated on these artificial lands. However, soft dredged deposits are intrinsically low in strength, and very high in compressibility. As a result of these inherently undesirable engineering characteristics, an appropriate ground improvement technique has to be employed so as to meet the engineering requirements necessary for the design and construction of overhead infrastructure facilities. To enhance the mechanical properties of the dredged sediments, several techniques are available in geotechnical engineering practices. One of the ground improvement schemes that may be adapted is chemical stabilization using cement or lime.

In recent years, a new soil improvement technique has been developed in Japan, named the "***Pneumatic Flow Mixing Method***" (PFMM), in which dredged soft soil is mixed with a small amount of stabilizing agent, usually cement, by way of compressed air in a pipe during transportation and then deposited in containment ponds for sea reclamation. The soil mixture deposited and cured on site can achieve relatively high strength so that no additional soil improvement is needed for building the overhead structure. This method requires only stabilizing agent supplier facilities to an existing pneumatic vessel and no mixing blade is used to mix soil and agent. This method is recognized as an economical technique for the construction of, for example, a man-made island, within a relatively short

period of time. It was found by the author that the only literature available in regard to the implementation of the PFMM consists of only a few journal and conference papers associated with the construction of the Central Japan International Airport (CJIA). This chapter presents the only available case history of the reclamation project where PFMM has been successfully executed in terms of relatively high shear strength development in cement-treated dredged mud. It has to be mentioned that whilst still significant, this thesis is not concerned with the development of shear strength of the treated-soft soil, as there are abundant investigations adopting various perspectives in studying this parameter of treated soil. In fact, the review of the case history of construction of the Central Japan International Airport (CJIA) merely improves our understanding about the mechanism of this method and the involved factors during its execution in the construction project of a man-made island. The insight into the mechanism of PFMM helps to detect the constraints and ultimate feasibility of the injection of a binder into dredged mud slurry in man-made island reclamation projects where only conventional dredging vessels are utilized for dredging purposes.

The ongoing man-made island reclamation project of the Port of Brisbane (PoB), characteristics of the employed dredge vessels, and the current ground improvement method used on the site are briefly presented in this chapter. Following that, the research question on which this study has been developed is discussed. This research aims to introduce and evaluate, in laboratory scale, a new approach of the chemical-clay mixing in ground improvement practices associated with construction of man-made islands. The feasibility of injection of the chemical binders into dredged mud slurry prior to discharging into the containment ponds in the Port of Brisbane is also discussed in this chapter.

2.2 Application of PFMM

The Pneumatic Flow Mixing Method (PFMM) has been recently employed in construction of man-made island for Central Japan International airport at Nagoya region. The construction project started in the year 2000 and was completed in 2005. During the reclamation phase, a total of 8.6 million cubic meters of dredged mud was stabilized by

the PFMM to create a part of the airport island (Kitazume and Satoh, 2005). This section explains the development of PFMM and its application to the Central Japan International Airport (CJIA) project as well as demonstrates some mechanical properties of the cement treated dredged soil.

2.2.1 Mechanism of the PFMM method

Conveying dense dredged mud with a low amount of dissolved air in a pipe requires high pressure due to the occurrence of friction between soil grains and the inner surface of the pipe. As a remedy, a relatively large amount of compressed air can be injected into the pipe frequently, so that soft soil is separated into small segments as it is moved throughout the pipe by the injected air. The separated soil segment or block is called a "*Plug*" and is continuously moved forward to an outlet by a force of compressed air. Figure 2.1 shows the schematic flow of plugs within a pipe.

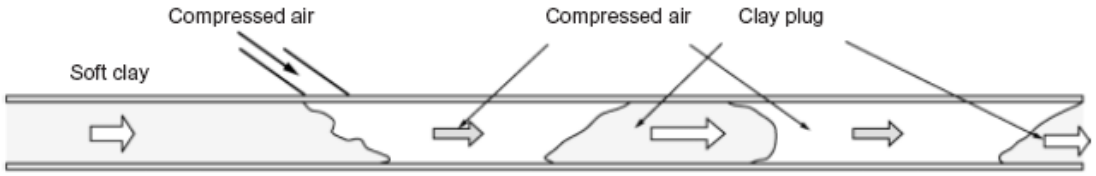

Figure 2.1 Schematic view of plug flow (Kitazume and Satoh, 2003)

The formation of plugs and air cushions together in the pipe reduces the degree of friction on the pipe's inner surface and consequently, lower air pressure would be required to transport the plugs. It should be noted that the characteristics of the plug is highly dependent on the mixing ratio of soil and air, also the diameter of the pipe. The required air pressure depends upon many factors, such as the properties of soil, volume of injected air, and diameter and length of the pipe (Kitazume and Satoh, 2005). In the CJIA project, an inlet air pressure of 400-500 kN/m^2 was frequently adopted. It was found that as the speed of clay plugs exceeded 10 m/s in a pipe, turbulent flow was generated within the plugs because of friction occurring on the inner surface of the pipe (Kitazume and Satoh 2005). Under turbulent conditions, the clay plugs and stabilising agent can be mixed. Kitazume and Satoh discussed that at least a minimum pipeline length of 50-100 m is necessary to

ensure appropriate mixing. It has been found that this method is applicable for the treatment of a large variety of soils with sand fraction content less than 30% (Kitazume and Satoh, 2005).

2.2.2 Characteristics of clay plugs

The properties of three clay plugs obtained from preliminary field tests are presented in Table 2.1.

Table2.1. Properties of clay plug measured in the field test (Mixing design for CJIA) (Kitazume and Satoh, 2003)

	Case 1	Case 2	Case 3
Test condition			
Soil volume: m^3/h	210	296	170
Water content: %	132·5	117·2	96·2
Liquid limit	70·5	77·6	81·5
Cement added: kg/m^3	38	78	52
Test results			
Plug speed: m/s	10·9 (1·6–25·0)	11·9 (1·5–25·0)	12·8 (1·9–25·0)
Plug volume: m^3	0·41 (0·23–0·52)	0·36 (0·25–0·45)	0·30 (0·18–0·36)
Plug length: m	4·3 (0·23–5·4)	3·7 (2·6–4·7)	3·1 (1·9–3·8)
Plug interval: s	7·1 (1·3–30·3)	4·4 (0·5–18·2)	6·4 (0·6–29·0)

It can be found that the clay plugs with an average volume of 0.36 m^3 are conveyed at an average speed of about 12 m/s and with an average interval of about 6 seconds. The field tests also demonstrated that these properties were almost independent of the transported soil volume and amount of cement added. Due to the relatively high speed of the plug in the pipe, and as a result of friction, turbulent flow was produced within the plugs. Under this turbulent condition, the stabilising agent can be added and mixed thoroughly. Former research efforts revealed that the uniform mixing of clay with an agent can be obtained under a flow condition where the Reynolds number lies in the range of 500 to 3000. The Reynolds number is identified as: $R_e = uD/v$

where u is the plug speed, D is the pipe diameter, and v is the viscosity of the plug.

2.2.3 Facilities for PFMM

Figure2.2 shows a group of barges with specific arrangements for the pneumatic flow mixing method utilised in Japan.

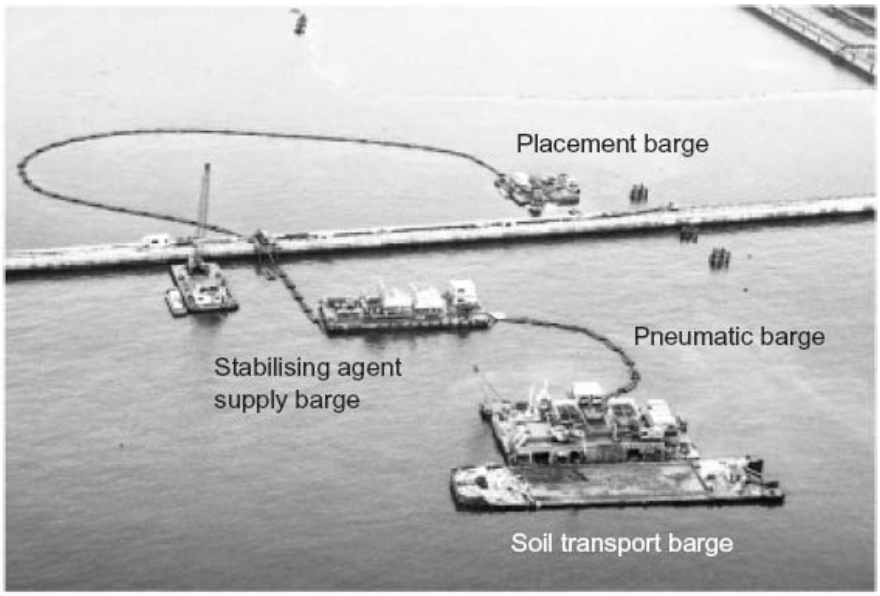

Figure 2.2 Group of barges for PFMM operation (Kitazume and Satoh, 2005)

To perform the Pneumatic flow mixing method in reclamation projects, a group of different barges should be employed. This includes a pneumatic barge, a stabilising agent supplier barge and placement barge. As the most common procedure, firstly, the dredged mud is loaded into the hopper of the pneumatic barge and is transported by means of compressed air to the supplier barge via a pipe (i.e. formation of plug). A stabilising agent, usually cement, in the form of slurry, is then injected to the soft soil in the stabilising agent supplier barge and mixed well in the pipe. In general, there are two major types of methods according to which the stabilising agent is injected; compressor addition and line addition. In the former method, the stabilising agent is injected to the soft soil before the compressed air is injected into a pipe.

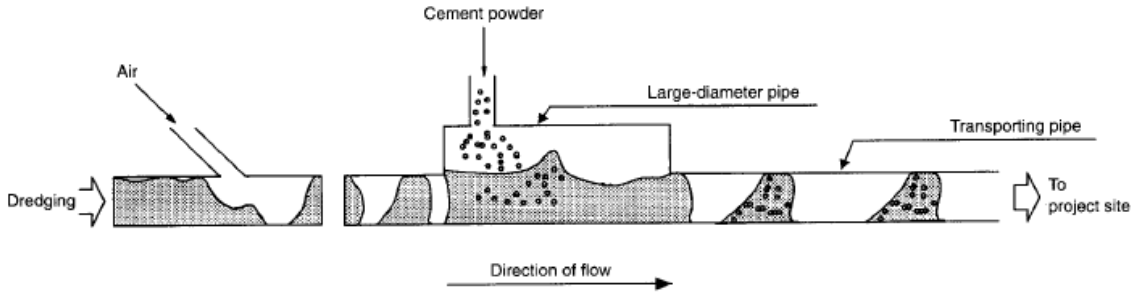

Figure2.3. Principles of pneumatic flow mixing method (Kitazume and Satoh, 2005)

In the later model of barges assembly however, the stabilisation agent is added to the pipe after air injection (Figure 2.3). In both techniques, the soil-additive mixture is allowed to be deposited in the reclamation site through a cyclone in the placement barge. The main function of the placement barge is to release the pressure transporting the soil plugs. A specific pipe is usually used to place the soil mixture under seawater. Care must be taken to avoid entrapping the seawater within treated soil plugs because seawater can cause a considerable decrease in treated soil strength.

There are various suggested methods in the stabilising agent injection technique and transporting technology to improve the efficiency of the clay-binder mixture. One is an additional device installed along the pipeline to detect the location of a plug and estimate its volume in order to inject a sufficient amount of slurry directly into clay plugs. Alternatively, a flexible wall tube, where the diameter or shape of pipe is changed locally, may be used to spot the soil plug.

2.2.4 Air pressure distribution in the pipe

The longevity of air pressure injected into a pipe to transport the soil plugs is dependent on many factors. These include the characteristics of clay, the volume of injected air, the diameter of the pipe, and its length. The variation of air pressure with the transport distance from the inlet, measured in the field test, is plotted in Figure 2.4.

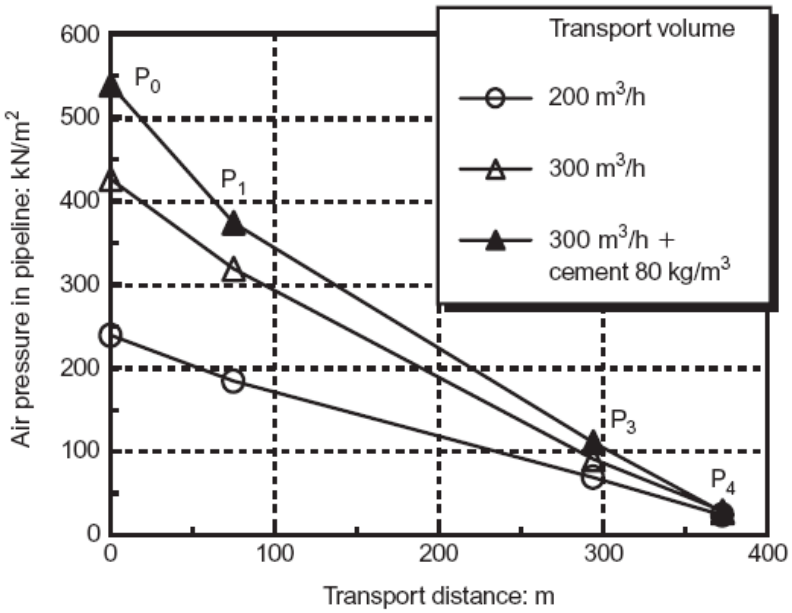

Figure 2.4 Variation of air pressure with distance from the inlet (Kitazume and Satoh, 2003)

In all three tests presented in Figure 2.4., a water content of soft marine clay was about 100% (Kitazume and Satoh, 2003). It can be seen that a relatively large reduction of pressure occurred between the pneumatic barge (P_0) and stabilising agent supply barge (P_1), and this was irrespective of the test condition. The large reduction of air pressure in the pipe in the short distance from P_0 to P_1 was attributed to the continuous presence of dredged mud in the pipe. In fact, between these two points the clay in the pipe was still in a transitional condition in the formation of plug flow. Within the distance between the stabilising agent supply barge and inlet of placement barge, P_1 to P_3, the air pressure decreases linearly and it reached almost zero at the outlet of the placement barge (P_4). The decrease in air pressure between P_1 to P_4, was thought to be attributed to the wall friction in the pipe.

Figure 2.4 also presents the affect of the volume of clay on the reduction of air pressure within the distance of transportation. It was found that with increasing volumes of transported soil, a higher air pressure needed to be produced at the pneumatic barge.

It was also found that the addition of cement causes an increase of pressure up to about 100 kN/m^3 ,at the inlet $P_{0,}$ which is due to an increase of the cohesion and adhesion of the cement –clay mixture.

2.2.5 Effect of amount of agent on strength properties

The extent of increased strength of the treated soil is governed by a range of factors, and in particular, the nature of the chemical reaction between soil and stabilising agent. These factors may be divided into four broad categories as shown in Table 2.2.

Table 2.2 Factors affecting the strength increase of treated soil (Terashi, 1997)

Characteristics of Stabilising agent	1- type of stabilizing agent, 2- Quality, 3- Mixing water and additives
Characteristics and conditions of soil (specially important for clays)	1- physical, chemical and mineralogical properties of soil, 2- Organic content, 3- pH of pore water, 4-water content
Mixing conditions	1-Degree of mixing, 2- Timing of mixing, 3- Quality of stabilizing agent
Curing conditions	1- Temperature, 2- Curing time, 3- Humidity, 4- Wetting and drying/ freezing and thawing

A series of laboratory and field tests was conducted by Kitazume and Satoh (2003) to investigate the strength increase and its deviation of treated soil for the mixing design of the Central Japan International Airport. The relationship between % cement and gained unconfined compressive strength, q_u, of treated soils (i.e. preliminary investigation) used in the Central Japan International Airport project are presented in Figure 2.5. Two types of field strengths are plotted and shown in the Figure; (a): treated soil discharged on dry land, and (b): treated soil placed under seawater. In this investigation, the amount of cement is defined as a dry weight of cement per one cubic meter of soil to be treated. The group of treated soil, named ‘laboratory’, refer to the samples prepared and cured in a laboratory. The specimens named ‘mold’ represent the soil-cement mixture obtained at the outlet of the

discharging pipe but having being cured in a laboratory. The specimens named as 'core' and 'L core' are in situ treated soil samples which were cured under field conditions. The specimens of 'core' were 5 cm in diameter and 10 cm in height, while the 'L core' was a cylindrical sample 50 cm in diameter and 100 cm in height.

Figure 2.5 shows that of the specimens prepared in the laboratory, as % cement increased, the unconfined compressive strength increased linearly. It was found in Figure 2.5(a) that in case of discharging the treated soil on dry land, the unconfined compressive strength of all the treated soil increased almost linearly with an increase in the amount of cement irrespective of specimen type. This figure also shows that the laboratory samples achieved the highest values of strength among all the test specimens. The samples obtained and cured in the field show a large increase in strength. However, it was found that the strength development in the 'L core' samples was relatively less than the 'core' samples. Figure 2.5(a) also reveals that the minimum amount of 40 kg/m^3 of cement lead to 100 kN/m^2 of gained unconfined compressive strength in the laboratory but the influence of such an amount of cement on strength development in the field were negligible. Figure 2.5(b) provides a comparison between strength development of treated soil in the field and laboratory in the case where treated soil is placed under seawater. This Figure shows that the strength of the field treated soil, 'core', was relatively small compared with the 'laboratory' specimen. This difference was likely attributed to entrapped seawater with treated soil during placement.

In order to compare the development of strength in cement treated dredged mud between laboratory and field-manufactured samples, the strength test results of field tests were normalised with laboratory results and the data are presented in Figure 2.6. It was found that the strength ratio of various specimens was not constant and rise with an increase in the amount of cement, irrespective of field soil type. Figure 2.6 indicates that an addition of cement less than 50 kg/m^3 in a practical operation in the field yielded a negligible increase of strength in comparison with the laboratory condition (strength ratio: 0.05-0.3). Figure 2.6(a) shows that the strength ratio of the core soil lied between 0.6-0.8 for placement on dry land when the amount of added cement was 60-80 kg/m^3. Figure 2.6(b) also presents

the strength ratio of the field core samples placed under seawater. Comparison of the figures 2.6(a) and 2.6(b) shows that with a certain amount of added cement, as a result of placement of the cured dredged mud under seawater, approximately 20% reduction of strength ratio of core samples was observed when compared with samples cured on dry land. This was likely due to increased water content of the treated soil as a result of entrapment of seawater during placement. This fact also indicates that during placement of plugs on the sea bed, great care should be taken to avoid entrapment of seawater.

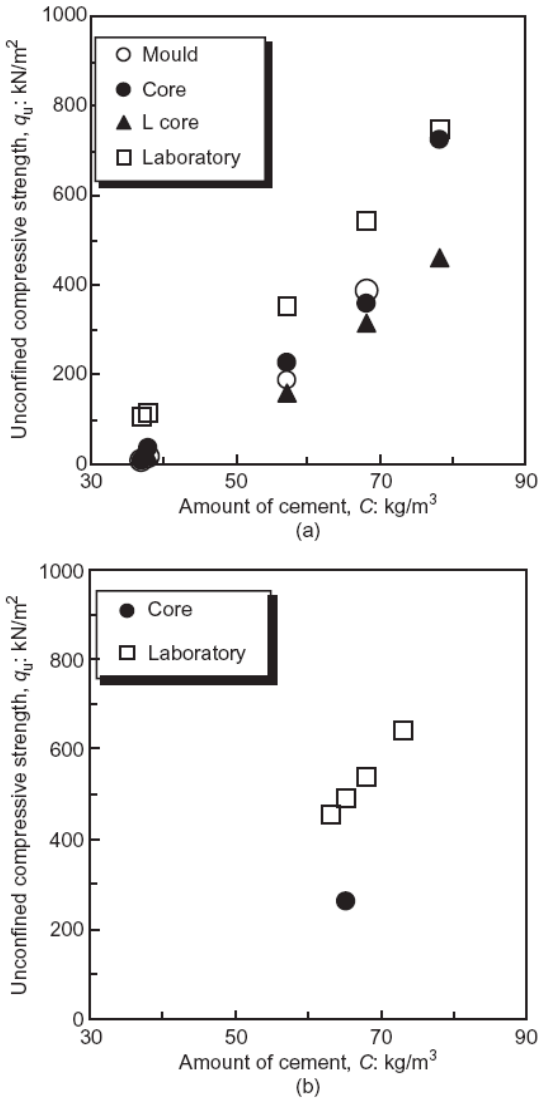

Figure 2.5 Variation of UCS with the amount of cement
(a) placement on land; (b) placement under seawater (Kitazume and Satoh, 2003)

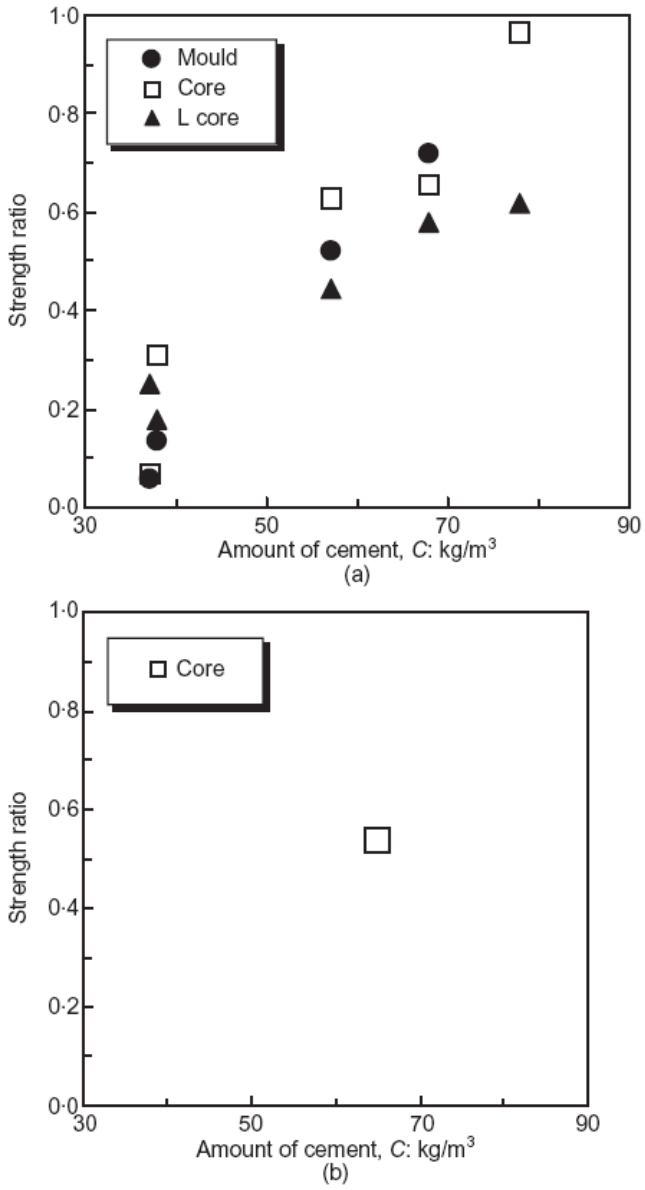

Figure 2.6 Strength ratio against the amount of cement
(a) placement on land; (b) placement under seawater (Kitazume and Satoh, 2003)

Figure 2.7 summarises the relationship between the amount of added cement and the coefficient of variation of unconfined compressive strength. It was noted that strength deviation was highly dependent on the amount of cement, the manufacturing technique, and the size of specimens. This figure presents the test results of several field-manufactured treated soils together with the specimens prepared under laboratory conditions. It was found that the coefficient of variation of laboratory specimens was relatively small and lied

in the constant range of approximately 15% irrespective of the amount of added cement. On the other hand, the field-manufactured treated soils demonstrated a relatively large coefficient of deviation compared with the laboratory specimens.

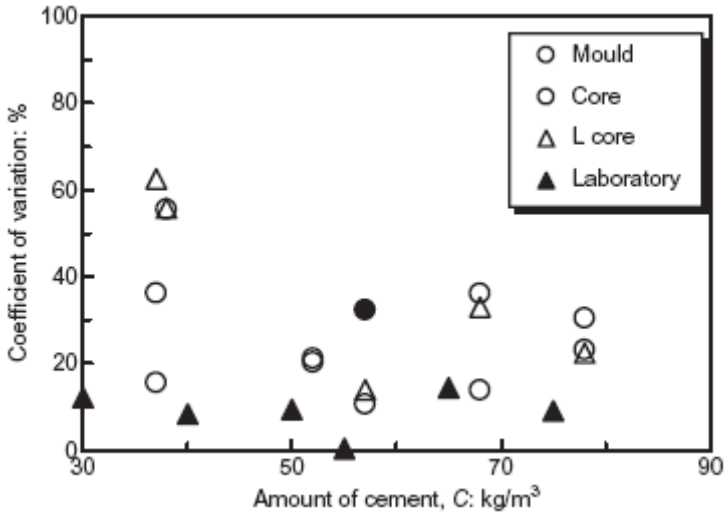

Figure 2.7 The correlation between coefficients of variation of strength with cement content (Kitazume and Satoh, 2003)

Figure 2.7 also shows that the average coefficient of variation of the small field specimen, termed 'core' is about 25% irrespective of the amount of stabilizing agent. The coefficient of variation of the large specimens termed 'L core' was almost the same as that of the core samples as long as the amount of cement exceeds the value of 50kg/m3. Figure 2.7 shows that for a small amount of cement i.e., 38 kg/m3, in the L core the coefficient of variation was relatively large - around 60%. Overall, this Figure indicates that a small amount of cement cannot be distributed properly within the mass of dredged mud by the pneumatic flow mixing method.

2.3 Construction of Central Japan International Airport

To construct the man-made island of CJIA, a total amount of 70 million cubic meters of various soils, of which, 8.6 million cubic meters dredged mud was used (Kitazume and Satoh, 2003). The island, with a plane area of 5.8 million m^2 has been constructed on the

seabed at about 3-10 m in depth (Ketazume and Satoh, 2005). The pneumatic flow mixing method was employed to enhance the mechanical properties of the dredged materials. Three sets of pneumatic execution systems including a pneumatic barge, a cement supply barge, and placement barge operated on the construction site to complete the project within the 15 months period (Figure 2.8).

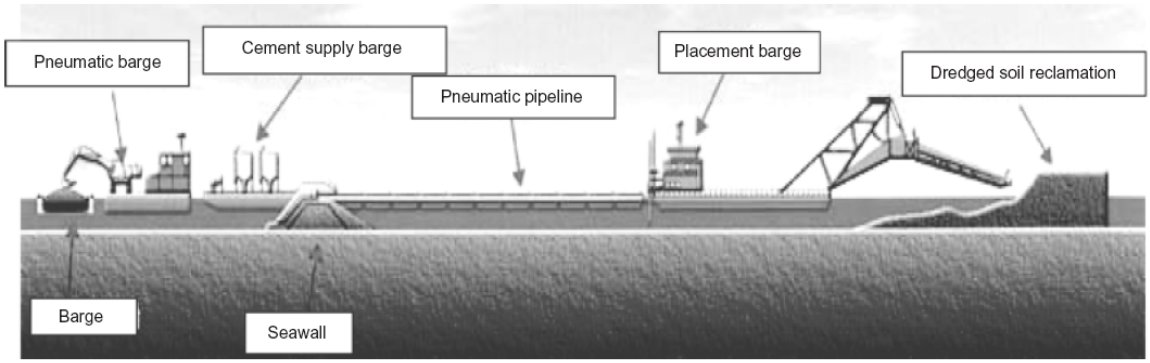

Figure 2.8 Schematic view of Pneumatic execution system
(Kitazume and Satoh, 2003)

A total of 8.6 million m^3 of dredged soil was excavated at 12 sites in Nagoya Port and transported by barge to the project site. After being premixed by a backhoe arm in the barge, the soft soil was poured into the hopper on the pneumatic barge. Ultra-large obstacles such as cobble and steel wire were removed by the sieve installed at the top of hopper. The soft soil was then mixed with an extra amount of seawater to adjust its initial water content to the target value in order to ensure transporting capacity and designed strength. The soil was moved forward using a sand pump and its density was measured by means of a γ-ray density meter. The water content of the soil was calculated based on the measured density to obtain the amount of cement slurry to be added, in accordance with the preliminary test results. Compressed air pressure between 390 to 490 kN/m^2 was injected into the transporting pipe with a diameter of 76 cm to form a plug flow and to transport the soil to the cement supplier barge. The cement slurry was manufactured at the batching plant on the cement supplier barge, with a water/ cement ratio of about 100%. After injection of cement slurry into the soil, the soil mixture was then transported towards the outlet by means of compressed air along a maximum 1500 m long pipeline (see Figure 2.9). A

cyclone was installed at the outlet on the placement barge to release the air pressure and for transporting energy (see Figure 2.10).

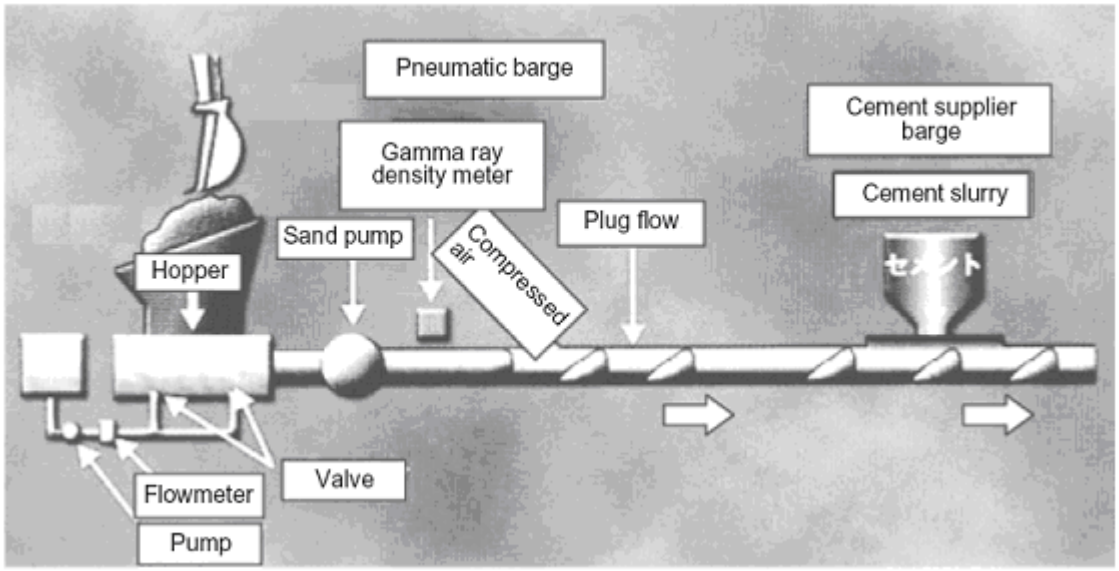

Figure 2.9 Schematic view of soil treatment in pneumatic and cement supply barge (Kitazume and Satoh, 2003)

The placement of treated soil was carried out in two stages:

Firstly, placement was made under water level at a reduced level between -1.5 and -5 m. During this operation, a tremie pipe was used to place the treated soil on the seabed, so only a little amount of seawater could be entrapped within the soil mixture. The utmost care to avoid entrapping water is necessary; otherwise a remarkable reduction in the shear strength will be expected.

Figure 2.10 The placement barge (Kitazume and Satoh, 2003)

After several weeks of curing, to ensure the strength development of the treated soil, a layer of soil mixture was placed on the previous layer to the design level of +2.5 m. Extra care was taken not to entrap seawater within the clay mixture. The sea reclamation with treated soil started in June 2001 and was finalised in October 2002 (Kitazume and Satoh, 2005).

2.3.1 Details of quality control of the treated soil

The type of dredged mud and initial moisture content always varies with location and depth of the dredged site. During construction of CJIA, a total of approximately 8.6 millions m^3 of soil was excavated at 12 sites in Nagoya Port (Kitazumeh and Satoh, 2005). The properties of the dredged soils differ from site to site as shown in table 2.3.

Table 2.3 Typical soil properties and mixing condition of excavated dredged soils (Kitazume and Satoh, 2005)

	Properties of dredged soils						Mixing condition		
			Particle size distribution						
Excavation site	Initial water content: %	Density: kN/m^3	Gravel content: %	Sand content: %	Clay content: %	Liquid limit: %	Water/cement ratio, w/c	Water content: %	Amount of cement: kg/m^3
A	74	1·57	0·0	6·8	93·2	75·6	14·0	105	54
B	81	1·58	0·0	8·0	92·0	74·3	13·4	97	55
C	75	1·56	0·0	5·6	94·4	85·5	13·8	113	56
D	84	1·51	0·0	2·4	97·6	88·3	13·8	116	56
E	68	1·57	0·1	8·7	91·2	72·7	13·8	101	54
F	75	1·56	0·0	2·7	97·3	78·3	14·1	100	53
G	67	1·65	0·0	18·0	82·0	55·3	8·5	64	87
H	62	1·67	0·0	5·0	95·0	67·1	13·8	88	52
I	54	1·72	2·3	29·3	68·4	59·3	13·2	80	53
J	48	1·79	0·0	19·3	80·7	49·2	11·4	65	57
K	78	1·59	0·0	14·6	85·4	75·5	13·8	101	54
L	82	1·56	0·2	8·3	91·5	76·8	13·8	101	54

The mixing conditions were required to be changed for each soil obtained from the particular excavated site. For ease of quality control of the treated soil, a new index, the water/cement (w/c) ratio, was introduced in the project (Kitazume and Satoh, 2005). The w/c ratio is defined as the weight of whole water, including what is apparent in both the soil and cement slurry, and the dry weight of cement. It is worthwhile mentioning that according to the preliminary test results, the unconfined compression strength, q_u, of the treated samples was almost inversely proportional to the w/c, and a unique relationship was obtained for each dredged soil (Kitazume and Satoh, 2005).

In order to maintain uniformity of the properties of cement treated soils obtained from various locations, a mixing control system was employed in the project as illustrated in Figure 2.11.

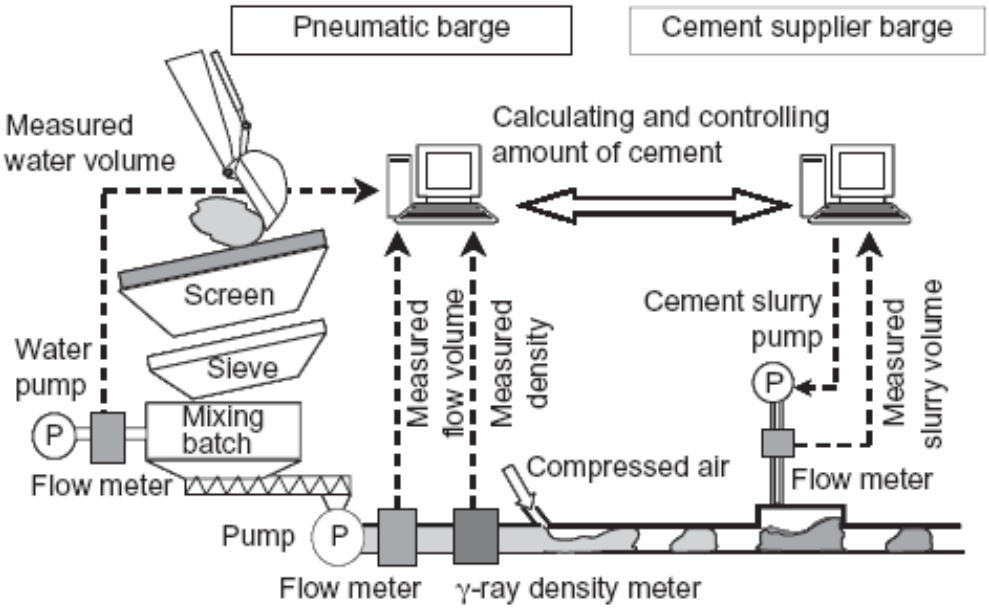

Figure 2.11 Mixing control system (Kitazumeh and Satoh, 2005)

The mixing control system operates as follows:

- First, the volume and density of the soft dredged mud in the pipe were determined by means of a flowmeter and a γ-ray densitometer respectively. The data logger acquisition unit continuously sends gathered information to the PC on the pneumatic barge.
- Secondly, the amount of required cement to be mixed was evaluated to obtain the target ratio of water content to cement, w/c., and then the PC computer stationed on the agent supplier barge controlled the amount of cement to be injected into a plug.

During execution of PFMM of the Central Japan International Airport, the density and amount of the water content were measured by means of the data acquisition unit at a time interval of 20 seconds to determine the required amount of cement to be mixed. Figure 2.12 shows a typical example of an execution chart of the dredged mud slurry properties and the amount of cement added, which was determined during the operation of one transporting barge. It is shown in Figure 2.12 that the water content of he treated soils varied over a range of 106-118%, whereas the target water content was designed to be around 110%. The amount of cement was controlled within the range of around 50-65 kg/m^3, depending on

the fluctuation of the water content in order to maintain w/c ratio of around 14.0. Figure 2.12 also shows the variation of water/cement ratio w/c, recorded at the same time. The w/c value was calculated from the measured volume of dredged soil and that of the injected cement slurry. Kitazume and Hayano (2007) pointed out the measured w/c was close to the targeted w/c of 14.0. A small fluctuation in w/c ratio proves the high accuracy in controlling w/c and it was expected that the strength variance of the cement-treated soil to be considered negligible.

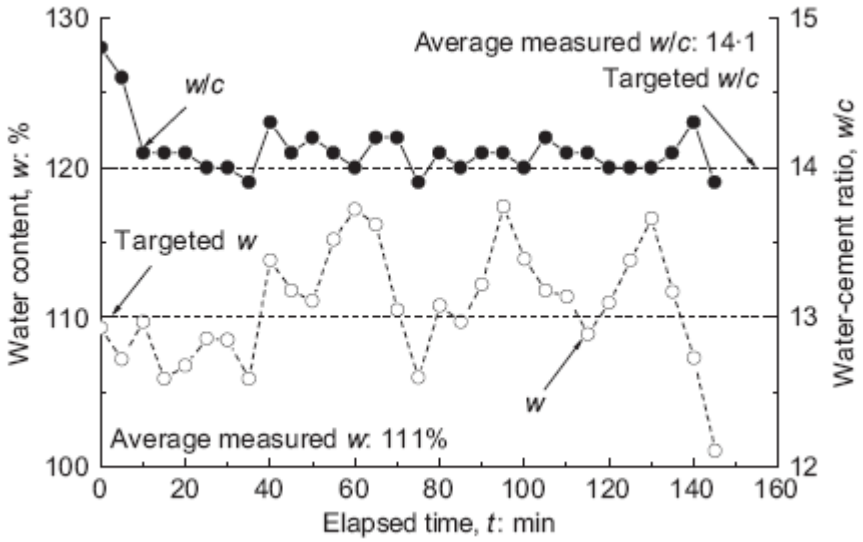

Figure 2.12 Mixing condition of the treated dredged mud
(Kitazume and Hayano, 2007)

To ensure the uniformity of the mixing process, the freshly treated soil was sampled on the placement barge every 15 minutes and was poured into a mould 5 cm in diameter and 10 cm in height. The samples were cured in a laboratory for 4 weeks and then subjected to an unconfined compression test. The test results of the unconfined compressive strength of typical specimens are shown in Figure 2.13. This figure also shows the envisaged values of the gained strength based on the measured w/c ratio (Kitazumeh and Satoh, 2005). It was found that the estimated values of strength fluctuates within the range of 225-420 kN/m^2, while the measured strength of the samples lies within the range 280-370 kN/m^2.

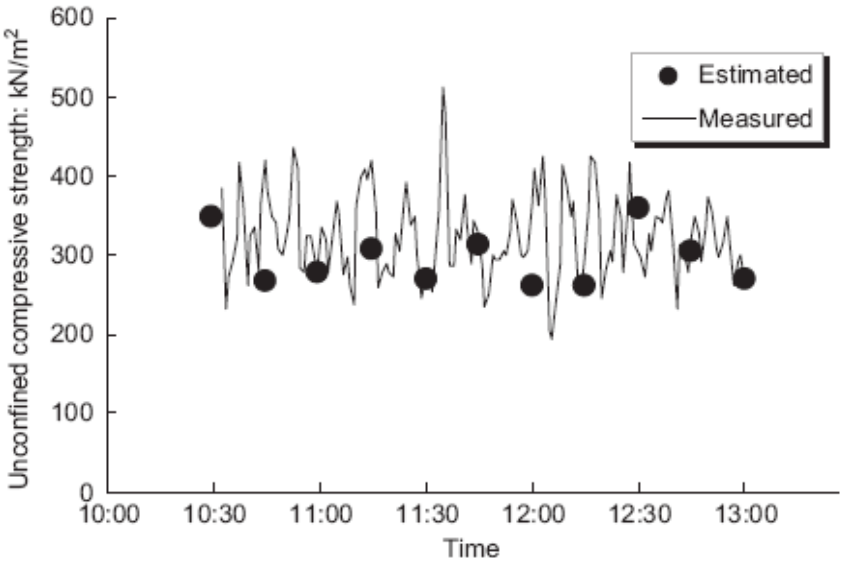

Figure 2.13 Quality control of treated soil strength (Kitazumeh and Satoh, 2005)

2.3.2 Strength of the fresh treated samples

During the construction period which lasted up to 1.5 years, freshly treated soil was sampled on the placement barge at regular intervals from every 25000 m^3 of produced dredged mud. The representative samples were poured into a mold of 5 cm in diameter and 10 cm height. After four weeks of curing in an air-conditioned laboratory, the unconfined compression test was conducted on the specimens. Figure 2.14 shows the frequency distribution of the measured unconfined compressive strength. The figure suggests that there was a relatively large scatter in the measured data, ranging from 150- 800 kN/m^2. However, the gained strength of the majority of the specimens lay between 300-450 kN/m^2 with an average value of $430kN/m^2$. The coefficient of variation was found at about 32.7%. These data proved that the manufactured process of treated dredged mud was well controlled. The measured average strength was about 37% higher than the design value of 314 kN/m^2 (Kitazume and Satoh, 2005).

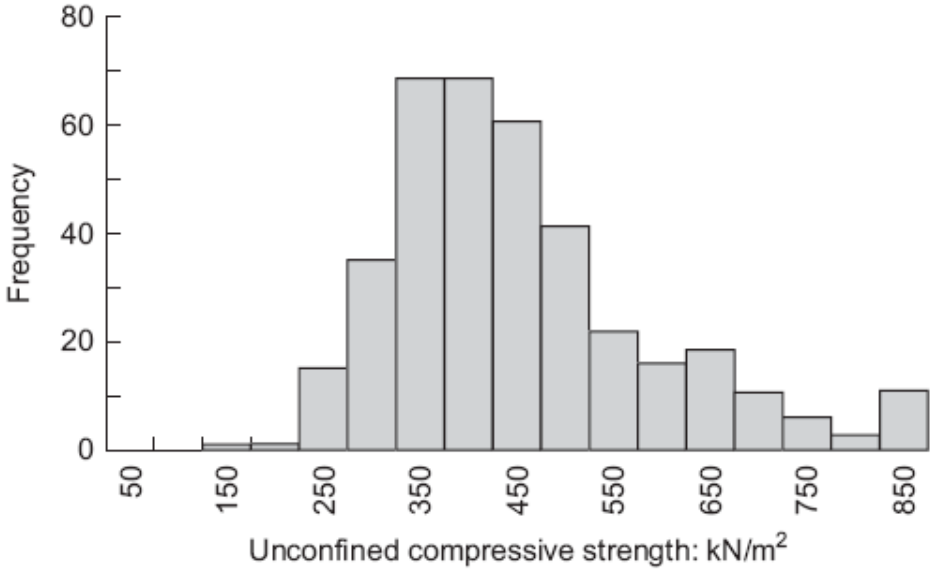

Figure 2.14 Frequency distribution of unconfined compressive strength of freshly treated soil (Kitazume and Satoh, 2005)

2.3.3 Strength of the stabilised ground

For the cement treated ground, a series of field cone tests and unconfined compressive strength tests on core samples were conducted on a regular basis. This was performed for every 25000 m^3 of the placed treated mud to ensure the design strength as well as to feedback to the mix design if it was necessary (Kitazumeh and Satoh, 2005). Figure 2.15 presents the depth profile of measured unconfined compressive strength. As it is shown, there was remarkable scatter in the measured data. However, the figure shows that the average gained strength of the treated soil was considerably higher than the target value of 120 kN/m^2. Figure 2.16 shows the depth profile of the sampled specimens with their associated moisture content of the samples. Again, there was considerable scatter in measured data with an average value of 105%. It was found that the average water content of the treated soils placed above and below water level were 97% and 107% respectively, which confirms the entrapping of seawater into treated soil during placement below water level. As a conclusion, it can be said that the entrapped seawater reduces the strength of treated soil placed below water level (Kitazumeh and Satoh, 2005).

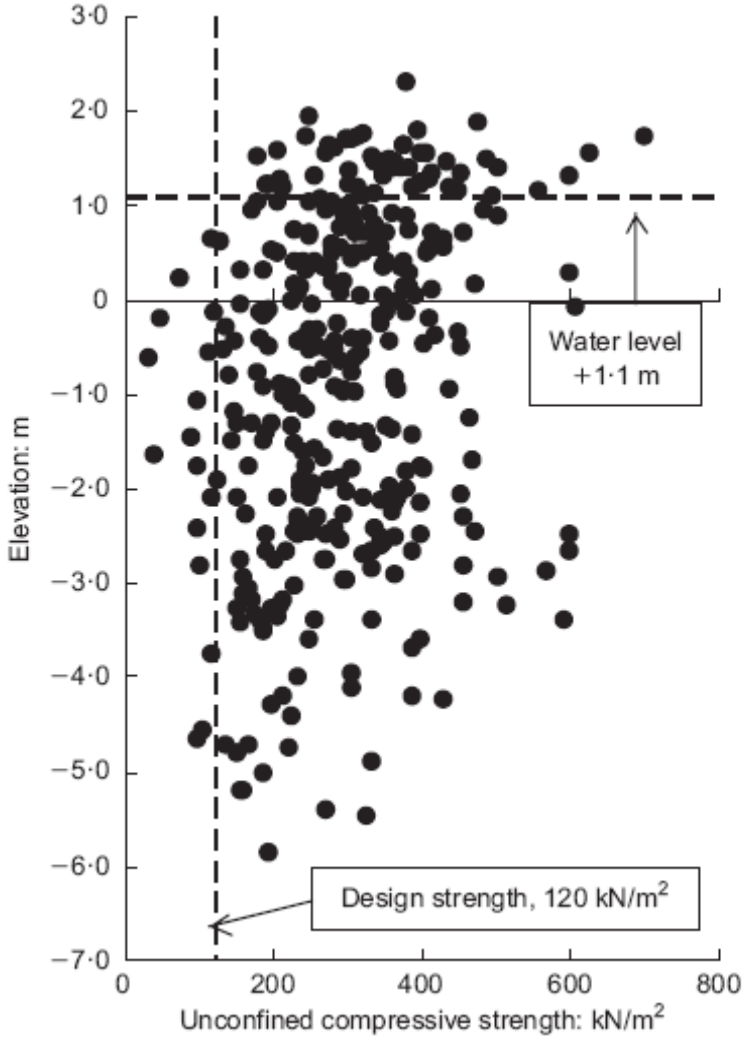

Figure 2.15 Unconfined compressive strength in field (Kitazumeh and Satoh, 2005)

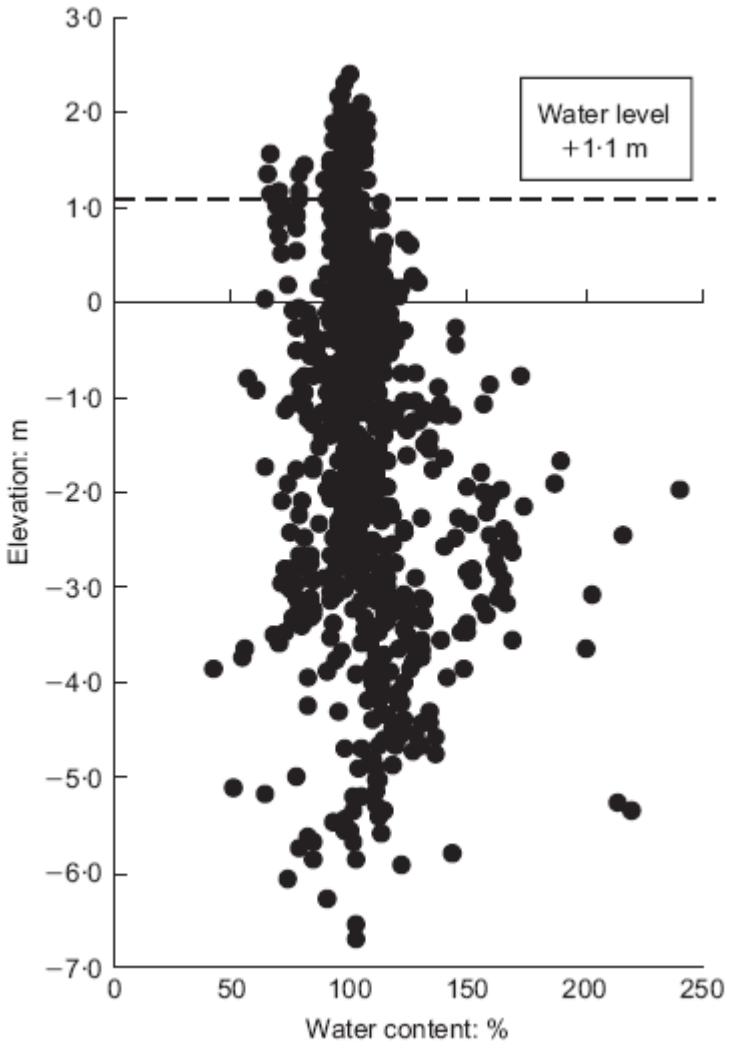

Figure 2.16 Water content profile of treated soil (Kitazumeh & Satoh, 2005)

2.4 Reclamation site at the Port of Brisbane in Australia

The Port of Brisbane is one of the growing Ports on Australia's east coast (Figure 2.117). Due to rapid commercial growth and high demand for space, the Port of Brisbane Corporation (PBC) has made a decision to locate all its facilities into one area on Fisherman Island and to expand this area over the period of 25 years.

Figure 2.17 Aerial view of the Port of Brisbane

To achieve this goal, POB is reclaiming a few paddocks (or containment ponds) to extend the length of Fisherman Island by 1.8 km and to create an extra 230 hectares of land. This conveyance gives the Port critical land and water area, creating an opportunity to develop significant improvements in the Port's capacity and efficiency of its marine terminals and in-house cargo transportation services. On Fisherman Island, Port land has been developed by reclaiming and filling land utilising materials dredged from the Brisbane River berths,

Moreton Bay and river shipping channels. Approximately 1.2 million cubic meters of mud is dredged out of the Brisbane River and Moreton Bay each year (Kinhill, 1999). This utilises a vast amount of containment area which is usually located in the nearby marine zones.

The reclaimed mud generally comprises silty clay, although a variation in material characteristics and occurrence of segregation across the paddocks are expected because of the single point discharge system, with coarser materials depositing closer to the discharge point. The utilization of this material for the reclamation project confirms that the material, that otherwise would have to be disposed of at great cost, can be used in a beneficial way. In fact, the use of this dredged material in the construction of the port reduces the demand for importing soil from inland precincts at higher price. However, it should bear in mind that the dredged materials consists of a high water content caused by the process of cutter and suction dredging. Due to high moisture content and presence of substantial fine fractions, the dredged material shows poor engineering characteristics. This material has to be settled for long periods before enough water has been squeezed out to achieve sufficient strength and stiffness.

Methods of improving the dredged mud's engineering characteristics would increase the possible uses of the material and ultimate value. Soil improvement can broadly be described as a countermeasure applied to soft soils to enhance the performance of the ground in terms of increasing strength, decreasing permeability or controlling deformation (Porbaha, 1998). The decision on which viable ground improvement technique to use depends generally on the future use, importance, and construction period of the project area.

The simplest ground improvement technique is to put a surcharge preload higher than the anticipated future load so as to preconsolidate the soil to the required effective stress (Terashi and Katagiri, 2005). It should be noted that the magnitude of surcharge defines the rate of post construction secondary compression settlement. In the past, the Port of Brisbane Corporation has adopted this technique to the west and north of the project site.

However, due to large vertical drainage paths of the thick reclaimed deposits, this technique often requires a long consolidation period, which is not ideal in many land reclamation projects. Therefore, the application of preloading alone may not be feasible with tight construction schedules and hence, a system of vertical drains is often introduced to achieve accelerated radial drainage and consolidation by reducing the length of the drainage paths (Lau et al. 2000). The rate of expelling the pore water is governed by the compressibility, permeability and length of the drainage path. Hence, to meet a tight construction schedule, the reduction of drain spacing might seem to be a viable solution to reduce the required time for preloading. However, one should note that the increase in number of installed vertical drains for the purpose of acceleration of consolidation may contribute a significant cost to the project development which may not be desirable. Hence, increasing the rate of soft ground settlement without reducing the drainage path necessitates research into other possible innovative technologies.

2.5 Introduction of dredging fleet in the Port of Brisbane

The principal type of dredging equipment used in the land reclamation works are the cutter-suction dredger, Bottom opening dredger, trailer suction hopper dredger and the bucket dredger. For the maintenance of the port and Moreton Bay, the Port of Brisbane Corporation currently utilizes a fleet of vessels for different dredging operations. A description of the dredges and their application are reviewed.

2.5.1 Suction Hopper Dredger

Brisbane is the POB's trailing suction hopper dredger and is the main and biggest dredger in the POB's fleet. *Brisbane* has the latest state-of-art automation control and navigation systems and is capable of performing capital and maintenance dredging in accordance with the latest environmental standards. It is used for maintenance and development dredging and reclamation works in the port.

Figure 2.18 Trailing suction hopper dredger

The suction dredger utilizes a hydraulic system that sucks up the material using large pumps as the dredge moves, scraping the material into the inlet pipe. The dredged material is pumped into the hopper, with a capacity of 2900 cubic meters, and is transported to the disposal site then pumped via a fixed or floating pipeline to the disposal area. Through this process the water content of the material is increased by as much as five times its in situ state. This technique utilizes the increase of water content so that the material can be pumped long distances. It also minimises the plumes of muddy water associated with excavation dredging.

2.5.2 Cutter Suction Dredger

The *Amity* is the POB's cutter suction dredger and is used for developing berths and associated reclamation at the river mouth. This dredger, like the trailing hopper suction dredge, utilizes a hydraulic system that sucks up the material using large pumps and with the assistance of the rotating auger tip, can cut through a wider range of materials. The dredged material can be transported via a fixed or floating pipeline to the disposal area in the same manner as the hopper suction dredger.

2.5.3 Bucket Dredger

The bucket dredger utilizes a bucket to excavate the material, like the common forward loading excavator on land. There are two main types of bucket for different types of dredging applications. The *Ken Harvey* is a clam bucket dredger used by the POB to dredge port berths and approaches, and is usually employed in small-scale dredging operations with a 3.25 cubic meters bucket. The material is placed into a barge or hoppers and transported to the disposal area. This type of dredging process takes the material in its current state and does not significantly increase the water content, allowing relatively easy manipulation.

Figure 2.19 Bucket Dredger in Operation

2.6 Development of the research question

The case history study of the construction of CJIA with the application of PFMM, revealed the feasibility of an injection of binder into the dredged mud slurry prior to discharging into a pond. However, as far as the development of shear strength of treated dredged mud is concerned, the successful application of a pneumatic flow mixing method is highly dependent on the degree of water content of the dredged mud slurry. Higher initial or final moisture content of dredged mud, results in a remarkable reduction of gained unconfined shear strength and consequently, unsuccessful application of PFMM.

It also can be understood that the sophisticated design of the PFMM system, which comprises a series of different linked barges, is considered suitable to deal with the low moisture content of dredged mud. As explained in the case history, the main reason for the injection of high air pressure into a system is to form discrete plugs of dredged mud in order to reduce friction between the dredged material and inner surface of the pipe as soil flows in. Besides, the installation of a cyclone at the outlet of a placement barge is also considered necessary to release the excess air pressure before the placement of plugs on the seabed. As a conclusion, it can been said that to execute the procedure of mixing dredged mud slurry with a binder, a simpler arrangement of operational vessels might be required once the slurry moisture content condition is not a factor to negatively affect the desired properties of treated soil. This research aims to define the different objective for the addition of binders into a dredged materials used in the Port of Brisbane. In fact, in spite of PFMM where improvement in shear strength of the treated soil is considered as a target, the current study tries to evaluate some other aspects of reactions which take place between clay particles and chemical binders and investigates the effects of the reactions on the consolidation properties of the dredged mud.

The study conducted here tries to blend the principles of both the surcharge preloading and PFMM techniques, in the laboratory scale, and then answer questions about the mechanical response of the treated sediment only from the point of view of consolidation and permeability and not other geotechnical aspects such as shear strength. However, to make the outcomes of this bench-scale research useful for the large industrial scale project like Port of Brisbane, high moisture content slurry is used throughout the experimental program in this study. This approach is adopted to ensure that on the basis of new defined objective, the high moisture content has no negative affect on the gained properties of the treated dredged mud. During the course of this research project, attention is directed toward the beneficial use of lime as a binder which possesses a power to modify the physico-chemical properties of clay particles. As dredged mud is mixed with certain amount of lime during a dredging operation, the clay particle surface properties would change significantly. Hence, one should expect different consolidation behaviour of a deposited reclamation layer when

it is later subjected to the external load of preloading during the ground improvement phase.

The literature survey shows that in the case of soft ground treated with a prefabricated vertical drain, the consolidation due to radial flow towards the vertical drain is proportional to both the coefficient of consolidation and inversely proportional to the square value of the diameter of influence zone of drain (Please refer to chapter 5 for further explanation). This fact indicates that under a certain diameter of influence zone of vertical drain, with an increase in the coefficient of consolidation of dredged mud, the degree of consolidation will increase within a specific elapsed time. The literature review (Chapter 3) shows that when lime is added to the clayey soil, as a result of flocculation, the permeability will increase which leads to an increase in the coefficient of consolidation. The implicit conclusion of the above two facts may now be drawn; that if lime is added to the dredged mud during the process of dredging, when it comes to ground improvement by application of preloading with a vertical drain, due to newly gained larger values of coefficient of consolidation, a smaller number of drains needs to be installed. In other words, adding lime into dredged mud slurry increases the coefficient of consolidation of clay, which in turn offsets the requirement for smaller drain spacing to meet a scheduled preloading time.

Furthermore, it is well known that the magnitude of surcharge defines the extent of post-construction secondary compression settlement (Chapter 5). Hence, as a second beneficial aspect of the injection of lime into the dredged mud, it is envisaged that the lime treated dredged mud will require a lower surcharge to present the allowable creep settlement under the final design load. This expectation is again attributed to the mechanism of flocculation, which is brought about by lime addition.

2.7 Feasibility of injection of binder into a dredged mud slurry in the Port of Brisbane

The study of the case history of the construction of Central Japan International Airport with the application of PFMM revealed the feasibility of utilizing current modern technology in the injection of the binder into the dredged mud slurry prior to discharging into a pond. However, even though the execution of this method may cut the need for further ground improvement techniques on the reclamation layer and eventually results in a shorter time period for completion of the project, this technology may attract little interest by project developers as it requires a new generation of execution vessels that may not be available for current ongoing man-made island projects around the world.

The application of PFMM requires a series of different linked barges to deal with low moisture content of dredged mud. This is because, as far as the development of shear strength of treated dredged mud is concern, the successful application of a pneumatic flow mixing method is highly dependent on the degree of water content of the dredged mud slurry. Hence, the invention of the PFMM system helps to inject high air pressure into a system to form the discrete plugs of dredged mud to mitigate the friction between the dredged material and inner surface of the pipe as soil flows in. Besides, the installation of a cyclone at the outlet of the placement barge is also considered to release the excess air pressure before placement of plugs on the bed.
For these reasons it can be said that when it comes to the improvement of problematic soft grounds, the application of commonplace practices like the surcharge preload may seem more desirable.

As a pragmatic proposal, it can be suggested that once the initial and final moisture content of slurry is not concerned, a simpler version of chemical injection system can be carried out to add the binder into the dredged mud slurry prior to discharging into the containment ponds. However it should be noted that this suggestion is made based on the philosophy on which this research study is established. According to the viewpoint of this study, the degree of initial moisture content of dredged slurry may not be a factor to govern the

alteration of the physico-chemical properties of the mud where it is treated with hydrated lime. On the other word, in spite of PFMM in which development of shear strength of cement-treated dredged mud is concerned, a chemical injection system may be considered in order to add small amount of chemical to the high moisture content dredged mud to only change the physico-chemical properties of the clay particles. The alteration of clay particles with the presence of lime is discussed in detail in chapter 3. According to this approach, it seems that with increasing initial moisture content to a high level (i.e. 350-550%), there is no further need for both the Pneumatic system, to reduce friction, and the placement barge with the cyclone system to carefully handle the treated plugs (Figure 2.20). This proposed method may now be called the "***Flow Mixing Method***" instead.

Figure 2.20 Discharging method for high moisture content slurry

Chapter 3

Chemical Additives in Soils

3.1 General:

Clay soils usually pose a challenge to both geotechnical engineers and developers due to short or long-term mechanical response when subjected to loading. The delayed deformation reaction to the applied load is often a manifested property of clay, which has the ability to develop high pore water pressures, both positive and negative (i.e. suction). The pore water pressure governs the stresses that clay can withstand in engineering practice, whether applied pressure is static or dynamic such as in cyclic loading. Hence, insights into the factors which govern the interaction of clay soils with pore water provide an adequate understanding of likely behaviour of the soil when it is subjected to loading.

The characteristics of clay soils are largely controlled by the amount and type of clay in the soil matrix, known as clay fraction and clay mineralogy respectively. The type of constituent mineralogy of clay fraction can considerably affect the way in which clay reacts to water. A clay soil containing significant quantities of Smectite minerals (e.g. Montmorillonite), has a tendency to be highly plastic. This is because this kind of mineral has an affinity to water molecules to become associated with it. The Atterberg Limits test which comprises both liquid limit and plastic limit is a laboratory tool by which the plasticity is measured. The difference between these two parameters is defined as the plasticity index which is a more precise parameter to present the plasticity of clay. Clay soils also have a high Cations Exchange Capacity (CEC), making them sensitive to the predominant cation existing in the soil water. CEC is the capacity of soil for ion exchange of positively charged ions (cations) between clay particles and pore water. The quantity of cations that a clay mineral can accommodate on its negatively charged surface is expressed as milliequivalent (meq) per 100g. Clay soils which contain mainly Kaolinite

show a much lower plasticity and cation exchange capacity. For those clay soils which predominantly contain Illite, these two parameters are even less than kaolinite.

Alteration or improvement to the properties of clay soils for construction purposes can be made by a variety of means, broadly divided in two categories:

- Mechanical improvement
- Chemical improvement

The economics of the alternative solution in ground improvement practices is always considered in an engineering design. In the case of clay soils, chemical improvement may be commonly most effective since it can be used to change the inherent nature of the material. Chemical additives can be used to not only strengthen the soil, but also to mitigate its problematic sensitivity both to water and subsequent stress development.

This chapter aims to provide useful information on the properties of the dredged mud used in this study, structure, and characteristics of clay fabric. The most common binders - cement and lime - and their reactions with clay soils will be discussed afterwards. Specific attention will then be directed towards the properties of lime which demonstrate some distinct features in comparison with cement when it reacts with soil pore water. This study emphasizes an important process of lime-clay reaction known as modification of clay soil; the addition of lime changes the fundamental nature of clay and creates a material with different characteristics. Literature review on the changes in permeability of clay soils treated with lime is presented. Finally, a laboratory test method to identify the quantity of lime required to modify the chemical properties of clay soils is proposed.

3.2 Constituents of mud

Mud is defined as a sediment mixture with particles smaller than $75\,\mu m$. It consists of organic and inorganic components, water and sometimes gas. The inorganic fractions include quartz, feldspar, clay minerals, calcite, dolomite, hydroxide, silicate, sulfides and small fractions of other minerals (Groenewold and Dankers, 2002). The organic material

in mud consists of living and dead material such as bacteria and remnants or products of phytoplankton, benthic algae, faecel pellets, peat and macromolecules produced by bacteria. The amount of organic material in mud strongly depends on the source and season. In intertidal areas it may amount to 10-20% of the dry weight of the sediment and due to the high level of absorbed water even 70-90% of the wet weight (Groenewold and Dankers, 2002). The water and organic material content decreases due to the drying and consolidation of the sediment layers. Therefore older mud differs strongly from the biologically active mud that lays at the surface. The resuspension of old mud layers due to dredging activities may thus have a different impact on the environment than the resuspension of the top-active layer (Groenewold and Dankers, 2002).

3.3 Structure of clay particles

The clay fraction, $< 2\,\mu m$, is the most important substance of mud as it exhibits typical properties. Two significant properties of clay are plasticity and cohesion (Partheniades, 1980). Plasticity is the ability of a clay mass to undergo substantial permanent deformation, at the proper water content, under stresses, without breaking (Partheniades, 1980). Cohesion is the property of a material to stick or adhere together.

Clay is essentially composed of one or more members of a small group of clay minerals. These minerals have predominantly crystalline arrangements; i.e. the atoms composing them are arranged in definite geometric patterns. Clayey materials can then be considered to be made up of a number of these clay minerals stacked on top of each other in the form of a sheet or layered structure (Partheniades, 1980). Chemically, clay consists of silicates of aluminum and / or iron and magnesium. These minerals form two fundamental building blocks which comprise the clay mineral. The silicon-oxygen sheet is one of these building blocks. It is formed by a SiO_4 tetrahedron (Figure 3.1). The other building block is the Al- and Mg-O-O-H sheet, which forms an octahedron (Figure 3.2). With these building blocks clay minerals are formed, of which Smectite, Illite, and Kaolinite are the most common. The differences between these clay minerals arise due to the different degree of weathering. Kaolinite is the youngest clay mineral and with increased weathering, over time changes from Illite to Smectite.

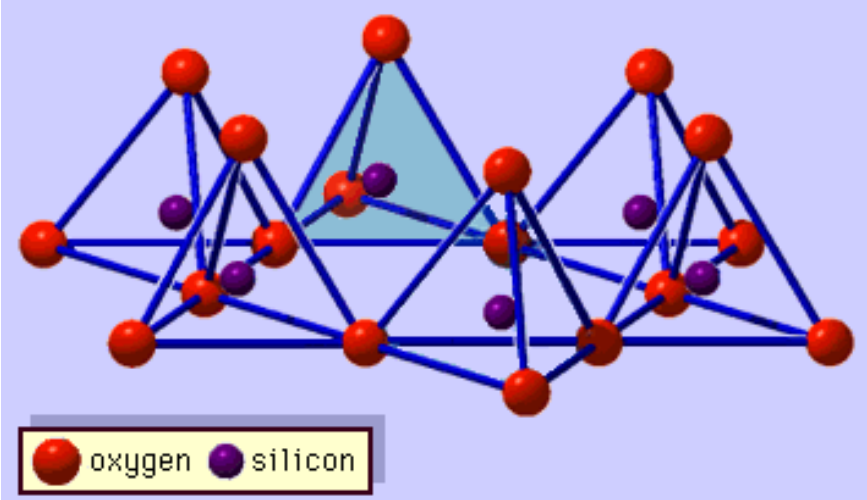

Figure3.1 Single silica tetrahedron (shaded) and the sheet structure of silica tetrahedrons arranged in a hexagonal network

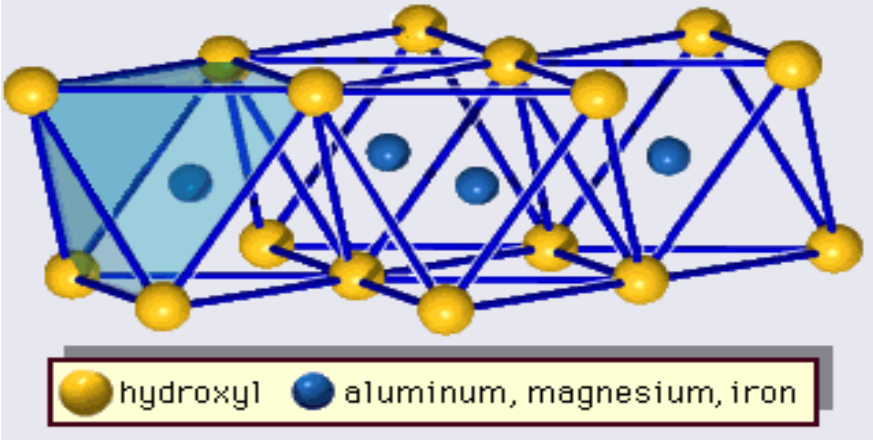

Figure 3.2 Single octahedron (shaded) and the sheet structure of octahedral units

Smectite is known as expanding three-layer clay and has a structure that consists of an octahedral sheet sandwiched between two silica sheets. A stack of such layers forms a Smectite particle. Minerals of the Smectite group are Montmorillonite, Hectorite and Laponite. Laponite has Lithium instead of Aluminum in its network and it forms irregular large transparent flocks. Smectites can double in volume, due to osmotic swelling (Mitchell, 1993) and the intrusion of water molecules between the layers. Another

characterization of Smectite is the extensive substitution of aluminum and silicon ions by magnesium, iron, zinc, and nickel; or aluminum in the silicon case.

Illite clays form a different class of the three-layer clays. These clays are distinguished from the Smectite clays primarily by the absence of the inter layers swelling with water. The minerals muscovite and phlogopite, for instance, are minerals of the Illite group (De Wit, 1995). In contrast with Illites and Smectite, Kaolinites have an almost perfect 1:1 layer structure. The main difference between the various species of Kaolinites is a difference in the layer stacking geometry. Members of this group are Kaolinite, Dictite, Nacrite and Hallogsite. The kaolinite clays are non-expandable in water.

3.4 Interaction of clay particles in suspension

It is known that the clay particles exhibit a negative charge on their surfaces. This is due to isomorphous substitution, incomplete occupation of the positions available for metal ions and release of protons from hydroxides (Lagaly and Köster, 1993). These negatively charged particles are assumed to be surrounded by ions of opposite charge at a fixed distance d, and they are held around the clay particle by electrostatic forces. Helmholtz (1897) proposed a model of a charged particle in suspension, in which oppositely charged layers of ions are separated by distance d (see Figure 3.3). The simple geometry of the particle and its surrounding ions assumed in the Helmholtz model allows straightforward calculation of the electrical potential of the charged particle with respect to its surroundings. This potential is referred to as the zeta potential ζ and is given by:

$$\zeta = 4\pi qd / \varepsilon \qquad \text{Eq. 3.1}$$

This equation is for two unit planes, each carrying a charge q and separated by a distance d in a medium of dielectric constant ε. Both the dielectric constant and product dq may be obtained experimentally (Bennett and Hulbert, 1986).

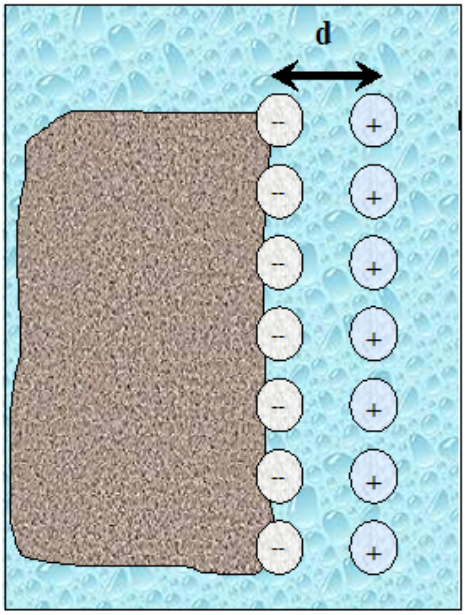

Figure 3.3 Helmholtz model of a charged particle in suspension

Application of the Helmholtz model to clay particles allows the zeta potential to be used in the quantitative description of some properties of clay suspensions or sediments which are fully saturated with water. If in clay suspension two similar particles approach each other, they will tend to adhere due to the strong, short-range attractive forces that hold the particles together internally. There are a few attractive forces act between silicate minerals, one of which is Van der Waals forces. These forces are effective over intermediate distances and are generated by the mutual influence of the motion of electrons of the atoms. The attractive potential of Van der Waals forces between two atoms is inversely proportional to the 7^{th} power of the distance. Hence, in order to become effective, particles must come very close to each other (Partheniades, 1980). In clay suspension more and more particles agglomerate as a result of attractive forces and form sediment in which all the interparticle spaces are filled with water. The tendency of the particles to agglomerate is opposed by the presence of the surrounding layers of positive ions adhered to a clay particle surface. Hence, it can be said that the interaction

between these two positive layers is repulsive. As a result of this phenomenon, the close approach of the particles is prevented (Figure 3.4).

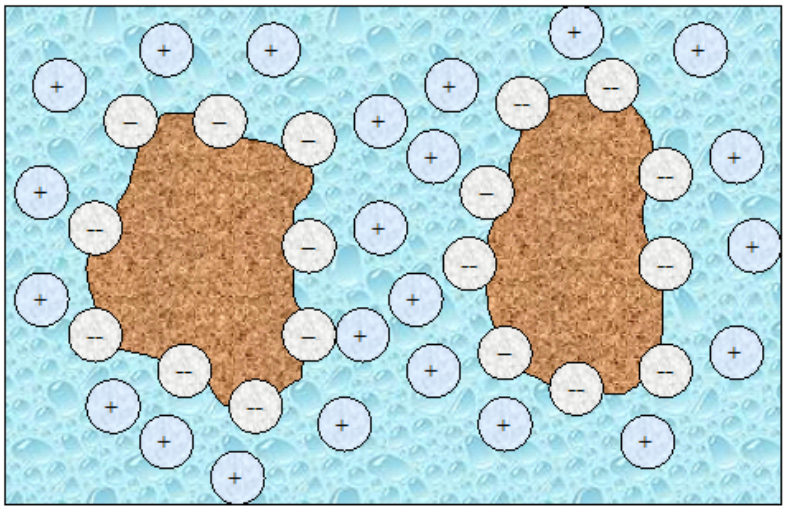

Figure 3.4 Electrostatic repulsion between the like-charged ion layers tends to hinder agglomeration of particle in suspension

The electrostatic repulsion increases with increasing charge density of the counter-ion layer (q) and decreases with increasing dielectric constant (ε) of the medium. Furthermore, the effectiveness of a given degree of repulsion in preventing particle to particle contact increases with increasing distance between each particle and its counter-ion layer (d). Based on the Eq. 3.1, the zeta potential responds in the same way to changes in q, ε, and d as does the stability (i.e. dispersion) against flocculation. Powis (1916) proposed that a "***critical zeta potential***" has to be exceeded in absolute value if a suspension is required to be stable (i.e. no settling or flocculation). It was suggested that this critical potential is of the order of 20-30 mV.

The importance of the counter-ion is expected if the Helmholtz description is appropriate. Ions of an added electrolyte that have the same negative charge as present on the suspended particles would be repelled electrostatically from the particle. Ions of the added electrolyte that have a charge opposite to that of the suspended particle however, would be appearing in the surrounding counter-ion layer. It is assumed that ions move

about freely in solution. Hence, all the counter-ions include those initially present in solution as well as those of the added electrolyte presented in the surrounding layer based on their proportion to the concentration in the solution. For those highly charged ions, fewer amounts would be required to neutralise the negative charge of a suspended particle. Accordingly, the thickness, d, of the counter-ion layer would be reduced, and the repulsive zeta potential would be smaller. Figure 3.5 shows the effects of added electrolytes on the stability of clay suspensions. This figure provides comparison between cations with different charge density on the zeta potential of a clay suspension.

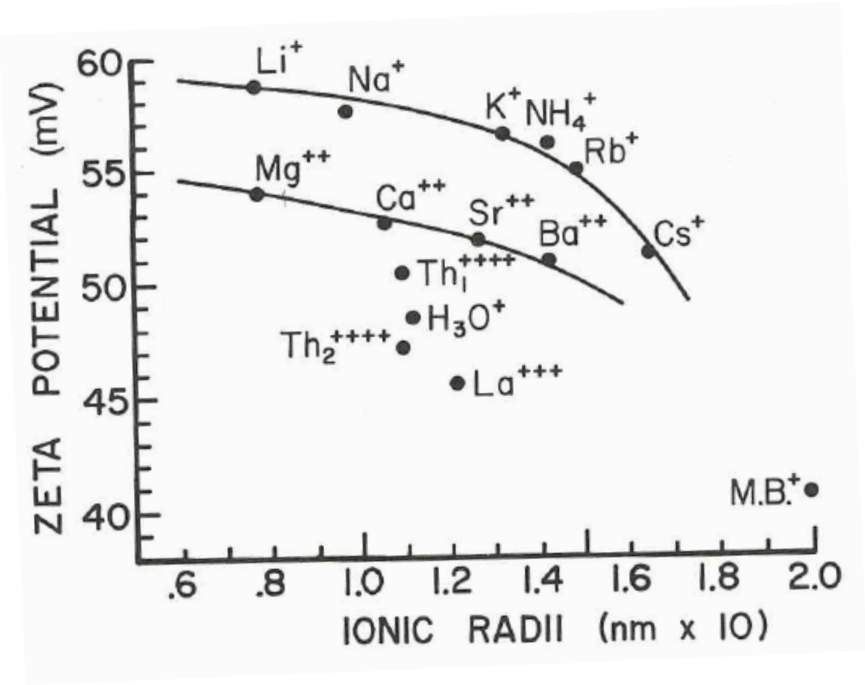

Figure 3.5 Dependence of the zeta potential of colloidal clay suspensions on charge and ionic radius of different counter-ions (Bennett and Hulbert, 1986)

It should be noted that although the Helmholtz model of charged particles proved to be helpful qualitatively, experimental evidence indicates that it is too simple to explain the behavior of suspensions. Gouy (1909) and Chapman (1913) proposed independently that the counter-ions are not held rigidly at a fixed distance from the clay particle surface, as

suggested by Helmholtz. They proposed that the counter-ions diffuse from the particle surface due to collisions with aqueous solution molecules.

Stern (1924) proposed the modern picture of charged particles in contact with an aqueous solution; he combined the Helmholtz and the Gouy-Chapman models. He argues that some counter-ions are held firmly at a fixed distance to the clay surface and other are held more loosely at a distance from the surface. Based on this model, the term "*Diffused Double Layer*" thickness may be used in the quantitative description of some properties of clay suspensions or sediments which are fully saturated with water.

3.5 Cation Exchange Capacity

The concept of Cation Exchange Capacity (CEC) basically requires understanding of the clay surface chemistry. Exchange in a clay particle refers to the capacity of colloid particles to change the cations which are adsorbed on the clay surface. Hence, hydrogen ions on a clay surface for example can be substituted by sodium due to the constant percolation of water containing dissolved sodium salt. The exchangeable ions are normally held around the outside of the silica- alumina clay mineral structure unit. Compositional variation in ionic or isomorphous substitution within the clay mineral crystal lattice can leave the structural unit of clay with a net negative charge. The presence of this net negative charge means that soluble cations in a suspension can be adsorbed on the surface of the clay mineral structural units. The ability of a clay soil to hold cations is termed "cation exchange capacity". The most common adsorbed cations on the clay surface are $Na^+, K^+, Ca^{2+}, Mg^{2+}, H^+$, and NH_4^+. Cation exchange capacity plays a significant role in determining properties of a clay mineral, particularly in regards to its affinity for water.

Cation exchange capacity is measured in terms of milliequivalent of the atomic weight of solvent per 100 grams of the dry solid. This parameter varies widely for different types of clay minerals. The CEC is usually measured as a function of the number of positively

charged cations which can be released from the clay surface once the clay particles encounter another salt solution in their vicinity. The general laboratory test procedure to measure CEC is as follows:

A given quantity of dry soil is immersed in an aqueous solution containing a salt, usually chloride or ammonium hydroxide. The quantity of exchanged ions which eventually are found in the solution will be measured as milliequivalent. The quantity of exchanged ions must be associated with 100 g of oven dried (110 ^{0}C) soil. Thus, the CEC is given in milliequivalent per 100 grams of dried soil (meq/100g).

The charge on the surface of clays of adsorbed sites is usually in the order of 5-10 meq/100g. The charge measured exchanged on sites between the layers of clays or within the structures units varies between 40 to 120 meq/100g. Table 3.1 shows the values of CEC for clays with different mineralogy.

Table 3.1 Cation Exchange Capacity of Clay Minerals (Grim, 1968)

Minerals	**CEC (meq/100 g)**
Kaolinite	3-15
Halloysite.2H_2O	5-10
Halloysite.4H_2O	40-50
Montmorillonite	80-150
Illite	10-40
Vermiculite	100-150
Chlorite	10-40

3.6 Principles of clay-binder reactions

Mixing the most common binders like cement or lime into a soil will affect the fundamental properties of the natural, untreated soil to varying extents. The strength and deformation properties are typically those factors of main interest when designing an extension of stabilization required for ground improvement. However, besides assessing

strength and deformation parameters from various laboratory tests, it is a matter of importance to consider the changes in other soil characteristics and their possible influence on the behavior of the treated soil. Furthermore, a basic understanding of the type of chemical reaction that takes place and the compounds formed when using binders is essential in analyzing the rate and type of changes in properties. This also applies to the durability of newly gained properties of treated soil.

The chemical reactions involved in the hydration of any different types of binders (e.g. cement, lime, flyash) have been described and discussed thoroughly in many papers and textbooks (Boynton, 1980; Taylor, 1997; Boardman et al., 2001). It should be noted that in almost all literature, the focus has mainly been on the two most common binders, cement and lime. The reactions generated when mixing various binders with soil vary by the process of mixing, the concentration of binders, and duration of time, but in general the reactions exhibit many similar characteristics. For example, as a binder is mixed into the soil, chemical reactions will start immediately. Cement will form a lattice among the soil particles due to the initial hydration process of cement. This differs with the addition of lime as it will react with the chemical components of the soil. Lime based binders will continue reactions with the soil for several months and even years. Initially, the moisture content will reduce in the clay matrix as a result of the hydration process. The further reaction will take between place clay minerals and calcium ion which is dissociated into the clay system.

The geotechnical characteristics of chemically improved soil highly depend on the type of binder. It is generally observed that the strength and brittleness of the improved soil increase with an increase in the amount of cement content whereas the ductility of the soil will increase with % lime content. The primary products of hydration are formed virtually immediately. Some reactions may involve cementation starting up directly, while others may lead to further reaction with the clay minerals. The abbreviations most often used to denote various compounds in the hydration process are given below.
The reaction products formed as a result of introducing binder into a wet soil are of somewhat different types. When using quicklime which contains a large amount of

calcium oxide (denoted by C), hydration will occur as the lime comes into contact with the pore water in the soil, resulting in the formation of calcium hydroxide (denoted by CH). Some of this calcium hydroxide will be absorbed onto the soil particles. Ion exchange will take place and the soil may be modified into a somewhat dryer and coarser structure due to the slaking process and flocculation of the clay particles that take place (Saitoh et al., 1985). The calcium hydroxide not consumed in this process is free to react with the silica (S) and alumina (A) contained in the minerals present in the soil. These reactions, termed pozzolanic reactions, will result in the formation of calcium aluminate silicate hydroxide (CASH), calcium silicate hydroxide (CSH), and/or calcium aluminate hydroxide (CAH) (TRB, 1987). When using cement, the primary products of hydration are formed almost immediately upon the mixing of two substances to produce the most substantial strength gains normally exhibited in cement stabilization. The secondary product of the hydration process of cement is hydrated lime, which induces a gradual rise in the soil-cement pH to finally dissolve and chemically alter clay minerals. This secondary reaction occurs over time to produce additional binding and strength. The reactions which take place in soil cement stabilization can be presented by the following qualitative equations (Bergado et al., 1996). It should be noted that only tricalcium silicate (C_3S) has been considered as it is the major cementitious constituent of Portland cement.

$$C_3S + H_2O \rightarrow C_3S_2H_x \text{ (Torbemorite Gel)} + Ca(OH)_2 \text{ (Hydrated Lime)}$$

$$Ca(OH)_2 \rightarrow Ca^{++} + 2(OH)^-$$

$$Ca^{++} + 2(OH)^- + SiO_2 \text{ (Soil Silica)} \rightarrow CSH$$

$$Ca^{++} + 2(OH)^- + Al_2O_3 \text{ (Soil Alumina)} \rightarrow CAH$$

The various other binders, for example fly ash, can be characterized with respect to the possible type and rate of reactions by looking at their content of CaO, Al_2O_3, and SiO_2. In general, the reactivity increases with total content of $CaO + Al_2O_3 + SiO_2$ of the binders (Taylor, 1997).

Lime, which contains a high proportion of CaO, has an elevated potential for forming large amounts of reaction products when mixed with soil. However, pozzolanic reaction with soil is normally relatively slow, due to the restricted accessibility of the silica and alumina contained in the soil whereas the reaction forming CSH upon hydration of cement involves minerals contained in the binder itself. Hence, more rapid pozzolanic reactions with the soil mineral are expected. In calcium aluminate cements, the high content of alumina will cause much faster reactions than those of Portland cements (Taylor, 1997).

3.7 Lime- the common binder

It is well known that the treatment of clays with lime leads to beneficial effects in terms of strength, compressibility, plasticity, permeability and workability of problematic soft clay (Kezdi, 1979). Lime stabilization has been extensively used for road construction purposes, where the bearing capacity of the soft subgrade is increased, resulting in reduction of the thickness of the base course (Chaddock, 1996; Holt and Freer-Hewish, 1998). The treatment needs intimate surface mixing of lime with soil and execution of compaction in order to produce the final dense product.

More recently, lime mixing has become established as a deep solidification technique via deep mixing to create lime columns (Broms and Boman, 1976). The present application of a lime column is to increase the bearing capacity, reduce the total and differential settlements of foundations, and to prevent the sliding failure of embankments. The column is created either by using slurry or powder placed into preformed holes to create lime piles (Broms, 1984) or via lime slurry pressure injection of intact soils.

Lime has also been used to treat chemical containment sites (Glendinning et al., 1998; Boardman, 1999). There are two aspects of this treatment that are a matter of interest: (1) the influence of the containments on the lime modification and solidification reactions, and (2) the ability of lime stabilization and solidification to reduce the availability of the containments of the surrounding environment.

Lime in broad terms is used to describe calcium oxide (CaO), calcium hydroxide $(Ca(OH)_2)$, and calcium carbonate $(CaCO_3)$. these three products are also known as quicklime, slaked or hydrated lime, and carbonate of lime respectively. The relationship between these three types of lime can be presented by the following equations:

$$CaCO_3 + HEAT \rightarrow CaO + CO_2$$

$$CaO + H_2O \rightarrow Ca(OH)_2 + HEAT$$

$$Ca(OH)_2 + CO_2 = CaCO_3 + H_2O$$

For many years lime, either in the form of quicklime (CaO) or as hydrated lime $(Ca(OH)_2)$, has been added to clay soils to enhance the physical properties of clay. When lime is added to a clay soil, it causes an immediate, profound alteration of the physico-chemical properties of clay particles. Once the lime is introduced into a wet clay system, the instant reaction is cation exchange which begins on a timescale of minutes to hours. The cation exchange takes place between metallic ions associated with the surface of the clay particles and the calcium ions of the lime. It is well understood that clay particles are surrounded by a diffused hydrous double layer which is modified by the ion exchange of calcium with sodium. The calcium cation sufficiently neutralised the negative charge of the clay particle, allowing minerals to adhere and flocculate. It is the mechanism which is primarily responsible for the modification of the engineering properties of clayey soils when they are treated with lime (Sherwood, 1993).

Furthermore, lime contains a high proportion of CaO with a high potential for forming large amounts of cementitious product when mixed with soil. However, pozzolanic reaction with soil is normally relatively slow, due to the restricted accessibility of the silica and alumina contained in the soil.

3.8 Mechanism of soil-lime interaction

The addition of lime either in the form of quicklime or as hydrated lime, to a soil system containing water results in several different chemical reactions that cause a profound alteration of the physico-chemical properties of clay soils. The reactions that occur bring about both immediate and long-term changes to the soil and have been described widely in the literature. In general, the lime addition to a soil initiates three reactions.

3.8.1 Hydration

A large degree of heat is produced when quicklime (CaO) is mixed with clay. This is due to the hydration of quicklime with the pore water of the soil. This reaction is highly exothermic, producing approximately 17×10^9 joules per kilogram of calcium oxide. The increase in temperature can somehow significant, so that the pore water starts to boil (Broms, 1984). Due to hydration of quicklime and heat generation, a considerable amount of pore water evaporates and therefore, the initial quantity of pore water is reduced. This drying action is particularly beneficial in the treatment of moist clays. Hence, if a reduction of the natural water content in a cohesive soil is desirable, instead of hydration lime, quicklime may be used as a dewatering agent.

The calcium hydroxide $(Ca(OH)_2)$, either resulting from the hydration reaction of quicklime or when using calcium hydroxide as the agent, dissociated in the water, results in high concentration of Ca^{++} and OH^- ions in the pore water of the soil. This dissociation of ions results in a sequence of reactions in soils that vary with soil composition, mineralogy, and pore water chemistry. The initial, immediate modification reaction occurs as a result of cation exchange of calcium ions for the existing cations at negative charge sites on the clay mineral lattice. The number of this charge sites is further enhanced in some clay minerals by the increase in pH caused by the presence of the hydroxide ions. The result of cation exchange is increased flocculation of mineral particles and changes in the plasticity properties of a soil.

3.8.2 Ion exchange and flocculation

This process is primarily responsible for the modification of the engineering properties of clay soils when they are treated with lime. The type of cations present in the soil determines whether a soil is dispersed or flocculated. Sodium cations cause dispersion while calcium or magnesium ions promote flocculation. As clay particle are simply large anions, they attract cations in order to neutralise their negative charge. Flocculating cations sufficiently neutralise the negative charge, allowing clay particles to adhere and flocculate. The attraction of particular cations to the negatively charged particle is a function of two things, the hydrated size of the cation and the charge of cation. These two factors combine to determine the charge density on the cation, which can also be explained as the distribution of charge over the surface of the cation. With the highly hydrated sodium ion, the hydrated size of the cation is relatively large, while its charge is only +1. As a consequence, that +1 charge has to be distributed over a relatively large area. With such a large cation having such a low charge, the negative charge on the clay particle is not sufficiently satisfied and the particles actually repel one another, resulting in dispersion structure of sediment.

When lime is mixed with clay, sodium and other cations initially absorbed to the clay mineral surfaces are exchanged with calcium which possesses the higher charge density. This reaction modifies the electrical surface forces of the clay minerals. As a result of the decrease of repulsive forces, the clay particles adhere together and larger sized aggregates or grains will be formed. This process is known as flocculation. The mechanism of flocculation and dispersion was discussed earlier in this chapter using the theory of the zeta potential.

3.8.3 Formation of pozzolanic products

The final stage of the lime-clay reaction process involves solidification which occurs over period of weeks or months. Sherwood (1993) defined the pozzolans as a material that is capable of reacting in the presence of water, at ordinary temperature and high alkalinity, to produce cementitious compounds. In order for pozzolanic reactions to take place, the soil must contain pozzolans, which are finely divided into silicaceous or aluminous

materials that will form cemented products. The addition of lime to clay in appropriate quantities raises soil pH and this promotes the dissolution of silica and alumina particularly at the edge sites of clay plates. The dissociated Ca++ ions react with the dissolved SiO2 and Al2O3 from the clay particle surface and form hydrated gels. The gel of calcium silicate (and/or aluminate hydrates) from the above reaction, is insoluble in water, binding the soil particles together.

The presence of gypsum or some other types of sulfates in combination with lime form ettringite. This product is a swelling mineral that utilizes large amounts of water to form its crystalline structure. The formation of ettringite is known to cause substantial heaving, and for this reason a successful use of lime stabilization in soil containing sulfate may require special consideration.

Thompson (1965) showed that presence of organic matter with a high exchange capacity retarded the strength producing pozzolanic reactions, probably due to the process of Ca lessening. However, a study by Arman and Murkhukh (1970) concluded that an organic soil-lime mixture produces cementitious products similar to those reported for inorganic soil-lime reactions, and that the organic matter does not appear to block the reaction that results in an increase in soil strength. A general statement can not be made regarding the appropriate binder or the amount thereof, as the degree of improvement is very dependant on the particular organic soil (Habib and Farrel, 2002). Clare and Pollard (1951) indicated that organic materials adversely effect pozzolanic reactions by attracting free calcium cations, therefore retarding the hardening of the soil-lime mixture.

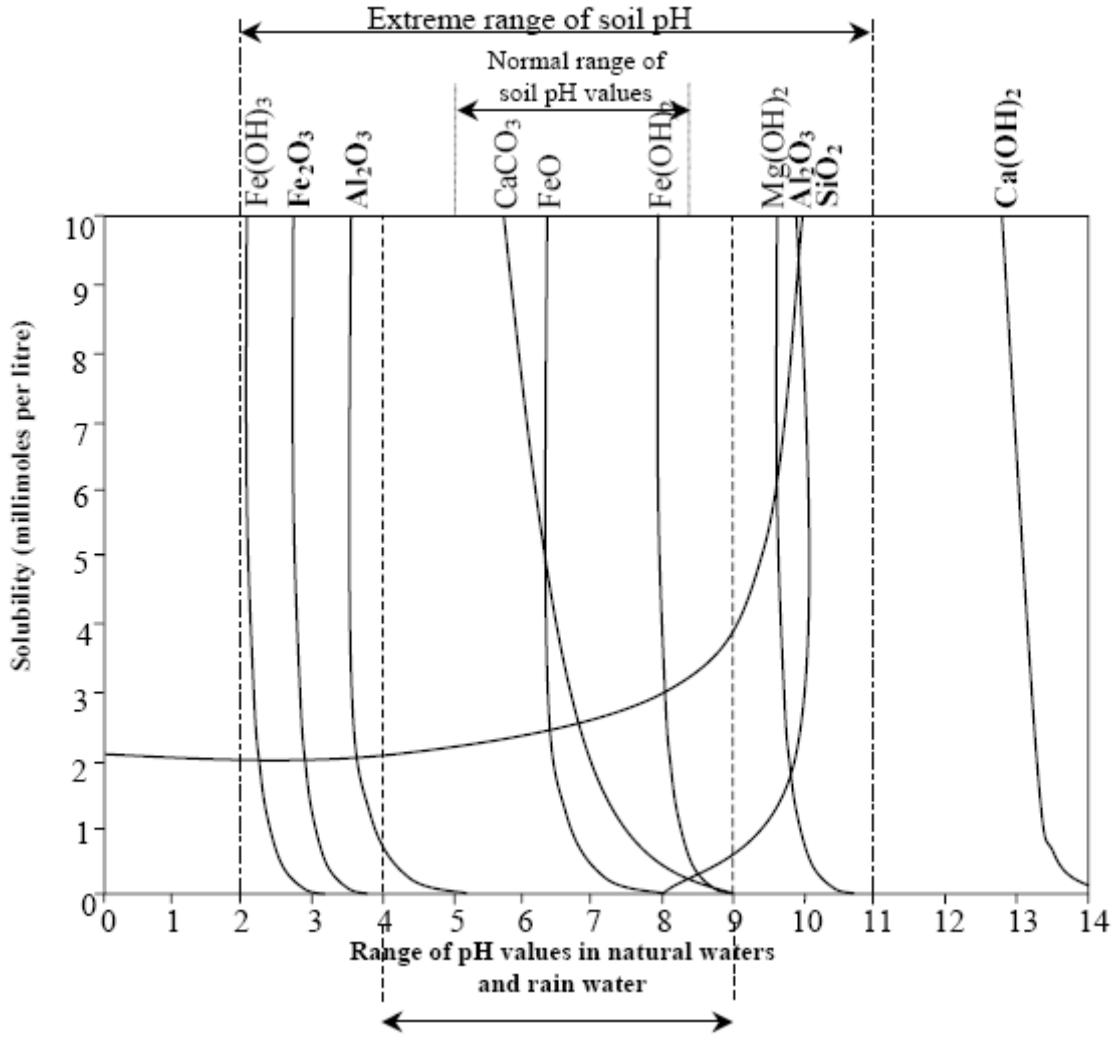

Figure 3.6 Solubility of some soil mineral species in relation to pH (Loughnan, 1969)

3.9 The threshold value of lime in soil

In the preceding paragraphs it was discussed that the hydration reaction of lime results in a high concentration of calcium and hydroxide ions in the pore water of particulate systems. The dissociation of ions leads to a series of chemical reactions that differ with the mineralogy and composition of soil, and pore water chemistry. An instant *modification* reaction would occur as a result of replacement of the calcium ions (Ca^{++}) for the existing cations at negative charge sites on the clay mineral lattice. With

increasing pH, caused by the presence of the OH^- ions, the number of negative charge sites will be further increased. This reaction induced the flocculation of clay particles and causes changes in the plasticity properties of the soil.

It was also noted that the longer-term physico-chemical alteration are brought about by a reaction termed *solidification*. Solidification occurs as a result of pozzolanic reactions, which are facilitated by the hydroxide ions, creating highly alkaline soil pore chemistry. The increase in pH promotes the dissolution of silicon and aluminium from the clay minerals (Sherwood, 1993). This is initiated at the edge sites of the clay plates. The new gel-like composites from the dissolved clay minerals react with the calcium ion in the water and form the calcium silicate hydrate (CSH) and calcium aluminate hydrate (CAH) products. These compounds crystallize over the course of time, resulting in considerable increases in shear strength and, normally, a reduction in soil permeability (El-Rawi & Awad, 1981).

The basic reactions described above are widely reported in the literature, but a fundamental question remains unanswered: whether the two reactions occur sequentially or take place concurrently. Additionally, the boundary condition between these two distinct reactions is less well established. There is some discrepancy between researchers when they address these issues. For example, Eades and Grim (1966) stated that a threshold value of pH 12.4 is required to dissolve silicates and aluminates in the clay in order to allow the formation of pozzolanic products. However, Diamond and Kinter (1965) discussed that lime adsorption and reaction at the clay plates give rise to instant local pozzolanic reactions at the clay surface. Bell (1988) found that the OH^- ions are more effective in modification of the clays surfaces; this reaction is quicker in expansive clays due to greater cation exchange capacity.

This lack of agreement between researchers is likely attributed to the complex nature and large diversity of combinations of minerals that form the clay particles, and the potential for varying reaction mechanisms to occur in these different minerals. For example, kaolinite and montmorillonite have obviously different mineral structures with cation

exchange sites in different positions within the clay lattice (Figure 3.7). Accordingly, the mechanism by which cation exchange takes place is almost different for the two minerals.

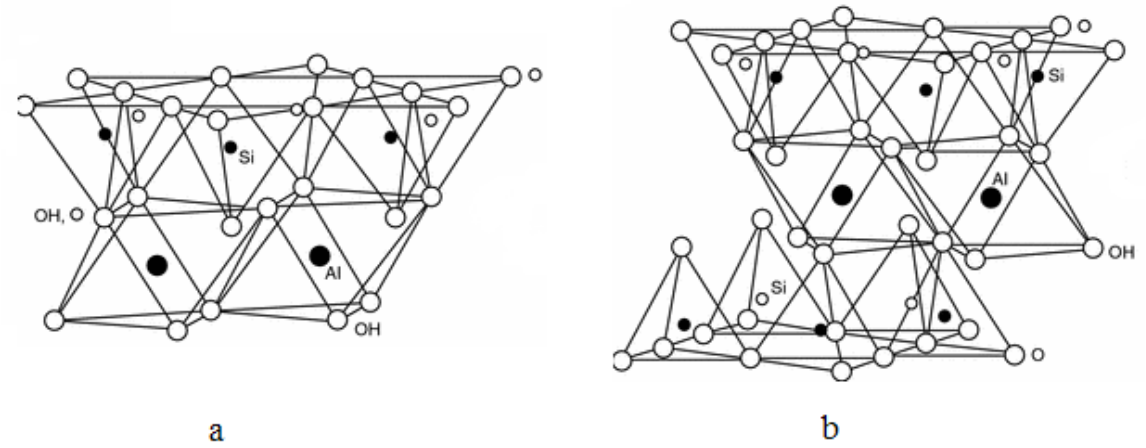

Figure3.7 Typical structure of (a) Kaolinite, and (b) Montmorillonite

The greater part of exchange sites on montmorillonite are due to isomorphous substitution caused by natural weathering processes. The development of this permanent positive charge dictates many aspects of physico-chemical behavior. The degree of cation exchanges on permanent charge sites is mainly governed by the ionic charge density (charge/radius) and ion concentration of the replacing ion relative to the existing ions on the exchange sites. Additionally, the exchange is also affected by the disorder of the particulate system, which is governed by the orientation of clay plates (McBride, 1994).
In kaolinite, the majority of variable charge, either negative or positive, is located on the edge sites of the clay mineral, mostly, hydroxyl groups on the mineral. These sites, which are responsible for inter-particle hydrogen bonding, are pH sensitive, and determined by:

$XOH + H^+ \Leftrightarrow XOH_2^+$ and $XOH \Leftrightarrow H^+ + XO^-$

where X is the mineral structure.

Research by Sparks (1995) shows that even though still significant, the cation exchange capacity developed on kaolinite (≈ 2-15 cmol/kg) is small compared with that of the of the permanently high cation exchange capacity of montmorillonite (≈ 80-150 cmol/kg). Consequently, as a result of higher cation exchange capacity, the changes in physico-

chemical properties of montmorillonite are likely to be more noticeable. Whereas, kaolinite minerals with surface pH-dependent charge sites, the cation exchange is highly dependent on the presence of the hydroxyl ion. Therefore, in kaolinite, where there are no permanent charge sites, the addition of $CaCl_2$ instead of $Ca(OH)_2$ will give rise to noticeably different immediate changes in clay properties as was demonstrated by Anson and Hawkins (1998).

The mechanisms of modification and solidification are associated with deciding how much lime to add to a clay soil in order to bring about the pozzolanic reactions. The current world-wide accepted methodology was derived from a test developed by Eades and Grim (1966). The principle of which is based on the philosophy that pore water pH will reach the value of a saturated solution of $Ca(OH)_2$ only when ion exchange is completed. However, some soils have been observed as never reaching the pH of a saturated lime solution. This phenomenon was reported by Eades and Grim (1966) for soils that are holding univalent ions such as Na^+ in the exchange position. As the monovalent ions are substituted by the Ca^{2+} ions in such soils, the pH electrode becomes sensitive to both Na^+ and H^+ ions therefore resulting in a misleading measurement as the solution becomes more acidic.

Boardman et al, (2001) conducted a laboratory experiment to investigate the time-dependent effects of mineral structural chemistry on lime-clay reaction. In their study two clays, representing the extremes of structural negative charge development used English China Clay (predominantly Kaolinite) and Wyoming Bentonite (Predominantly Montmorillonite). Kaolinite was used because it predominantly has a pH variable surface charge, while sodium montmorillonite was selected because it shows a very high permanent charge deficit as well as a pH variable surface charge similar to Kaolinite. As part of their investigation, they performed the Initial Consumption of Lime (ICL) test (or pH test) on the two representative clays. With the addition of lime to the two samples, prepared in slurry form, they found that the maximum increase in pH occurred at 1.5% and 7.0% lime addition in English China Clay (ECC) and Wyoming Bentonite (WB) respectively (see Figure 3.8). Based on the test results they concluded that the minimum

of lime (carbonate oxide, CaO, in their study) required to bring about the solidification, termed ICL, is greater for WB than ECC.

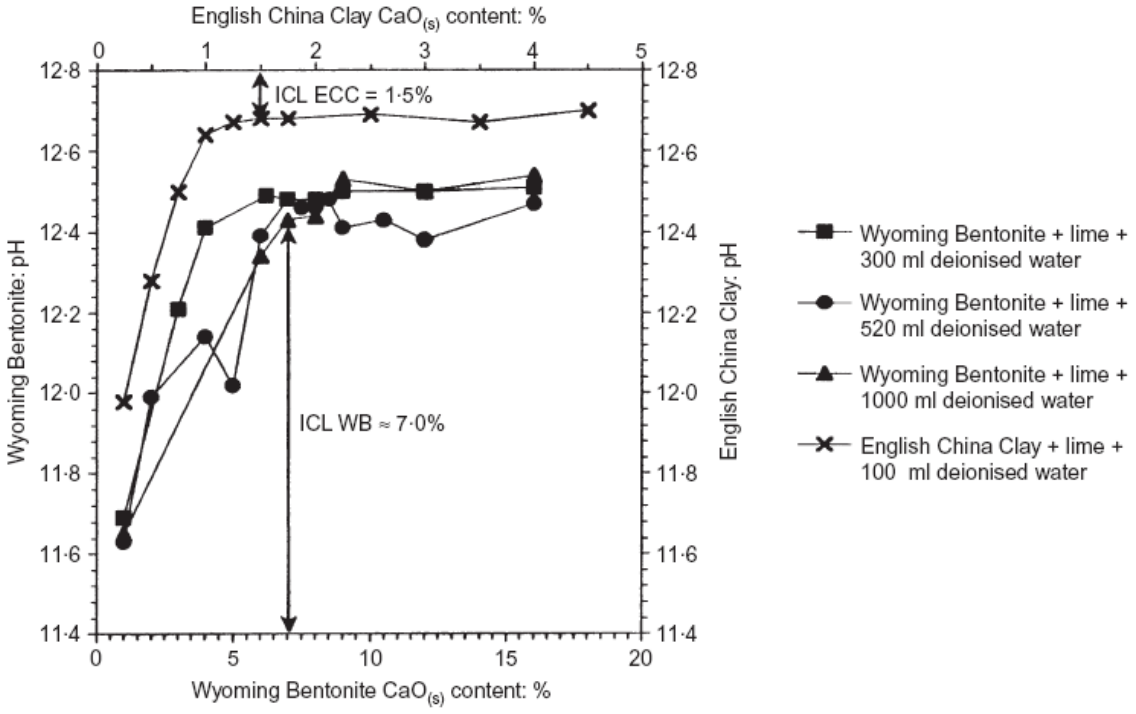

Figure 3.8 Initial consumption of lime of ECC and WB (Boardman et al, 2001)

As reported by Boardman et al, (2001), it can been seen from figure 3.8 that the initial state of the water content of the clay-lime slurry for both clays had an effect on the values of pH measured, but not significantly on the quantity of lime required to cause no further rise in pH. This finding may lead to a conclusion that the mechanism of lime-clay modification for a variety of soils is independent of the state of water content. This finding is the basis for the hypothesis from which the current thesis has been developed. To ascertain certainty however, this thesis aims to perform a set of different laboratory experiments to evaluate the accuracy of the above statement. The details of the experimental work are reported in chapter 4.

Rogers et al, (1997) recommended an alternative approach for enhanced analysis of the pH test data. There is a dearth of literature on the changes in soil properties wrought by

very low percentages of lime, the significance of which being that a very small addition of lime may be sufficient to profoundly change the apparent nature of the soil. They therefore suggested that plasticity changes should be considered to confirm the minimum lime requirement for solidification, and also the strength determination should be used for design.

There are a few incidences in the literature showing that with the addition of lime to a clay system, as a result of flocculation and coagulation, void ratio and consequently permeability will increase (Rajasekaran and Narasimha Rao, 2002; Cassia de Brito Galvao et al., 2004). The work conducted by Locat et al, (1996) on an inorganic dredged mud (Louiseville clay) sample revealed that the maximum flocculation of dredged mud was observed at the *Lime Modification Optimum* (LMO). The lime modification optimum concept was first introduced in the literature by McCallister and Petry (1992) based on a leach test program on lime treated clays. Based on this concept, at LMO, the maximum consumption of calcium ion in clay soil occurs, resulting in the maximum induced flocculation of clay particles. Thus, the change in permeability and void ratio can be used as indicators instead of a change in pH. However, it can be said that both the ICL and LMO represent the same reaction between lime and clay particles. In the research by Locat et al, (1996), the value of the lime modification optimum was already determined for Louiseville clay by the pH method and reported at 2% lime. They studied the microstructure of treated and untreated clay by using scanning electron microscopy. Their investigation showed that at a lime concentration of 2%, the average pore radius increases as a result of flocculation where no secondary minerals due to solidification reactions were visible. This finding was in accord with previous laboratory results which were observed by McCallister and Petry (1992). They measured and reported significant increases in permeability at LMO for three soil sites that comprised different clay minerals. Based on these test results they concluded that the maximum value of permeability of the soils is attributed to the large degree of flocculation and agglomeration that eventually increase the size of flow channels, hence increasing permeability.

The author believes that the basic immediate phenomenon of clay flocculation has been neglected so far as to propose a new technique to determine the lime modification optimum. It is postulated that if lime in varying percentages is blended with a clay slurry sample and allowed to settle, at the lime modification optimum, sediment exhibits a maximum value of void ratio and permeability. To verify this hypothesis, a laboratory setup was developed in the study to evaluate the effect of varying % lime on the fabric of the dredged mud sediment fabric (Figure 3.9). The fabric refers to the particular distribution, orientation, and particle to particle relations of the soil grains of sediment which are broadly divided in the two categories, flocculated and dispersed (Bennett and Hulbert, 1986).

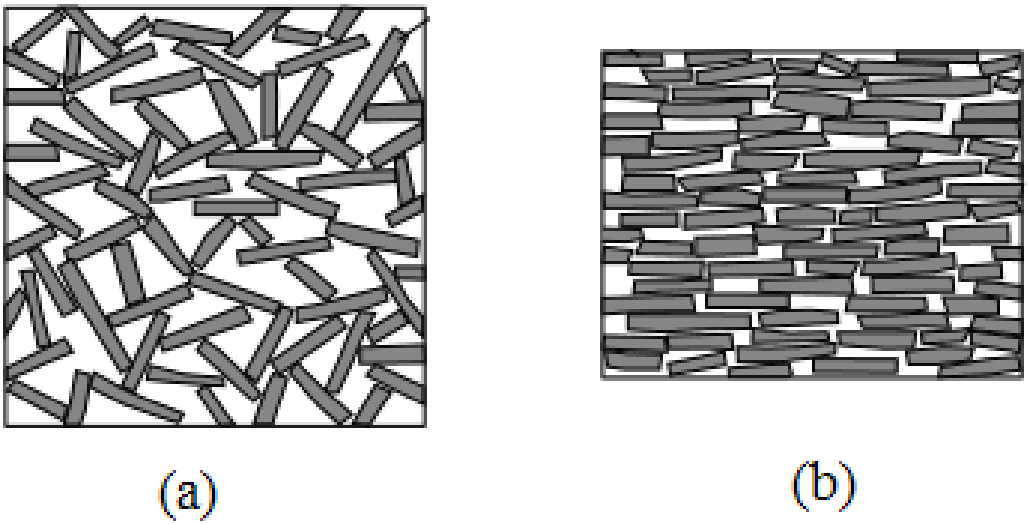

Figure 3.9 (a) Flocculated and (b) dispersed fabric of clay sediment (Bennett and Hulbert, 1986)

Mitchell (1956) pointed out three important distinctions between dispersed and flocculated clays in relation to their geotechnical behaviour:

1- For any given consolidation pressure and mass of clay sample, material with dispersed fabric occupies a smaller volume than those with flocculated fabric.

2- Dispersed clay particles are distributed more uniformly within a given volume than those particles in flocculated sediment.

3- For a given increment of stress, the shifting of particles relative to one another is greater in flocculated clay than in a dispersed one.

According to the above three facts, the following conclusions are made by the author:

1. Under a given applied consolidation pressure, a lower void ratio is expected for the clay sediment with dispersed fabric.

2. Dispersed clay fabric may hinder the free flow of water through the mass of soil in perpendicular direction towards orientation of the particles. Thus, dispersed fabric may cause reduction in the permeability of soil.

3. Larger degree of deformation of clay sediment will be expected in clays with flocculent fabric.

Based on the above conclusions, together with other research evidences about changes in soil permeability as discussed previously, it is envisaged that if lime is added to slurry and the slurry is allowed to settle, as a result of formation of flocculent sediment fabric, both the void ratio and permeability of the treated mud will be altered. To propose a new laboratory method to determine the LMO in clay, the author defined an innovative application for the adopted technique known as the hydraulic consolidation test of soft sediment which was primarily devised by Imai (1979) and later simplified by Sridharan and Prakash (1999a).

The test procedure, results, and details of the equipment used in this study will be explained in both chapters 4 and 6 where the experimental program conducted as part of this thesis is presented. The principle of the method is described herein.

3.10 Hydraulic consolidation test

The very soft consistency of the recent sediment poses a real problem in studying compressibility behavior by way of conventional laboratory oedometer apparatus. The soft recent sediment forms during, for example, the natural process of sedimentation in rivers and sea or as a result of human activities like dredge and sludge disposal projects. According to the test method proposed by Imai (1979), the soil sediment formed due to sedimentation is subjected to a seepage force of known magnitude. As water flows through the soft sample, the sediment undergoes consolidation. During consolidation the water content of a soil decreases as effective stress due to seepage force increases. The moisture content in the specimen varies with depth z, where coordinate z being measured is from the top of the specimen. In this method, immediately after the applied seepage force is removed, three measurements are made within a short period of time: flow rate v, distribution of pore water pressure u_z, and distribution of moisture content w_z by the method of slicing the specimen. From the gained moisture contents and pore water pressure distribution over the depth of the specimen, the consolidation curve in the whole range of the consolidation stresses found in the specimen can be obtained. Since the velocity of flow is constant throughout the length of the specimen and the water head gradient, i, is calculated from the water pressure distribution, the value of the coefficient of hydraulic conductivity (permeability), k, can be determined as a function of the effective applied pressure.

3.11 Simplified hydraulic consolidation test

The hydraulic consolidation test has proved to be a useful tool to study the compressibility behaviour of soft sediment. However, the test procedure suggested by Imai (1979) appears to be very tedious and it requires sophisticated instrumentation for the measurement of variation both the pore water pressure and moisture content over the

length of the specimen. Sridharan and Prakash (1999a) proposed a simplified consolidation test apparatus as shown in Figure 3.10.

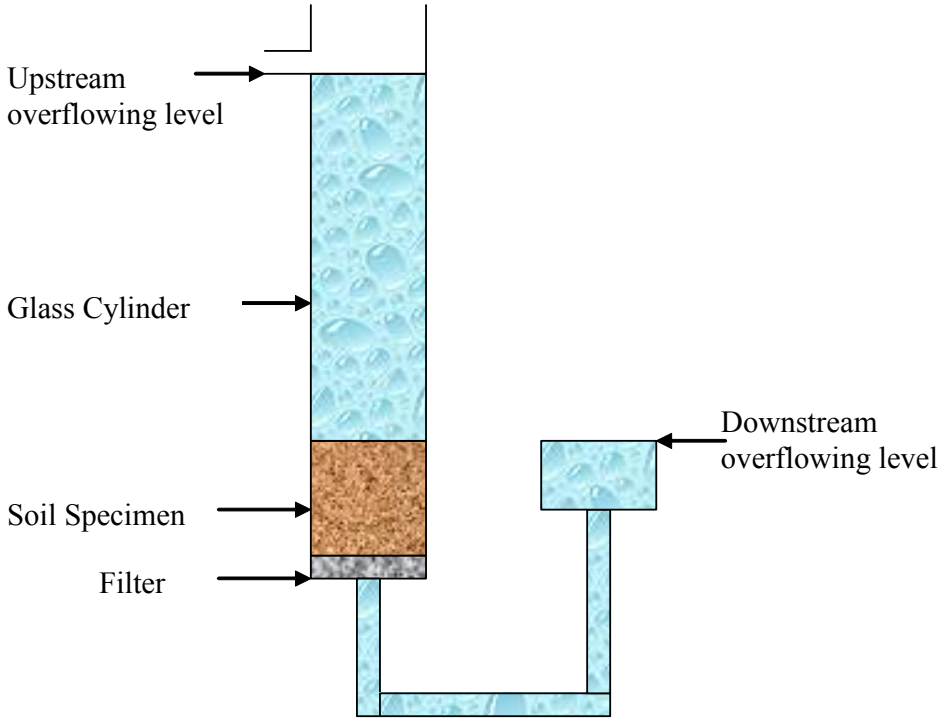

Figure 3.10 Schematic view of the simplified seepage consolidation test proposed by Sridharan and Prakash (1999a)

In this model, due to the difference between the hydraulic heads on the upstream and downstream sides of the specimen, as water is made to flow through a sample, the seepage force consolidates every element of the slurry sample. Sridharan and Prakash (1999a) proposed the following equations to explain the mechanism which is responsible for the consolidation of the slurry sample in the seepage-induced consolidation test. Let γ_w, γ_{sat}, and γ_{sub} represent the unit weight of water and the saturated and submerged unit weight of the slurry specimen respectively. If $d\sigma'$ is change in effective stress, and

du is the change in the pore water pressure due to the seepage force induced by downward water flow through a specimen of thickness dz then:

$$d\sigma' = \gamma_{sat} dz - du \quad \text{(Eq.3.2)}$$

The change in hydraulic head between the top and bottom surfaces of the specimen is presented by:

$$dh = \frac{1}{\gamma_w}\left(du - \gamma_w . dz\right) \quad \text{(Eq.3.3)}$$

Substitution of Eq.3.3 in Eq.3.2 results in:

$$\frac{d\sigma'}{dz} = -\gamma_w \frac{dh}{dz} + \gamma_{sub} \quad \text{(Eq.3.4)}$$

Seepage force is defined as the force induced by the flow of water per unit volume of soil and is given by:

$$j = \gamma_w i = -\gamma_w \frac{dh}{dz} \quad \text{(Eq.3.5)}$$

Eq.3.4 can now be written as:

$$\frac{d\sigma'}{dz} = j + \gamma_{sub} \quad \text{(Eq.3.6)}$$

Eq.3.6 shows that the seepage force and submerged weight of the soil brings about an effective stress gradient. In other words, the seepage force is responsible for induced effective consolidation pressure. Hence, for the case of steady flow, the effective applied pressure at the base of the specimen can be given by:

$$\sigma' = \gamma_{sub} L + \gamma_w h \quad \text{(Eq.3.7)}$$

where h is the head that causes the flow and L is the thickness of soil sample.

Sridharan and Prakash (1999a) discussed that in spite of the hydraulic consolidation test invented by Imai (1979), which considers varying void ratio with depth, with the simplified proposed apparatus, the thickness of the specimen is relatively small. Hence one can assume a constant void ratio throughout the length of the specimen.

To determine the consolidation parameters of soft sediment using the seepage-induced consolidation test successfully, the following test procedure is suggested by Sridharan and Prakash (1999a):

1. The flow of water through a soft sample is initiated once the settling and self-weight consolidation of the slurry is practically ended (i.e. the downward movement of the top surface of the soft slurry specimen is negligible).

2. To introduce varying seepage forces to the system, a known hydraulic head difference between the upstream and downstream overflowing level is gradually increased. Due to induced seepage force, the height of the specimen decreases.

3. Once a steady state is reached and no more apparent reduction in height of the specimen is observed, the height of the sediment is noted and the average void ratio, e, is calculated (Please refer to Eq.4.4 in chapter 4). The effective stress at the base of the sediment is determined using Eq. 3.7, which has two components, one as a result of buoyant weight of the specimen and other due to the action of the seepage force. The test result can be presented as a plot of the average void ratio versus the average of the effective stress developed over the depth of the specimen.

4. upon completion of consolidation of the sediment at each single stage, and once a steady state is reached, either a constant head or falling head permeability test may be conducted to measure the average coefficient of permeability, k, of the sediment. During the permeability test, care must be taken to not to adopt a hydraulic gradient greater than the one adopted while conducting seepage consolidation. Under this situation, the gradient in excess of that already applied, will cause further consolidation of the specimen.
5. The hydraulic head difference between the upstream and downstream can now be increased gradually and slowly to a new value, which in turn results in an increase in the seepage force. This leads to more consolidation of the sediment. Corresponding to the consolidated sediment, a second set of void ratio, effective stress and permeability values is calculated.

3.12 Summary and conclusion

This chapter provides comprehensive information about clay surface chemistry and its significant role in controlling physico-chemical properties of clay soils. It was discussed that the nature of the counter-ions governs the mechanism of interaction between clay particles in an aqueous solution and defines whether the suspension solution tends to flocculate or disperse. Later, the properties of the two common chemical binders, cement and lime, were broadly presented. It was found that once it reacts with pore water, lime manifests features of the three distinct reactions which include: hydration, ion exchange and flocculation, and formation of pozzolanic reactions. The different reactions are observed in cement when it mixes with wet clay soils. The literature survey showed that there is a threshold value in the lime addition, below which only hydration and flocculation take place. This threshold value is termed 'Lime Modification Optimum' or 'Initial Consumption of Lime'. The common methods by which this threshold value is determined was discussed.

Insight into the responsible factors involved in flocculation of clay particles, together with some evidence in the literature in regard to lime-clay reactions led the author to propose a new laboratory technique to determine lime modification optimum. The principle of the seepage induced consolidation test was discussed in detail. This study aims to introduce a new application for this laboratory setup to determine the LMO.

Chapter 4

Experimental Program -1

4.1 General

This chapter deals with a part of the experimental program which was undertaken through the course of the study. The program commenced with a field trip to the reclamation site at the Port of Brisbane to gather information about the general dredging operation of the project and perform sampling. Attention was directed towards accumulating data about the original sources of dredged materials utilized in the project. In an attempt to collect the right dredged mud sample from the site, a brief meeting was arranged between the author, staff of Coffey Ltd Pty, and technical personnel who were affiliated to the Port of Brisbane Corporation to identify a location on the project site where sampling could be conducted. A bulk sample of the existing dredged material was eventually recovered from containment pond locally termed paddock S3b. The samples bags then where transferred to the Geotechnical Laboratory at James Cook University where a basic study on the properties of the dredged mud was conducted. The prime objective of this chapter is to assess the basic engineering behavior of the dredged mud in its natural state and when mixed with lime. The properties of the hydrated lime and seawater used in this study are also presented. In this chapter a seepage-induced consolidation test is employed as a reliable and fast laboratory technique to determine the threshold value of lime into a clay soil, below which the maximum physico-chemical alteration to the clay particles would take place without allowing the formation of the pozzolanic products. This study also tries to assess the dependency of lime-clay reaction (modification) on the state of initial moisture content of the dredged mud slurry. The details of the procedures and the properties of the lime-treated dredged mud are given herein.

4.2 Project site

The field trip was made in May 2007 to the project site within the Port of Brisbane to perform sampling. The project area is located on the eastern end of Fisherman Island. Fisherman Island Port land has been developed by reclaiming and filling land, utilizing materials dredged from the Brisbane River berths, River shipping channels and Moreton Bay. With the knowledge of the officer affiliated to the Port of Brisbane Corporation, the specific containment pond, which is locally termed "paddock", was selected for the sampling purpose. The author was advised that the deposited sediment in paddock *S3b* has been obtained as part of the maintenance strategy for the Brisbane River channel.

The dredged material originating from Brisbane River poses a significant problem for the developer and engineers, due to high compressibility and low shear strength. The current method of material deposition is by pumping and discharging the dredged material from one corner of the paddock, allowing the soil to settle slowly. This type of discharging, however, inevitably results in coarser particles depositing in the vicinity of the pipe outlet and finer particles being transported with water and settling over time. This leads to variable properties in the dredged material across the deposition area. At the time of sampling no white sand capping covered the zone of paddock *S3b* where sampling was conducted (Figure 4.1).

It has been mentioned that vacuum preloading is currently implemented in a few paddocks which are already filled with the similar sediment excavated from the Brisbane River channels or berths. Based on the visual observation of the project site, the author noticed that there were few other paddocks which were filled with granular or coarser particle soils. According to the verbal information provided by the officer, the granular sediment was a result of dredging the shipway navigation channels in Moreton Bay where the sea bottom is mostly dominated by Upper Holocene stratum which comprises of coarser sediment in comparison with sediment from the river bottom (Figure 4.2).

Figure 4.1 Sampling location in the Fisherman Island project site

Figure 4.2 Paddock in the Port of Brisbane filled with dredged mud from Moreton Bay

It is worth mentioning that the review of onshore reclamation study of paddocks S2, S3a, and S3b in the PoB conducted by Coffey geosciences (2004) confirms that the dredged material obtained as part of the maintenance program of the river channel is generally silty clay, although a variation in material characteristics across the paddocks is expected because of the single point discharge system, with coarser material depositing closer to the discharge point. This report also shows that the Holocene sediment is subdivided into an upper and lower layer of normally consolidated, low strength silty clay with a shell band, separated by a few discontinues layers of sand. The upper layer generally consists of sand layers interspersed with layers of soft clays and silts (Figure 4.3).

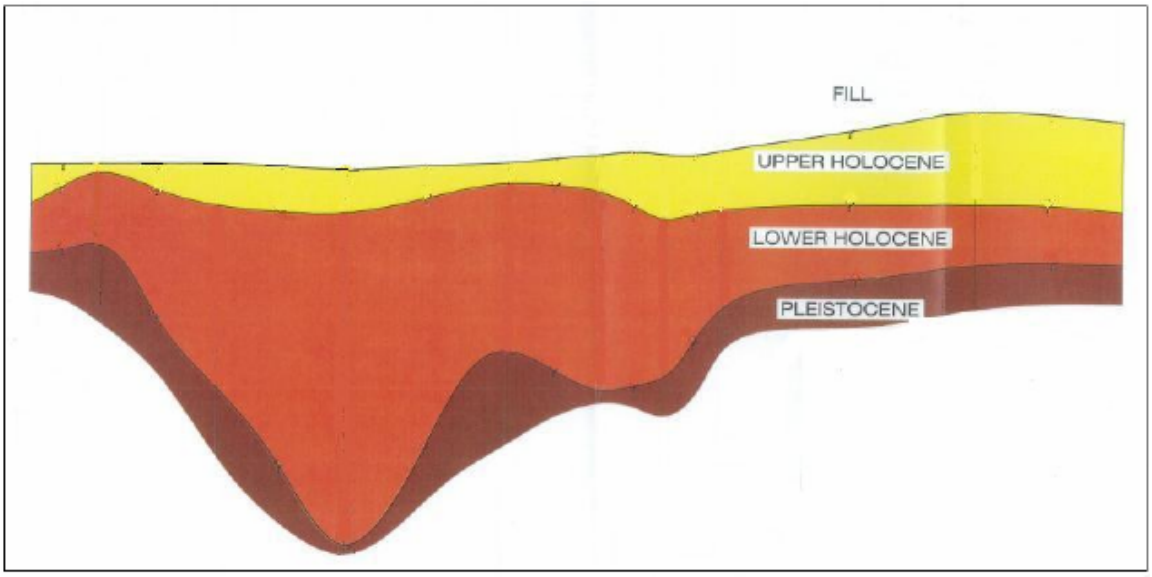

Figure 4.3 Typical geological profiles in the extension project of the Port of Brisbane (Coffey, 2004)

4.3 Sampling method

Undisturbed samples of the compressible foundation soils can usually be obtained using conventional soil sampling techniques and equipment. In this study, the major problem in retrieving the undisturbed samples from the nominated paddock (S3b) was that the surface crust did not support conventional drilling equipment and therefore a personal manual sampling in this area was selected as appropriate, to be applied cautiously. This is because below the surface crust, fine grained dredged mud was found to be very soft with a high moisture content and any equipment taken onsite was expected to sink rapidly. Unfortunately, due to soil consistency and high plasticity of the soft dredged mud, even the employment of lightweight drilling equipment like a manual auger supported by matt appeared to be ineffective. Under such circumstances, the shoveling method of sampling was chosen to be performed by the author as shown Figure 4.4.

Figure 4.4 Shoveling method was conducted for sampling in the paddock of S3b

Fresh samples of the dredged mud were collected from a shallow depth in the north-east corner of the paddock, after removal of 30 to 40 centimeters of the dry hard crust. About 12 bags with an approximate weight of 20 kg each were filled with the mud. Upon completion of the sampling, an arrangement was made with Queensland Rail to transfer the collected mud samples to James Cook University in Townsville, a distance of 1400 km from the extraction site.

Once the samples were received in the geotechnical laboratory in School of Engineering at JCU, the determination of in situ moisture content was promptly made for each individual bag in accordance with the oven method stated in AS 1289.2.1.1. The test results of determined initial moisture content are presented in Table 4.1.

Table 4.1 Initial moisture content of the dredged mud under 35 cm dry crust (S3b)

Bag Number	MC%	Bag Number	MC%	Bag Number	MC%
1	98	2	102	3	106
4	103	5	99	6	103
7	103	8	104	9	100
10	103	11	100	12	99

As it can be seen from the table, even though some variation of initial moisture content were observed in several bags, the average value of 102% moisture content can be reported as in situ moisture content of paddock S3b below approximate 35 cm of crust layer.

4.4 Particle Size Distribution

The determination of the mass of material containing only particles of certain sizes is termed Mechanical analysis. Mechanical analysis is one of the oldest and most common forms of soil analysis. It provides the basic information for revealing the uniformity or gradation of the materials within established size ranges and for textural classification. The normal method adopted for separation of particles in a fine grained soil mass is the hydrometer analysis and for the coarse grained soils the sieve analysis. In this study, the standard method of "Analysis by sieving in combination with hydrometer analysis" was used to determine the grain size distribution of the dredged mud sample. This method covers the quantitative determination of the grain size distribution in a soil down to the N.200 sieve (75 μm), in which the material washed out during the fine sieving analysis is kept as the sample for particle size distribution analysis by hydrometer in accordance with AS 1289.3.6.3. Figure 4.5 shows the particle size distribution for the dredged mud sample.

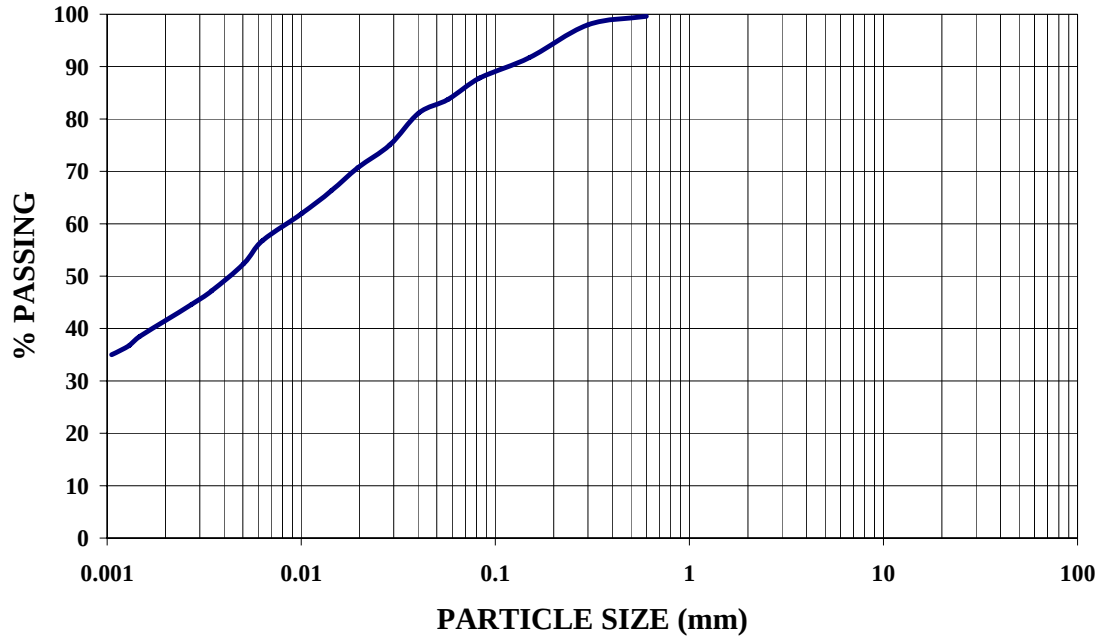

Figure 4.5 Particle size distribution of the dredged mud from Paddock of S3b in PoB

Figure 4.5 shows that almost 14% of the grains are classified as medium to fine sand (600 - 75 μm), about 46% of the particles represent the silt size(75-2 μm) and the rest of about 40% of fractions, are clay size particles (< 2 μm).

4.5 Atterberg Limits

It is well known that while the general engineering behavior of coarse grained soil is controlled by particle size distribution, the performance of the cohesive fine grained soils (silt and clay) is governed mostly by the presence of water in the voids of the soil. The Atterberg limits of a fine soil are defined as the average moisture content between various phases in soil behavior (Holts and Kovacs, 1981). They are used to subdivide the clays and silts. The limits are based on the concept that a fine grained soil can exist in any of four phases depending on its water content. Initially soil is solid when it is dry, and with the addition of water its state changes to semi-solid, plastic, and finally liquid states. The

moisture content at the boundaries between adjacent phases are termed shrinkage limit, plastic limit, and liquid limit. In particular, the determination of the liquid limit of a soil as an index property is now widely used in geotechnical engineering. This parameter of soil may be use alone or in conjunction with other index properties to supply many functional engineering correlations (Prakash and Sridharan, 2002).
The common procedure for determining the liquid limit, plastic limit and shrinkage limit are outlined in Australian Standards As1289.3.1.1, AS1289.3.2.1, and AS1289.3.3.1 respectively.

Liquid limit of cohesive soils may be determined using one of two devices- the Casagrande percussion liquid limit device or fall cone apparatus. The Casagrande percussion apparatus is the one used in this study. This method is detailed in AS 1289. 3.1.1. Based on this method, the liquid limit is defined as the moisture content at which a groove cut into the soil placed within the cup will close over a distance of 12.5 mm after 25 blows. It is required by the standard method that at least four tests need to be undertaken at different moisture contents to correspond to different blow counts. The test results are then presented on a semi-logarithmic paper in which the points present the different values of moisture content with an associated number of blows. A straight line of best fit will be drawn between the points to determine the water content which corresponds to the 25 blows.

The plastic limit is rather a manual technique and it defines the moisture content at which a thread of soil crumbles when rolled out to a diameter of 3mm. The standard specifies that the crumbled threads should be 3-10 mm long.
After determination of the liquid limit and plastic limit, the plasticity index of soil is calculated from the following formula:

$$PI = LL - PL \qquad \text{Eq.4.1}$$

where:
LL = liquid limit and,
PL = plastic limit

The linear shrinkage (LS) test is a method to determine the shrinkage of the soil due to loss of its moisture content. The standard method of LS is outlined in AS 1289.3.4.1. With this method, the linear shrinkage mold is lightly greased before use. The mold is then filled by compressing the paste of soil, at the liquid limit state, slightly with a spatula. The mold is tapped gently to remove air bubbles. The level of sample is smoothed off and the specimen is then allowed to dry at room temperature for 24 hours. It is then transferred to the 105-110 ^{0}C oven until shrinkage was ceased. Once this process completes, the total longitudinal shrinkage is recorded to the nearest millimeter. The linear shrinkage of the specimen is calculated as follow:

$$LS = \frac{L_s}{L} \times 100 \qquad \text{Eq.4.2}$$

where:

L_s = longitudinal shrinkage of the specimen in millimeters

L = length of mold in millimeters

It is worth to mention that the author accidentally encountered a phenomenon in which the plasticity properties of the dredged mud altered significantly due to the method of sample preparation. According to Australian Standards (1289.1.1), the fine grained soil must first become air dried or low-temperature (50^{0}C) oven dried before passing through the sieve, 425 μm, to prepare for liquid limit, plastic limit and linear shrinkage test procedures. In this study the author examined the effect of varying degrees of temperature during sample preparation of the dredged mud on index properties. To assess the Atterberg limits of the dredged mud in its own natural moisture state, the paste material with an approximate moisture content of 102% was gently past through the sieve 425 μm to remove the oversize particles. The passing fraction was then used to determine the liquid and plastic limit and linear shrinkage in accordance with standard procedures. The second series of the dredged mud samples was prepared exactly in accordance with the procedure stated on the standard. The last series of the samples however, followed the same test procedure but was dried out under an influence of 110±5 degree Celsius during preparation. The obtained results are outlined in Table 4.2.

Table 4.2 The effects of temperature on Atterberg Limits of the dredged mud

Parameters	Natural state	@50 ^{0}C	@105 ^{0}C
LL	88%	63%	56%
PL	26%	23%	21%
PI	62%	40%	35%
LS	21%	18%	16%

The test results suggest that the maximum liquid limit, plastic limit, plasticity index, and linear shrinkage values were obtained where the sample was tested under its in situ moisture condition. The table shows that following the procedure of the sample preparation outlined in standard method (i.e. preparation at 50^{0}C) brings about a remarkable reduction in liquid limit from 83% to 63% associated with in situ moisture content and low-temperature oven dried respectively.

The table suggests that should the sample prepared in a higher temperature of 105 ^{0}C, the further decrease in liquid limit to 56% will occur. The results also show that in comparison with liquid limit values the variation of temperature slightly affects the plastic limit of the dredged mud with values changing from 26% to 21% in line with increasing temperature. The reduction trend of the linear shrinkage with temperature varies from 21% to 16%. The change in plasticity index lies along a wide band from 62% to 35%. Further in this chapter, the state of plasticity of these three samples is presented on Casagrande's plasticity chart.

4.6 Specific Gravity

Specific gravity of soil (G_s) defines the ratio of density of a material to the density of water. The test procedure to determine the specific gravity of soil is described in Australian Standard, AS 1289.3.5.2. According to the standard method, at least two sub-samples of the same origin have to be tested to ensure consistency between results. The

acceptable toleration between the test results is outlined in the method. This method requires the sample to first be dried out in the air or low temperature oven.
Intuitively, the author decided to evaluate the effect of sample preparation (varying degree of temperature) on the gained value of specific gravity. Thus, three sets of samples (two representative sub-samples of each) were considered; natural, air dried, and oven dried.

The representative natural state sample appeared in the form of mud paste with an approximate moisture content of 100%. Before starting the test procedure the mud test was whisked thoroughly to ensure that it was quite uniform. About 250 grams of the mud paste was then carefully poured into two 250 ml density bottles (250 g each). Distilled water was then added until each bottle was approximately two thirds full. Next, each single bottle was placed in a desiccator under a vacuum of about 700 mm of mercury at room temperature for about 12 hours. A representative sub-sample of about 200 grams was also taken from the remaining mud paste and was placed in the oven to measure its moisture content. Specific gravity of the specimens was then calculated by the specified formula, taking into account the initial moisture content to find the initial dry mass of the wet samples. For every two representative sub-samples the test results showed the variation less than 0.03. The quoted specific gravity was the average of these two results. The same test procedure was also undertaken for the oven dried and the air dried dredged mud specimens and the average specific gravity was determined from the two representative sub-samples. The results of the specific gravity tests are presented in Table 4.3.

Table 4.3 Variation of specific gravity with degree of temperature

Natural state	@ 50 ^{0}C	@ 105 ^{0}C
2.73	**2.61**	**2.52**

Results showed that the specific gravity of the dredged mud is extremely affected by the temperature during the sample preparation phase. The reduction from the natural state to

oven dried state is about 0.21 which is quite considerable. It should be noted that this parameter plays a significant role in the computation of the particle size distribution by hydrometer analysis and also one-dimensional consolidation test so as to determine the void ratio of a sample. In particular for one-dimensional consolidation where the clay sample has to be tested in its original in situ condition, the utmost care must be taken toward selecting the right value of specific gravity which normally is determined under dry conditions in the soil laboratories worldwide.

4.7 Quantitative assessment of the mineralogy

In order to evaluate the quantity of the constituents of the dredged mud, a quantitative XRD analysis was conducted in the Advance Analytical Centre at James Cook University. The full report of the analysis procedure is presented in appendix 1. The quantitative XRD results are presented in Table 4.4.

Table 4.4 The quantitative XRD results of the dredged mud

Phase	Weight%
Plagioclase feldspar (albite)	37
Quartz	22
Kaolinite	16
Illite	12
Smectite (Montmorillonite)	5
Amphibole	4
Halite	4

The above results show that feldspar and quartz are the major constituents of the dredged mud which comprise about 59 % of the total minerals. The percentage of the clay particles (Kaolinite, Illite, and Smectite) is about 33 %. Additionally, Amphibole

contributes 4% of the total weight. Amphibole defines an important group of generally dark-colored rock-forming inosilicate (tetrahedral) minerals, composed of double chain SiO_4 tetrahedral, generally containing ions of iron and magnesium in their structure. It has to be mentioned that the contribution of the Halite mineral (defined as rock salt or table salt) in the total weight of sediment should be neglected as it is likely attributed the presence of seawater between grain particles which obviously contain high salinity and result in crystallized salt after being dried for preparation purposes.

4.8 Specification of the hydrated lime

The hydrated lime used throughout this research study was manufactured by Cement Australia. Based on the information provided on the material safety data sheet of the product, the composition of the product is summarized as shown in Table 4.5.

Table 4.5 Composition of the hydrated lime used in the study

Chemical Name	Proportion %
Calcium hydroxide $Ca(OH)_2$	**80 - 90**
Magnesium hydroxide $Mg(OH)_2$	**0 - 6**
Silicon dioxide SiO_2	**2 - 6**
Aluminium oxide Al_2O_3	**0.2 – 0.6**
Iron oxide Fe_2O_3	**0.1 – 0.3**

4.9 Characteristic of the seawater

The seawater was used in this study for the purpose of sample preparation for various laboratory tests. The fresh seawater was collected manually by means of gallon from the surface of sea on the border of Townsville city. The chemical characteristic of seawater is

summarized in Table 4.6. It is assumed that the composition of seawater remains almost constant in a specific region; hence, this table which has been obtained from the New-Zealand governmental website may enable us a rough estimation of the properties of seawater in the North Queensland region where Townsville city is located.

Table 4.6 The properties of seawater

Ion	Valence	Concentration (ppm)	Part of salinity%	mmol/kg
Cl	**-1**	**19345**	**55.03**	**546**
Na	**+1**	**10752**	**30.59**	**468**
SO_4	**-2**	**2701**	**7.68**	**28.1**
Mg	**+2**	**1295**	**3.68**	**53.3**
Ca	**+2**	**416**	**1.18**	**10.4**
K	**+1**	**390**	**1.11**	**9.97**
HCO_3	**-1**	**145**	**0.41**	**2.34**
Br	**-1**	**66**	**0.19**	**0.83**
BO_3	**-3**	**27**	**0.08**	**0.46**
Sr	**+2**	**13**	**0.04**	**0.091**
F	**-1**	**1**	**0.003**	**0.068**

Source: www.seafriends.org.nz

4.10 Proposed method for LMO

In chapter 3, the concept of Lime Modification Optimum was extensively discussed. This is a threshold value of lime in a clay soil, below which the maximum flocculation of the dredged mud occurs. The principle of the seepage induced consolidation method was also explained in detail. According to this method, when water is made to flow through soft sediment due to the difference between the hydraulic heads on the upstream and downstream sides of the sediment, the seepage force exerted by the flowing water

consolidates every element in the sediment. This technique is adopted here to be used to determine the threshold value of lime in soil, termed lime modification optimum. It is postulated that if lime in varying percentages, blended with a clay slurry sample and allowed to settle, at lime modification optimum, sediment exhibits a maximum value of void ratio and permeability as described below. It has to be noted that by performing the following test the author has attempted to evaluate not only the lime modification optimum of the dredged mud but the affect of high initial moisture content of the specimens on the lime-clay reactions. The extent by which the test results are impacted by the initial state of the moisture content of the slurry helps to discern whether or not the mechanism of lime-clay modification (stage, during which ion exchange takes place) is moisture content dependent.

In order to verify the effect of the initial moisture content on the test results, the test procedure described below was conducted twice on the two representative sub-samples with initial moisture content of 350 and 550% respectively. To avoid repetition, the following procedure only outlines the test method performed with the initial moisture content of 350%. However the test results of the representative sample with initial moisture content of 550% is presented thereafter.

The dredged mud with initial in situ moisture content of around 100 percent was passed through a 2.35 mm sieve in order to remove the possible presence of shells and oversize particles. The water content of the sediment was then brought up to 350% using sea water and mixed thoroughly to ensure an uniform slurry. Various lime contents from 0 to 6% (dry weight basis) were then mixed with slurry in separate buckets. Once homogenized, the slurry samples of natural and treated mud were poured into a falling head permeability cell, with the top and bottom of the sample covered by filter paper. After assembly of the mold, the inlet on the top cap was connected to a water reservoir filled with seawater. Because water comes through the small hole in the middle of the cap in the permeability cell, it is essential to use filter paper on the top of the slurry sample to avoid formation of a crater in the centre and localized flow channels along the side of the sample. The permeability mould was then immersed in a stainless steel container, 30 cm deep and filled with water, to ensure that the bottom of the specimen was not in contact

with the atmosphere and the whole specimen remained fully saturated. Consolidation initiates once water is allowed to pass through the sample. During consolidation, the level of water in the upstream reservoir was maintained constant to ensure a steady seepage force on the samples. As a result of this seepage induced consolidation, the height of the sediment gradually reduced. The seepage-induced consolidation of slurry samples was maintained for one day. After day one, the water flow was temporarily disconnected and the top cap of the mold was removed. The perforated disk with a thickness of 2 cm and diameter of slightly smaller than the mould's diameter was placed on the top of the specimen over the filter paper (see figure 4.6). The perforated disk was light in weight and applied only 0.3 kPa pressure on the sample. The placement of the disc on top of the sample helps to slightly consolidate the loose section of the top of specimen. This pressure is necessary for accurately measuring the final thickness of the specimen. After placement of a disk, the system was reassembled and the water was allowed to run through for another 24 hours until no further apparent reduction of height was observed in the permeability cells. The inner surface of the mold was marked using a ruler so that the observation of the change of sample thickness was made through the transparence top cap of the mold. Once a steady state was reached, the upstream water supply was disconnected and the top cap of the cell was connected to the falling head permeability standpipe panel. Unless otherwise stated, to measure the permeability by the falling head method, the standard method of hydraulic conductivity of clay was adopted in accordance with the procedure stated in Australian Standards, AS 1289, 6.7.2.

In order to measure permeability, at regular time intervals, the drop in the standpipe connected to each single mold containing dredged mud with a specific amount of lime was measured over a period of 24 hours to ensure that the values were consistent (see Figure 4.7). It should be noted that even though the standard method specifies at least 3 days of percolation to ensure saturation of clay, this period of time was reduced to one day as the slurry sample was presumed to be 100% saturated. Hence, once a steady state in the rate of standpipe water height drop was observed and no further large fluctuation was encountered, the test was stopped and the final height of the samples was recorded.

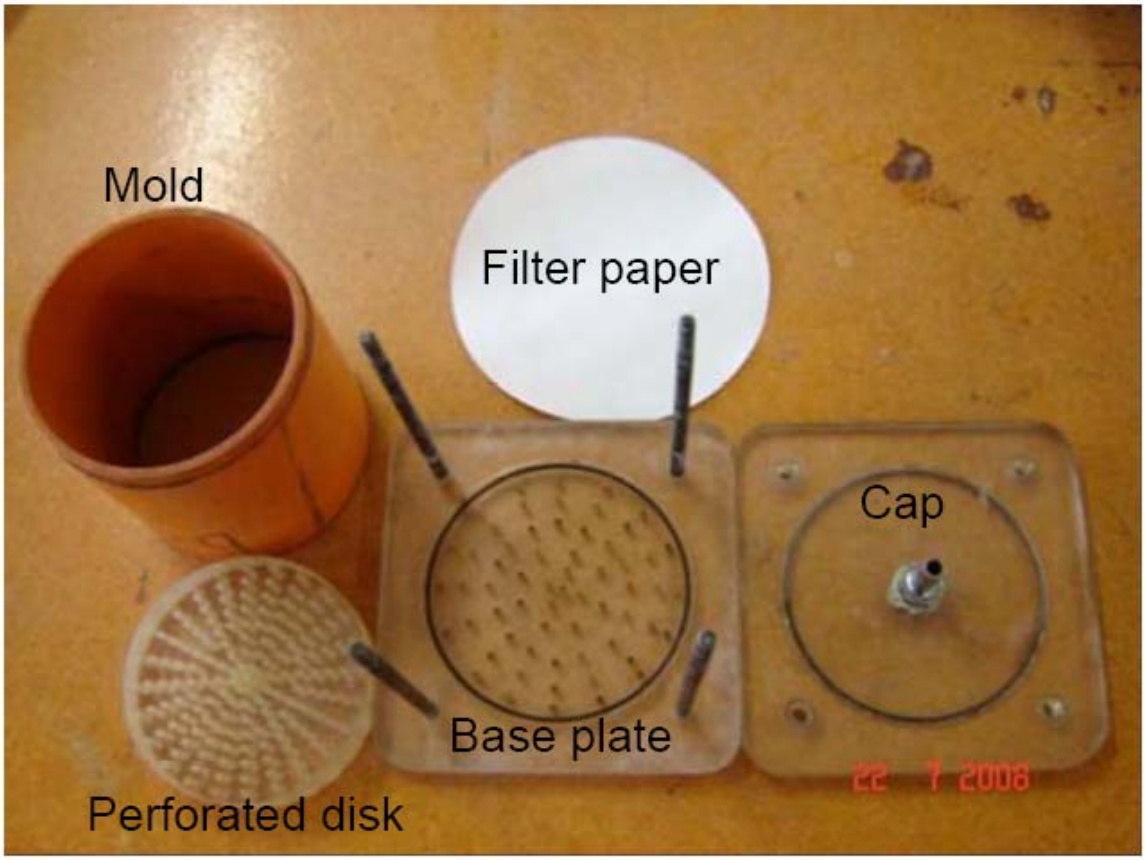

Figure 4.6 The components of the proposed seepage-induced consolidation apparatus for determination of Lime Modification Optimum

Upon completion of the test, the permeability mold was extracted from the container. The top cap was then removed and the excess water on the top of specimen was discarded. Care was taken to not press the perforated disk down as it may have caused more consolidation of the soft sample. While the mold still remained in its position on the base plate, it was placed on the bench on a piece of paper towel to lose it excess moist from the bottom. It was left on the laboratory bench for a few minutes before transferred to the digital scale for weighing. The net weight of the soil specimen was determined by subtracting the weight of the whole assembly from the weight of the mold, base plate and perforated disk. At this stage, the whole specimen was removed from the mold and transferred to the oven to measure the moisture content. By having the final height of the

specimen at the end of the permeability test, plus the diameter of the mold and net weight of the specimen, the average wet density of the specimen was calculated.

Figure 4.7 Falling head permeability apparatus

After determination of moisture content, the average dry density of the specimen was calculated as follows:

$$\rho_d = \frac{\rho_m}{1 + w/100} \qquad \text{Eq.4.3}$$

where: ρ_d = dry density of the dredged mud after consolidation

ρ_m = bulk density of the dredged mud after consolidation

w = final moisture content of the specimen after consolidation

the determined values of dry density together with the value of specific gravity of the material used to calculate the void ratio as follows:

$$e = \frac{G_s}{\rho_d} - 1 \qquad \text{Eq.4.4}$$

Where, e is the void ratio, and G_s is the specific gravity.

As a final stage, the average permeability of each mold was calculated as follow:

$$k_\theta = \frac{3.84 a_s h}{At} \times \log_{10}\left[\frac{h_i}{h_f}\right] \times 10^{-5} \qquad \text{Eq.4.5}$$

where

k_θ = Coefficient of permeability at test temperature (θ), in meter per second

a_s = Cross-sectional area of standpipe is square millimeters

h = Thickness of specimen, in millimeters

A = Cross-sectional area of specimen, in square millimeters

t = Time interval for measurement, in minutes

h_i = Initial height in the standpipe, in millimeters

h_f = Final height in the standpipe after time interval (t), in millimeters

θ = Temperature of outflow water, in degrees Celsius

During the test program the temperature of the outflow water was measured regularly and it was found to have an average value of 23 ^{0}C. This measurement is necessary because the calculation of permeability (k_T) shall be corrected to that at 20 ^{0}C by using the following equation:

$$k_T = k_\theta \left(\frac{\eta_\theta}{\eta_{20}} \right) \qquad \text{Eq.4.6}$$

where

k_T = coefficient of permeability at 20 ^{0}C, in meter per second

k_θ = coefficient of permeability at temperature (θ), in meter per second

η_θ = dynamic viscosity of water at θ ^{0}C

η_{20} = dynamic viscosity of water at 20 ^{0}C

θ = temperature of outflow water, in degrees Celsius

The values of dynamic viscosity of water at different degrees of temperature are tabulated in AS 1289.6.7.2 and used for computation purposes.

The test results of the first series of the lime treated dredged mud samples prepared at 350% moisture content are presented in Figure 4.8. These results show that the coefficient of permeability, along with average void ratio, gradually increased as lime was added from 0 to 4 % and maximum permeability and maximum average void ratio were achieved in the sample containing 4 percent of lime. The coefficient of permeability and void ratio slightly dropped in the sample with the lime content of 5 percent and theses values remained almost constant with the addition of lime to 6%.

Figure 4.9 shows the test results obtained from the same procedure conducted on the lime treated material prepared with an initial moisture content of 550%. It can be seen that the general trend in increase of void ratio and permeability with increasing % lime is almost similar to those which were obtained previously with 350% moisture content. According to these findings, it was concluded that the state of initial moisture content has no significant role in controlling the chemical reactions in terms of ion exchange on the clay surface lattice as a results of addition of hydrated lime into a soil system. Based on the above test result, the lime percentage of 4 percent was considered as a threshold value (i.e. Lime Modification Optimum) at which the maximum permeability and void ratio in treated dredged mud was achieved.

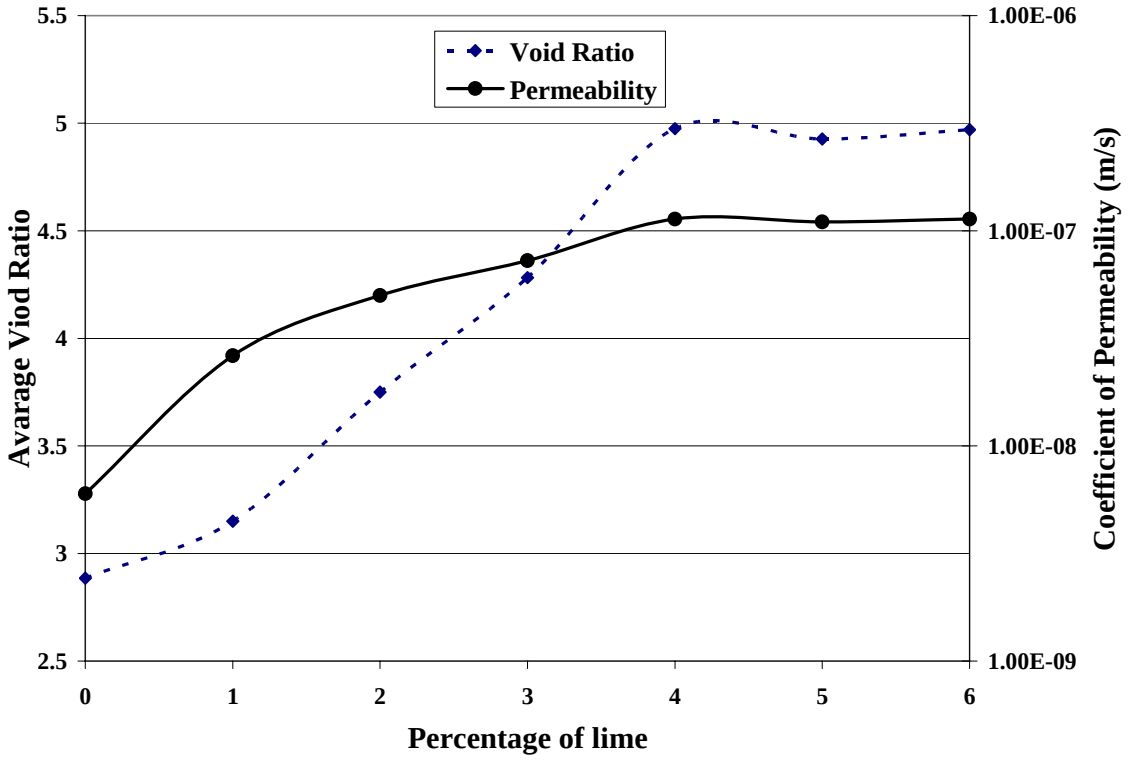

Figure 4.8 Variation of coefficient of permeability and average void ratio with % lime in seepage induced consolidation test (MC=350%)

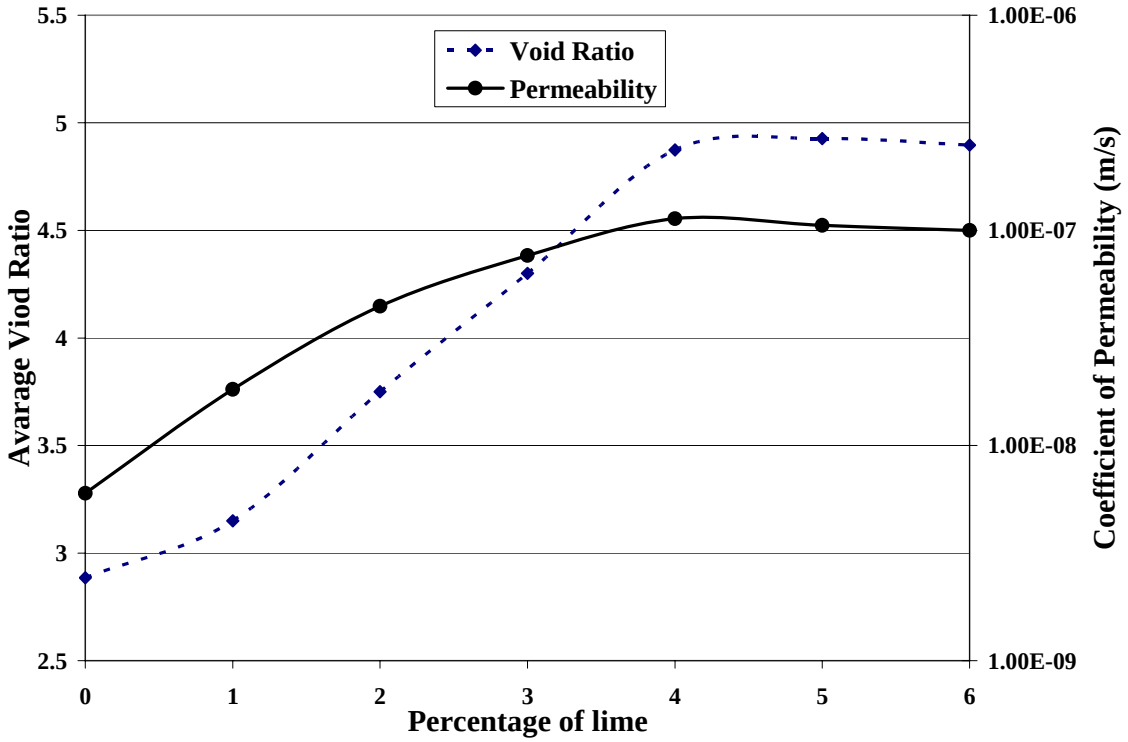

Figure 4.9 Variation of coefficient of permeability and average void ratio with % lime in seepage induced consolidation test (MC=550%)

4.11 Scanning electron microscopy

Scanning electron micrograph was used to evaluate the modification effect of lime on the microstructure of the dredged mud. This investigation was conducted in Advance Analytical Centre in JCU. The samples of the lime-treated and natural dredged mud were obtained from the seepage-induced consolidation test program once the experiment was completed. Two representative small samples from natural and treated specimens with 4% lime were collected. The samples were left to dry out in the laboratory at room temperature. After drying, the chunky samples were broken down to a size suitable for the scanning electron microscope. Figure 4.10 shows the SEM images which were taken from the natural and lime treated dredged mud. The photograph of the natural dredged mud (a) presents a uniform laminar structure, as if particles tend to lie on each other exhibiting the same pattern and orientation. The inter-aggregate pores in this pattern are

expected to be small in size. In addition, this pattern is likely responsible for low void ratio and permeability of the non-treated dredged muds as particles are stacked on each other in consistent order resulting in the highly dense arrangement of the particles. Particle orientation which is perpendicular to the flow path notoriously hinders the water flow and the actual flow lines must bypass theses particles. The photograph of lime-treated dredged mud is shown in Figure 4.10 (b). It appears that with addition of lime, particles are oriented more randomly in the sample interior which is likely attributed to the flocculation of the particles. Obviously, water flow is easier if the sample has larger pores and if the particles are randomly oriented (Stepkowska et. al. 1995).

As a conclusion it can be said that the difference in microstructure of non-treated and lime treated dredged mud may explain differences in soil behavior in terms of permeability and void ratio. In other words, microstructural arrangement of soil particles and soil pores arrangement influence the permeability of fine grained soil (Ranganatham, 1961). When lime is added to a clay soil, due to the ion exchange phenomenon, several changes take place in the soil system. The extent of the induced changes depends on the mineralogical composition, exchangeable cations and pore system fluid chemistry of a soil system. The reaction of calcium ion with clay particles reduced the diffused double layer thickness and induces flocculation. Hence, the change in the dispersed arrangement of particles (e.g. Figure 4.10- a) to the flocculation pattern (e.g. Figure 4.10-b) is a factor in increasing the void ratio and permeability of the soil.

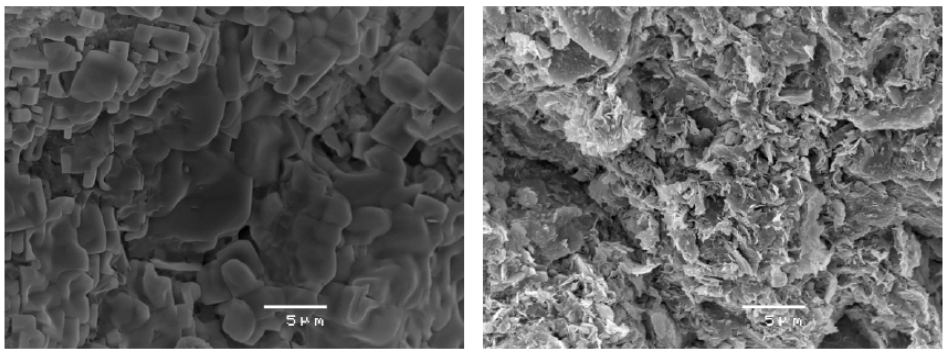

(a) (b)

Figure 4.10 Scanning electron microscope photographs of (a) non-treated and (b) lime-treated dredged mud

4.12 Effect of % lime on the sedimentation columns

The results obtained from the seepage induced consolidation test showed that as % lime increases from 0 to 4%, both the void ratio and permeability increase accordingly. The results suggested that extra addition of lime up to 6% brings about no further remarkable changes on the void ratio and permeability. It is clear that in the seepage induced consolidation test, any excess of calcium or hydroxide ions as a result of dissociation of hydrated lime are washed out from the particulate system. Thus, no distinction between the properties of lime treated dredged mud will be expected as % lime exceeds the threshold value. To evaluate the accuracy of this statement a simple alternative laboratory setup is proposed to investigate the effect of % lime on the dredged mud in the enclosed system where no excess ions are removed from the system. It is envisaged that if lime is added to clay soil in an enclosed system beyond the threshold value, the pozzolanic product will be formed in the course of time. These newly formed materials eventually fill the interparticle spaces between the soil grains and causes reduction in void ratio. The laboratory setup is designed as follows:

The dredged sediment with initial in situ moisture content of around 100 percent was passed through a 2.35 mm sieve in order to remove the shells and oversize particles. The water content of the sediment was then brought up to 400% using seawater and mixed thoroughly to ensure uniform slurry. Various lime contents from 0 to 5% (dry weight basis) were then mixed with slurry in separate buckets. Once homogenized, the contents were carefully poured into 6 glass measuring cylinders with the capacity of 1000 ml (Figure 4.11). The sediments were allowed to settle under their self weight for a period of 6 months. During this time, the distilled water was added to each cylinder to maintain the water surface at the initial level of 1000 ml. it was found that in all cylinders, as a result of self-weight consolidation, the interfacial clay-water surface moved downward rapidly for the first few days. The pace of settlement however, gradually reduced as time passed by. It was observed that the pace of settlement was reduced significantly in all cylinders after 5 months and no remarkable change in height of specimens were monitored after elapsed period of between 5 to 6 months. At this stage, the excess water above the interfacial clay water surface of the sediment columns was removed by means of a

burette. Care was taken not to disturb the specimens in the cylinders in order to avoid expansion or reduction in their volume. The final volume of the specimens in the measuring cylinders was recorded. Then, the mass of a cylinder including its content was measured using the digital scale. At this stage, the content was emptied into a tray and placed in the high temperature oven for determination of its moisture content.

The cylinders were then hosed with water and dried to measure their weight in order to determine the net weights of the specimens accordingly. By having net weight, moisture content and volume of the specimens the dry density of the specimens were calculated and the void ratio was obtained. Figure 4.12 shows the variation of void ratio with % lime in the sedimentation column experiment. It can be seen that void ratio increased from 5.5 to 8.8 as % lime increased from 0% to 4% respectively. Once the lime percentage increases to 5% the void ratio reduces to 8.3. This reduction is likely attributed to the formation of pozzolanic products during the course of the experiment (6 months) which filled the space between the particles and eventually reduces the void ratio.

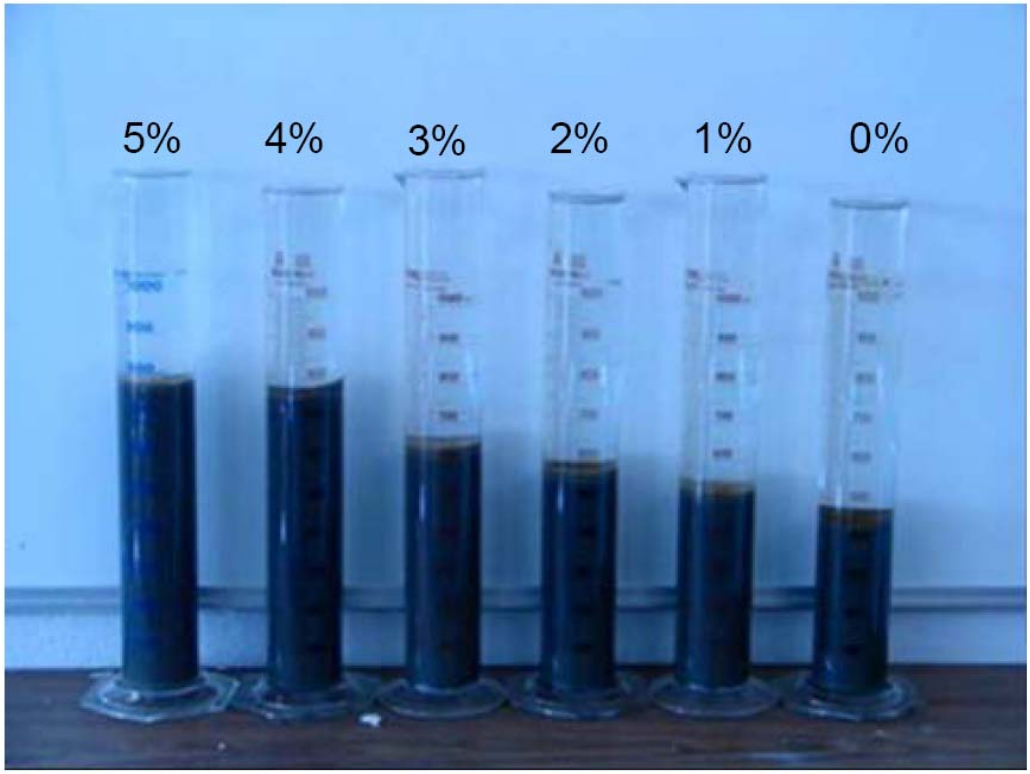

Figure 4.11 Effect of % lime on the sedimentation of the dredged mud

The test results obtained from the sedimentation column experiment may be discussed against the results of the seepage-induced consolidation test program. In the former, the lime treated specimens were subjected to water flow continuously and hence, once substitution of calcium ions with existing cations on clay particle lattice were completed, any remaining calcium ion was washed out from the system as water flows in. In the sedimentation column experiment however, the presence of the excess hydroxide ion (OH) had a significant role to increase alkalinity which led to dissolving the amorphous material on the edge of the clay particles. These gel-like materials have a potential to react with excess calcium ions in the system and form pozzolanic products as explained in chapter 3.

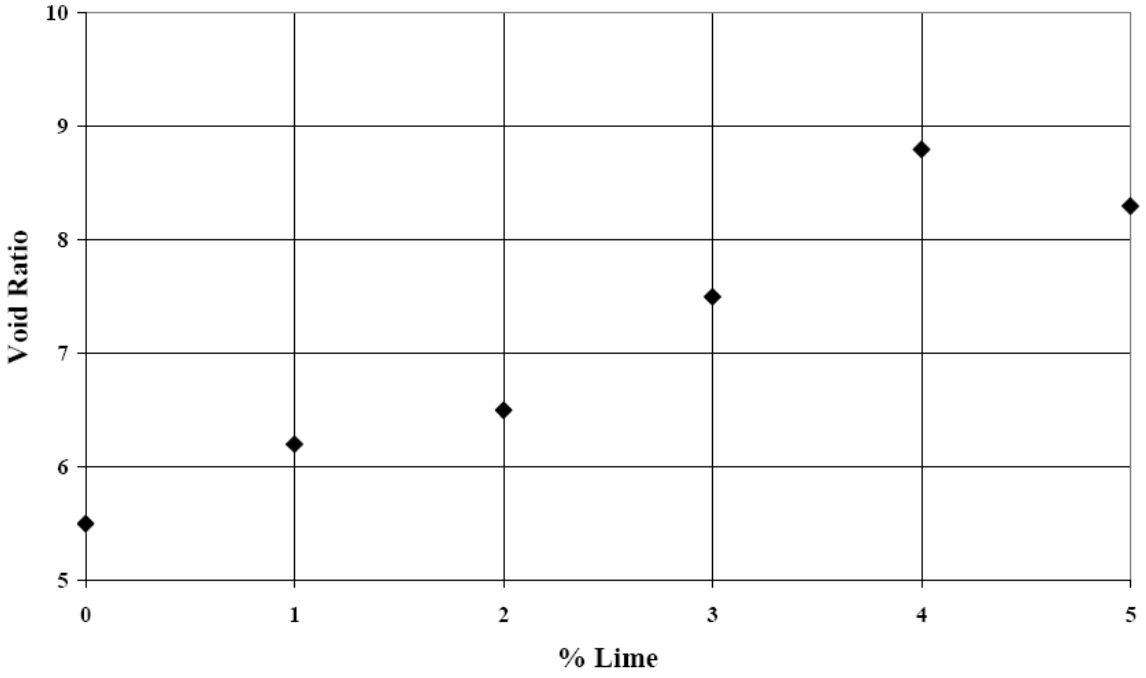

Figure 4.12 Variation of void ratio with % lime in enclosed system

Considering the test results obtained from both the seepage-induced consolidation test and the sedimentation column setup, it can be concluded that the seepage- induced consolidation test can be adopted as a reliable and fast tool, to evaluate the lime modification optimum of the clay soils with varying mineralogy from different origins.

4.13 Atterberg Limits of the lime treated dredged Mud

To asses the effect of % lime up to LMO on the index parameters, a set of the Atterberg Limit tests was conducted on the treated samples. For this purpose, the natural dredged mud with initial moisture content was first passed through a sieve of 425 micron to remove the oversize particles. A fraction of the sample was placed in the oven for moisture content determination. Four large glass beakers were partially filled with the natural dredged mud paste and extra seawater was added to each to increase the moisture content to 350%. The pastes on the different beakers were mixed thoroughly with water to ensure uniform slurry. Based on the determined initial moisture content a different amount of lime was added to each beaker to represent 1,2,3, and 4 % lime respectively (dry weight basis). The contents of the beaker were mixed again to ensure uniform distribution of lime through the samples. At this stage, a vacuum filtration flask was employed to filtrate the slurry samples in order to expel the excess water and bringing down the moisture to a level suitable for conducting the liquid limits (Figure 4.13). The slurry samples were poured into a funnel and then connected to the top of vacuum filtration flask as shown in Figure 4.13. The filtration flask was then connected to the vacuum pump. A high vacuum pressure of about 80 kPa was gradually applied to induce filtration. As a result of filtration, the moisture content gradually decreased within a few hours. For the lime treated samples this process was quicker as they presented the better porosity and water channels due to lime modification. At this stage the contents remaining in the funnel were collected and liquid limit, plastic limit and linear shrinkage limits were carried out in accord with Australian Standards as stated previously in section 4.5. The test results are tabulated in table 4.7.

Figure 4.13 Vacuum filtration flask

Table 4.7 Atterberg Limits of lime treated dredged mud

Parameters	0% Lime	1% lime	2% lime	3% lime	4% lime
LL	88	92	96	102	105
PL	26	27	28	34	36
PI	62	65	68	68	69
LS	22	23	24	23	24

The test results show that both the liquid limit and plastic limit gradually increase as % lime increases from 0 to 4% resulting in almost equal value for the plasticity index (PI). The plasticity index of the sample with 1% lime however, is slightly lower than those with 2% to 4% lime. Furthermore, it was found that linear shrinkage (LS) of treated samples is independent of the % lime and remains almost constant for all cases. Figure 4.14 shows the locations of the natural and lime treated dredged mud on the Casagrande's plasticity chart. It can be seen that all samples lay in the high plasticity clay zone (CH).

For the samples prepared under air or oven temperature, both the plasticity index and liquid limit, dropped significantly resulting in a lower plasticity of the materials. Plasticity indexes of the natural sample, tested on its in situ moisture content, is slightly less than those treated with lime. However, these parameters remain almost constant when the percentage of lime exceeds 2%. The change in liquid limit however, is affected by the lime content and gradually increased from 88% to 105% as % lime increases from 0 to 4%.

Figure 4.15 shows the Atterberg Limits test results of the dredged mud which was conducted earlier in 2001 and reported by FPE Seawall Alliance and URS (Coffey, 2004). The figure shows that the LL values generally vary between 80% to 100%, and PI values vary from 55% to 75%. These finding were in agreement with the in situ test results obtained in the current study.

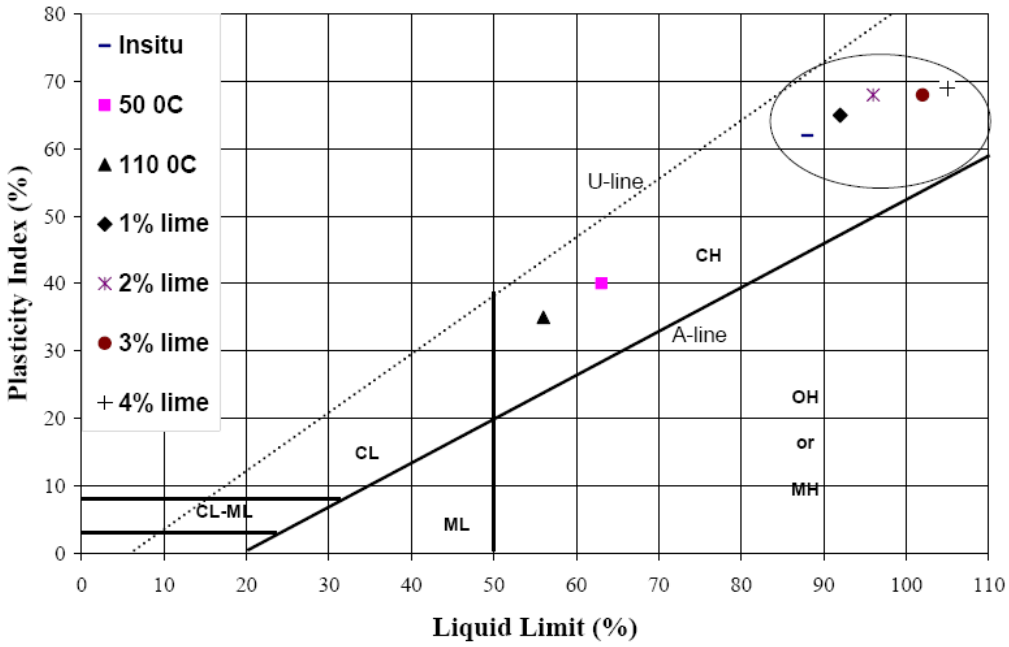

Figure 4.14 Casagrande's chart of plasticity

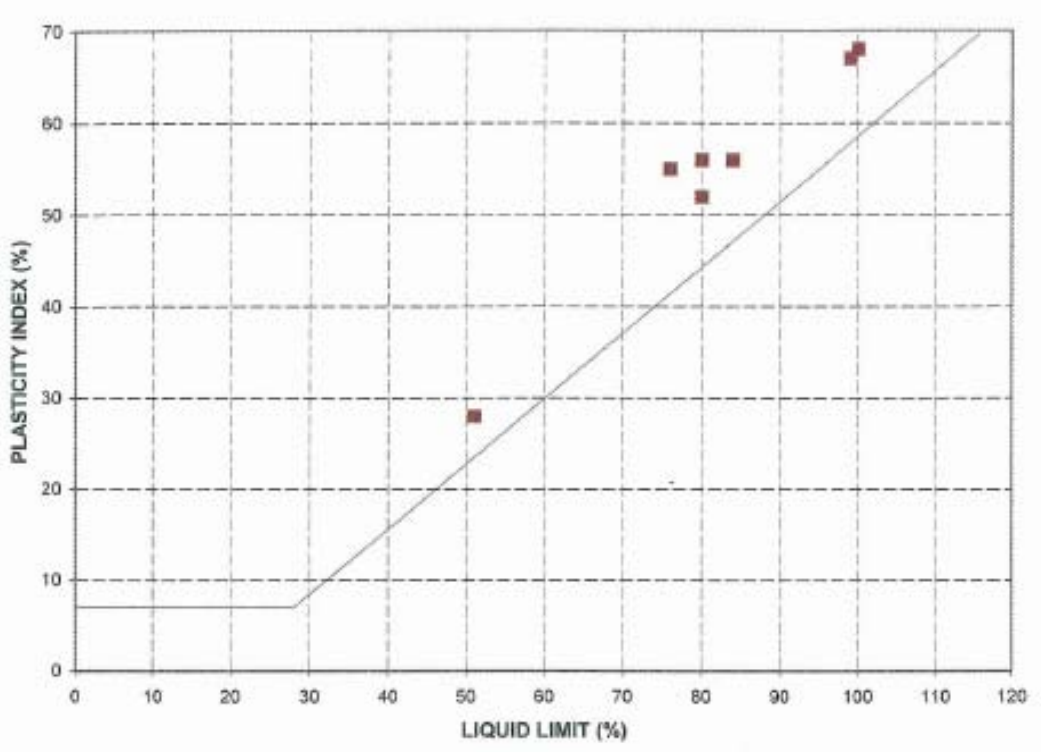

Figure 4.15 Atterberg Limits- Dredged Material (Coffey, 2004)

4.14 Summary and conclusion

This chapter provides comprehensive information about the properties of the various materials used throughout this research study. A series of laboratory studies were undertaken on the dredged mud sample obtained from the reclamation site of the Port of Brisbane in Australia to evaluate both chemical and mechanical properties of the dredged mud. it was found that the index properties and specific gravity of the base sample were drastically affected by the method of preparation. The liquid limit, plastic limit and specific gravity reduce as the samples are dried out for preparation purposes. The extent of these changes increase as higher temperatures is applied during preparation.

One of the main objectives was to introduce a new laboratory technique to determine the threshold value of lime in clay soil, below which only flocculation of particles takes place. This threshold value is termed “Lime Modification Optimum” and was first introduced to the literature by McCallister and Petry (1992). This technique is known as

the seepage-induced consolidation test which is primarily devised to study the consolidation behavior of the soft clay. This research however, proposed a different application for this laboratory setup aimed at evaluating the lime modification optimum (LMO) for the clay soil. The experimental data showed that for the type of clay soil used in this study, the maximum flocculation and permeability of amended soil was achieved when 4% of lime is added. To evaluate the accuracy of the data obtained from the seepage-induced consolidation test another laboratory setup known as a sedimentation column was employed to investigate the percentages of lime which contribute towards modification (i.e. flocculation) of the clay particles. The test results obtained from this laboratory arrangement showed that the addition of 4% lime should be considered as a threshold value, below which maximum flocculation takes place in the type of material used in this study. These findings, together with a study of the photographs taken by the scanning electron microscope suggested that the proposed seepage-induced consolidation test can be used as a reliable and fast laboratory technique to determine the LMO.

It is interesting to note that addition of lime to the dredged mud induced flocculation and caused both the void ratio and permeability to gradually increase with % lime. The higher capacity in holding water as a result of changing the fabric was also observed in the liquid limit of the lime treated dredged mud which showed increase as % lime increased.

The most significant interpretation which can be made from the seepage-induced consolidation test results is that the modification affect of lime on clay particles is independent of the degree of initial moisture content. In the experimental program, two representative lime-treated sub-samples were tested with high moisture content (350% and 550%) in order to evaluate the effect of moisture content on the lime-clay modification reaction. It was found that in the both sub-samples the similar results in terms of void ratio and permeability were achieved, indicating that the mechanism of lime-clay modification is not negatively affected by the degree of moisture content. These bench-scale findings may be considered as supporting the pragmatic proposal of injection of lime into the high moisture content dredged mud slurry in the Port of Brisbane.

Chapter 5

Surcharge Preload with Vertical Drains

5.1 General:

Previously in chapters 1 and 2 and 4, a discussion ensued as to the ultimate aim of the injection of lime into dredged mud slurry being to improve the consolidation behavior of the dredge sediment when it is subjected to surcharge preloading with vertical drains. It was stated that with addition of lime into a dredged mud, the increase in rate of the primary consolidation and reduction in the rate of secondary compression settlement were envisaged. Hence, a through understanding of the preloading technique is prerequisite to this study. Insight into a surcharge preloading technique and the function of vertical drains helps to develop an effective laboratory test program and also assist in the application of an appropriate constitutive model to predict the consolidation behavior of lime treated dredged mud on a large industrial scale.

This chapter outlines important concepts associated with the surcharge preloading technique with the aid of vertical drains. The aspects of surcharging along with vertical drain history and development are considered within the chapter. The method of converting an axisymmetric vertical drain system into an equivalent plane strain drain is also discussed in detail. This conversion is used in most finite element packages in analysing preloading with vertical drains. This chapter also provides a brief review of critical state soil mechanics and the soft clay model of Cam-clay is also incorporated in the constitutive model.

5.2 Introduction of the surcharge preloading technique

Surcharge preloading generally refers to the process of compressing the soft soil under applied vertical stress, prior to construction and placement of the final construction load. Construction of the embankment (surcharge preload) on a soft foundation aims to consolidate ground under a load intensity higher than the final construction load (i.e. infrastructure facilities) to compensate or minimise post-construction settlement. When the preload is placed on soft soil, it is initially carried by the pore water. When the soil is of low permeability, which is normally the case with clays, the water pressure will decrease gradually because the pore water is only able to flow away very slowly in a vertical direction. Because of its low permeability, the period for consolidation settlement of soft clays is protracted. To shorten the consolidation time, vertical drains are installed prior to preloading. Vertical drains are artificially created drainage paths which are inserted into the soft clay subsoil. Thus, the pore water squeezed out during consolidation of the clay due to the hydraulic gradient created by the preloading flows faster in the horizontal direction toward the vertical drains. Subsequently, the pore water can flow freely along the vertical drains. With installation of vertical drains, the consolidation process will accelerate and will allow the clay to gain rapid strength to carry the new load. The schematic view of surcharge preloading with the installation of vertical drains is shown in Figure5.1.

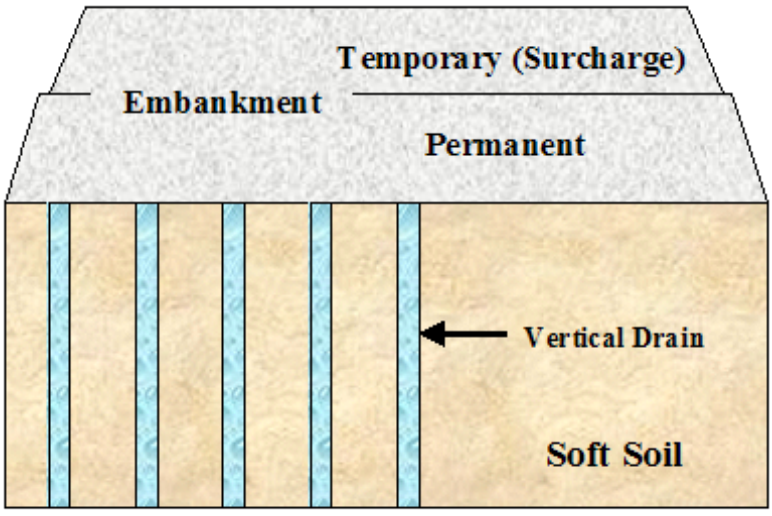

Figure5.1 Surcharge preloading with vertical drains

At the end of the preloading period, the temporary part of the embankment, termed surcharge, is removed and the soil beneath the permanent embankment becomes overconsolidated. The removal of surcharge fill should preferably not take place before the remaining excess pore pressure is below the stress increase caused by the temporary load. The final design load (i.e. construction of infrastructure facilities) can now be placed on the embankment. It should be noted that by increasing the preloading time (i.e. achieving a higher degree of consolidation), or the size of the temporary surcharge, the post construction secondary compression settlement can be reduced significantly. Using a surcharge higher than the final design load, the soil will always be in overconsolidated state and the secondary compression for overconsolidated soil is much smaller than that of normally consolidated soil. Hence, this will greatly benefit the subsequent geotechnical design.

The following section helps to improve understanding the influence of preloading with surcharge on the post-construction secondary compression settlement.

5.3 Introduction of the concept of aging in clay consolidation

There is extensive literature on clay consolidation, beginning with Terzaghi's initial work. Terzaghi (1925) published one article on the "Settlement and Consolidation of Clay" in Vienna of '*Erdbaumechanic*'. He recognized the similarity of moisture flow in soils to heat flow through materials and consequently developed the theory of consolidation. He also designed the first consolidation apparatus named an 'oedometer' (from the Greek *oidema*, swelling). Following Terzaghi's experimental works, Taylor at the Massachusetts Institute of Technology (1942), helped to increase understanding of the consolidation phenomenon in soils. His study was directed mainly at the difference between the rates of compression observed in laboratory specimens and the theoretical rates. Taking into consideration the time-dependent plastic resistance of the soil structure, Taylor developed a modification to Terzaghi's theory. This is illustrated in Figure 5.2 in which the upper line approximately presents the end of primary consolidation and the

lower lines corresponds to the stress/void ratio after increasing degrees of secondary compression.

Twenty-five years later Bjerrum, in the Seventh Rankine Lecture, provided a useful analysis to the observation of Taylor. Bjerrum introduced the term “delayed consolidation” which occurs in natural deposits under constant effective stress.
In his state-of-the-art report to the 8th International Conference on Soil Mechanics and Foundation Engineering (1973), Bjerrum elaborated his own views expressed earlier in the Rankine lecture.

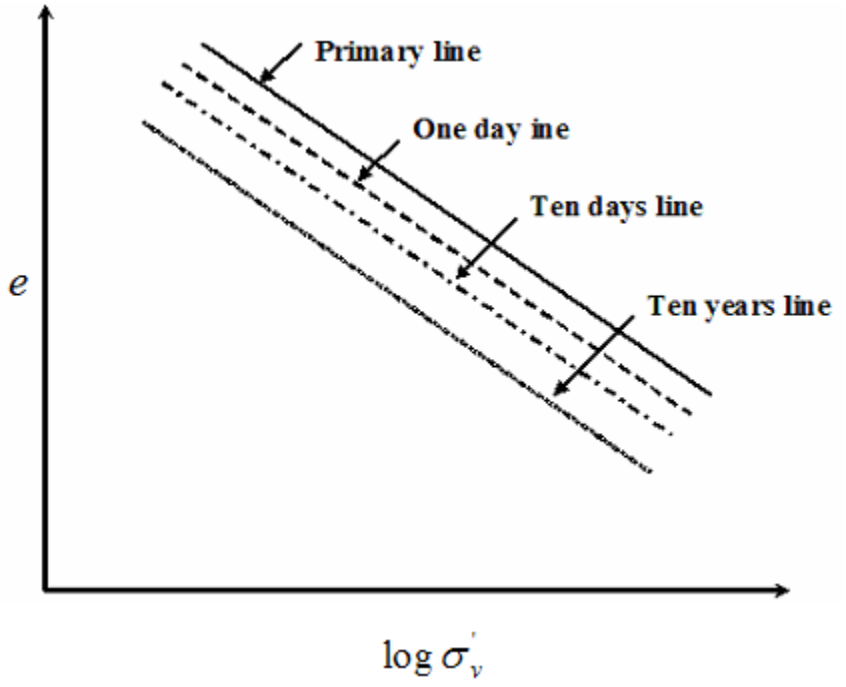

Figure5.2 Semi-logarithmic plot of pressure versus void ratio
(Redrawn after Taylor, 1942)

It is worthwhile mentioning that his discussion was limited to homogeneous, flocculated soft clays, classified as:

- Normally Consolidated (NC) young clays, most recent deposits of equilibrium condition under self-weight, but as yet not having experienced significant delayed or secondary consolidation.

- Normally consolidated aged clays, placed under constant effective stress for centuries or thousands of years having experienced a considerable delayed consolidation.

- Overconsolidated clays, already subjected to a load larger than the current effective overburden pressure.

The behavior of clay deposits associated with the first of the two categories (above) is presented in Figure 5.3. An intact specimen of'young' NC clay would lay on the upper bold curve, with a preconsolidation pressure (P_C or σ'_p) equal to the current effective over burden pressure (P_0 or σ'_{v0}). If the young normally consolidated clay (NC) is left undisturbed for centuries or thousands of years, the process of consolidation would continue, under constant effective stress, achieving a more stable arrangement of grains with more significant strength against further compression.

If an undisturbed specimen of this aged NC clay is loaded in the consolidation apparatus, it would follow the lower line (in bold) with a measured $P_C > P_0$ ($\sigma'_p > \sigma'_{v0}$). This reasoning helps to understand the phenomenon; in which P_C values are greater than P_0 when there is no other satisfactory geological explanation.

Bjerrum also reported that the P_C / P_0 ratio of clay is highly dependent on its plasticity and for the clay deposits of the same age, under 'delayed consolidation', this ratio increases with an increasing plasticity index. The relationship between the P_C / P_0 ratio with the plasticity index observed in a few normally consolidated late glacial and post-

glacial clays is shown in Figure 5.4. It should be noted that the ratio of P_C / P_0 is also known as the "*Over Consolidated Ratio*" (OCR), a terminology which will be used in this thesis hereafter.

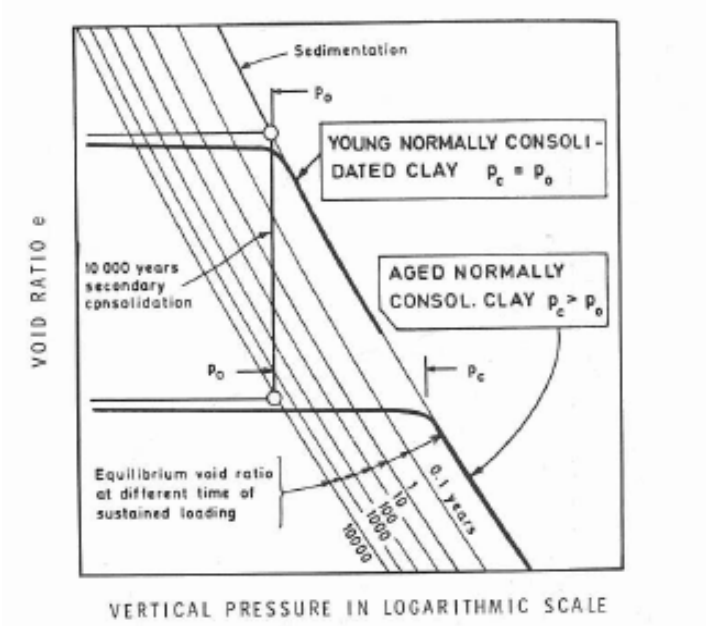

Figure 5.3 Geological history and compressibility of a 'young' and'aged' normally consolidated clay (Bjerrum, 1973)

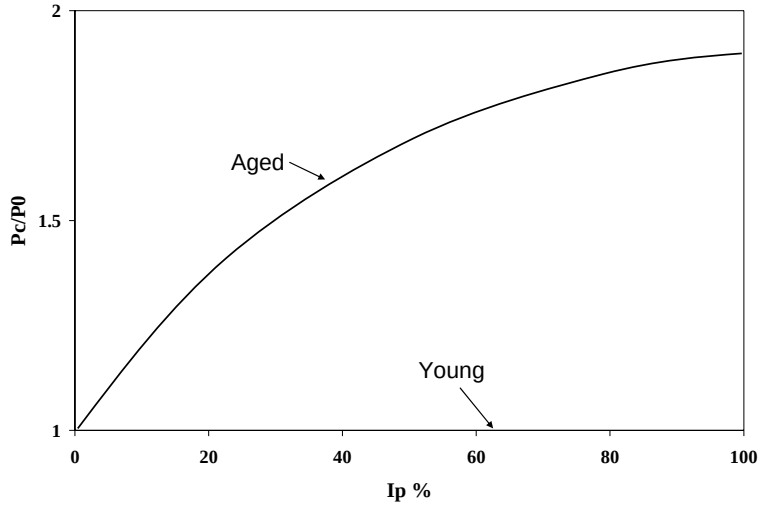

Figure 5.4 Typical values of P_C / P_0 observed in normally consolidated late glacial and post-glacial clays (Bjerrum 1973)

For the specific clay deposits which have been subjected to pressure greater than the current overburden stress during their geologic history, the pressure/void ratio is presented in Figure 5.5. In this case, the previous maximum effective pressure is denoted as P_1. Again, like aged NC clay, the delayed consolidation occurred over a long period e.g. 10000 years, and present effective in situ stress is P_0. When an intact specimen of such clay is loaded in the oedometer apparatus, due to the 'reserve resistance' build up before the geological erosion which led to unloading, the measured P_C exceeds the previous maximum effective stress(P_1).

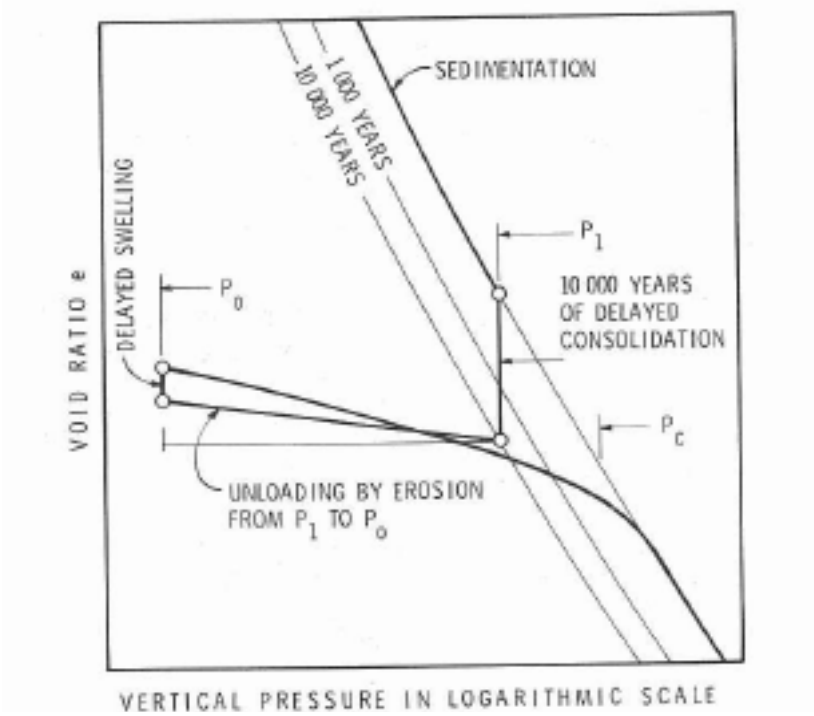

Figure 5.5 Geological history and compressibility of overconsolidated clay

5.4 Application of the concept of aging in preloading technique

For soft soils, it is well known that the compression ratio $C_R = C_c/(1+e_0)$ is remarkably larger than the recompression ratio $C_{RR} = C_r/(1+e_0)$. The ratio of C_{RR}/C_R normally lies in the range of 0.1-0.2. Hence, in case surcharge preload where the soft clay foundation has previously been loaded beyond the final design load (i.e. after removal of the surcharge and construction of infrastructure facilities), the amount of expected settlement due to primary consolidation when the final design load is applied will only be 10-20% of that of normally consolidated clay. However, if the final design load is at or close to the preconsolidation pressure, considerable creep or secondary compression settlement will take place over the course of time, and this kind of settlement may not be tolerated over the design life of the project (Mesri et al. 2001). The usual principle of preloading is therefore to surcharge the soft foundation beyond the target construction load, such that secondary compression settlement will also be reduced to a desirable limit. Planning the required surcharge for a specific soft foundation to reach satisfactory preloading is a function of soil characteristics, post-construction settlement limits, schedule of project, and whether the preloading will be facilitated by artificial drain paths (vertical or horizontal drains) or some other method of accelerating the rate of consolidation.

There is one common method by which the required surcharging effort in the preloading technique is assessed. This method is explained in section 5.5 and then will be further interpreted in section 5.6.

5.5 Engineering Judgment

Quite often, an initial estimate of the required surcharge load could be achieved by relying on the engineering judgment. This could be made by multiplying the final design load by a factor 1.5 to 2.0. This technique is limited to a condition where the entire layer is to be subjected to a uniform load in order to reach the same degree of consolidation of the entire soil profile during preloading and where more than 90% of primary consolidation will be achieved before removal of surcharge (Wong, 2005). Under application of this approach, post-construction settlement is normally evaluated by taking

into account the reload (recompression) primary consolidation only. This approach however suffers from ignorance of the fact that creep settlement still occurs even under applied stress in the recompression range. The implicit assumption of this approach is that the secondary compression settlement only abruptly increases when the preconsolidation pressure is reached. This presumption does not quite sound because the secondary compression settlement occurs under whatever overconsolidation ratio. However, it is true to state that the type of secondary compression settlement gradually increases as the applied design load reaches close to the preconsolidation pressure.

5.6 Role of surcharge in secondary compression settlement

This section mostly deals with the law of compressibility or concept of C_α / C_c ratio initially introduced and later developed by Professor Mesri's group in Illinois University, USA (Mesri and Godlewski 1977, 1979; Mesri and Castro 1987; Mesri 1987; Mesri, 1991; Mesri et al, 1994, 1997, 2001; Mesri and Ajlouni, 2007). According to the literature corresponding to the law of compressibility, the compression index C_c, denotes the slope of the $e - \log \sigma_v^{'}$ curve in both the compression and recompression range whereas in conventional literature and textbooks, the specific term of recompression index, C_r, denotes the slope of the $e - \log \sigma_v^{'}$ curve in the recompression range. The current chapter however, adopts the former approach where C_c is the constant term used to refer to the two states of compressibility.

The key parameter for quantitative analysis of secondary compression settlement is the secondary compression index, C_α, which can be expressed in terms of void ratio or volumetric strain change per log cycle of time. On the settlement-log time plot it is possible to separate the end of the primary consolidation stage from the inflection points appearing on the consolidation curves (Figure 5.6).

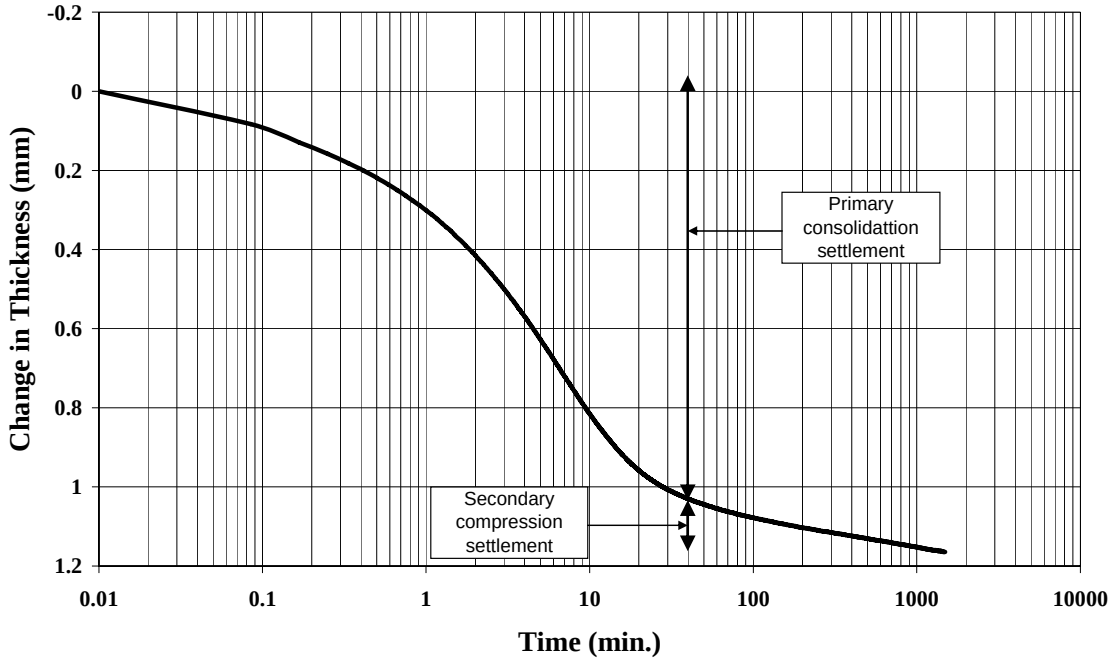

Figure 5.6 Typical settlement- log time consolidation curve

Mesri and Godlewski (1977) made a detailed study of the relationship between C_α and C_c, and concluded that the volume changes during secondary compression and primary consolidation phases are essentially due to the same mechanism. They proposed the concept of C_α / C_c where C_c is the compression index, i.e. the slope of void ratio, e, against the logarithm of effective stress, $\sigma_v^{'}$, curve in the virgin loading range. According to this concept, for any one soil the ratio of C_α / C_c is constant for any time, effective stress, and void ratio. It was also found that the ratio of C_α / C_c lies within a narrow range of 0.02- 0.1 for a number of soils (Mesri and Godlewski, 1977; Mesri and Castro, 1987).

Table 5.1 Values of C_α / C_c for different soils (Mesri and Godlewski, 1977)

Soil	C_α / C
Organic silts	0.035-0.06
Amorphous and fibrous peat	0.035-0.085
Canadian muskeg	0.09-0.10
Leda clay (Canada)	0.03-0.06
Post-glacial Swedish clay	0.05-0.07
Soft blue clay (Victoria, B.C.)	0.026
Organic clays and silts	0.04-0.06
Sensitive clay, Portland, ME	0.025-0.055
San Francisco Bay Mud	0.04-0.06
New Liskeard (Canada) varved clay	0.03-0.06
Mexico City clay	0.03-0.035
Hudson River silt	0.03-0.06
New Haven organic clay silt	0.04-0.075

Settlement due to secondary compression can be calculated as:

$$S = \frac{C_\alpha}{1+e_0} L_0 \log \frac{t}{t_p} \qquad \text{Eq. 5.1}$$

where, e_0 and L_0 are the void ratio and thickness of layer corresponding to the end of primary consolidation (EOP). t_p is the time corresponding to EOP, and t is any elapsed time beyond t_p.

The Eq. 5.1 suggests that for a given void ratio and thickness, at any time beyond t_p, the secondary compression settlement is governed by the secondary compression index, C_α.

In a preloading technique, the magnitude of the post construction secondary compression settlement can be gradually reduced by increasing the surcharge. The fact that the surcharge controls the size of the post-construction secondary compression settlement can be explained by the law of compressibility or ratio of C_α / C_c, as elaborated herein:

Surcharging produces a preconsolidation pressure, $\sigma_{vs}^{'}$, greater than the final permanent effective vertical stress, $\sigma_{vf}^{'}$. The surcharging effort can be expressed as the 'total surcharge ratio' (Terzaghi et al, 1996):

$$R_s = \left(\sigma_{vs} / \sigma_{vf}^{'}\right) - 1 \qquad \text{Eq. 5.2}$$

where $\sigma_{vf}^{'}$, is the final effective vertical stress after removal of surcharge, σ_{vs} is equal to $\sigma_{vf}^{'} + \Delta\sigma_{vs}$ and $\Delta\sigma_{vs}$ is the total surcharge pressure.

As an alternative, the surcharging effort can be presented as the 'effective surcharge ratio':

$$R_s^{'} = (\sigma_{vs}^{'} / \sigma_{vf}^{'}) - 1 \qquad \text{Eq. 5.3}$$

where $\sigma_{vs}^{'}$, is the maximum effective vertical stress achieved before removal of surcharge.

Figure 5.7 shows the typical effect of surcharging on a clay sample under laboratory conditions. The ratio of C_α / C_c in this example is 0.06 for the compression and recompression range as well. This figure shows that without surcharging, secondary compression of a clay sample at $\sigma_{vf}^{'} = 50$ kPa begins at point (a) and develops the length of (al). As can be seen, at point (a) the compression index, C_c, is high, and because the ratio of C_α / C_c is constant, C_α is accordingly larger.

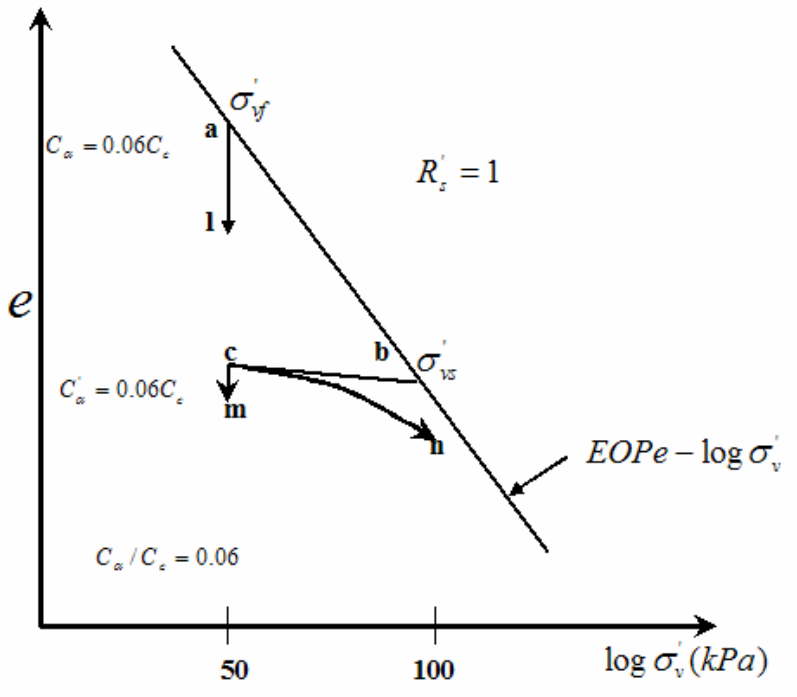

Figure 5.7 Interpretation of secondary compression behavior in terms of C_α / C_c law of compressibility using laboratory data (Redrawn after Mesri & Ajlouni, 2001)

On the other hand, after surcharging, post surcharge (or post-construction) secondary compression begins at point (c) and developed along (cm). In this state, C'_α denotes post surcharge secondary compression index, which is again proportional to C_c values related to the slope of the recompression curve (i.e. cn). Since C'_α / C_c in the recompression range remains constant (i.e. 0.06) and C_c is small, C'_α is modest. Figure 5.7 also suggests that the recompression curve (cn) starts with a very small slope at point (c) and the slope continuously increases with an increase in σ'_v until it merges with the virgin compression curve. Attention to this behavior is essential to understanding the effectiveness of varying surcharging efforts on post-surcharge secondary compression behavior. Actually, once the final permanent effective vertical stress, σ'_{vf}, is close to preconsolidation pressure, σ_{vs}, the slope of recompression curve, C_c, increases and post-surcharge secondary compression, C'_α, increases accordingly. However, with increasing surcharge effort

(i.e. $\sigma_{vs}^{'} \rangle\rangle \sigma_{vf}^{'}$), the compression index reduces and consequently the post-surcharge compression index will decrease.

The removal of the surcharge load leads to a rebound, including primary rebound up to t_{pr} and secondary rebound that levels off at t_l, followed by post-surcharge (or post-construction) secondary compression settlement (Mesri et al., 2001). Both t_{pr} and t_l are calculated from the time at which the surcharge load is removed. Figure 5.8 shows the general consolidation and rebound behaviors of a soft deposit subjected to surcharge preloading with an effective surcharge ratio of 0.6.

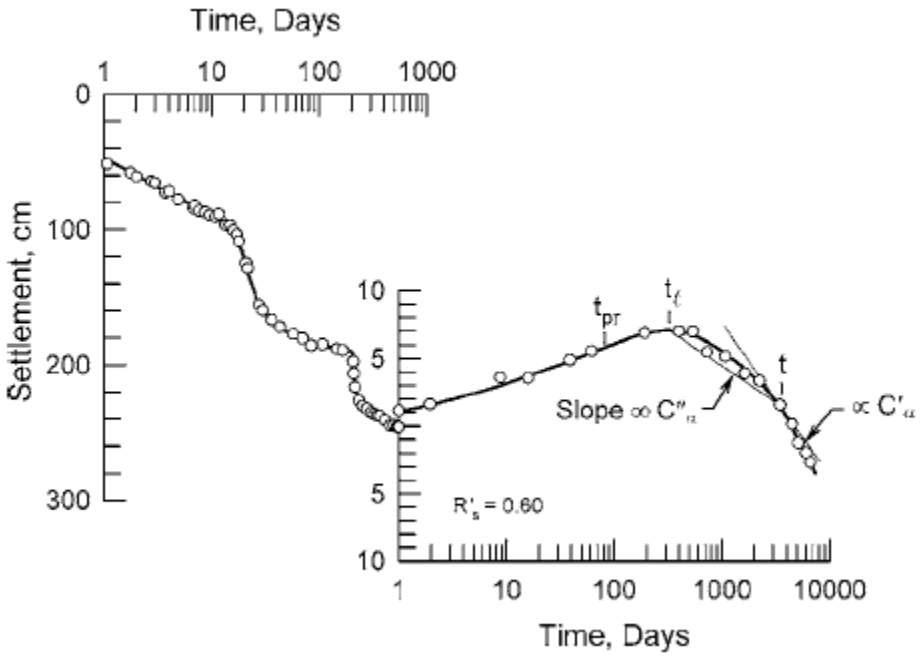

Figure 5.8 Settlement behaviors before and after surcharging
(Mesri and Ajlouni, 2007)

Figure 5.8 also shows that post-surcharge (or post-construction), secondary compression index $C_\alpha^{'}$ does not remain constant with time and therefore for a realistic settlement study, a secant $C_\alpha^{''}$ is defined from the time t_l, at which post-surcharge secondary

compression settlement appears to any instant t at which secondary compression is to be determined.

Figure 5.9 illustrates the post surcharge rebound, and secondary compression behavior of inorganic soft clay. This figure shows that for small values of effective surcharge ratio, $R_s^{'}$, time for secondary rebound, t_l, is small and post surcharge secondary compression settlement appears soon after the removal of surcharge. At a lower value of effective surcharge ratio, post-surcharge secondary compression rate increases rapidly with time. On the other hand, once the effective surcharge ratio increases, time for secondary rebound, t_l, is large and post-surcharge secondary compression appears long after the removal of surcharge and secondary compression rate is very low.

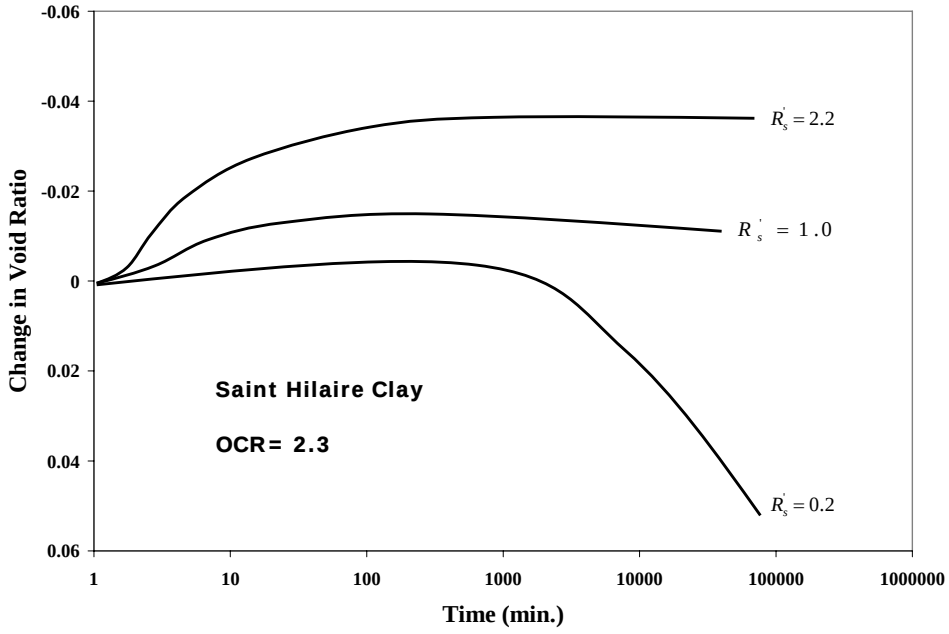

Figure 5.9 Post-surcharge rebound, and secondary compression behavior of inorganic soft clay, as a function of effective surcharge ratio
(Refined and redrawn after Mesri et al., 2001)

The post-surcharge of a soft sediment as shown in figure 5.9 can be explained by the $C_{\alpha}^{'} / C_c$ law of compressibility. Referring to figure 5.7, as effective surcharge ratio, $R_s^{'}$, increases, the horizontal distance between points (b) and (c) certainly increases. When point (c) is distant enough from (b), the slope of the recompression curve (cn) starts with a small value. When point (c) is closer to (b), C_c becomes larger and $C_{\alpha}^{'}$ is expected to increase thereof.

As discussed, the successful application of a preload surcharge to minimize the magnitude of post-surcharge or post-construction secondary compression settlement is highly dependent on the degree of effective stress achieved before removal of the surcharge load (i.e. higher effective surcharge ratio, $R_s^{'}$). The increase of effective stress however is related to the rate of excess pore water pressure dissipation which is initially developed by the surcharge preload. It is known that the consolidation of soil is a process of decreasing the volume in saturated soil by pressing out the pore water. The consolidation rate is governed by soil compressibility, permeability and length of drainage paths. The review of a few case histories indicates that in almost all cases, the natural permeable boundaries are not sufficient enough to provide satisfactory drainage paths for soft clay deposits when they are subjected to preloading. Therefore artificial drainage paths such as vertical drains might be employed to accelerate the rate of dissipation of excess pore water pressure.

Overall, the use of artificial drainage paths can benefit a reclamation project in several aspects as summarized below:

- To decrease the time for preloading and achieving a higher value of the final effective stress in a shorter period.

- To lessen differential settlement that normally ensues during primary consolidation settlement of soft ground.

- To enhance the shear strength of soil as a result of reduced moisture content and void ratio.

- To reduce the height of surcharge fill needed to achieve desired preconsolidation.

5.7 Function of vertical drains

The one-dimensional consolidation settlement behavior of clay is described by Terzaghi (1925). In the case of one-dimensional consolidation, based on the Darcian flow, the relationship between excess pore water pressure u and consolidation time t at different depths z is given by the Eq. 5.4:

$$\frac{\partial u}{\partial t} = \frac{k}{\gamma_w m_v} \frac{\partial}{\partial z}\left(\frac{\partial u}{\partial z}\right) \qquad \text{Eq. 5.4}$$

where k is the permeability, m_v is the coefficient of volume compressibility, and γ_w is the unit weight of water.

The permeability, k, generally decreases as strain, ε, continuously occurs as a result of increased applied stress. The linear relationship can therefore be observed in the $\log k / \varepsilon$ curve (Hansbo, 2005). Accordingly, k is a function of the effective stress $\sigma_v^{'}$ or on the other hand is the function of the excess pore water pressure u.

In reality, the decrease in k with increasing the effective stress is generally counteracted by a reduction of coefficient of volume compressibility m_v. Hence, it can be concluded that that the coefficient of consolidation $c_v = \frac{k}{\gamma_w m_v}$ of normally consolidated clay is usually found to be fairly constant under a moderate increase of strain ε.

With the application of vertical drains where the drainage paths are provided laterally, Rendulic (1936) suggested the differential equation for one-dimensional vertical compression by radial flows.

$$\frac{\partial u}{\partial t} = c_h \left(\frac{\partial^2 u}{\partial r^2} + \frac{1}{r} \frac{\partial u}{\partial r} \right) \qquad \text{Eq. 5.5}$$

where, r is the radial distance from the drain centreline (Figure 5.10) and c_h is the coefficient of consolidation in the horizontal direction $c_h = \frac{k_h}{\gamma_w m_v}$.

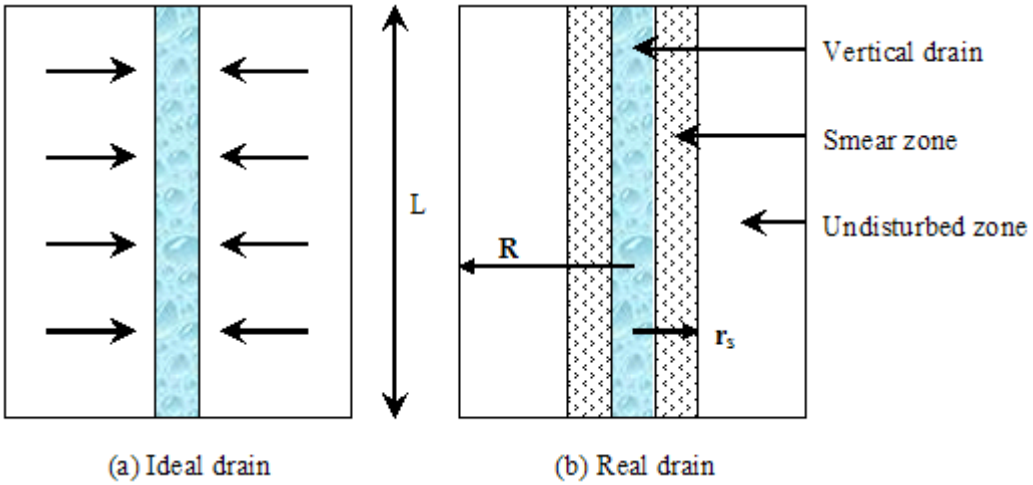

Figure 5.10 Unit-cell model of vertical drain in soil (after Barron, 1948)

In the case where the both radial and vertical flows occur, the dissipation of excess pore water pressure can be computed by the equation suggested by Carrillo (1942).

$$\frac{\partial u}{\partial t} = c_h \left(\frac{\partial^2 u}{\partial r^2} + \frac{1}{r} \frac{\partial u}{\partial r} \right) + c_v \frac{\partial^2 u}{\partial z^2} \qquad \text{Eq. 5.6}$$

$$\overline{U}_{tot} = \frac{u_r u_z}{u_0} \qquad \text{Eq. 5.7}$$

where, u_r and u_z are excess pore water pressures due to radial and vertical flow respectively, and u_0 is the initial pore water pressure.

It has to be mentioned that the installation of vertical drains is only performed in places where the thickness of the fine-grained soil layer is so large that the effect on the consolidation process - due to the one-dimensional consolidation by pore water pressure dissipation in a vertical direction between the drains - is insignificant. However, the contribution of vertical flow to the total consolidation can be based on the classical Terzaghi solution with the Darcian flow as expressed below and is only valid when $\overline{U}_z \leq 50\%$.

$$\overline{U}_z = \frac{2}{l}\sqrt{\frac{c_v t}{\pi}} \qquad \text{Eq. 5.8}$$

The consolidation due to radial flow toward the vertical drains can be expressed as:

$$\overline{U}_r = 1 - \exp\left(-\frac{8c_h t}{\mu D_e^2}\right) \qquad \text{Eq. 5.9}$$

This equation proposed by Hansbo (1981) will be detailed in the following sections.
The average degree of consolidation of the compressible soft layer can now be obtained by combining U_r and U_z therefore:

$$\left(1-\overline{U}_{tot}\right) = \left(1-\overline{U}_z\right)\left(1-\overline{U}_r\right) \qquad \text{Eq. 5.10}$$

where, $\overline{U}_{tot}$ is the average degree of consolidation of the clay at time t for combined radial and vertical flow, and $\overline{U}_r$ and $\overline{U}_z$ are the average degree of consolidation at time t for radial and vertical flow respectively. It is important to note that the solution presented

by both Redulic and Carillo are suitable for "ideal" drains only in which the discharge capacity of the drain is infinite and there is no smear zone.

5.8 Efficiency of vertical drain

The efficiency of the prefabricated vertical drains (PVD) is governed by the two distinct factors as explained herein:

5.8.1 Smear zone

A vertical drain inserted into a steel mandrel is pushed into a soft ground by means of static or dynamic force. Upon reaching the desired depth, the mandrel is withdrawn, leaving the drain in the subsoil. This process of installation brings about the remolding of the subsoil, particularly in the immediate vicinity of the mandrel. As a result of fabric disturbance in the smear zone, the lateral permeability reduces which adversely affects the consolidation process. As remolding retards the rate of the consolidation process of the subsoil, the effect of permeability and compressibility within the smear zone has to be considered in any theoretical solution. Both the diameter and permeability value of the smear zone is difficult to determine from laboratory experimental works and so far no standard method has been suggested to measure them. It can be said that the extent of the smear zone and its permeability is influenced by the installation procedure, size and shape of the mandrel, and sensitivity of soil.

Holts and Holm (1973) together with Akagi (1977) proposed that the diameter of the smear zone (d_s) and the cross section area of mandrel can be related as follows:

$$d_s = 2d_m \qquad \text{Eq. 5.11}$$

where d_m is the diameter of the circle with an area equal to the cross sectional area of the mandrel.

Jamiolkowski and Lancellotta (1981) proposed the different relationship as being:

$$d_s = (2.5 - 3.0)d_m \qquad \text{Eq. 5.12}$$

According to Hansbo (1987), Bergado et al. (1993), and Cortlever and Hansbo (2004), within the smear zone, the $k_h^{'}/k_v^{'}$ ratio was found to be close to unity, which is in agreement with the results of the study of Indraratna and Redana (1998).

5.8.2 Well resistance

The resistance to water flowing in the vertical drains is known as well resistance. The well resistance increases with an increase in the length of the drain and reduces the consolidation rate. On the other hand, well resistance reduces the discharge capacity of the drain and therefore hinders the excess pore water pressure dissipation. There are a few main factors which are responsible for well resistance as described briefly herein:
Firstly, the filter sleeve surrounding the core of the prefabricated vertical drain must be strong enough to resist tension and wear and tear to avoid infiltration of fine particles into the drain. Furthermore, the pore size of the filter has to be small enough to prevent intrusion of fine clay particles into the channels of the cone, which eventually lead to clogging of the channel. Besides, in organic soil, the deterioration of the filter may also cause reduction of the discharge capacity (Hansbo, 1987).

Secondly, the lateral earth pressure causes a reduction of the drain cross section area which reduces drain discharge capacity. However, the effect of lateral confining pressure varies for different drains (Hansbo 2005).

Thirdly, Possible folding, bending, and crimping also reduces the discharge capacity of the drains (Indraratna et al. 2005).

The effect of well resistance varies with the permeability of the adjacent soils, the discharge capacity and the length of the vertical drain drainage paths. Accordingly, well resistance may affect the excess pore water pressure distribution with depth and distance from the vertical drain during the consolidation phase. Based on the previous analysis of the field performance of vertical drains in soft clay deposits, Lin et al (2000) reported that

well resistance is negligible when the well resistance factor, R is greater than 5 as defined in the following equation:

$$R = \frac{q_w}{k_h \times I^2} \qquad \text{Eq. 5.13}$$

where:

q_w is the discharge capacity of the vertical drain in m^3/s

k_h is the horizontal permeability of the undisturbed soil in m/s

I_m is the length of the vertical drain in m

5.9 Diameter of the influence zone of the drain

The equivalent diameter of the influence zone D_e is the function of enclosed cross section area A between four drains as follows:

$$D_e = 2\sqrt{\frac{A}{\pi}} \qquad \text{Eq. 5.14}$$

For more simplicity, Hansbo (1981) proposed the correlation between influence zone D_e and drain spacing S for two different patterns of drain installation as shown in Figure 5.11:

$$D_e = 1.13S \text{ for drains installed in a square pattern} \qquad \text{Eq. 5.15}$$

And

$$D_e = 1.05S \text{ for drains installed in a triangular pattern} \qquad \text{Eq. 5.16}$$

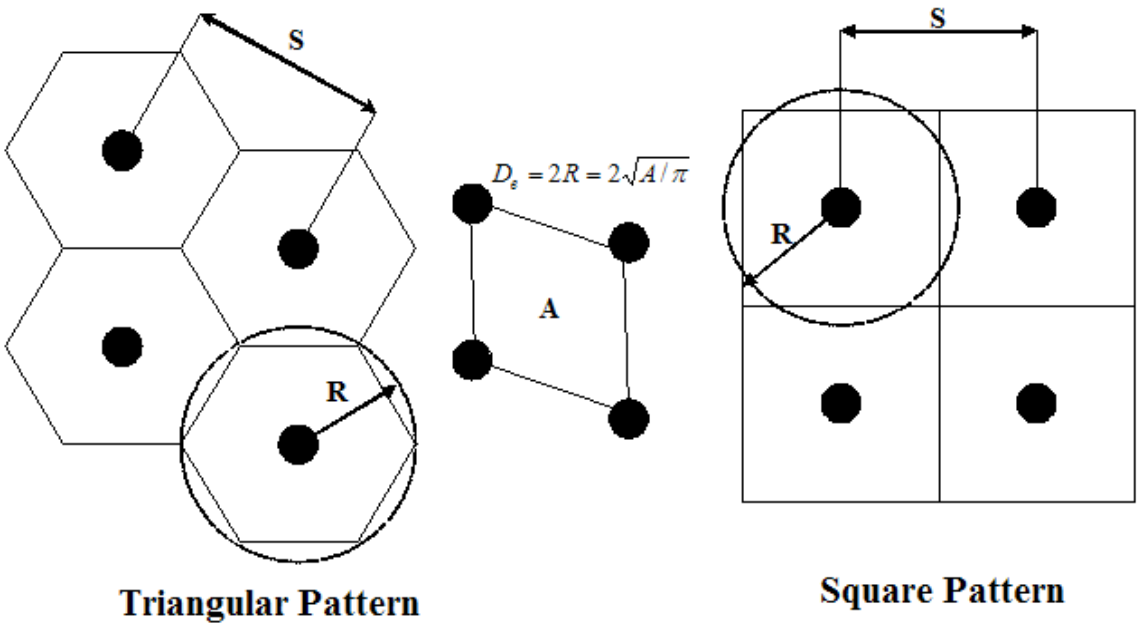

Figure 5.11 Typical drain installation patterns and the equivalent diameter (Hansbo,1981)

Even though the square pattern of the drain installation in the field seems to be easier to arrange and control, the triangular pattern normally provides a more uniform settlement between the drains (Indraratna et al, 2005).

5.10 Equivalent diameter of band-shaped drain

The conventional theory of consolidation with vertical drains assumes that the vertical drains are circular in cross-section. Hence, a band-shaped drain dimension (width a, thickness b) have to be converted to an equivalent circular diameter d. There are few typical equations which are used to determine the equivalent drain diameter.

Hansbo (1979) introduced the equivalent diameter for a prefabricated vertical drain as:

$$d_w = r_w = 2(a+b)/\pi \qquad \text{Eq. 5.17}$$

Taking into consideration the corner effect, where the flow lines rapidly converge, Rixner et al (1986) proposed the equation below:

$$d_w = (a+b)/2 \qquad \text{Eq. 5.18}$$

Pradhan et al (1993) proposed that the equivalent diameter of a band-shaped PVD should be approximated by considering the flow net around the soil cylinder of diameter d_e as shown in Figure 5.12. The average square distance of their flow net is calculated as:

$$s^{-2} = \frac{1}{4}d_e^2 + \frac{1}{12}a^2 - \frac{2a}{\pi^2}d_e \qquad \text{Eq. 5.19}$$

Then:

$$d_w = d_e - 2\sqrt{\left(s^{-2}\right)} + b \qquad \text{Eq. 5.20}$$

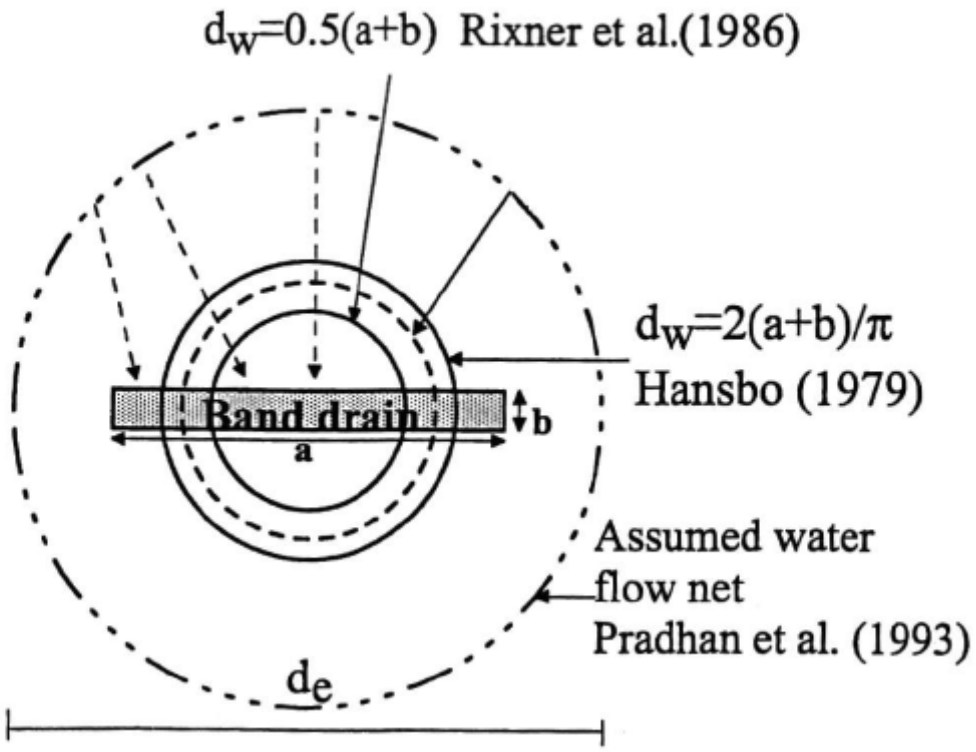

Figure 5.12 Equivalent diameters of band-shaped PVD from various researchers

5.11 Revising one-dimensional consolidation with radial flows

As discussed previously, Rendulic (1936) suggested the differential equation (Eq. 5.5) for one-dimensional vertical compression by radial flows for an ideal well. After Rendulic, Barron (1948) proposed a new equation with consideration to the smear and well-resistance effects on efficiency of vertical drains. He showed closed form solutions for two extreme cases for radial drainage-induced consolidation, the so-called “free strain” and “equal strain” and showed that the average consolidation obtained in both cases is approximately the same.

The equal vertical strain assumes that arching occurs in the upper layer during the consolidation process without any differential settlement in the clay layer between the immediate vicinity of the drain and the centre between the drains. In fact, the arching effect implies a more or less stable boundary at the surface of the soil layer being consolidated with vertical drains. This means that the vertical strain is uniform along the horizontal section of the soil. The free stain hypothesis on the other hand implies that the load is uniform over a circular zone of influence for each vertical drain and that the differential settlement occurring over this zone has no effect on the redistribution of stresses by an arching of the fill load.

Figure 5.13, shows a schematic illustration of a soil cylinder with a central vertical drain, where r_w is the radius of the drain, r_s is the radius of smear zone, R is the radius of soil cylinder and l is the length of the drain installed into soft ground.

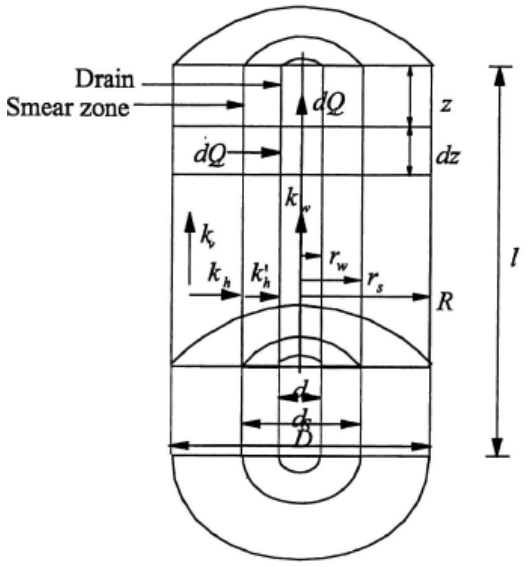

Figure 5.13 Schematic of soil cylinder with vertical drain (Hansbo, 1997)

Barron's (1948) analytical solution of the excess pore pressure for radial flow based on Rendulic's (1936) differential equation for an ideal drain is given by:

$$u_r = \frac{4\bar{u}}{D_e{}^2 F(n)}\left[R^2 \ln\left(\frac{r}{r_w}\right) - \frac{r^2 - r_w^2}{2}\right] \qquad \text{Eq. 5.21}$$

where:

D_e, is the diameter of soil cylinder, and the drain spacing factor, $F(n)$ is given by:

$$F(n) = \frac{n^2}{n^2 - 1}\ln(n) - \frac{3n^2 - 1}{4n^2} \qquad \text{Eq. 5.22}$$

where:

$n = R / r_w$, is drain spacing ratio

The average excess pore water pressure is given by:

$$\bar{u} = u_{av} = u_0 \exp\left(\frac{-8T_h}{F(n)}\right) \qquad \text{Eq. 5.23}$$

The average degree of consolidation, $\overline{U}_h$ in the soil body is given by:

$$\overline{U}_h = 1 - \exp\left(\frac{-8T_h}{F(n)}\right) \qquad \text{Eq. 5.24}$$

where, the time factor T_h is defined as:

$$T_h = \frac{c_h t}{D_e^{\,2}} \qquad \text{Eq. 5.25}$$

The coefficient of radial drainage consolidation; c_h is represented by:

$$c_h = \frac{k_h(1+e)}{a_v \gamma_w} \qquad \text{Eq. 5.26}$$

where:

γ_w, is unit weight of water, and a_v is the coefficient of compressibility of the soil, e is the void ratio, and k_h is the horizontal permeability of the soil.

5.11.1 Analysis with smear and well resistance

Hansbo (1981) presented an approximate solution for a vertical drain based on equal strain by taking both smear and well resistance into account. The average degree of consolidation $\overline{U}_r$ can be expressed as:

$$\overline{U}_r = 1 - \exp(-8T_h / \mu) \qquad \text{Eq. 5.27}$$

where:

$$\mu = \ln\left(\frac{n}{s}\right) + \left(\frac{k_h}{k_h^{'}}\right)\ln(s) - 0.75 + \pi z(2l - z)\frac{k_h}{q_w} \qquad \text{Eq. 5.28}$$

The effect of the smear zone only is given by:

$$\mu = \ln\left(\frac{n}{s}\right) + \left(\frac{k_h}{k_h^{'}}\right)\ln(s) - 0.75 \qquad \text{Eq. 5.29}$$

And the effect of well resistance only is given by:

$$\mu = \ln(n) - 0.75 + \pi z(2l - z)\frac{k_h}{q_w} \quad \text{Eq. 5.30}$$

If both smear and well resistance effects are ignored the above parameter becomes:

$$\mu = \ln(n) - 0.75 \quad \text{Eq. 5.31}$$

5.12 Simple 1-D modeling of PVD improved subsoil with horizontal drainage boundary

The normally used consolidation theory for designing prefabricated vertical drain (PVD) improvement is the 1-D unit cell solution which was considered by researchers and explained previously. Because the solutions in considering both vertical and horizontal drainage are complicated, commonplace solutions used in practice are those that ignore the effect of vertical drainage, such as Barron's and Hansbo's solutions. A simple approximate method for modeling PVD improved subsoil is suggested by Chai et al. (2001). Because PVD increases the mass permeability of subsoil in the vertical direction, it is deemed rational to establish a value for vertical permeability which approximately represents the effect of vertical drainage of natural soft ground and horizontal permeability toward the vertical drain. Under this condition, the sub-ground improved with a vertical drain can be analyzed in the same way as the unimproved ground. This equivalent vertical permeability (k_{ve}) was derived from an equal average degree of consolidation under the 1-D condition. To obtain a simple expression for k_{ve}, an approximate equation for consolidation in the vertical direction was suggested:

$$U_v = 1 - \exp(-C_d T_v) \quad \text{Eq. 5.32}$$

Where T_v is the time factor for vertical consolidation, and C_d =constant=3.54.

The equivalent vertical permeability, k_{ve}, can be presented as:

$$k_{ve} = \left(1 + \frac{2.5 l^2 k_h}{\mu D_e^2 k_v}\right) k_v \qquad \text{Eq. 5.33}$$

Where l is drain length (Figure 5.14), D_e the equivalent diameter of unit cell and:

$$\mu = \ln\left(\frac{n}{s}\right) + \frac{k_h}{k_s}\ln(s) - \frac{3}{4} + \frac{\pi 2 l^2 k_h}{3 q_w} \qquad \text{Eq. 5.34}$$

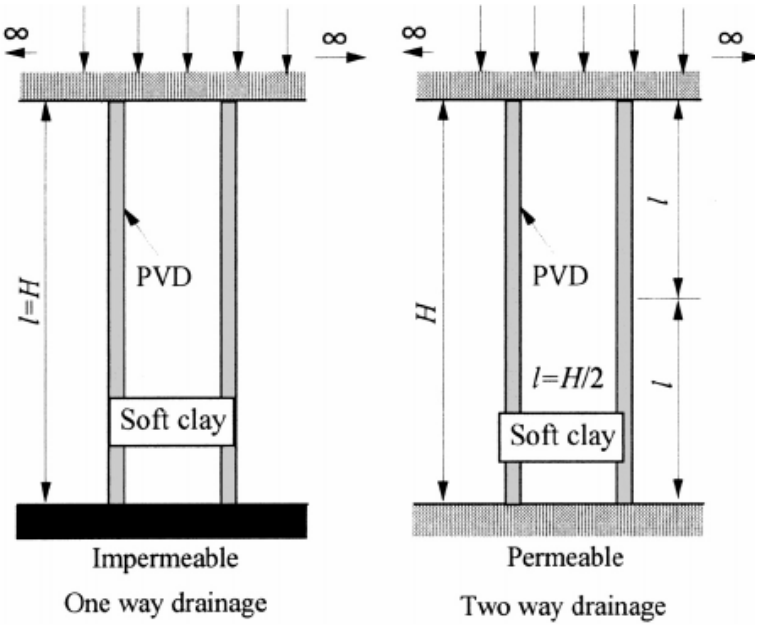

Figure 5.14 Schematic view of one or two way drainage conditions (Chai et al. 2001)

5.13 Assessment of ground settlement records

Due to uncertainty of boundary conditions, it is difficult to precisely estimate the ultimate settlement of the ground using laboratory test data. To remedy this problem Asaoka (1978) proposed a graphical procedure as one possible and practical way to predict the magnitude and rate of settlement of the ground under preloading. The steps in the graphical procedure are as follows:

1- The observed time-settlement curve plotted to an arithmetic scale is divided into equal time intervals, Δt for the constant load. It is common to take Δt between 30 and 100 days. The settlements $S_1, S_2 \ldots$ corresponding to the time $t_1, t_2, \ldots$ are read off and tabulated.

2- The settlement values $S_1, S_2 \ldots$ are plotted as points (S_{i-1}, S_i) ,for a best fit line, in the coordinate system with axes S_{i-1} and S_i, as shown in Figure15. The 45^0 line is also drawn to present $S_i = S_{i-1}$.

3- A strength line is fitted through the points; the point at which this line intersects the 45^0 line gives the final consolidation settlement, S_{100}.

It has to be mentioned that the longer the time interval is, the higher the accuracy of settlement prediction. Figure 5.15 shows a typical graphical illustration of Asaoka's method. Deviation from Asaoka's method may occur when the one-dimensional theory is not fully applied. This specific circumstance refers to consolidation due to immediate settlement and also secondary compression settlement as a result of creep.

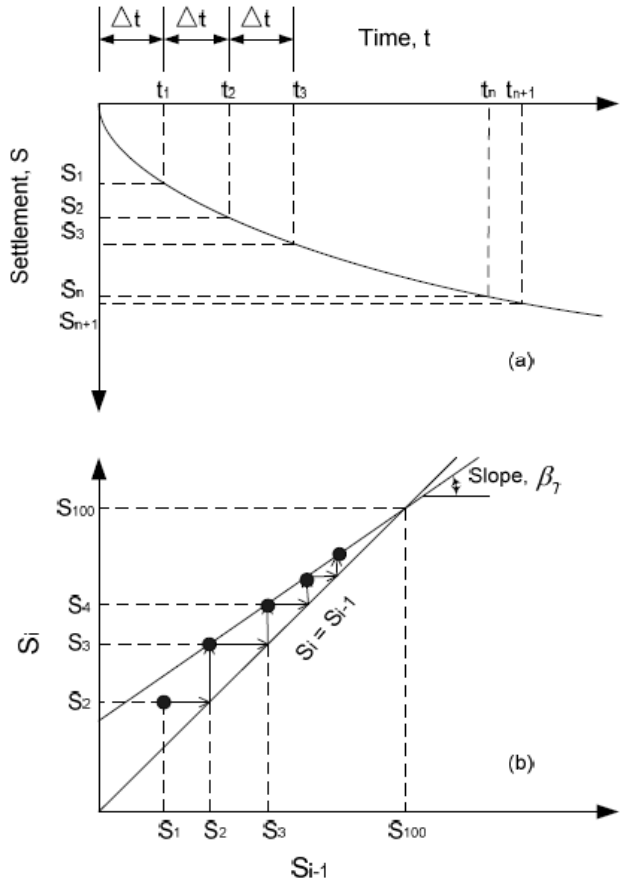

Figure 5.15 Graphical illustration of Asaoka's method

The values of coefficient of consolidation in both the horizontal and vertical direction can be obtained by using Asaoka's graphical method as follow:

For c_v (one-dimensional consolidation):

$$c_v = \frac{5}{12} h^2 \frac{\ln \beta_1}{\Delta t} \qquad \text{Eq. 5.35}$$

And for c_h (Radial flow with vertical drain):

$$c_h = \frac{F(n) \ln \beta_1}{8 \Delta t} \qquad \text{Eq. 5.36}$$

Where, β_1 is the slope of the settlement-time curve from Asaoka's method; Δt is the time interval in settlement-time curve.

5.14 Back-calculation of c_h values from pore pressure measurement

From the Hansbo (1979) equation, the following equation can be derived to estimate the coefficient of radial consolidation of a soft ground treated with prefabricated vertical drains (PVD).

$$1-\frac{\Delta u_t}{\Delta u_0}=1-\exp(-\alpha t) \qquad \text{Eq. 5.37}$$

$$\alpha=\frac{8c_h}{D_e} \qquad \text{Eq. 5.38}$$

where, Δu_0 is the excess pore pressure at reference time (t=0); Δu_t is the excess pore pressure at reference time t; D_e is the effective diameter of unit drain; α is the resistance factor for the effects of spacing, smear and well resistance.

Eq. 5.37 can also be written as:

$$\ln\left(\frac{\Delta u_0}{\Delta u_t}\right)=\alpha t \qquad \text{Eq. 5.39}$$

The values of α are therefore obtained as the slope of the plot of $\ln\left(\frac{\Delta u_0}{\Delta u_t}\right)$ versus time.

Now by having the value of α, c_h can be computed from Eq. 5.38.

5.15 Plane strain consolidation model

Most finite element analyses on preloading of soft ground treated with vertical drains are conducted based on the plane strain assumptions. However, this kind of analyses pose a problem as the consolidation around a vertical drain is axisymmetric. Hence, to employ a realistic 2-D finite element analysis for vertical drains, the equivalence between the plane

strain and axisymmetric analysis needs to be established. The matching of axisymmetric and plane strain conditions can be carried out in three ways:

1- Geometric matching approach, i.e. the spacing of the drains is matched while keeping the permeability the same.

2- Permeability matching approach i.e. permeability coefficient is matched while keeping the spacing of drains to be same.

3- Combination of permeability and geometric matching approach i.e. plane strain permeability is calculated for convenient drain spacing.

It should be mentioned that the conversion method which was adopted and employed in the constitutive model throughout the current research was permeability matching. Indraratna and Redana (1997) converted the vertical drain system into an equivalent parallel drain well by adjusting the coefficient of hydraulic conductivity of the soil and by assuming the plane strain cell to have a width of 2B as shown in Figure 5.16.

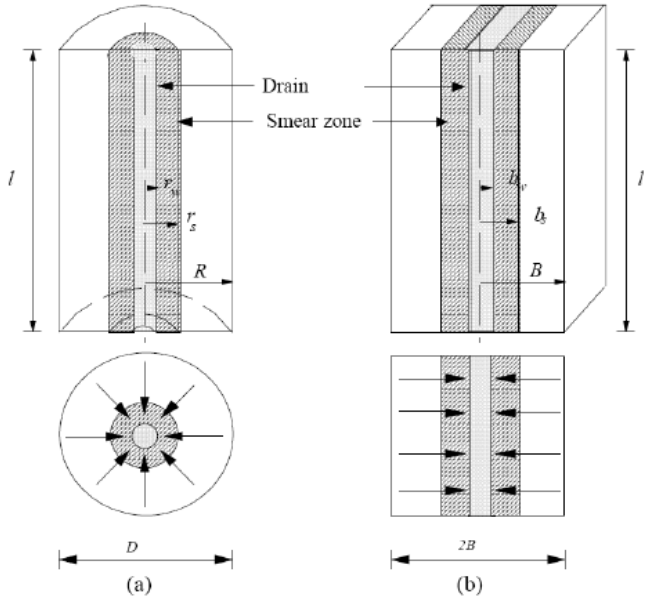

Figure 5.16 Conversion of an axisymmetric unit cell into plane strain condition (Indraratna and Redana, 1997)

The half width of drains b_w and half width of the smear zone b_s may be taken to be the same as their axisymmetric radii r_w and r_s respectively, which gives:

$$b_w = r_w \text{ and } b_s = r_s \qquad \text{Eq. 5.40}$$

The equivalent drain diameter (d_w) or radius (r_w) for band drains can be determined using equation 5.18 proposed by Rixner et al (1986).

Indraratna and Redana (1997) represented the average degree of consolidation in a plane strain condition as follows:

$$\overline{U}_{hp} = 1 - \frac{\overline{u}}{\overline{u}_0} = 1 - \exp\left(\frac{-8T_{hp}}{\mu_p}\right) \qquad \text{Eq. 5.41}$$

where, $\overline{u}_0$ = initial pore pressure; $\overline{u}$ = pore pressure at time t (average values); T_{hp} = time factor in plane strain.

And,

$$\mu_p = \left[\alpha + \beta\frac{k_{hp}}{k_{hp}^{'}} + \theta\left(2lz - z^2\right)\right] \qquad \text{Eq. 5.42}$$

where, k_{hp} and $k_{hp}^{'}$ are the undisturbed horizontal and corresponding smear zone permeability respectively. The geometric parameters α and β, and the flow term θ are given by:

$$\alpha = \frac{2}{3} - \frac{2b_s}{B}\left(1 - \frac{b_s}{B} + \frac{b_s^2}{3B^2}\right) \qquad \text{Eq. 5.43}$$

$$\beta = \frac{1}{B^2}(b_s - b_w)^2 + \frac{b_s}{3B^3}\left(3b_w^2 - b_s^2\right) \qquad \text{Eq. 5.44}$$

$$\theta = \frac{2k_{hp}^2}{k_{hp}^{'} q_z B}\left(1 - \frac{b_w}{B}\right) \qquad \text{Eq. 5.45}$$

where, q_z = discharge capacity of the equivalent plane strain.

At a given stress level and each time step, the average degree of consolidation for both equivalent plane strain and axisymmetric conditions are made the same, therefore:

$$\overline{U}_h = \overline{U}_{hp} \qquad \text{Eq. 5.46}$$

Now with combination of Eq. 5.27 and Eq. 5.41, the time factor ratio can be given by the following equation:

$$\frac{T_{hp}}{T_h} = \frac{k_{hp}}{k_h}\frac{R^2}{B^2} = \frac{\mu_p}{\mu} \qquad \text{Eq. 5.47}$$

By assuming the magnitudes of R and B to be the same (permeability matching approach), Eq. 5.47 can be rewritten as:

$$\frac{k_h\left[\alpha + \beta\frac{k_{hp}}{k_{hp}^{'}} + \theta\left(2lz - z^2\right)\right]}{\left[\ln\left(\frac{n}{s}\right) + \frac{k_h}{k_h^{'}}\ln(s) - 0.75 + \pi\left(2lz - z^2\right)\frac{k_h}{q_w}\right]} \qquad \text{Eq. 5.48}$$

If well resistance is ignored in Eq. 5.48 by omitting all terms containing l and z, the influence of the smear effect can be represented by the ratio of the smear zone permeability to the undisturbed permeability as follows:

$$\frac{k_{hp}^{'}}{k_{hp}} = \frac{\beta}{\frac{k_{hp}}{k_h}\left[\ln\left(\frac{n}{s}\right) + \frac{k_h}{k_h^{'}}\ln(s) - 0.75\right] - \alpha} \qquad \text{Eq. 5.49}$$

If both well resistance and smear effect are ignored, then the simplified ratio of plane strain to axisymmetric permeability is readily obtained (Hird et al., 1992):

$$\frac{k_{hp}}{k_h} = \frac{0.67}{\ln(n) - 0.75} \qquad \text{Eq. 5.50}$$

The well resistance is derived independently and yields an equivalent plane strain discharge capacity of drain (Hird et al, 1992):

$$q_z = \frac{2}{\pi B} q_w \qquad \text{Eq. 5.51}$$

5.16 Soft clay modeling

In order to predict the consolidation behavior of a soft reclamation layer subjected to preloading and treated with vertical drains, it is necessary to use an appropriate constitutive model, which represents the stress deformation response of the material. Deformation analysis in geotechnical engineering often assumes a linear elastic material in a small stress state. This hypothesis possibly holds true for overconsolidated clay, on the other hand, most soils exhibit plastic behavior at increased stresses. The theories of critical state soil mechanics have been developed based on the application of the theory of plasticity in the form of a Cam-clay model to represent the behavior of clay (Wood, 1991). The Cam-clay model has attracted wide acceptance due to its simplicity and accuracy to model clay behavior, especially for normally and lightly overconsolidated clay. In this model, the shear strength of the soil is related to the void ratio. To explain the state of soil during triaxial testing, the following critical state parameters are defined as:

$$p' = \frac{\sigma_1' + 2\sigma_3'}{3} = \frac{\sigma_1 + 2\sigma_3}{3} - u \qquad \text{Eq. 5.52}$$

and

$$q = \sigma_1' - \sigma_3' = \sigma_1 - \sigma_3 \qquad \text{Eq. 5.53}$$

where, $\sigma_1^{'}$ shows the effective vertical stress, $\sigma_3^{'}$ represents the effective confining stress and u is the pore water pressure.

According to critical state theory, the virgin compression, swelling and recompression lines are assumed to be straight lines in $\left(\ln p^{'} - v\right)$ plots with slopes of $-\lambda$ and $-k$ for compression and recompression lines respectively (see Figure 5.17).

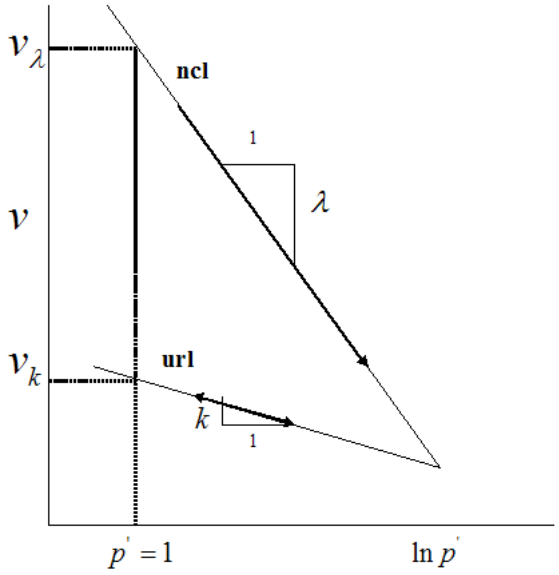

Figure 5.17 Isotropic normal consolidation line (NCL) plot in critical state theory

The isotropic virgin compression line or isotropic normal consolidation line (NCL) is presented by the equation below:

$$v = N - \lambda\left(\ln p^{'}\right) \qquad \text{Eq. 5.54}$$

where, N is the value of v when $\ln p^{'} = 0$ or $p^{'} = 1$.

The swelling or recompression line is expressed as:

$$v = v_K - k\left(\ln p^{'}\right) \qquad \text{Eq. 5.55}$$

where, v_k is the value of v when $\ln p^{'} = 0$ or $p^{'} = 1$.

The correlation between compression and recompression slope of $e - \log \sigma'$ plot with $v - \ln p'$ curve can be expressed as:

$$\lambda = \frac{Cc}{2.307} \qquad \text{Eq. 5.56}$$

$$k = \frac{Cr}{2.303} \qquad \text{Eq. 5.57}$$

The initial void ratio can be estimated at any given depth below the ground level. The $e - \ln p'$ plot is shown in figure 5.18. The parameter e_{cs} is defined as the void ratio on the critical state line for the value of $p' = 1$. The intersection between the swelling line and the in-situ stress line is assumed to be at point a and given by coordinates e_A and p'_A. Point P represents the intersection between the initial void ratio (e) and the effective mean normal stress (p'). The following relation may be established:

$$e_A = e_{cs} - \lambda \ln p'_A \qquad \text{Eq. 5.58}$$

where, $p_A = p'_c / 2.718$ for Cam-clay.

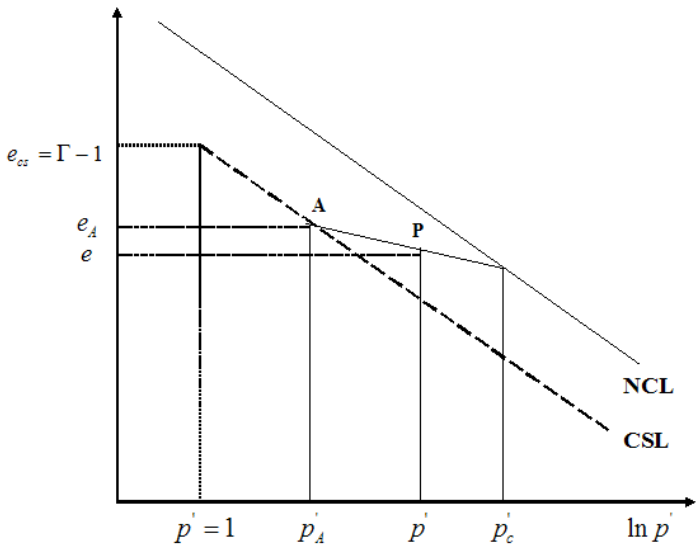

Figure 5.18 Position of the initial void ratio on critical state line

Along the swelling line passing through the initial stress state at point P, the following relation is applied:

$$e - e_A = k(\ln p' - \ln p'_A) \quad \text{Eq. 5.59}$$

Substituting e_A from Eq. 5.58 gives:

$$e_{cs} = e + (\lambda + k)\ln p'_A - k \ln p' \quad \text{Eq. 5.60}$$

5.17 Summary and conclusion

This chapter provides information about the principles of the surcharge preloading technique with vertical drains. The concept of aging and delayed consolidation of soft ground under a constant effective stress was presented in detail. It was found that with an application of surcharge which is defined as a temporary extra load beyond a final construction load, the post surcharge or post-construction secondary compression settlement decreases. The extent of the reduction in secondary compression however, depends on the surcharging effort which is defined as the effective surcharge ratio.

The mechanism of consolidation as a result of dissipation of excess pore water pressure due to the installation of vertical drains in the soft foundation was discussed. It was found that two factors, including the smear zone and well resistance, control the efficiency of vertical drains in terms of expelling the water from a particular system. The effect of smear however, may not be significant in fresh sediment as clay structure has been developed yet. According to the general theory of consolidation with horizontal drainage, for any given soil, the rate of consolidation is mostly governed by the diameter of influence zone of vertical drains. The larger the size of the diameter, the slower the ground reaches its ultimate consolidation. The current methods utilized in the prediction of a coefficient of consolidation based on settlement observation of ground over the course of time were discussed. It was realized that the graphical and pore pressure measurement methods are the most common techniques in back calculation of the coefficient of consolidation. The requirement for converting the axisymmetric vertical

drain to plain strain analysis was presented. Finally, the basic theory of stress-strain behavior of soft clays based on the critical state theory was briefly discussed.

As a conclusion it can be said that the salient aspects and concepts of surcharge preloading with a vertical drain presented in this chapter help the author to establish and orientate a laboratory test program to investigate the beneficial aspects of lime treatment on consolidation behavior of the dredged mud. The subsequent chapter presents the second round of experimental program conducted as part of this research study.

Chapter 6

Experimental Program-2

6.1 General

This chapter provides information about the second round of the laboratory test program undertaken on the natural and lime treated dredged mud. The effects of lime percentages up to LMO on both the primary consolidation and secondary compression behavior were evaluated by means of the oedometer test. The oedometer test is the basic method for determining the consolidation characteristics of fine grained soils. The oedometer tests conducted in this study followed a specific manner slightly different to that stated on the Australian Standard method AS1289. The alteration to the conventional test procedure was considered in order to produce test data to be appropriately discussed by means of the concept of the C_α/C_c ratio. The law of compressibility or C_α/C_c ratio was detailed in chapter 5 and is discussed further herein.

It can be said that the consolidation test is a model test in which a representative specimen of soil is subjected to pressure in order to help envisage the strain that would occur on a layer of soil under similar loading in the ground. A successful application of the test depends on how well the model test represents a real situation in nature. The loading and deformation in the conventional consolidation test, using the oedometer apparatus, is for example unidirectional. However, this simulation may not truly represent the situation in the field. It is not uncommon for a specimen 85 cm^3 in volume (Approximate value for the retaining ring with dimensions of 19 mm × 76 mm) to be used to represent the properties of soil mass of 850 m^3, a mass ten million times as great. Furthermore, in reclamation projects where dredged mud is discharged into a containment pond, a segregation of the materials is likely to occur across the pond. On the other hand, the specimens in the laboratory are expected to show uniform

characteristics as they are prepared and tested under controlled conditions in the laboratory. Thus, prediction of ground settlement by means of laboratory test data may not be quite sound. However, it should be noted that estimation of a ground's behavior utilizing the laboratory data is currently the only tool used worldwide.

6.2 Variables used in the settlement analyses of clay

In the consolidation progress of clayey soils, to obtain the required soil properties in terms of the stress-strain-time response, appropriate boundary conditions must be considered. It is almost commonplace to use effective stress as the independent variable, and search for stress-strain and stress-permeability correlations. Properties are conventionally defined in terms of the vertical effective stress and strain. Vertical effective stress is denoted by $\sigma_v^{'}$ which can be defined as follows:

$$\sigma_v^{'} = \sigma_v - u \qquad \text{Eq. 6.1}$$

where $\sigma_v^{'}$, σ_v, and u, are effective stress, total stress, and excess pore water pressure respectively.

Strain, ε, is conventionally defined in the usual engineering sense as $\Delta L / L_0$, where L_0 is the original height (length) and ΔL is the change of length with a positive value for compression.

The results of a one dimensional consolidation of clay may be plotted as a stress-strain curve on a natural scale, and have a local slope of m_v which is termed as the coefficient of volume compressibility where:

$$m_v = \Delta\varepsilon / \Delta\sigma_v^{'} \qquad \text{Eq. 6.2}$$

The definition of strain as $\frac{\Delta L}{L_0}$ apparently has not been favoured by many engineers and researchers. As an alternative, a different strain scale may be defined as:

$$\frac{\Delta e}{1+e_0} = \frac{\Delta L}{L_0} \qquad \text{Eq. 6.3}$$

where Δe is modified in the void ratio due to an increase of stress and defined as the strain of soil, and e_0 is the initial void ratio of the soil. It should be noted that the values of both ΔL and Δe are negative for compression or incremental loading phases. The revised stress-strain curves can be plotted to the natural $(\Delta e - \sigma_v^{'})$ or semi-logarithmic scale $(\Delta e - \log \sigma_v^{'})$. The stress-strain relationship presented on the natural scale demonstrates the local slope which is known as "coefficient of compressibility" and is denoted by a_v:

$$a_v = \frac{\Delta e}{\Delta \sigma_v^{'}} \qquad \text{Eq. 6.4}$$

Eq. 6.2 may now be written as:

$$m_v = \frac{a_v}{1 + e_0} \qquad \text{Eq. 6.5}$$

In the case when the stress-strain results are plotted on the semi-logarithmic scale, the local slope is defined as a compression or recompression index as shown below:

$$C_r \text{ or } C_c = \frac{\Delta e}{\log \frac{\sigma_2^{'}}{\sigma_1^{'}}} \qquad \text{Eq. 6.6}$$

The coefficient of consolidation (c_v) is the soil parameter that governs the rate of consolidation. The value of c_v depends on the permeability (k) and the compressibility of the soil skeleton (m_v) and is given by:

$$c_v = \frac{k}{m_v \gamma_w} \qquad \text{Eq. 6.7}$$

where γ_w is the unit weight of water.

In a laboratory oedometer test, for a given load increment on a clay specimen, there are two commonly used graphical methods for determining the coefficient of consolidation. One is the logarithm-of-time method proposed by Casagrande and Fadum (1940) and the

other is the square-root-of-time method proposed by Taylor (1942). Both methods usually do not provide the same values of c_v. However, if the shapes of the laboratory time curves were exactly comparable to the theoretical shape, Casagrande's and Taylor's methods would result in the same value of c_v.

Secondary compression is a volume change under load that takes place at constant effective stress. The secondary compression index, C_α, can be defined in a similar way to that of determination of the compression index, except that the parameter is now related to time instead of pressure. The secondary compression index can be obtained by means of the Casagrande graphical method and is given by:

$$C_\alpha = \frac{\Delta e}{\Delta \log t} \qquad \text{Eq. 6.8}$$

where Δe is the change in void ratio over any elapsed time interval, Δt, in the secondary compression zone beyond the time for cessation of primary consolidation.

6.3 Sample preparation for the oedometer test

In chapter 4 the seepage induced consolidation test setup was explained. The primary aim of performing that laboratory test was to identify the lime modification optimum of the dredged mud. The second round of the seepage induced consolidation test with an equivalent quantity of lime added (0-4%), and following the same procedure, is performed here. However, once the consolidation process under seepage flow is concluded, the test assembly is dismantled and the residual compressed samples in the mould are used as specimens for use in the oedometer test. The advantage of this technique is that the moisture content of the slurry sample gradually reduces as water flows through, and the sample remains fully saturated. It is well known that saturation of a clay sample is necessary to ensure validity of Darcy's law and applicability of the general theory of clay consolidation. Furthermore, as water flows, any possible presence of excess Ca^{2+} and OH^- ions are removed from the particulate system. The removal of the possible presence of excess ions is essential in order to prevent creation of high alkaline

soil pore chemistry and formation of pozzolanic products. This is because the primary aim of the research is to investigate the modification and not solidification affect of lime on compressibility characteristics of clay. The procedure was as follows:

A slurry sample was poured into the permeability mold. Sufficient time was given to the slurry to partially undergo its self-weight consolidation in order to achieve the re-sedimentation structure. This condition lasted for approximately 24 hours before placing the top cap on the mold and connecting it to the water reservoir for consolidation purposes. The water flow was allowed to continually pass through the specimen for one day. Following, the top cap of the mold was temporarily removed and a perforated disk was placed of the top of the dredged mud sample. The seepage consolidation process was resumed again and allowed to run for another 24 hours. The water reservoir in upstream was placed in a level to induce the seepage force of about 10 kPa. Once consolidation of the sample in the permeability mould under constant flow of water was completed, the water supply was disconnected and the top cap of the mould was removed. At this stage a light surcharge load was placed on the perforated disk to apply 2 kPa pressure on the specimen in the mould (Figure 6.1).

Figure 6.1 Preparation and recovering of a sample for oedometer test

This kind of loading caused further consolidation and helped the specimen to reach a consistency suitable for recovery of the sample for the oedometer test. The mould was then turned inverted and 76 diameter and 19 mm height retaining ring was pushed carefully into the bottom of the sediment to extract the undisturbed oedometer sample (Figure 6.1). Once the sample was obtained it was trimmed and covered with semi-wet filter paper and glass plates on both the top and base. Masses of the combined specimen, retaining ring, filter papers and glass plates were then recorded. The excess mud remaining as a result of treatment of the sample in the ring was then collected for determination of the initial moisture content of the specimen. By using the net weight of the specimen, initial moisture content and specific gravity, the initial void ratio of the specimen was calculated.

The retaining ring containing the dredged mud specimen was then placed on the saturated porous plate, both of which were carefully placed in the oedometer cell. On completion of this stage, it was then feasible to assemble the cell by placing the saturated top porous plate/load cap on the specimen and fill the cell with water. The cell was then placed in the loading frame (Figure 6.2). At this stage the top arm or hanger of the loading frame was balanced by means of the sliding mass. After balancing the hanger, the digital dial gauge of the apparatus was set to zero to present the starting value. The apparatus was now ready and the test could be initiated.

6.4 Data logger system

The MUX-10F (Mitutoyo) is an advanced data acquisition unit, capable of scanning analogue channels hundreds of times a second. The system was used in combination with the PC using the menu driven software. The data logger interface was in steady communication with the digital dial gauge, keeping up to date with any change in specimen thickness as the dial's gauge sensor traveled downward or upward. An interface to a PC-Host program (PRECISION DAQ & CONTROL) allows the user to control the operation of the logger unit. The system recorded the time and date when the logging

process started. This information appears in the final documentation of results. Compiled data can be recalled for further analysis with a spreadsheet.

Figure 6.2 Oedometer Apparatus with data acquisition unit

6.5 Consolidation test program

The experimental program that deals with the conventional oedometer test and described hereafter comprises two different series of tests that were performed on remoulded samples of the dredged mud. In the first series, the primary and secondary consolidation parameters of the natural and lime treated dredged mud were investigated in the compression range. The compression range is also defined as the normally consolidated state in which the clayey soil has not previously experienced pressure higher than the

current sustained stress. In the additional test program, the primary and secondary parameters were evaluated when the samples were standing in a recompression or artificial overconsolidated state. During this phase, the samples were first compressed in the oedometer under certain values of applied pressure. The initial load was then removed and the consolidation parameters were evaluated with an implication of a smaller load on overconsolidated samples.

6.5.1 The test procedure and results in NC state

A total number of 20 incremental loading one-dimensional consolidation tests were conducted on resettled dredged mud without and with varying percentages of lime. Unless otherwise stated, the test procedure accorded with Australian Standard AS 1289.6.1.1. Samples were loaded in a series of increments, from 10 kPa to 640 kPa, where each load was twice that of the preceding load, with a load increment ratio (LIR) of unity. Preliminary consolidation tests revealed that with an increase in the percentages of lime, the elapsed time to reach the end of primary consolidation becomes shorter. Hence, to maintain equivalent conditions between the different samples, successive loads were applied after the end of primary consolidation (EOP). For this purpose, the data acquisition unit of PRECISION DAQ & CONTROL was employed to continuously monitor the deformation against time. As data were gradually compiled on an individual Notepad file on a computer, the file was regularly copied and pasted to a pre-developed spreadsheet. The spreadsheet helped to produce a settlement-log time plot in accord with Casagrande's t_{50} approach in order to determine the time when EOP is achieved. According to this technique, the end of primary consolidation (more than 95%) is assumed to have been reached when a nonlinear transition zone between the primary and secondary phase travels most of its distance. At this point, the successive load increment was added.

- **Coefficient of consolidation**

Upon completion of each single load increment, the log time-settlement curve was utilized to evaluate the coefficient of consolidation. Based on this method, the time associated with 50% of deformation is measured (t_{50}) and the following equation is employed to calculate the c_v:

$$c_v = \frac{0.026\overline{H}^2}{t_{50}} \qquad \text{Eq. 6.9}$$

where, c_v is the coefficient of consolidation in square meters per year, t_{50} is time elapsed at 50% consolidation in minutes, $\overline{H}$ is average thickness of specimen for the load increment, in millimeters.

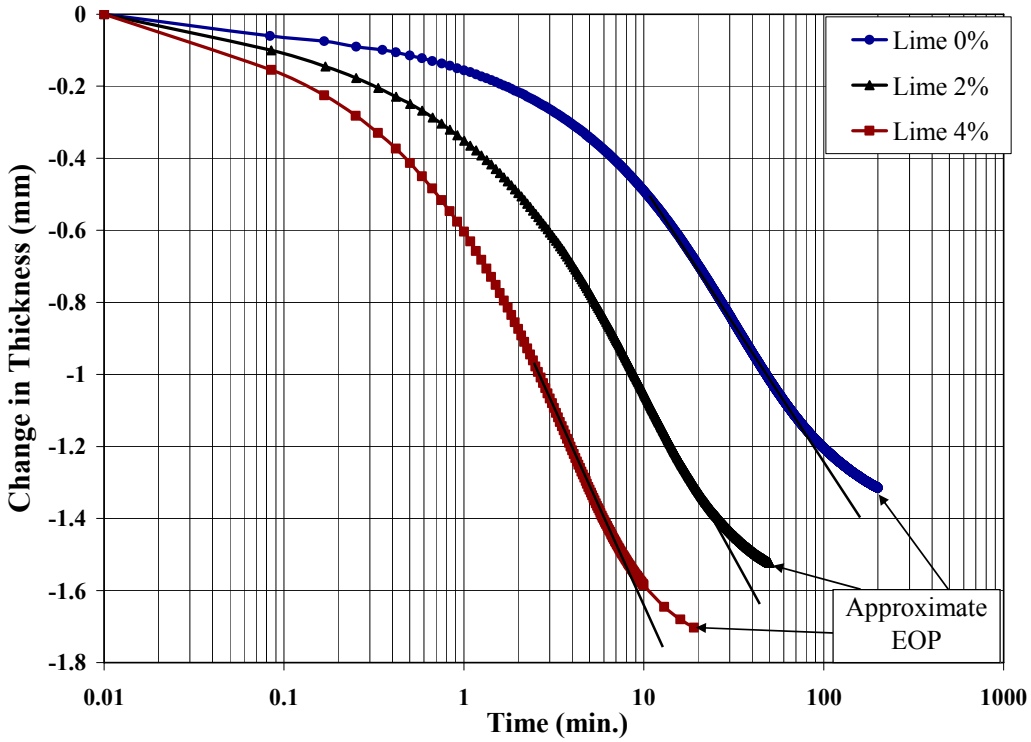

Figure 6.3 Rapid-loading approach adapted in this study

The above equation shows that for a given mean thickness of specimen, as time decreases, results in the value of c_v increases. It is interesting to note that with increasing lime content, the samples required less time to reach the end of primary consolidation,

resulting in an increase in the coefficient of consolidation. This improvement in c_v was observed in all load increments and has been presented in Figure 6.4.

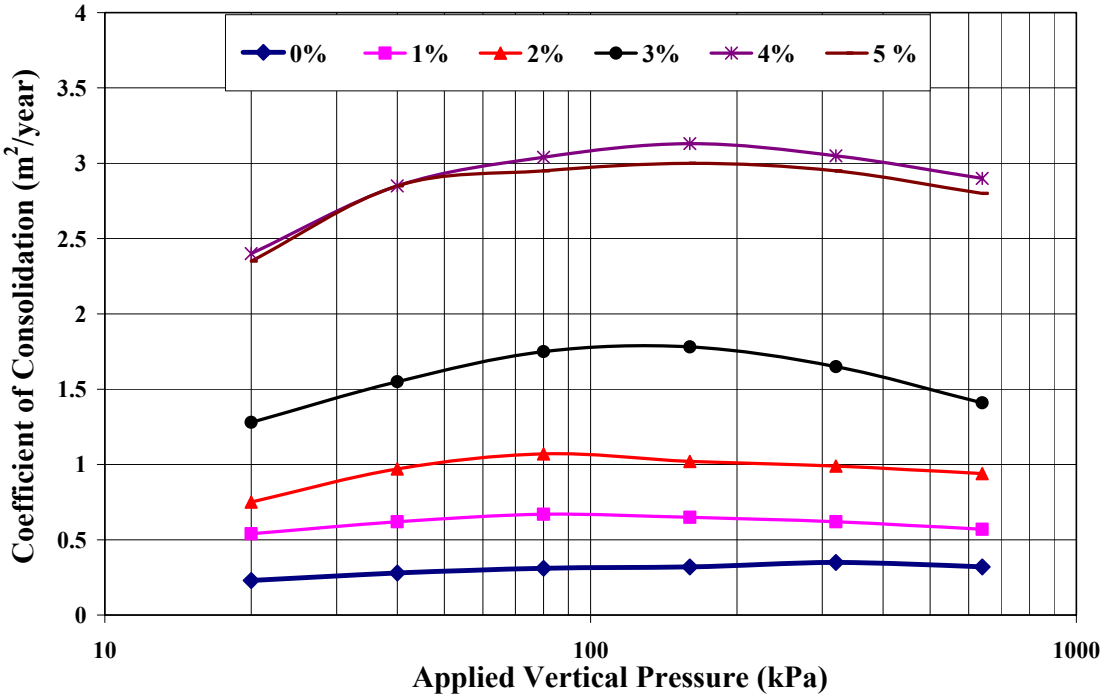

Figure 6.4 Variation in coefficient of consolidation with % lime

The results show that when the lime content increases from 0 to 4%, the average value of c_v increases considerably, by an order of magnitude, from the average of 0.3 to $3.0\,m^2/year$. This figure indicates the coefficient of consolidation for the sample containing 5 % of lime is almost equal to that of 4 % lime. This finding, together with other results obtained during the permeability test program, indicating that 4 percent of lime must be considered as LMO for the dredged mud sample used in this research. Hence, to avoid complexity, the following tests are limited to the samples which were treated with up to 4 % lime.

- **Primary consolidation settlement**

The data obtained from the above test procedure are presented to display the relationship between void ratio and applied vertical pressure (Figure 6.5). The rapid loading

procedure of the oedometer test adopted throughout this study helps to produce the virgin e-log pressure curve. This curve presents the correlation between applied pressure and corresponding void ratio at the end of primary consolidation (EOP). Figure 6.5 shows that the initial void ratio increases with % lime, and under all values of applied vertical pressure, the material with a higher percentage of lime exhibits a higher void ratio. Figure 6.5, shows the initial void ratio of the specimens defined at the instigation of the tests where the top cap was placed on the specimens in the retaining ring. The apparent preconsolidation pressure at around 10 kPa is attributed to the sample preparation in the permeability mould in which seepage induced force, approximately 10 kPa in magnitude, was applied to compress and consolidate the slurry samples. The consistency of the all specimens allows the initial load to increase from 1 to 10 kPa. An observation of Figure 6.5 suggests that that compression index, $C_c (= \frac{\Delta e}{\Delta \log \sigma_v^{'}})$, of the mud is not constant and is higher in samples containing more percentages of lime, indicating the additional compressibility characteristics of lime treated dredged mud.

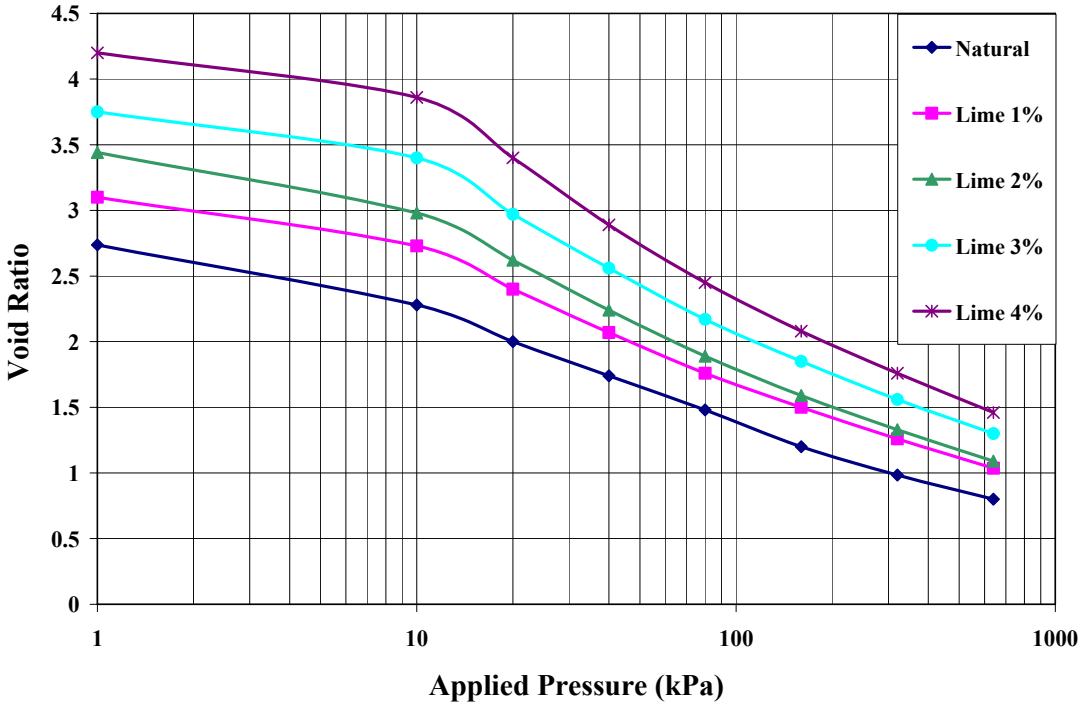

Figure 6.5 Effect of % lime on $e - \log \sigma_v^{'}$ curves

Figure 6.6 presents the variation of the compression index of the natural and lime treated dredged mud with various percentages of lime for the range of applied pressure from 10 to 640 kPa. It can be observed that the compression index increases from 0.82 to 1.33 as % lime increases from 0 to 4% respectively. The compression index plays a significant role in controlling the magnitude of ground settlement when it is subjected to an external load. This means that for any given of thickness of stratum, with an increase in the compression index, the extent of primary consolidation will increase. However, it should be considered that with addition of lime to the dredged mud, the void ratio is also increased. The settlement of the ground under application of external load and in compression range of compressibility is given by:

$$S_t = \frac{C_c}{1+e_0} H \log \frac{\sigma'_{v0} + \Delta\sigma'_v}{\sigma_{v0}} \qquad \text{Eq. 6.10}$$

According to this equation, for any given thickness of the clay stratum, with increasing % lime, both the void ratio and compression index increase. Hence the ratio of $\frac{C_c}{1+e_0}$ may increase or even remain constant (see Table 6.1). As a conclusion, it can be said that with increasing the lime content into the dredged mud, for a given thickness of dredged deposit, due to application of the external load, the settlement of the soft ground may slightly increase or even remain constant. It is important to note that the initial state of void ratio, e_0, in Table 6.1 was arbitrarily chosen at 10 kPa applied pressure.

Table 6.1 The relationship between C_c and $(1+e_0)$ obtained from Figure 6.5

% Lime	C_c	$(1+e_0)$ @ 10 kPa	$\frac{C_c}{1+e_0}$
0	0.82	3.28	0.25
1	0.94	3.73	0.25
2	1.05	3.98	0.26
3	1.16	4.4	0.27
4	1.33	4.86	0.28

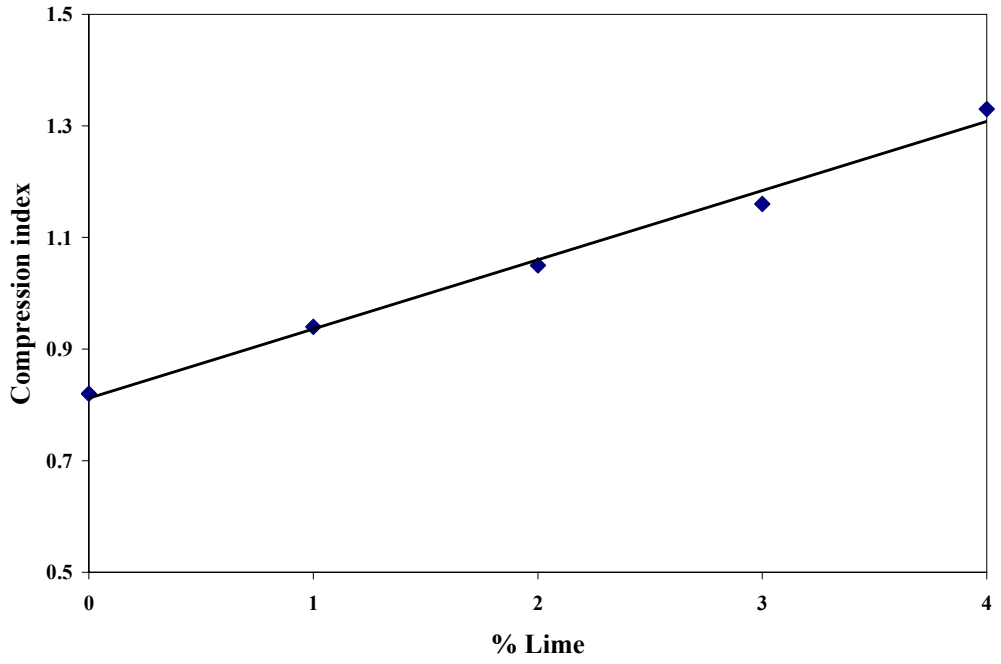

Figure 6.6 Variation of Compression index with % lime (10-640 kPa applied pressure)

- **Coefficient of volume compressibility**

Figure 6.7 presents the variation of coefficient of volume compressibility of the dredged mud with effective stress and % lime. It can be seen that for the all specimens, the values

of coefficient of volume compressibility lies in a narrow band in all states of effective stresses. This finding shows that even though addition of lime gradually increases, void ratio and the coefficient of consolidation of dredged mud indicates no significant effect on the coefficient of volume compressibility as % lime increases.

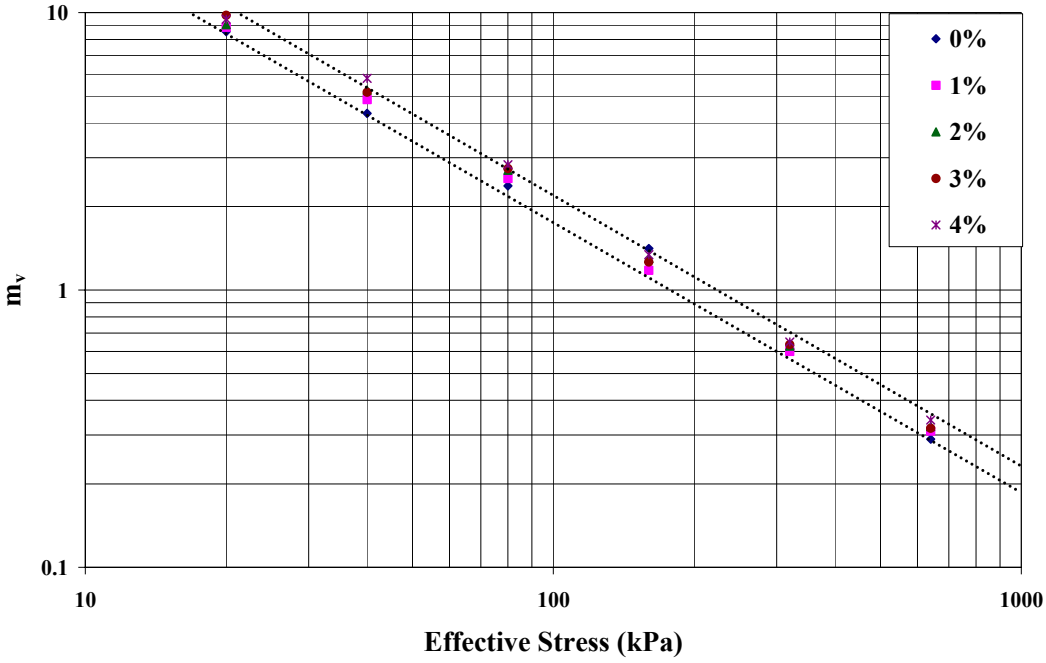

Figure 6.7 Variation of coefficient of volume compressibility with the effective stress and % lime

- **Coefficient of permeability**

Earlier in this chapter, it was shown that the coefficient of consolidation is proportional to the coefficient of permeability and is inversely proportional to the coefficient of volume compressibility, i.e. $c_v = \frac{k}{m_v \gamma_w}$. Hence, the values of the coefficient of permeability can be simply obtained by multiplying the values of the coefficient of consolidation and coefficient of volume compressibility together with the unit weight of water. Figure 6.8

illustrates the values of the coefficient of permeability of the natural and lime treated dredged mud obtained empirically using the above equation for the range of effective stress from 20 kPa to 640 kPa. This figure illustrates that for any state of effective stress, with increasing % lime, the permeability increases. Figure 6.9 presents the variation of permeability with void ratio for various specimens. This figure suggests that with increasing void ratio, the permeability of the clay soil increases. This figure suggests that for any void ratio, the value of permeability is almost constant and only slightly increases as % lime increases.

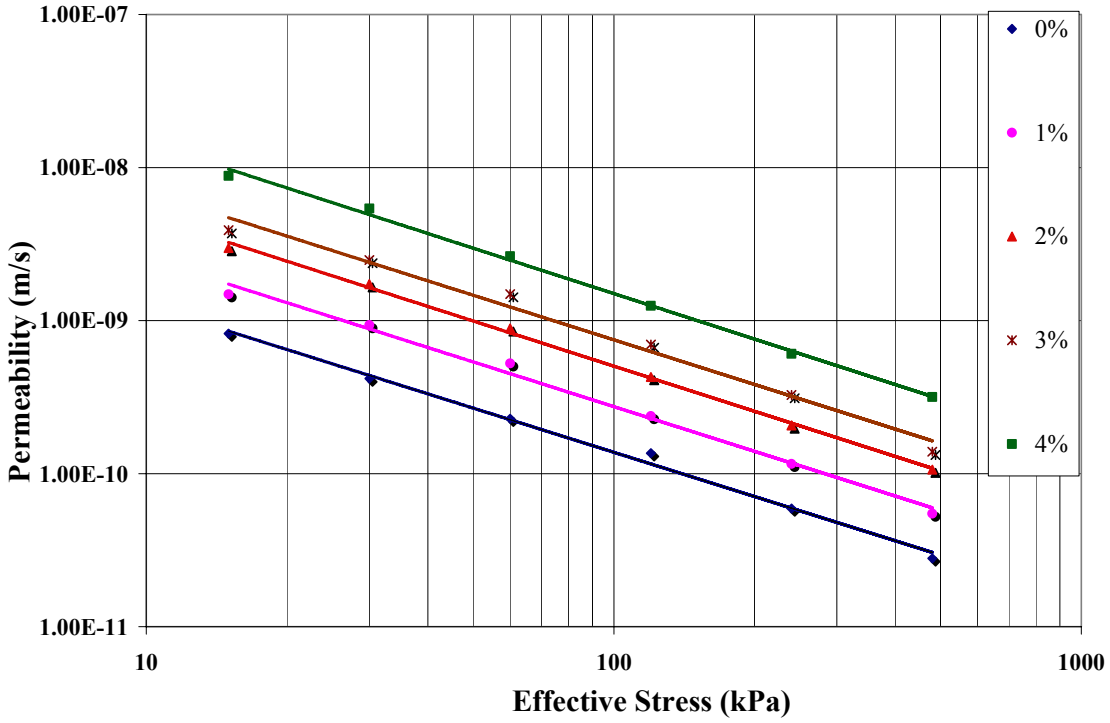

Figure 6.8 Variation of Coefficient of permeability with the effective stress and % lime

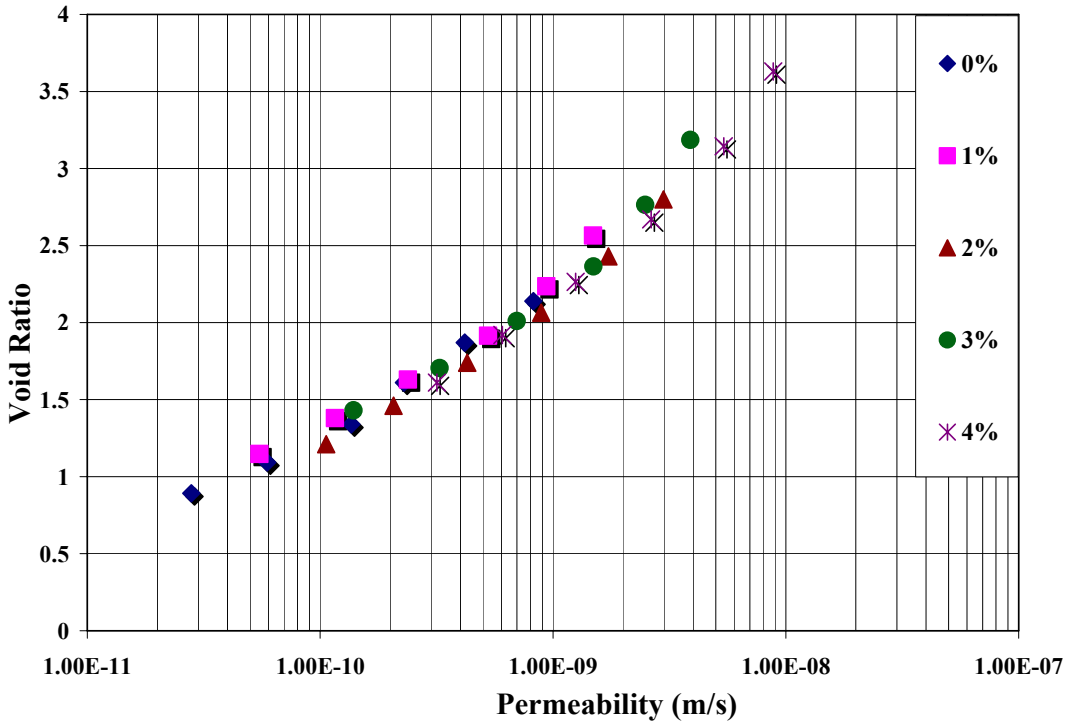

Figure 6.9 Variation of permeability with void ratio for different lime-treated samples

Previously in chapter 4 it was revealed that with an increase in the % lime the fabric or orientation of the particle changes. It was discussed that as a result of the alteration in the clay fabric both the void ratio and permeability increase. According to the data (Figure 6.9), for the overlapping range where the void ratio of the various specimens lie in the vicinity of each other, the permeability values slightly increase as % lime increases. This behavior may be explained by the theory of isotropy and anisotropy of the clay soil and is evaluated and broadly discussed later in this chapter.

- **Secondary Compression**

To evaluate the secondary consolidation behavior of the dredged mud in the compression range, a series of tests were conducted on successive load increments from 10 to 80 kPa in the samples containing varying the amounts of lime. Each pressure increment remained to the end of primary consolidation before the next increment was applied.

However, under a vertical compressive stress of 80kPa, the tests were allowed to continue beyond 100% of primary consolidation in order to evaluate the deformation of clayey samples in the secondary phase (Figure 6.10).

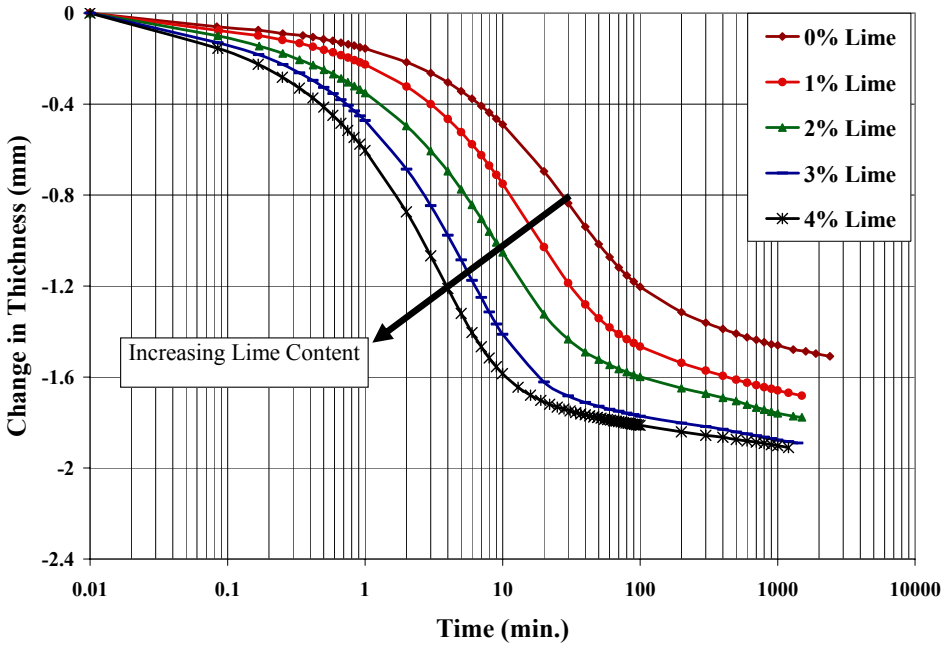

Figure 6.10 Primary consolidation and secondary compression behavior of the dredged mud with varying amount of the lime under 80 kPa applied pressure

During this experimental program, the secondary compression index was calculated as follows: $C_\alpha = \frac{\Delta e}{\Delta \log t}$ where, C_α is the secondary compression index and, Δe is change in void ratio per one log cycle time in the secondary phase.

Figure 6.11 illustrates the change in C_α together with C_c as % lime increases. The test results show that the slope of secondary segment of consolidation curves $(e - \log t)$, defined as the secondary compression index, is about 0.04 for dredged mud containing 0, 1 percent lime, and reduced to 0.035 at 2% lime, further decreasing to an average value of 0.026 for mud containing 3% with a little fluctuation at 4% lime. It can be seen from

Figure 6.11 that the values of the compression index, C_c, in the range of applied pressure from 10 kPa to 80 kPa, drastically increased from 0.83 to 1.44 as % lime increases from 0 to 4.

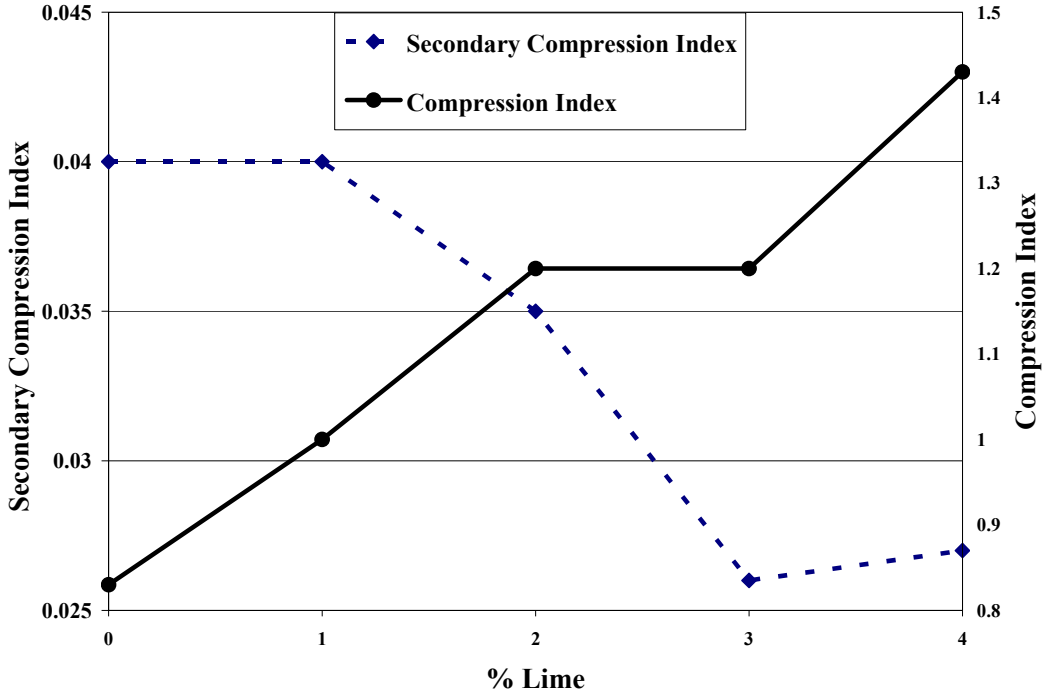

Figure 6.11 Variation of the secondary compression index and compression index with % lime at effective pressure increment from 40 - 80kPa

Figure 6.12 presents the variation of the secondary compression index together with time associated to the end of primary consolidation at 80 kPa. It is shown that time for EOP gradually decreases with % lime and its period reduced to one tenth as lime content increased from zero to four percent. Figure 6.12 also suggests that time for EOP has no negative impact on the secondary compression index in terms of increasing this parameter.

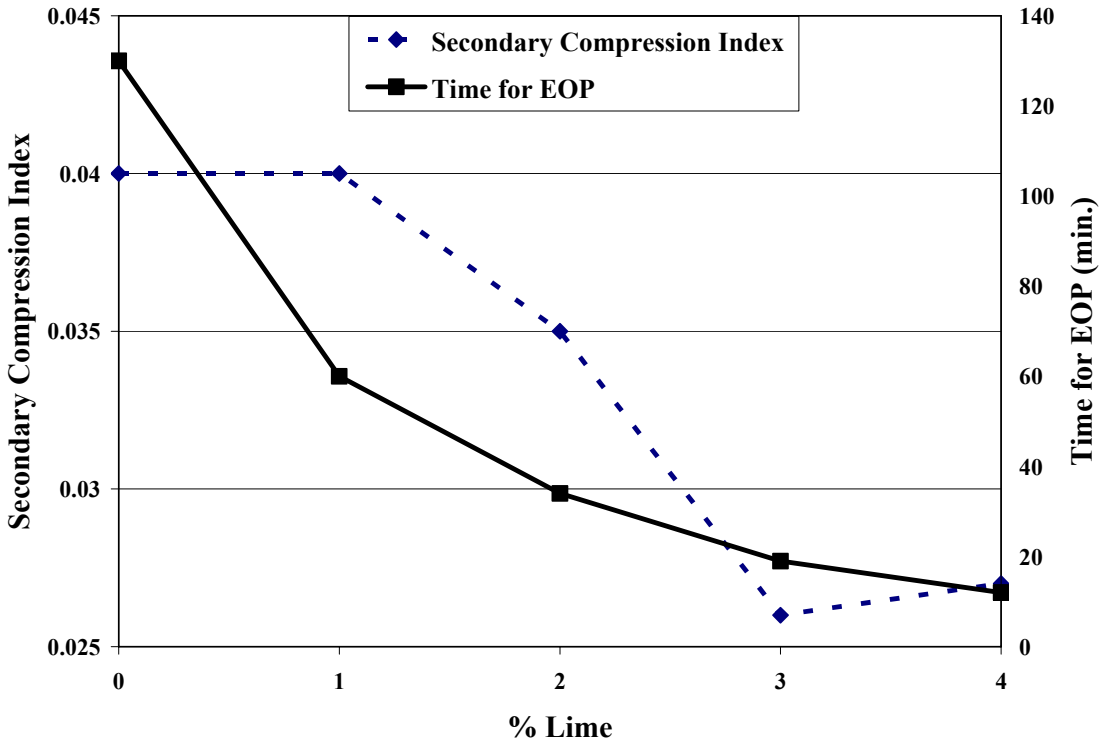

Figure 6.12 Variation of the secondary compression index and time for EOP consolidation with % lime at effective pressure increment from 40- 80 kPa

It is believed that for any one soil there is a constant ratio between the secondary compression index and compression index, C_α / C_c, (Mesri and Godlewski 1977; Mesri and Castro 1987; Mesri et al. 1997). On the basis of the C_α / C_c approach, for the range of applied pressure, if C_c increases, decreases, or remains constant, the corresponding C_α, increases, decreases or remains constant with time. It can be concluded that in a normally consolidated state, as soil exhibits a higher value of C_c, a greater value of C_α is achieved. Figure 6.13 presents the variation of C_α/C_c against percentages of lime. It was found that as the lime content increased, the value of C_α/C_c decreased from the initial value of 0.046 at natural dredged mud to 0.02 at modified dredged mud treated with 4 % lime. This figure indicates that as mud is treated with lime, for the same value of applied pressure, the value of C_α / C_c, is not constant and gradually decreases with increasing % lime.

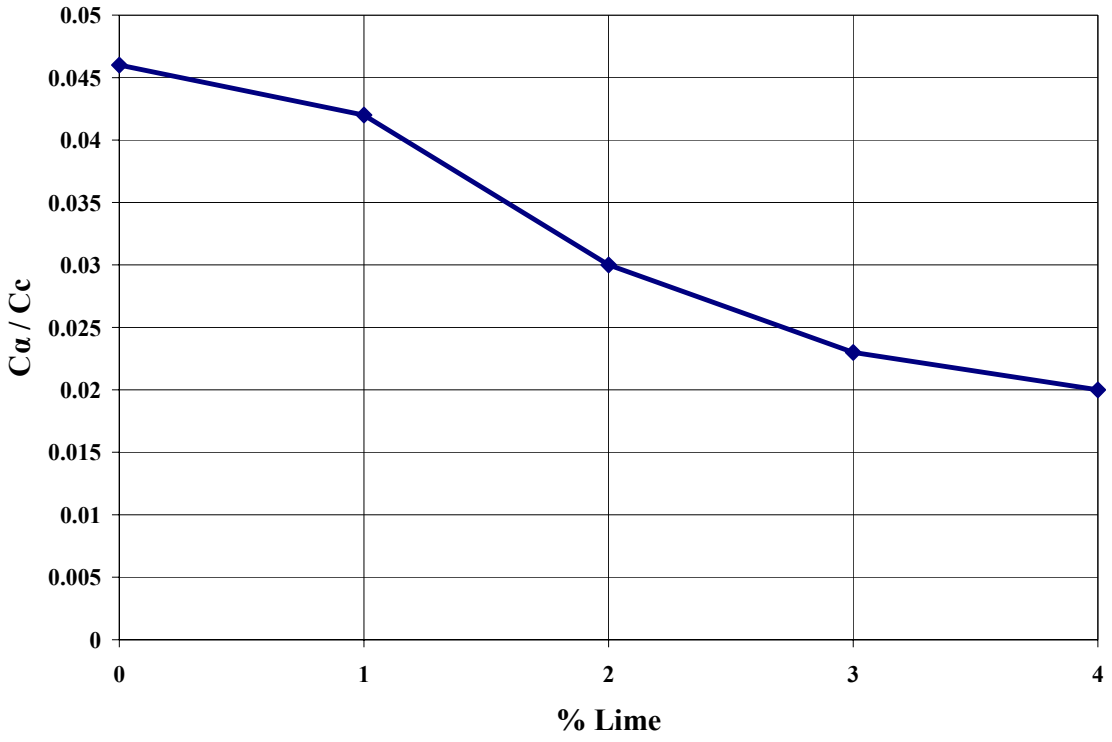

Figure 6.13 Variation of C_α / C_c with % lime at effective pressure increment from 40- 80 kPa

As a summary of the general consolidation behavior of the natural and lime treated dredged mud in a compression range, the following details are outlined:

- The coefficient of consolidation drastically increases with increasing % lime
- The addition of lime into the dredged mud increases the compression index resulting in more compressibility with increasing lime.
- As lime content increases, the secondary compression index gradually decreases.

The significant increase of the coefficient of consolidation in a vertical direction is likely attributed to the change in natural clay fabric. It is known that substitution of monovalent ions (sodium or potassium) by divalent ion (calcium), artificially introduced into a soil,

results in several changes in the soil system (van Olphen 1962). The replacement of calcium ion on the clay surface decreases the interparticle repulsive forces between soil plates, and brings about flocculation (Sridharan and Prakash 1999b). Under the natural condition of sediments, the dispersed arrangement of particles resists water flow in a vertical direction; however, the newly gained flocculated structure, as a result of edge to face particle arrangement, increases the pore volume (Townsend and Kylm 1966) and provides a better channel flow for water to expel vertically.

This change in clay fabric due to the new particle arrangement and flocculation also explains the higher void ratio and compressibility of lime treated dredged mud in comparison to natural sediment.

The reason for producing Figure 6.12 is to provide a comparison between consolidation behaviors of lime treated dredged mud with other highly compressible materials such as peat. In peat, the significant primary consolidation settlement occurs in a very short time followed by a substantial amount of secondary consolidation settlement (Mesri et al. 1997). Whereas in lime treated dredged mud, the rate of primary consolidation increases with % lime while the rate of secondary consolidation settlement decreases.

The test results demonstrate that the value of C_α / C_c of the natural dredged mud remains within a narrow range of 0.04 ± 0.01 which is valid for the majority of inorganic clays (Mesri and Godlewski 1977). However, further reduction of this ratio with increasing % lime is likely attributed to the action of lime in the flocculation and agglomeration of clay particles (Feng, 2002).

- **Empirical relationship for coefficient of consolidation, C_v**

The results obtained from the oedometer test program suggest that with increasing lime percentages, both the void ratio and coefficient of consolidation increase. It was also found that with increasing lime percentage, the coefficient of volume compressibility remains almost constant. The consistency in the coefficient of volume compressibility implied that addition of lime into a dredged mud solely brings about an increase in the soil permeability. In fact, the change in permeability is responsible for the change in the

coefficient of consolidation. Intuitively, in an attempt to find a useful empirical correlation between the changed parameters, the coefficient of consolidation is plotted against the void ratio corresponding to EOP under specific order (Figure 6.14). In Figure 6.14, each regression line is fitted through the points of void ratio and coefficient of consolidation for the five specimens (0, 1, 2, 3, and 4% lime) corresponding to similar effective stress. As shown, six regression lines are plotted for various effective stresses (i.e. 20, 40, 80, 160, 320, and 640 kPa). The general form of the logarithmic regression line is defined as:

$$e = a\ln(c_v) + b \qquad \text{Eq. 6.11}$$

where a and b are empirical coefficients.

For instance, the uppermost line graph presents the void ratio and coefficient of consolidation that achieved at 20 kPa in the five different specimens. This kind of presentation is repeated for the other values of the effective stress up to 640 kPa accordingly.

Figure 6.14 shows that for the void ratio vs coefficient of consolidation, logarithmic regression line provides the best fit for all states of effective stresses. Table 6.2 shows the values of the empirical coefficients together with R-squared values for the six regression lines.

The variations of “a” and “b” with effective applied pressures are presented in Figure 6.15.

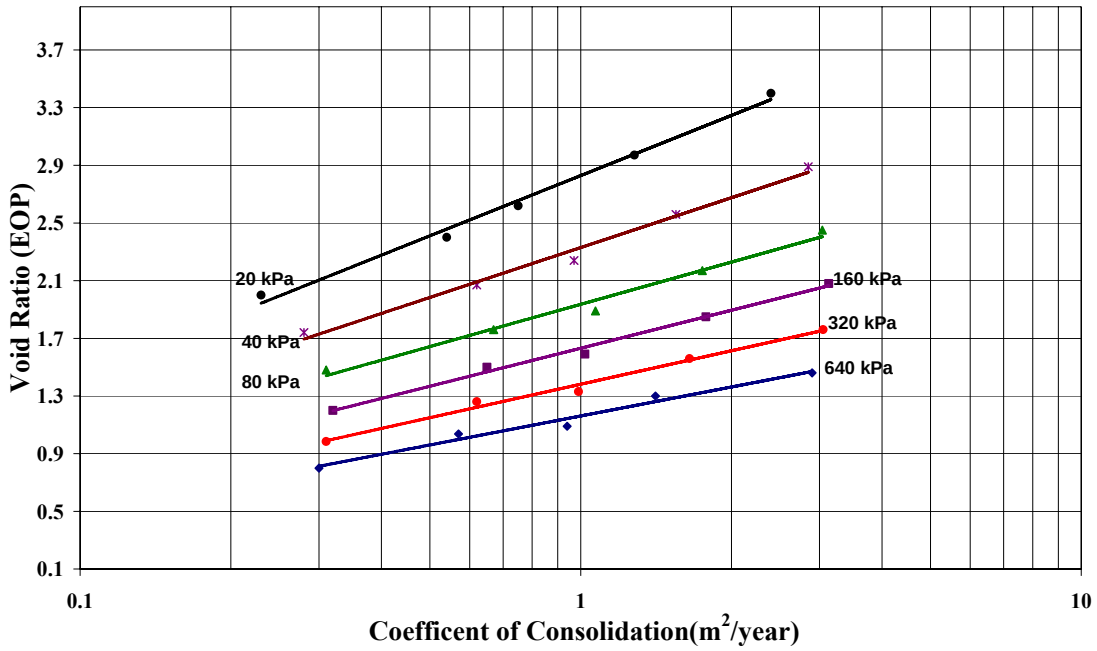

Figure 6.14 Relationship between e vs c_v for various specimens

Table 6.2 Empirical coefficients and R-squared values of figure 6.15

Pressure (kPa)	a	b	R^2
20	0.602	2.83	0.99
40	0.499	2.33	0.99
80	0.422	1.94	0.98
160	0.380	1.63	0.99
320	0.335	1.38	0.99
640	0.290	1.16	0.98

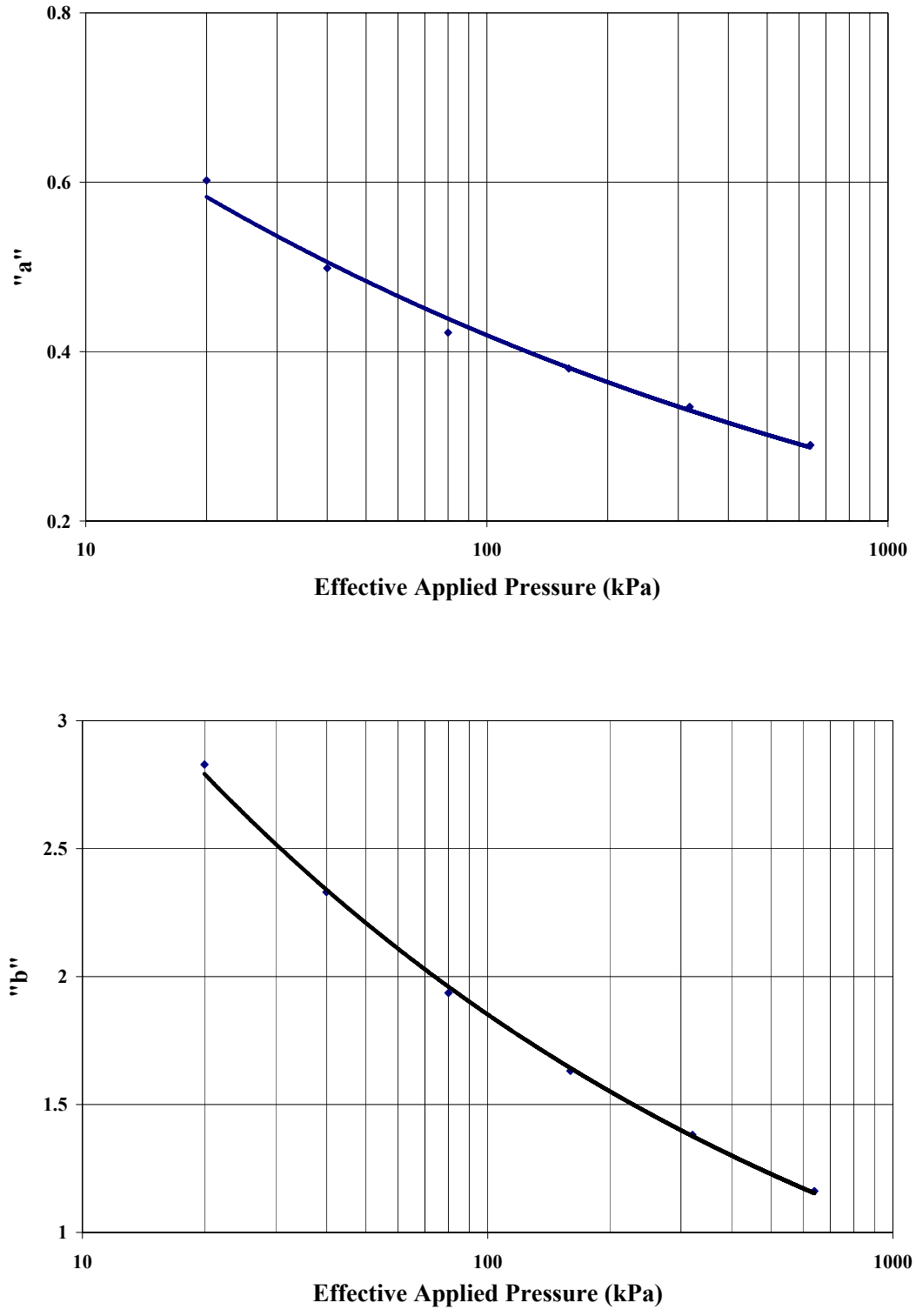

Figure 6.15 Variation of "a" (top), and "b" (bottom), with effective applied pressures

The regression line associated with $a - \log \sigma_v^{'}$ suggests the following power equation:

$$a = 1.0749(\sigma_v^{'})^{-0.2044} \text{ and } R^2 = 0.99 \quad \text{Eq. 6.12}$$

The regression line corresponding to $b - \log \sigma_v^{'}$ suggests the power equation as:

$$b = 5.9953(\sigma_v^{'})^{-0.2551} \text{ and } R^2 = 0.99 \quad \text{Eq. 6.13}$$

The values of empirical coefficients obtained by Eq. 6.12 and Eq. 6.13 can be replaced on the Eq. 6.11. Thus:

$$e = 1.0749(\sigma_v^{'})^{-0.2044} \ln(c_v) + 5.9953(\sigma_v^{'})^{-0.2551} \quad \text{Eq. 6.14}$$

Eq. 6.14 may now be rewritten in the form of exponential equation as:

$$c_v = \exp^{\frac{(e - 6.0\sigma_v^{'-0.25}) \times \sigma_v^{'0.20}}{1.075}} \quad \text{Eq. 6.15}$$

Previously it was explained that the Eq. 6.15 was derived using the values of void ratio corresponding to the end of primary consolidation together with the values of coefficient of consolidation. Hence, this equation holds true, once for any load increment the maximum effective vertical pressure is obtained (i.e. at EOP). In attempt to evaluate the applicability of Eq. 6.15 in any instance when the primary consolidation is still in progress, the following approach is proposed:

The $e - \log t$ curve of the three specimens that were treated with 0, 1 and 4 percent of lime and consolidated under different effective applied pressures are randomly selected and shown in figures 6.16, 6.17 and 6.18 respectively. The load increment for the specimens containing 0, 1 and 4 % lime are 12.5 to 25 kPa, 40 to 80 kPa, and 80 to 160 kPa respectively.

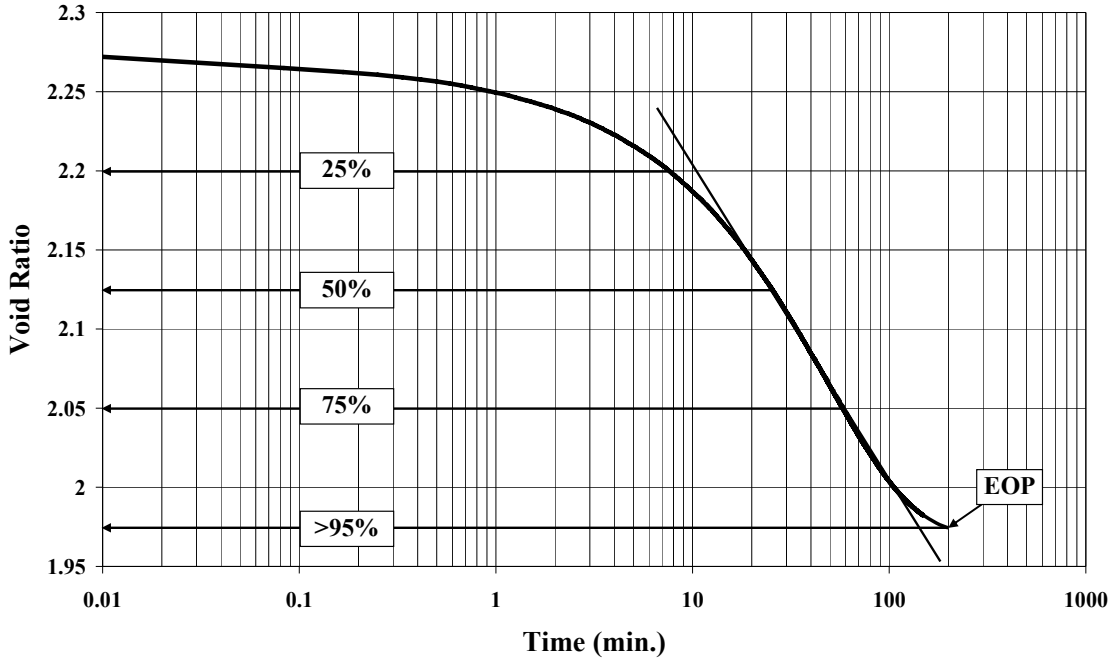

Figure 6.16 Void ratio vs log-time curve at 25 kPa for the treated specimen (0% lime)

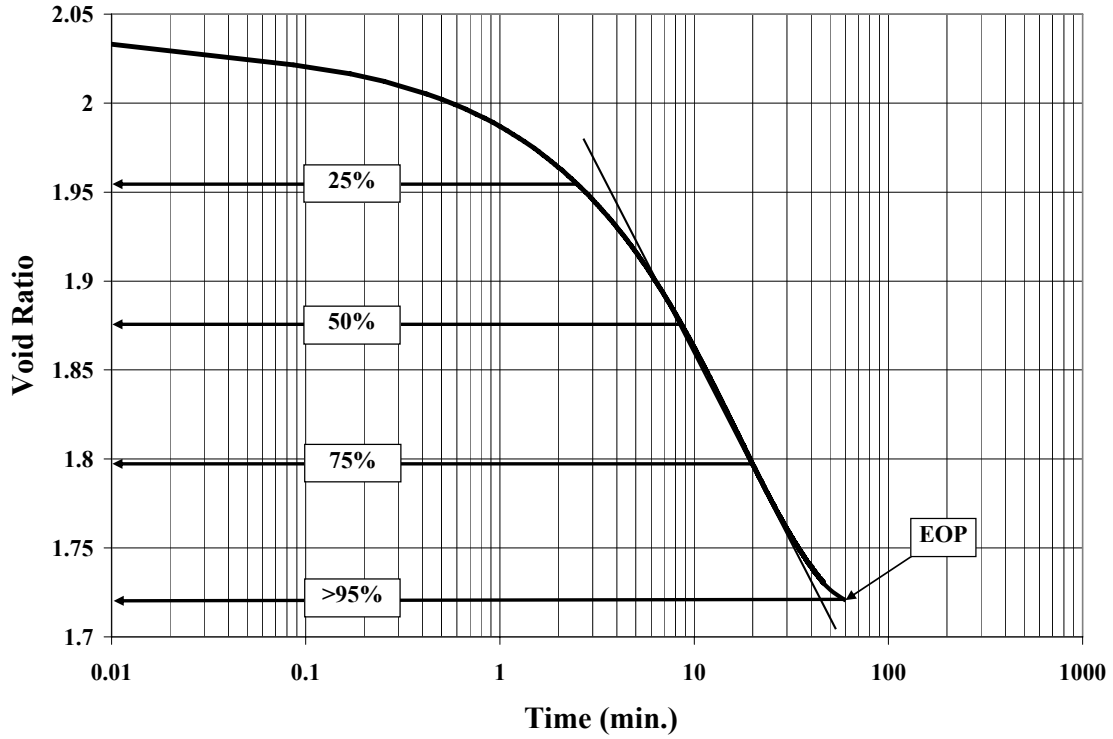

Figure 6.17 Void ratio vs log-time curve at 80 kPa for the treated specimen (1% lime)

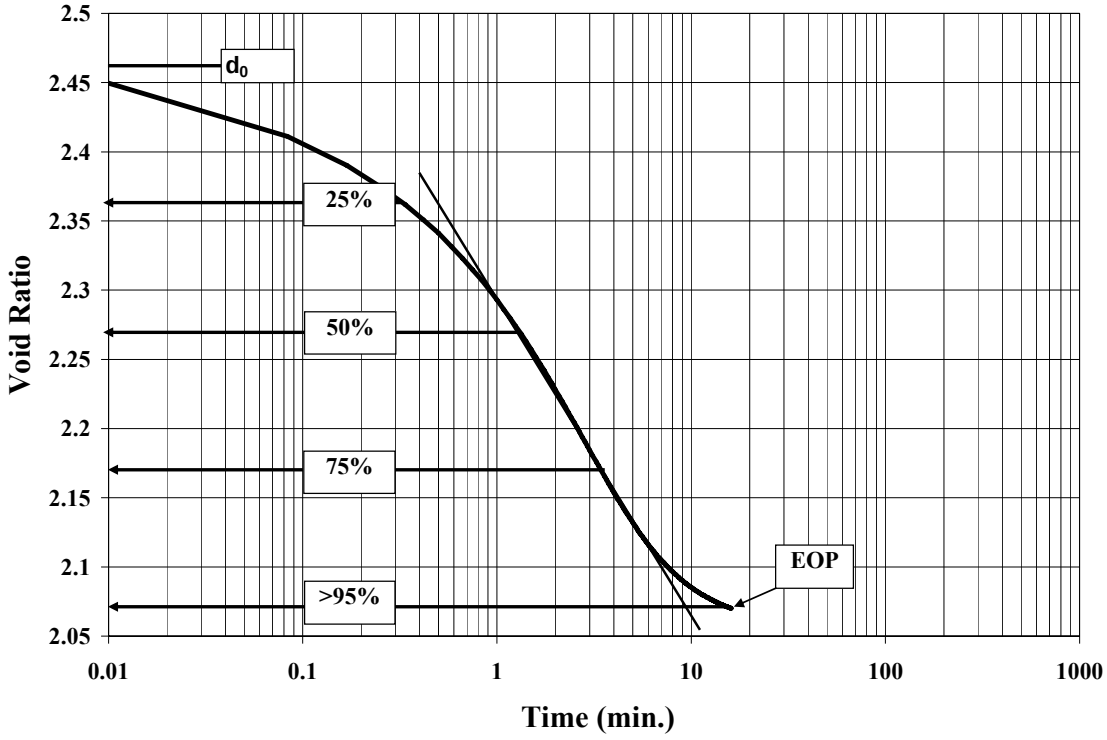

Figure 6.18 Void ratio vs log-time curve at 160 kPa for the treated specimen (4% lime)

In the three cases, the total deformation of the materials (i.e. reduction in void ratio) is considered between the theoretical zero point denoted by d_0 (usually lies on elapsed time of 0.01 minute), to the time for the end of primary consolidation as is indicated. The total reduction is then divided into the four equal segments to represent the state of void ratios at 25, 50, 75, and >95% of consolidation of the specimen. The values of effective applied pressure were then calculated accordingly. For example, in the case of the specimen with 1% lime, the load increment takes place from 40 to 80 kPa. For the instance when the specimen experiences 25% of its total consolidation, the actual effective stress is defined as:

$$\sigma_v^{'} = (\sigma_v \times 0.25) + \sigma_{v0}^{'}$$

where σ_v is the increase in total pressure for the specific load increment.

Thus,

$$\sigma_v^{'} = (40 \times 0.25) + 40 = 50kPa$$

Table 6.3 summarized the values of void ratio and effective applied pressure for the four instances during the consolidation process of the two specimens. This table also presents the calculated values of coefficient of consolidation which are obtained using Eq. 6.15.

Table 6.3 Coefficient of consolidation values at different stages of consolidation

Specimen- Stage of Consolidation	Void ratio	Effective Stress kPa	c_v m^2/year
0% lime @ 25%	2.2	15.63	0.28
0% lime @ 50%	2.125	18.75	0.30
0% lime @ 75%	2.05	21.88	0.31
0% lime @ 95%	1.98	25	0.31
1% lime @ 25%	1.953	50	0.59
1% lime @ 50%	1.875	60	0.60
1% lime @ 75%	1.798	70	0.60
1% lime @ 95%	1.720	80	0.55
4% lime @ 25%	2.36	100	3.36
4% lime @ 50%	2.27	120	3.38
4% lime @ 75%	2.17	140	3.33
4% lime @ 95%	2.07	160	3.08

Table 6.3 suggests that for any single specimen, the estimated values of the coefficient of consolidation in four stages are in good agreement with each other. A slight discrepancy observed between the data obtained from various stages of consolidation of the single

specimen is likely attributed to the degree of precision of the method by which the oedometer test program was controlled. As explained previously, the oedometer samples were loaded in a series of increments where the successive loads were applied after the end of primary consolidation (EOP). The end of primary consolidation is associated with the total dissipation of excess pore water pressure which is developed into a sample as a result of the application of external loading. In the case when the new load increment is initiated before allowing the full dissipation of excess pore water pressure corresponding to a former load, on a few occasions the new state of excess pore water pressure is higher than the total applied pressure. This fact indicates that utmost care must be taken once Casagrande's graphical method is used as a tool to perform the oedometer test in the rapid loading manner.

As a conclusion it can be noted that for the type of the dredged mud used in this study, the empirical relationship - that proposed by Eq. 6.15 - can be used as a reliable tool in the estimation of coefficient of consolidation at any instance of the consolidation process. At any moment, the state of void ratio and effective applied pressure (i.e. $\sigma_v - u$) are the sole input data required for the above equation.

6.5.2 The test procedure and results in OC state

A total number of 18 samples of the dredged mud treated with 0, 2 and 4 percent of lime and a limited number of samples with 1 and 3% lime were tested to investigate the primary and secondary consolidation behaviors under different surcharging efforts. As discussed in chapter 5, surcharging effort is quantified by the effective surcharge ratio (Mesri and Feng, 1991) as follows:

$$R_s^{'} = \frac{\sigma_{vs}^{'}}{\sigma_{vf}^{'}} - 1$$

where $\sigma_{vs}^{'}$ is the maximum effective vertical stress achieved before removal of surcharge, and $\sigma_{vf}^{'}$ is the ultimate effective stress after removal of surcharge. In this experimental

setup, the different samples were first loaded in successive load increments up to 80 kPa, 100 kPa, or 120 kPa (σ'_{vs}). Upon completion of primary consolidation (EOP), the pressure was reduced to 20 kPa. For all series of tests, a 24 hour period was given to the samples to rebound under 20 kPa of applied pressure. Once a state of equilibrium was achieved, another extra 40 kPa was added, representing the final pressure (σ'_{vf}) of 60 kPa. Initial consolidation of samples to σ'_{vs} of 80 kPa, 100 kPa, and 120 kPa reflected the effective surcharge ratio of 0.33, 0.66 and 1 respectively. It should be noted that the above manner of loading- unloading- reloading was chosen to simulate the conceptual reclamation site where the final design load (e.g. 40 kPa) was applied after removal of the surcharge.

The secondary compression index corresponding to the artificial overconsolidated state due to the application of surcharge is denoted as C'_{α}, which has the same meaning as C_{α}. Some reports in the literature show that the value of C'_{α} is significantly larger if the final design load is close to the preconsolidation pressure (Mesri et al. 1997; Mesri et al. 2001), Therefore, with an increase in the surcharge effort, the post construction secondary consolidation settlement accordingly reduces.

Figures 6.19, and 6.20 show the primary and secondary consolidation settlement of samples with varying amounts of lime with effective surcharge ratios of 0.66 and 0.33 respectively. Both figures 6.19, and 6.20 display that the rate of primary consolidation settlement in the OC state increases as % lime increases. This behavior is similar to the consolidation behavior observed in the NC state. It was also found that in spite of the NC range where the magnitude of primary consolidation increases with % lime, in the OC state, with increasing % lime, the primary consolidation settlement decreases. The effect of % lime on the recompression index of natural and lime treated dredged mud is presented in Figure 6.21. This figure shows that the recompression index gradually decreases with increasing % lime from 0.1 to 0.038 for natural and 4% lime respectively.

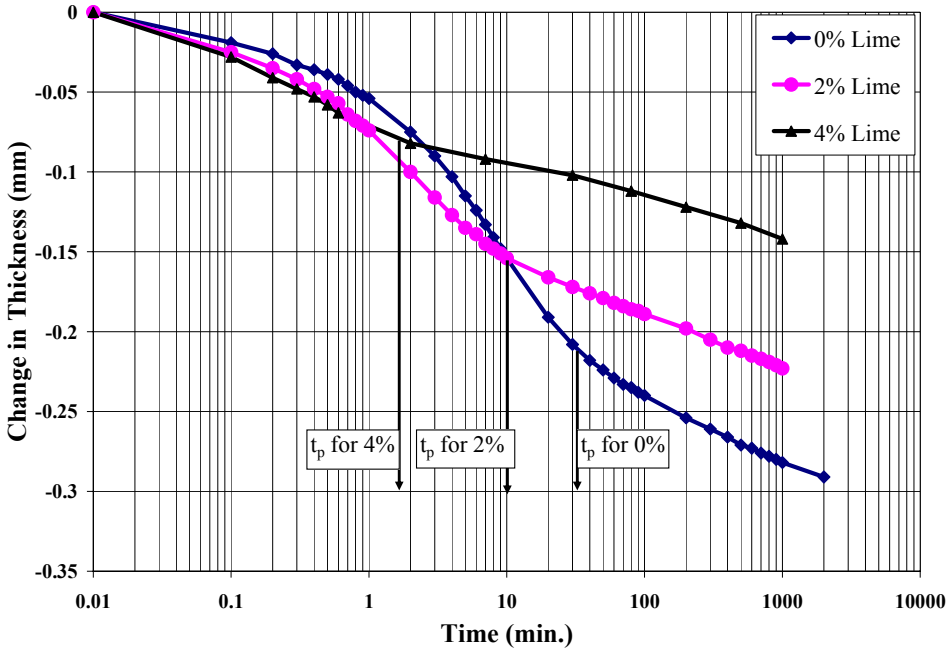

Figure 6.19 Variation of primary consolidation and secondary compression settlement with % lime after the effective surcharge ratio of 0.66

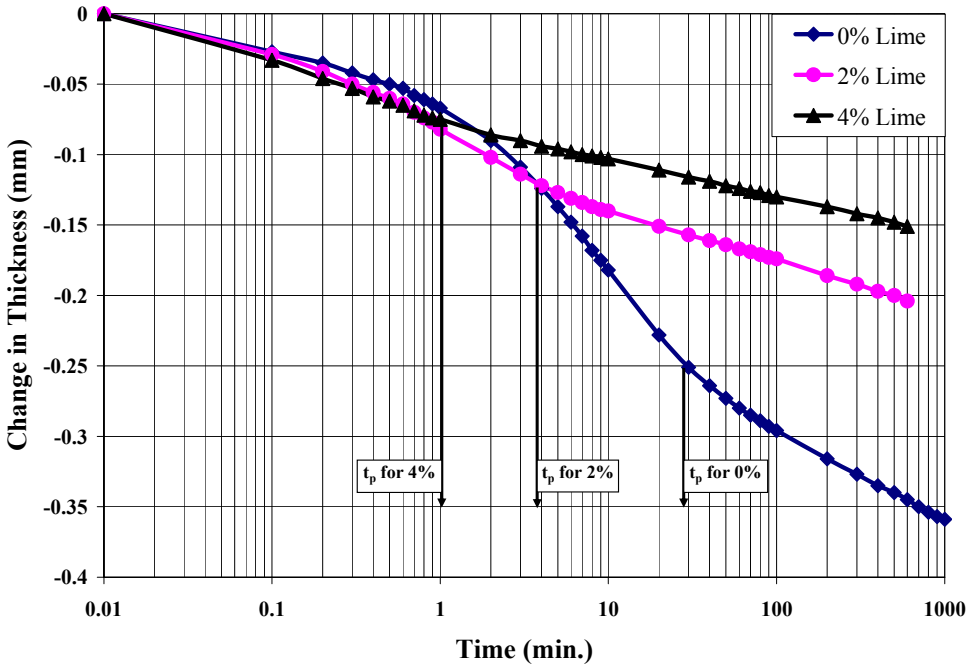

Figure 6.20 Variation of primary consolidation and secondary compression settlement with % lime after the effective surcharge ratio of 0.33

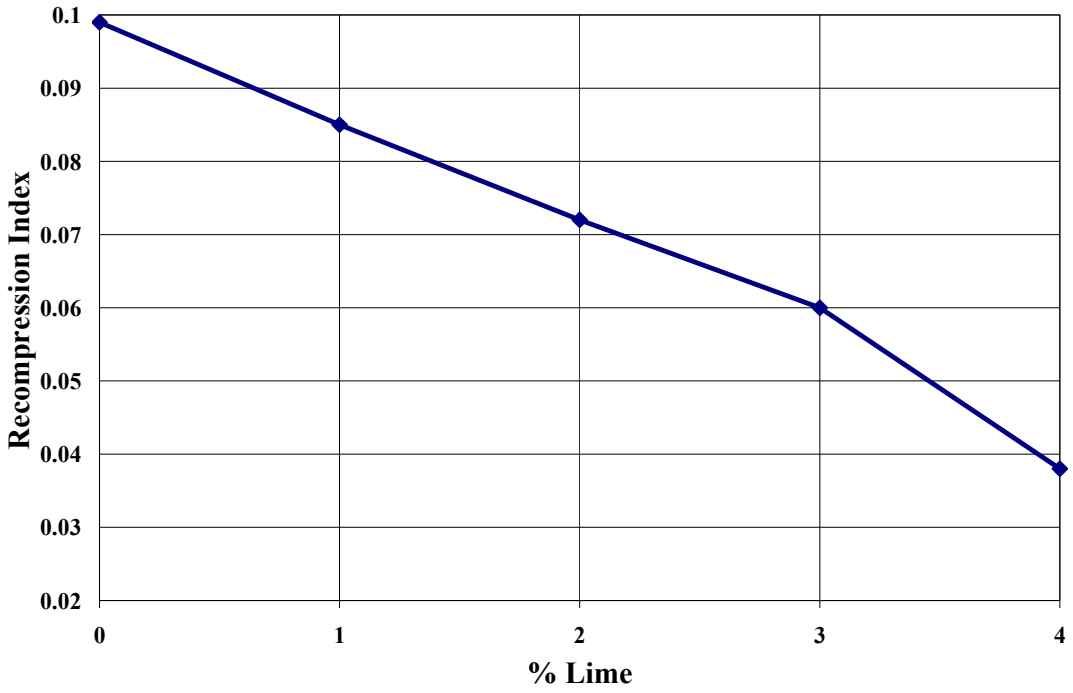

Figure 6.21 Variation of recompression index corresponding to the end of primary consolidation with % lime

The values of coefficients of secondary consolidation under varying effective surcharge ratios are presented in Figure 6.22. The results show that extra addition of lime to dredged mud caused a significant reduction in $C_{\alpha}^{'}$ values. This figure suggests that the coefficient of secondary consolidation for natural material gradually decreases with an increase in the effective surcharge ratio. It is interesting to note that under the same effective surcharge ratio, as the % of lime increases, the secondary compression index decreases. Figure 6.22 suggests that increasing the surcharging effort is more effective for the natural dredged mud samples and the values of $C_{\alpha}^{'}$ gradually decrease as the effective surcharge ratio increases. However, it was found that the reduction of $C_{\alpha}^{'}$ with an increasing effective surcharge ratio is less for the dredged mud samples treated with 2 and 4% lime. Figure 6.22 illustrates that the material with four percent of lime exhibited

no further reduction in $C_{\alpha}^{'}$ beyond the effective surcharge ratio of 0.66. In the case of 2% lime, no reduction of the secondary compression index was observed as the effective surcharge ratio increases from 0.33 to 0.66.

In summary it was found that in the recompression range, both the recompression index and secondary compression index decreases with increasing % of lime. Furthermore, the effective surcharge ratio has less effect as the amount of lime increases.

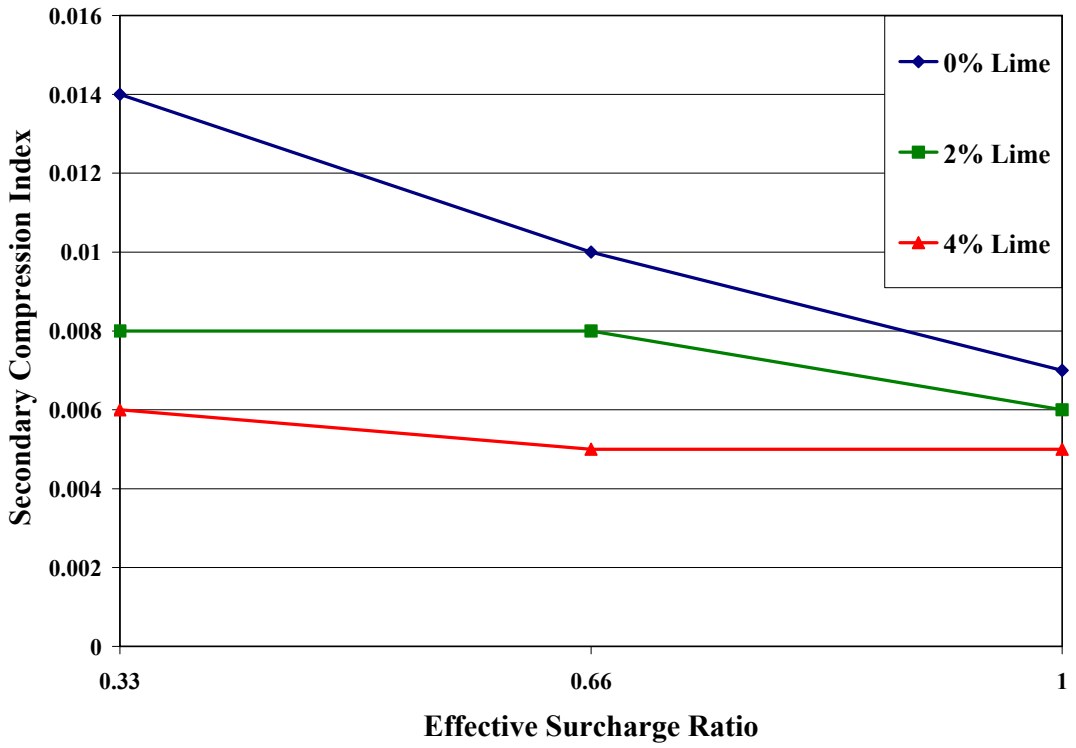

Figure 6.22 Variation of secondary compression index with % lime and different effective surcharge ratio

6.6 Anisotropy of the dredged mud

A particulate soil system is said to be anisotropic when it displays directional variation of its properties. It has been found that anisotropy in strength, consolidation, and permeability is an inherent characteristic of the clay deposits (Sivakugan et al., 1993). During the sedimentation, particles tend to become oriented in such a way that the long axis is perpendicular to the major principal stress during deposition. It is also a general belief that during one-dimensional consolidation, the clay particles gain an orientation that induces cross-anisotropic properties. Hence, the rate of consolidation is often expected to be greater for horizontal than for vertical drainage conditions. However, it is important to note that in the case of the soft clay deposits, it is quite common to assume that the ratio of k_h / k_v is almost unity (Bergado et al., 1991; Indraratna et al., 1998). The experimental program conducted so far has revealed that with addition of lime into a dredged mud, the void ratio or in general the fabric of the material is changed. The results obtained from the conventional oedometer test showed that the increase in effective vertical stress has no negative effect on the lime treated dredged mud in terms of deteriorating the new gained fabric and water flow characteristics of the specimens. On the other hand, for any state of the applied effective stresses, the materials with higher percentages of lime exhibited the higher void ratio. As far as this study is concerned, the effect of % lime on horizontal flow of the specimens and stability of the newly gained properties under varying effective stresses should be evaluated. Furthermore, it is worthy to assess the effect of % lime on the ratio of c_h / c_v or k_h / k_v to provide deep understanding of the mechanism and features of the lime-clay modification.

In this section, an attempt has been made to quantify the horizontal coefficient of consolidation of the natural and lime treated dredged mud. In reclamation projects, accurate prediction of the amount, and in particular, the rate of settlement of the ground under applied load is necessary since geotechnical design is largely driven by serviceability limit state conditions. The measuring of horizontal coefficient of consolidation is important because, this feature has a significant role in controlling the rate of ground settlement where vertical drains are employed. Hence in order to produce a

meaningful research outcome, it is a matter of importance to ensure that the hydraulic characteristic of the dredged mud in the horizontal direction is also improved when it is treated with hydrated lime. The current research defines anisotropy of the dredged mud as the ratio of c_h / c_v, where c_h is the coefficient of consolidation in horizontal direction. In the current research, a modified oedometer cell was designed and used to measure the coefficient of consolidation in the horizontal direction (Figure 6.23).

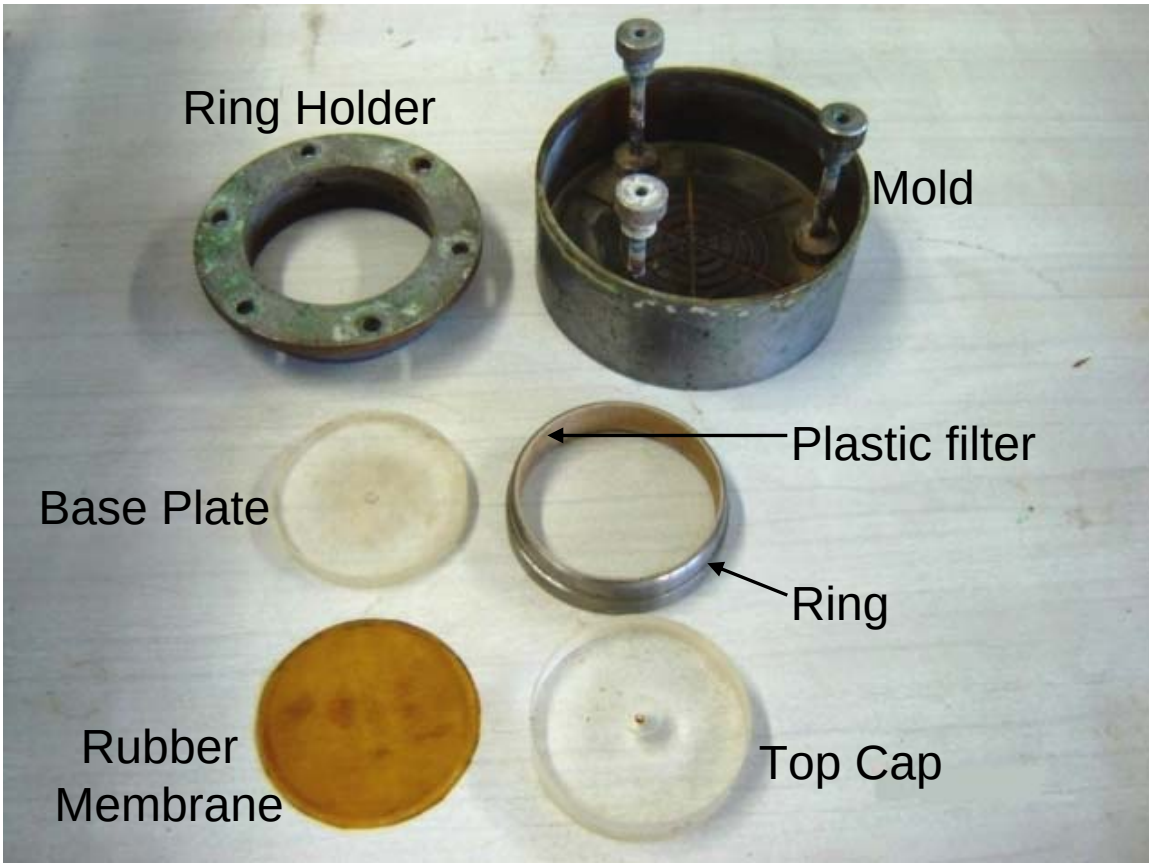

Figure 6.23 Components of the modified Oedometer apparatus

The modified oedometer shown in Figure 6.23 slightly differs to the conventional oedometer used in soil laboratories. This apparatus was designed to provide the radial drainage path instead of the vertical when the dredged mud specimen is subjected to the

incremental loading. For this purpose, a band-shaped plastic filter with a width equal to the height of the ring (19 mm) was carefully cut and fitted to cover the inner surface of the ring. The porous plastic filter allows the water to be drained horizontally when the vertical load is applied on the specimen. It should be noted that in the proposed system, once the water molecule exits the soil mass and reaches the filter, it moves vertically upward through the filter to eventually leave the system.

The sample preparation for the modified oedometer test is almost similar to the one explained earlier in section 6.3. However, instead of recovering the oedometer sample at the end of seepage consolidation, in the new manner, the modified ring was first placed on the base of the permeability mold prior to pouring the slurry into the mold. This approach was taken because the presence of the plastic filter inside the ring means no sharp edge for the ring to penetrate in the specimen as described in 6.3. Once consolidation of the slurry sample in the permeability mold was completed, the mold was dismantled and the trapped modified ring was recovered. After treating the specimen, it was placed into the oedometer mold. To obstruct the of water flow in a vertical direction, two impermeable disks were used as a “top cap” and “base plate”. The diameter of the top cap was quite close to the inner diameter of the modified ring (76 mm) to ensure that it fitted properly. However, due to the smoothness of the plastic filter, the top cap could still move freely inside the ring with only a small fraction of space between the two surfaces. The bottom of the specimen was covered with a rubber membrane with the impermeable disc underneath. The rubber membrane was used to ensure that all small gaps between the base plate and ring were filled and the vertical water flow path was appropriately clogged.

The test program was carried out on two specimens containing 0, and 4% lime. Again, samples were loaded in a series of increments, from 10 kPa to 640 kPa, where each load was twice that of the previous, and successive loads were applied after the end of primary consolidation (EOP). Figures 6.24 and 6.25 identify the settlement-log time curves of the natural and lime-treated specimens. It can be seen that the elapsed time to reach the end

of primary consolidation in the natural specimen is much higher than the treated dredged mud with 4% lime. An observation of these two figures also suggests that for both specimens, the required time for EOP in the modified cell is larger than one which is obtained by means of the conventional cell (see Figure 6.10).

In order to evaluate the horizontal coefficient of consolidation of the specimens, the author adapted the equation proposed in the British Standard (BS 1377-6: 19990; 3.7.8.3).

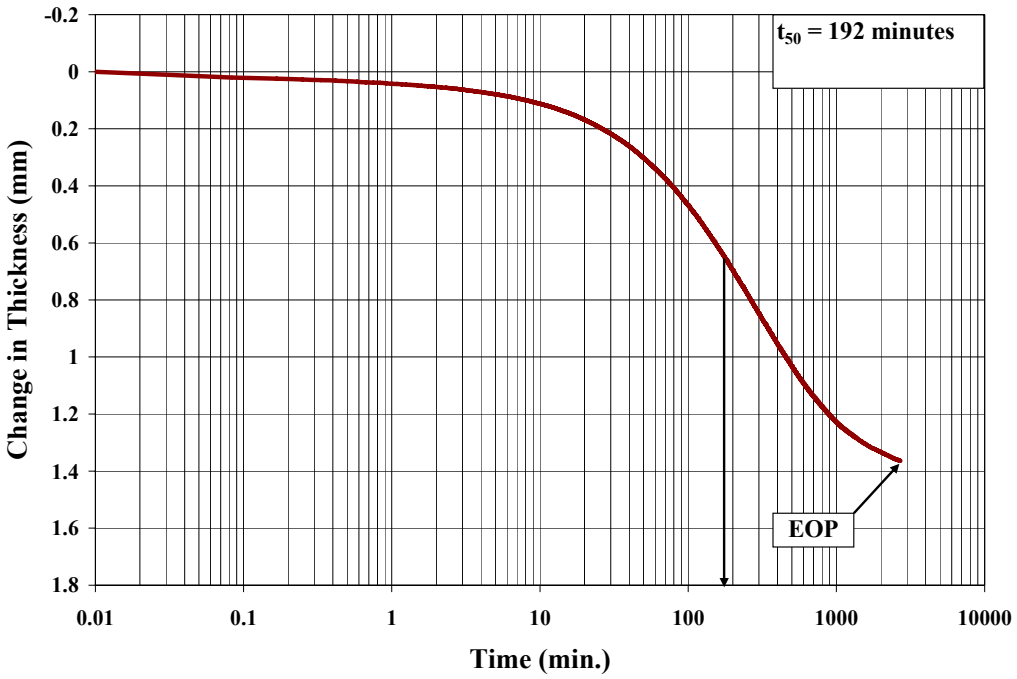

Figure 6.24 Oedometer test with outwards radial drainage for the natural dredged mud under effective applied pressure of 160 kPa

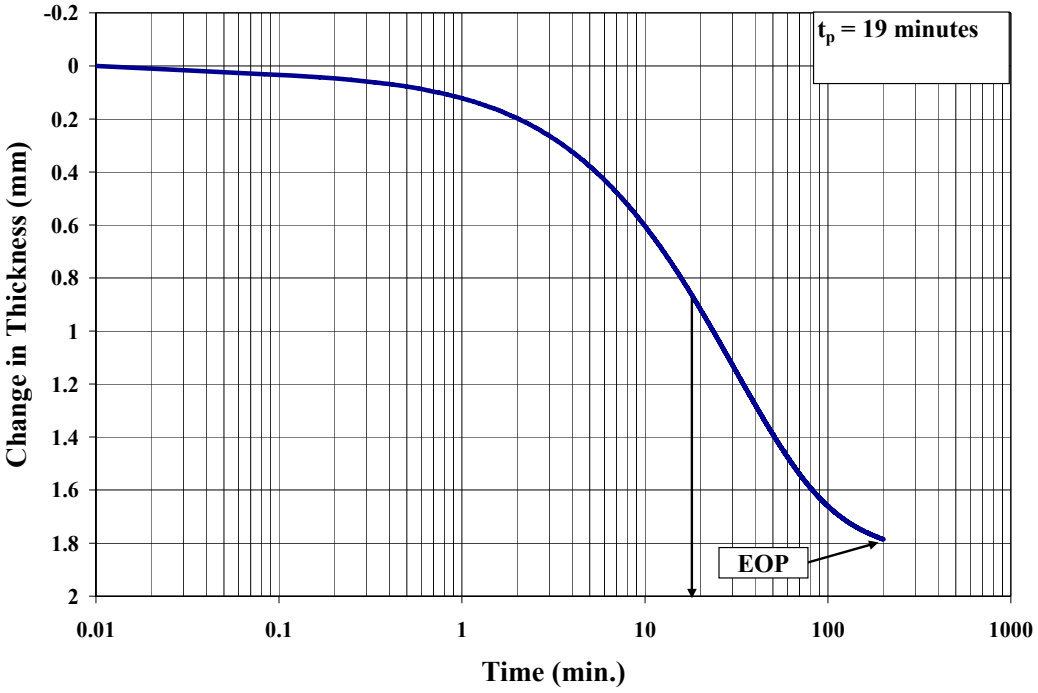

Figure 6.25 Oedometer test with outwards radial drainage for the lime-treated dredged mud (4% lime) under effective applied pressure of 80 kPa

The adapted equation is initially proposed for the consolidation test with radial outward drainage in hydraulic cell (Rowe Cell) under equal strain loading. These test conditions are quite similar to the one applied in the modified oedometer cell. The method of calculation corresponds to the settlement-log time curve and is defined as the following:

$$c_h = \frac{0.011 D^2}{t_{50}} \qquad \text{Eq. 6.16}$$

where:

c_h is the horizontal coefficient of consolidation (m^2/year).

t_{50} is the time corresponding to a pore water pressure dissipation of 50% (in min.).

D is the specimen diameter (76 mm).

Table 6.4 The values of c_h and c_v and state of anisotropy of the natural and lime treated dredged mud

Specimen- Loading stage	c_h	c_v **From section 5.1.1**	$\frac{c_h}{c_v}$
Natural- 20 kPa	0.26	0.23	1.13
Natural- 40 kPa	0.34	0.28	1.2
Natural- 80 kPa	0.35	0.31	1.13
Natural- 160 kPa	0.33	0.32	1.05
Natural- 320 kPa	0.38	0.35	1.09
Natural- 640 kPa	0.34	0.32	1.06
4% lime- 20 kPa	2.9	2.4	1.2
4% lime- 40 kPa	3.6	2.85	1.26
4% lime- 80 kPa	3.34	3.04	1.1
4% lime- 160 kPa	3.7	3.13	1.18
4% lime- 320 kPa	3.34	3.05	1.1
4% lime- 640 kPa	3.2	2.9	1.1

It is important to note that according to the British standard, t_{50} in Eq. 6.16 is time corresponding to $U_{ave} = 50\%$. The standard method states that:

In the consolidation test with outwards radial drainage, pore water pressure is measured at the centre of the bottom face, and it is assumed that at any instant, the pore water pressure distribution along any vertical line is uniform. This statement confirms that the adoption of equation 6.16 for the purpose of determination of c_h in the modified oedometer ring is sound and appropriate.

Table 6.4 presents the values of the coefficient of consolidation in both vertical and horizontal directions of the natural and lime treated dredged mud. The illustrated data suggests that with an addition of lime into the dredged mud, the horizontal coefficient of consolidation increases up to ten fold as % lime increases from zero to 4 percent. This behaviour was similar to the one observed in the vertical coefficient of consolidation obtained by means of the conventional oedometer test. The data also shows that the improvement in c_h values remains almost constant under varying effective applied pressure. This table also illustrates the ratio between the two parameters to demonstrate the state of anisotropy for the natural and the treated specimen prepared at lime modification optimum. According to the information outlined in Table 6.4, the anisotropy of the both specimens at all load increments remains within the narrow band (1.05 -1.26) and no significant differences are observed between the average values of c_h / c_v corresponding to each specimen. As shown in chapter 4 and earlier in this chapter, for the type of the dredged material used in this study, the fabric anisotropy (i.e. increase in void ratio at given effective stress) is apparent as % lime increases. However, though somewhat counter-intuitive, by considering $c_h / c_v \approx 1$ in both specimens (see Table 6.4), one may assume that the initial permeability isotropy of the dredged mud remains unchanged as % lime increases. On other words, since the values of m_v in the oedometer moulds with horizontal and vertical drainage are same, therefore $k_v = c_v m_v \gamma_w$ and $k_h = c_h m_v \gamma_w$, results in $c_h / c_v = k_h / k_v \approx 1$ for both the natural, and lime treated dredged mud specimens. As a conclusion, it may be assumed that for the same void ratio, the efficiency of the water flow channels does not correlate strongly with the alignment of the individual soil grain. This assumption may be employed to explain the permeability behaviour of the dredged mud as shown in Figure 6.9. The $e - \log k$ curves associated to the different treated and non-treated specimens, lie in close vicinity to each other (i.e. almost overlapping), so that for the single value of void ratio the corresponding permeability is approximately similar for all specimens. Based on this characteristic (i.e. same permeability at the same void ratio) it may suggest that permeability of the dredged mud can be attributed to the size of the effective pores (i.e. void ratio) rather than the

shape of the water channels. However, the author wishes to strongly advise that this behaviour (i.e. same permeability at same void ratio) should not be confused with the fact that with increasing lime content, at any given effective stress, a higher void ratio and consequently higher permeability is achieved.

6.7 Summary and conclusion

This chapter deals with the second round of the experimental program conducted during the course of the study. The main objective of the laboratory test program in this section was to evaluate the effect of % lime up to the lime modification optimum, on consolidation parameters of the dredged mud.

A set of oedometer tests was conducted in both normally consolidated and artificially overconsolidated stages on both natural and lime treated samples. It was found that the new fabric of sediment under varying percentages of lime affects the consolidation behavior of the lime treated dredged mud to varying extents. The laboratory findings revealed that in both compression and recompression states, the coefficient of consolidation drastically increases. In the compression range, the increase of c_v was observed up to ten fold, with an increase of lime up to 4 percent. The coefficient of consolidation governs the rate of ground settlement. The higher the values of the coefficient of consolidation, the faster the ground reaches its ultimate primary consolidation settlement.

Observation of the test results suggests that in the compression range, the values of the compression index increase when increasing the lime content whereas in the recompression range, the value of the recompression index gradually decreases with increasing % lime. This finding indicates that with increasing % lime, the magnitude of primary consolidation in the NC state increases while in the OC state it decreases.
It is interesting to note that the secondary compression index in both the compression and recompression range decreases with increasing % lime. In the compression range the

decreasing of C_α together with an increase of C_c, results in a gradual reduction of C_α / C_c as the amount of lime increases. It is worthwhile stating that the surcharging effort was found to be more effective in a further reduction of the secondary compression index of the natural dredged mud in comparison with lime treated dredged mud.

The above laboratory findings highlight the beneficial effects of lime modification on improving the consolidation behavior of the dredged mud. This study may lead to consideration of an innovative ground improvement technique in construction of man-made islands in which dredged mud becomes mixed with lime prior to discharging into a containment pond. The advantages of this pre-treatment may later appear in improving the effectiveness of preloading on a deposited dredged mud layer.

The empirical correlation between coefficient of consolidation, void ratio and corresponding effective stress was proposed and evaluated in this chapter. It was found that for the type of the dredged mud used in this study, irrespective of the percentages of added lime, the coefficient of consolidation can be obtained by knowing the state of void ratio and effective stress at any instance during consolidation. Even though this equation holds true for all natural and lime treated specimens in the laboratory however, the applicability of the equation in predicting the coefficient of consolidation of the soft ground in the field requires more assessment.

The modified oedometer apparatus with horizontal drainage was developed to determine the horizontal coefficient of consolidation and evaluate the state of anisotropy of the natural and lime treated dredged mud. The anisotropy was defined as a ratio of c_h / c_v. It was found that with increasing the % lime, the horizontal coefficient of consolidation increases in the same manner of vertical coefficient of consolidation, resulting in c_h / c_v ratio almost being in unity. Since the coefficient of volume compressibility is independent to the drainage condition, $k_v = c_v m_v \gamma_w$, and $k_h = c_h m_v \gamma_w$. Therefore, the ratio of c_h / c_v is similar to the ratio of k_h / k_v. Because $k_h / k_v \approx 1$ is valid for the natural and lime treated specimens, it was concluded that in spite of the change in the fabric (i.e.

increase in void ratio at the same effective stress), with increasing % lime, the state of the permeability isotropy remained unchanged.

Chapter 7
Modeling of the Reclaimed Layer

7.1 General

Previously in this dissertation, the pretreatment of the dredged mud with hydrated lime was proposed as an effective approach to enhance the physico-chemical properties of the dredged fill used in the construction of a man-made island. It was suggested that the treatment of the dredged material, together with an application of surcharge preload aided by vertical drains may benefit the project from both the engineering and economical aspects. In chapters 4 and 6 the laboratory test results showed that with addition of lime, the rate of primary consolidation settlement increases while the rate of secondary compression settlement decreases. In order to make the laboratory outputs more meaningful, this chapter aims to develop the three conceptual reclaimed layers in the man-made island with materials containing 0, 2, and 4 % of lime by means of oedometer test results. Once the reclaimed layers are created, their consolidation behavior in conjunction with prefabricated vertical drains will be modeled. One of the objectives of this modeling is to assess the relationship between % lime and vertical drain spacing to achieve a specific preloading time. Modeling of the consolidation behavior of the dredged layer with installed prefabricated vertical drains (PVD) under surcharge preload is carried out by the finite element modeling (FEM) method. The modeling software, Plaxis Version 8 (Netherland, 2008) is used in this study.

As a second objective, the effect of % lime on the development of lateral displacement of the three models during the construction of embankment is evaluated by full scale analysis method using a 2D model. The necessity of this analysis has arisen due to hazardous potential of this phenomenon on the surrounding sea-wall. Actually, when soft

soil is present, the lateral soil displacement is particularly large, and may pose quite significant stress to adjacent structure (e.g. sea-wall). In fact, when a load is applied to the soil surface, the vertical stress within the soil mass is increased and expands indefinitely in all directions. The induced lateral soil displacement will consequently generate passive stresses on nearby structure. (Indraratna et. al., 2005) reported that the extent of heave at the toe of embankment on soft ground is governed by the construction rate of embankment. It was reported that the slow rate of construction allows a larger embankment height at failure, because due to gradual rate of construction, the soft soil gains shear strength upon pore pressure dissipation. In this study, an attempt has been made to evaluate the lateral displacement at the toe of embankment at the end of construction periods of 30 and 90 days respectively.

As a third objective, the beneficial effect of lime on the secondary compression settlement of the modeled layers is also evaluated by means of the analytical method for the design project life of 100 years.

7.2 Construction sequence of a man-made island

The construction process and elevation of the ground in a man-made island is schematically shown in Figure 7.1. The interpretation of the figure is as follows.

The construction of a seawall on the sea bottom is a basic requirement for reclaimed land. The seawall defines the border of the reclamation project and provides enclosure for disposal of the dredged material. Upon completion of the seawall, the reclamation phase begins with discharging of the dredged material into a pond. During this reclamation stage, suspended clay particles settle loosely in the seawater. While discharging continues, the surface elevation of the dredged clay layer gradually increases as a result of the combined process of sedimentation (i.e. increasing elevation) and self-weight consolidation (i.e. decreasing elevation).

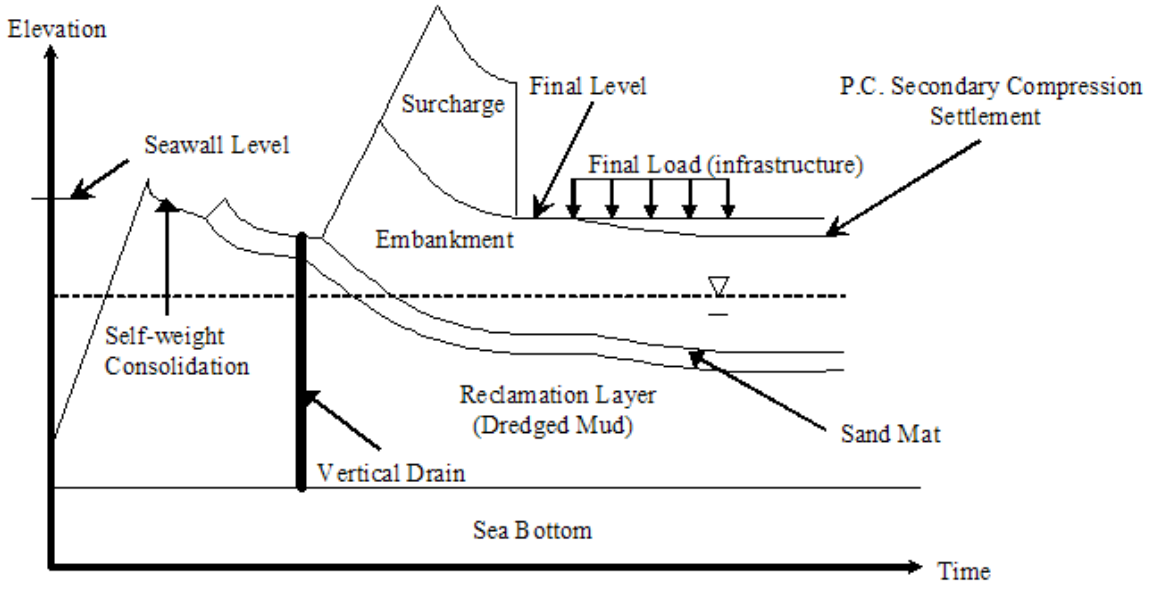

Figure 7.1 Construction sequence of a man-made island

At a time when the dredging process is over and the settlement due to self-weight consolidation is still in progress, the reclaimed dredged soil may be covered by a net for the surface stabilization (Terashi and Katagiri, 2005). At this stage a sand mat can be placed on the dredged layer to create a reliable foundation at a specific level. Quite often when a rapid construction is required, to increase the consolidation rate, following the placement of a sand mat, the prefabricated vertical drains are installed throughout the entire compressible layer down to the sea bottom. The spacing of the vertical drains is determined to achieve a certain degree of consolidation (e.g. 90%) within a given duration. During installation of PVDs, the self-weight consolidation of the reclaimed clay layer, and the consolidation induced by the sand mat, still continues. Once the installation of PVDs is complete, the placement of the permanent (embankment) and temporary (surcharge) fill on the sand mat will proceed. The main consolidation of the soft dredged layer takes place under the surcharge preload which is defined as a combination of both the surcharge and embankment fill. It has to be noted that typically, due to large ground settlement, part of the fill used as an embankment would gradually sink below the water level. The submergence effect accounts for a reduction of effective stress of surcharge preloading. After achieving of the required degree of consolidation,

the surcharge is removed and construction of infrastructure facilities (i.e. final load) is initiated. The elevation of the ground under the final design load may still continue to reduce creep or secondary compression settlement over an infinite period of time.

7.3 Prediction of a ground condition using the laboratory data

A systematic procedure for an estimation of the condition of the conceptual soft dredged layer under application of a surcharge preload is developed. The method for estimating the field responses of the natural and lime treated dredged mud is developed by utilizing the laboratory test data produced by means of a series of oedometer tests. The simplified method of analysis supposes that the amount of primary consolidation settlement of these sites can be estimated assuming a similar EOP $e-\log\sigma_v^{'}$ relationship between laboratory and field behavior. Taking the above assumption into account, Figure 6.6 in the previous chapter is considered here to define the $e-\log\sigma_v^{'}$ relationship in the conceptual sites.

Firstly, given a wide containment pond, it is required to estimate the initial height and state of effective stress in the middle of the reclaimed dredged layer when it is initially covered with a sand mat. Based on the analytical method proposed here, the ground condition in terms of void ratio and height, under the application of surcharge preload is evaluated first, and then the initial ground condition under application of the sand mat is back calculated. Figure 7.2 presents the typical schematic vertical profile of a containment pond in the two different stages of the ground improvement phase before and after placement of the surcharge preload.

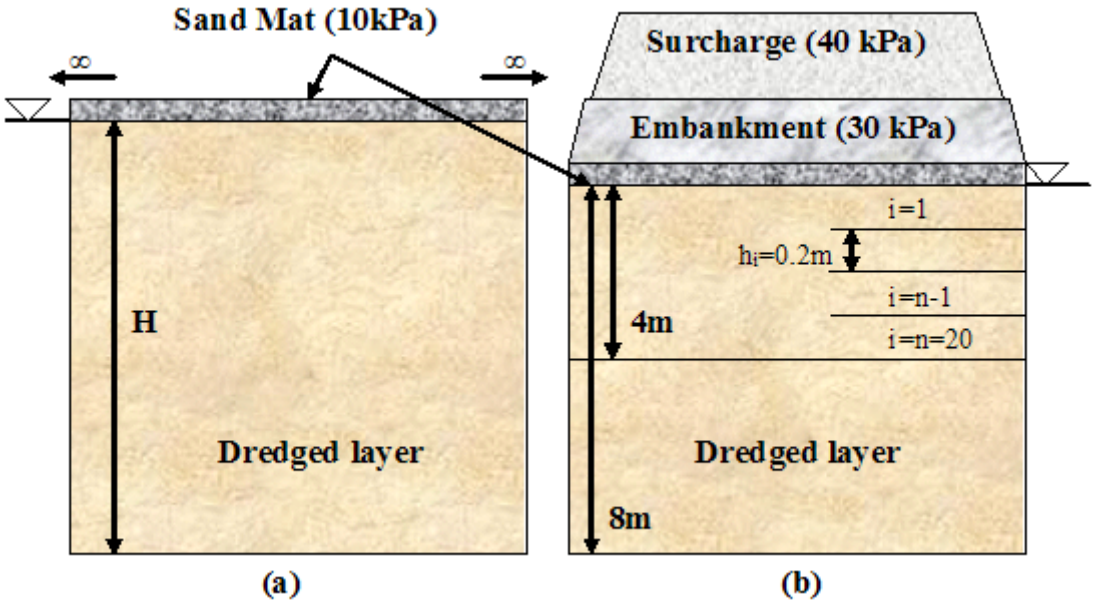

Figure 7.2 Schematic view of the containment pond before and after the placement of surcharge preload

The following assumptions are made for the conceptual site shown in Figure 7.2:

- The dredged layer is homogenous and consists of uniform material within the entire volume.

- Prior to the placement of the surcharge preload on the soft foundation (Figure 7.2 a), the excess pore pressure within the mass of the dredged layer due to the placement of the sand mat is totally dissipated and the layer is normally consolidated.

- The final design elevation of the dredged layer under application of the surcharge preload and completion of > 95% of consolidation is 8 m (Figure 7.2 b).

- The effective loading due to the combined sand mat, embankment, and surcharge fills is 80 kPa where the surcharge accounts for 40 kPa.

- The water table moves vertically downwards as ground gradually settles.

- The rebound of the ground after removal of the surcharge is negligible.

- The final design load (i.e. due to infrastructure facilities) of 20 kPa is applied once the surcharge fill is removed.

The weight of the surcharge preload causes an increase in the vertical stress in the soft dredged layer. It was assumed that the conceptual site is infinite horizontal dimensions. Thus, the increase in stress and/or incremental stress ($\Delta\sigma_v^{'}$) is constant within the entire height of the dredged mud layer. Figure 7.2 (b) demonstrates the final stage of consolidation (i.e. more than 95% of consolidation) where the ultimate ground settlement has occurred and the final design height of 8 meters has been achieved. Accordingly, the dredged mud layer is divided into 20 sub-layers for upper half of its thickness, with each sub-layer 20 cm in thickness. This division is made to precisely calculate the effective overburden pressure which is applied at the centre of the dredged layer. For the condition of one-dimensional consolidation, the total effective overburden pressure in the dredged mud layer is the summation of the self-weight effective overburden pressure and effective vertical pressure due to the surcharge preload.

Let $e_{i=1}$ = void ratio at top of layer 1 corresponding to 80 kPa obtained from the EOP $e-\log\sigma_v^{'}$ curve shown in Figure 6.6. The submerged unit weight of layer 1 is given by:

$$\gamma_{b(i=1)}=\frac{G_s-1}{1+e_{i=1}} \qquad \text{Eq.7.1}$$

The total effective overburden pressure at the bottom of layer 1 is given by:

$$\sigma_{v(i=1)}^{'}=\gamma_{b(i=1)}\times h_i+80 \qquad \text{Eq. 7.2}$$

where h_i is the thickness of layer equal to 0.2 m.

With increasing total effective overburden pressure, a further reduction in void ratio of the below layers occurred. Hence for the second layer, the state of void ratio at top is defined by:

$$e_{i=2} = e_{i=1} - (C_c \times \log \frac{\sigma'_{v(i=1)}}{80})$$

where C_c is a compression index drawn from EOP $e - \log \sigma'_v$ curve (80-160 kPa) in Figure 6.6.

The new void ratio accounts for a further increase in effective overburden pressure due to self-weight. The total effective overburden pressure at the bottom of layer 2 is a sum of the two components; the total effective overburden pressure at layer 1 and the contribution of self-weight of layer 2 (i.e. self-weight effective overburden pressure of layer 2). Hence, the total effective overburden pressure at the bottom of layer 2 is given by:

$$\sigma'_{v(i=2)} = \gamma_{b(i=2)} \times H_i + \sigma'_{v(i=1)}$$

Therefore, the following general equations can be used to estimate the void ratio and corresponding effective overburden pressure at a specific depth of the dredged layer:

$$e_i = e_{i=1} - \left(C_c \times \log \frac{\sigma'_{v(i-1)}}{80} \right) \quad \text{Eq. 7.3}$$

And,

$$\sigma'_{vi} = \gamma_{bi} \times H_i + \sigma'_{v(i-1)} \quad \text{Eq. 7.4}$$

It should be noted that all the above equations are suggested based on the assumption that the value of void ratio corresponding to the top of each sub-layer is applicable for the entirety of thickness and increases sharply at the bottom (i.e. the top of the below layer).

Figure 7.3 shows the state of the total effective overburden pressure of the middle of three conceptual dredged layers with 0, 2, and 4% of lime. It can be seen that for the same thickness of the dredged layer, with increasing % lime, the total effective overburden pressure is less. This behavior is attributed to the status of the fabric of the materials. In the other words, as % increases, the void ratio increases, resulting in the lower value of submerged unit weight and consequently lesser self-weight effective overburden pressure.
Figure 7.3 suggests that the increases in effective overburden pressures attributed to the self-weight of the dredged mud layers down to half of the thickness are 28, 24, and 20 kPa for layers containing 0, 2, and 4% lime respectively.

It was assumed that the conceptual layers stand in the normally consolidated state under the sand mat (10 kPa). Thus, it is concluded that before and after the placement of surcharge preload the self-weight effective overburden pressure at the middle of the layer is the same for Figure 7.2(a) and 7.2 (b). Therefore self-weight effective overburden pressure at the half depth of the layers subjected to the placement of the sand mat (Figure 7.2 a) and containing 0, 2, and 4 % of lime is 28, 24, and 20 kPa respectively.

Since the sand mat was assumed to apply 10 kPa of effective stress on the top of the dredged layer (i.e. at EOP), the total effective overburden pressure at the middle of the layer with thickness H, is 38, 34, and 30 kPa for the models containing 0, 2, and 4% lime respectively.

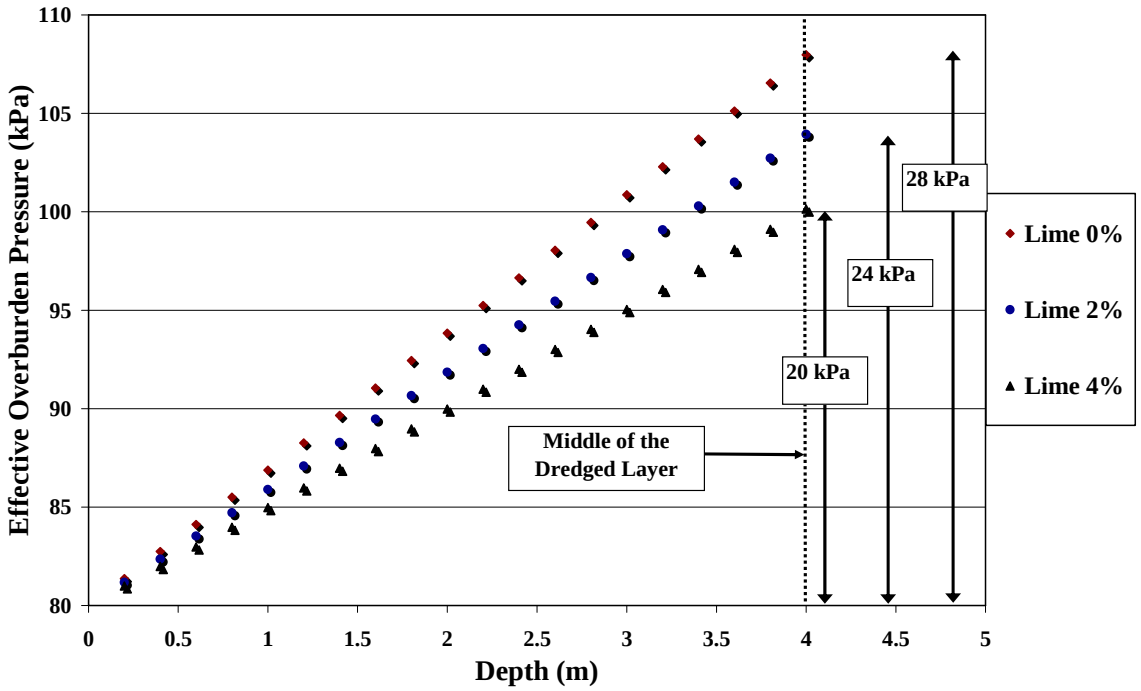

Figure 7.3 Development of the total effective overburden pressures from surface to the middle of dredged layers under application of the surcharge preload (see Figure 7.2 b)

The initial height, H, of the dredged layers before application of the preload surcharge is estimated using the equation below:

$$S_t = H - 8 = H \times \frac{e_0 - e_1}{1 + e_0} \qquad \text{Eq. 7.5}$$

where:

S_t is the total ground settlement and is defined by: H-8 (m);

e_0 and e_1 are void ratio corresponding to the middle of the layer in Figure 7.2 (a) and 7.2 (b) respectively.

Table 7.1 summarizes the data obtained from Eq. 7.5 and used in the three models of the dredged layer containing 0, 2, and 4% lime.

Table 7.1 Characteristics of the three models of dredged mud layer

Model % lime	σ'_{v0} kPa	e_0	σ'_{v1} kPa	e_1	C_c	H m
0%	38	1.75	108	1.38	0.82	9.3
2%	34	2.35	104	1.79	1.15	9.6
4%	30	3.1	100	2.34	1.45	9.8

7.4 Finite element model (PLAXIS analysis)

The performance of the surcharge preload on the three conceptual sites of the dredged mud layer with the aid of vertical drains is evaluated using the finite element modeling (FEM) method with PLAXIS Version 8 (Netherland, 2008). The analyses pursue two different objectives:

- To assess the effect of % lime on drain spacing for the given preloading time.
- To evaluate the effect of % lime on lateral displacement for a given construction time of embankment.

Modeling of the conceptual dredged mud layers were carried out by the plane strain unit cell and full scale analyzing methods using the 2D model. Previously in chapter 5, it was discussed that most finite element analyses on preloading of soft ground treated with vertical drains are conducted based on plane strain assumptions. This kind of analysis may pose a problem as the consolidation around vertical drains is axisymmetric. Hence, to employ a realistic 2-D finite element analysis for vertical drains, the equivalence between the plane strain and axisymmetric analysis needs to be established. The matching of axisymmetric and plane strain conditions can be carried out in three ways:

- Geometric matching approach, i.e. the spacing of the drains is matched while keeping the permeability the same.
- Permeability matching approach, i.e. coefficient of permeability is matched while keeping the spacing of drains the same.

- Combination of permeability and geometric matching approach, i.e. plane strain permeability is calculated for convenient drain spacing.

In this study, the conversion approach of permeability matching was employed in the modeling program. Indraratna and Redana (1997) successfully converted the vertical drain system into equivalent parallel drains by adjusting the coefficient of permeability of the soil. Details of the permeability conversion approach were broadly presented in chapter 5.

For modeling the plane strain unit cell, the ideal drain condition was considered and both the well resistance and smear effects were ignored. In this study, the Eq.5.50 is incorporated in the numerical analysis employing Plaxis to analyze the three conceptual dredged mud layers.

Eq.5.50 is recalled and presented here:

$$\frac{k_{hp}}{k_h} = \frac{0.67}{\ln(n) - 0.75}$$

Based on the laboratory test result obtained in chapter 6 (section 6.6), the coefficient of horizontal permeability, k_h, is considered to be approximately 1.2 times k_v (i.e. $k_h = 1.2k_v$). The coefficient of vertical permeability itself is obtained from Figure 6.9. That figure shows the values of permeability based on the correlation of: $k_v = c_v \times m_v \times \gamma_w$.

The equations for the regression lines corresponding to 0, 2, and 4% lime are $k_{0\%} = 2E^{-8}\sigma_v^{'\,-0.9603}$, $k_{2\%} = 6E^{-8}\sigma_v^{'\,-0.9804}$, $k_{4\%} = 2E^{-7}\sigma_v^{'\,-0.9872}$ respectively.

7.4.1 Plane strain unit cell analysis of vertical drain

The geometry tool available in the Plaxis version 8 finite element program was used by the author to draw the plane strain vertical drain. The length of the drain was equal to the height of the conceptual dredged mud layers shown in Table 7.1. Since each single dredged mud model posses a different permeability value, the width of the drain element in the three mentioned layers was iteratively adjusted to meet equal time for the excess pore pressure dissipation at a certain point.

The 15-node triangular element was adopted in the analysis. The powerful 15-node element contains 12 stress points that provide a precise calculation of stresses. In analysis, the dredged mud layer was simulated by way of the Soft Soil Model and the sand fill layer was simulated, using the Mohr-Coulomb Model.

Figure 7.4 demonstrates a typical unit cell vertical drain modeled by Plaxis in this study. As can be seen, the right hand side enclosed boundary is the centerline of the dredged mud body between two adjacent drains. The dredged mud layer is characterized by drained conditions at both the upper and lower boundaries. The material above the phreatic level on the upper boundary represents the fill sand with a high level of permeability. The excess pore water pressure is set to zero along the drain boundary to simulate complete dissipation. Effects of both smear zone and well resistance is neglected.

In the unit cell model, the change in pore pressure is registered at the middle of the dredged layer, in the vicinity of the enclosed boundary.

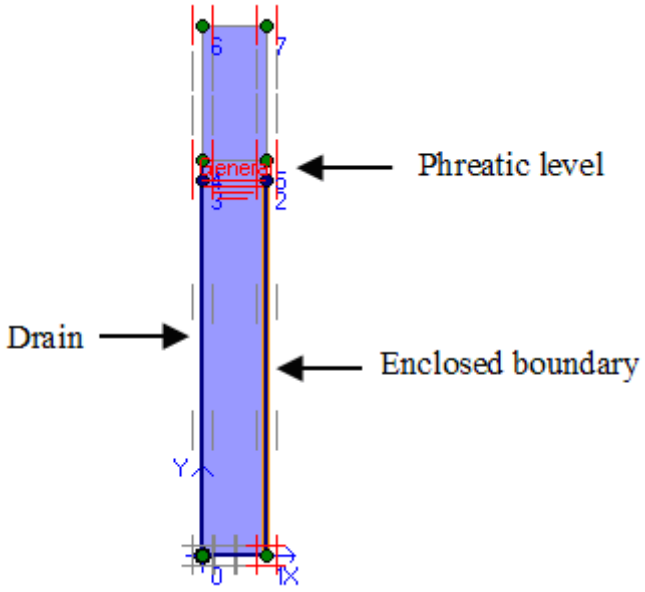

Figure 7.4 One-half of the unit-cell vertical drain

The properties of the three unit cell models corresponding to the three conceptual dredged mud layers are tabulated in Table 7.2. As discussed earlier, the main objective of this modeling exercise is to evaluate the effect of the different material properties on the drain spacing under equal preloading time. In this study, the time period of two years or 1095 days was chosen as a target preloading time to achieve more than 95% of consolidation. With increase in lime percentage the permeability of the treated dredged mud increases, hence, a bigger drain influence zone for the material with a higher percentage of lime was expected to be attained. As mentioned earlier, the width of the drain elements was adjusted through trial and error to achieve a similar consolidation period of the 1095 days. Table 7.2 summarizes the data used for converting the axisymmetric to the plane strain model. The coefficient of horizontal permeability in the three proposed models was assumed to be 1.2 times the coefficient of vertical permeability.

Table 7.2 The input parameters for permeability conversion approach

Model % Lime	k_v m/day	k_h m/day	d_w m	D_e m	n	F_n	k_{hp} m/day
0	0.000054	0.000065	0.05	1.2	24	2.43	0.000018
2	0.00016	0.00019	0.05	2.0	40	2.94	0.000045
4	0.0005	0.0006	0.05	3.4	68	3.47	0.00011

In this table d_w and D_e, represent an equivalent diameter of band-shape drain and diameter of unit-cell (i.e. influence zone of drain) respectively. n and F_n denote the drain spacing ratio and drain spacing factor respectively.

Previously in chapter 5 it was shown that the drain spacing ratio, n ,can be given by:

$$n = \frac{D_e}{d_w}$$

The drain spacing factor is also given by:

$$F_n = \ln(n) - 0.75$$

The converted value of the horizontal coefficient of permeability was obtained by:

$$k_{hp} = \frac{k_h \times 0.67}{F_n}$$

The values of k_v and k_{hp} were used as the input parameters in the Plaxis program.

Tables 7.3 and 7.4 summarise the soil parameters used in the program for sand fill and three dredged mud models. The data presented in Table 7.3 are adapted from the literature. The data shown in Table 7.4 are mostly obtained from the laboratory test program conducted in this research study (except those marked with +).

Table 7.3 Soil parameters of sand fill

Mohr-Coulomb	**Sand fill**
Type	Drained
γ_{unsat} $[kN/m^3]$	17.00
γ_{sat} $[kN/m^3]$	20.00
k_h $[m/day]$	1.000
k_v $[m/day]$	1.000
E_{ref} $[kN/m^2]$	13000
ν ***	0.300
G_{ref} $[kN/m^2]$	5000
E_{oed} $[kN/m^2]$	17500
c_{ref} $[kN/m^2]$	1.0
φ $[^0]$	31
ψ $[^0]$	0.00

Notations:

γ = Soil unit weight

k = Permeability

E_{ref} = Young's modulus

ν = Poisson's ratio

G_{ref} = Shear modulus

E_{oed} = Oedometer modulus

c_{ref} = Cohesion

φ = Friction angle

ψ = Dilatancy angle

λ^* = Modified compression index

k^* = Modified swelling index

Table 7.4 Soil Parameters for the dredged mud models

Soft- Soil	**0% Lime**	**2% Lime**	**4% Lime**
γ_{unsat} $[kN/m^3]$	15.98	14.88	13.97
γ_{sat} $[kN/m^3]$	15.98	14.88	13.97
k_{hp} $[m/day]$	0.000018	0.000045	0.00011
k_v $[m/day]$	0.000054	0.00016	0.0005
λ^* ***	0.130	0.149	0.156
k^* ***	0.032	0.018	0.009
+ c $[kN/m^2]$	1	1	1
+ φ $[^0]$	27	27	27
+ ψ $[^0]$	0	0	0
+ ν_{ur} ***	0.150	0.150	0.150
+ K_o^{nc} ***	0.546	0.546	0.546

The total vertical displacement of the three unit-cell drain models with varying lengths and widths corresponding to the materials with 0, 2, and 4% lime are shown in Figure, 7.5. The figure shows that the all three cases follow the similar pattern in settlement and more than 95% of consolidation achieved within the period of 1095 days. The deformed mesh of unit cells associated with the models containing 0, 2, and 4% lime are shown in Figures 7.6, 7.7, and 7.8 respectively. The observation of these three figures suggests that for a given preloading time (i.e. 1095 days), with increasing permeability of the dredged mud, the influence zone of the prefabricated vertical drain increases. Based on these findings, the influence zone of 1.2, 2.0, and 3.4 m was considered for the unit-cell models, containing 0, 2, and 4% lime respectively.

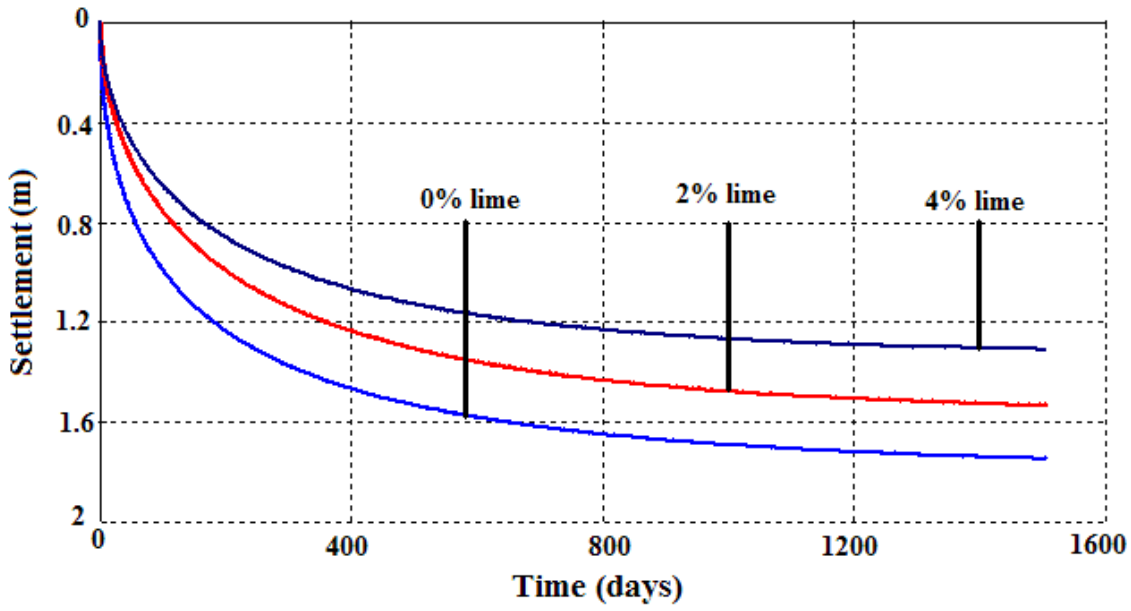

Figure 7.5 Settlement versus time for three unit-cell models (Plaxis)

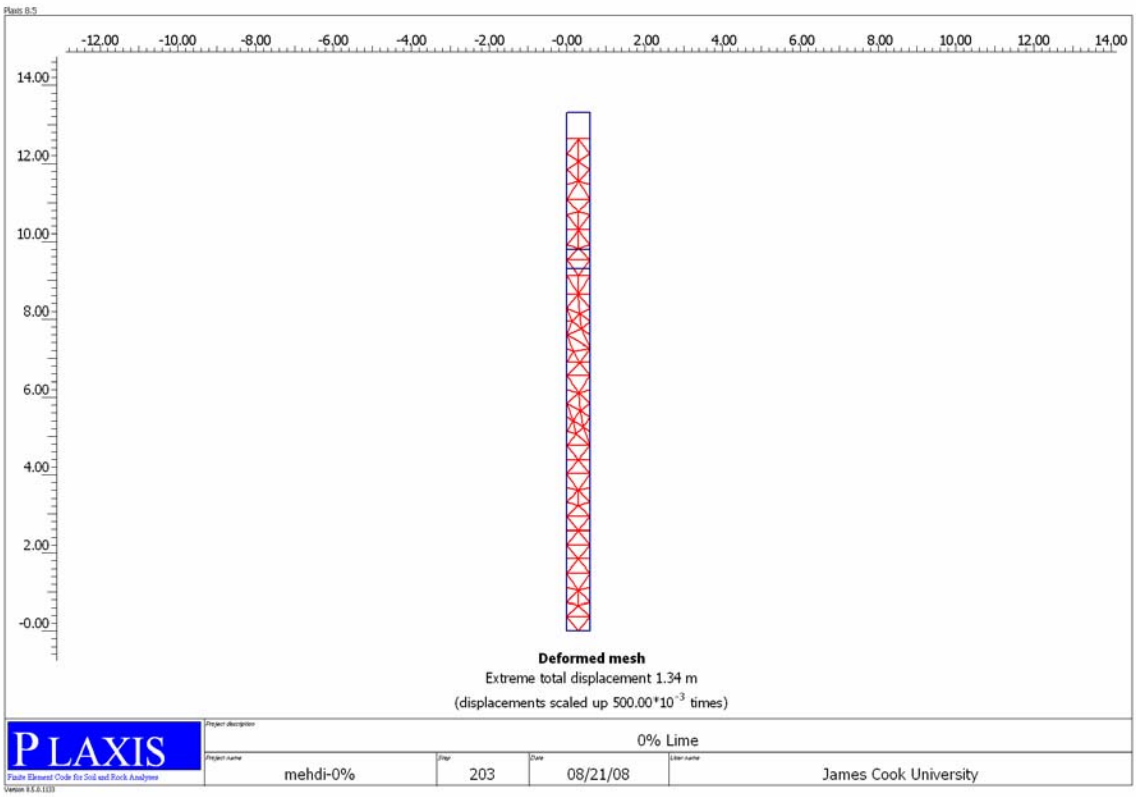

Figure 7.6 Deformed mesh of unit cell with 0% lime

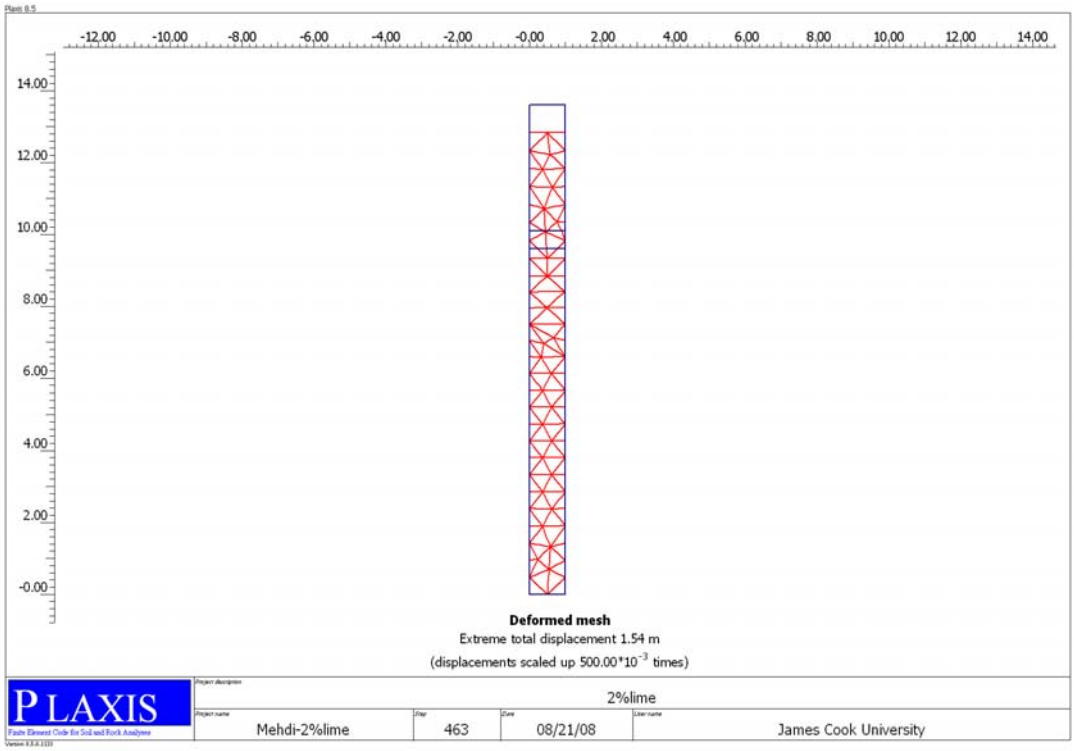

Figure 7.7 Deformed mesh of unit cell with 2% lime

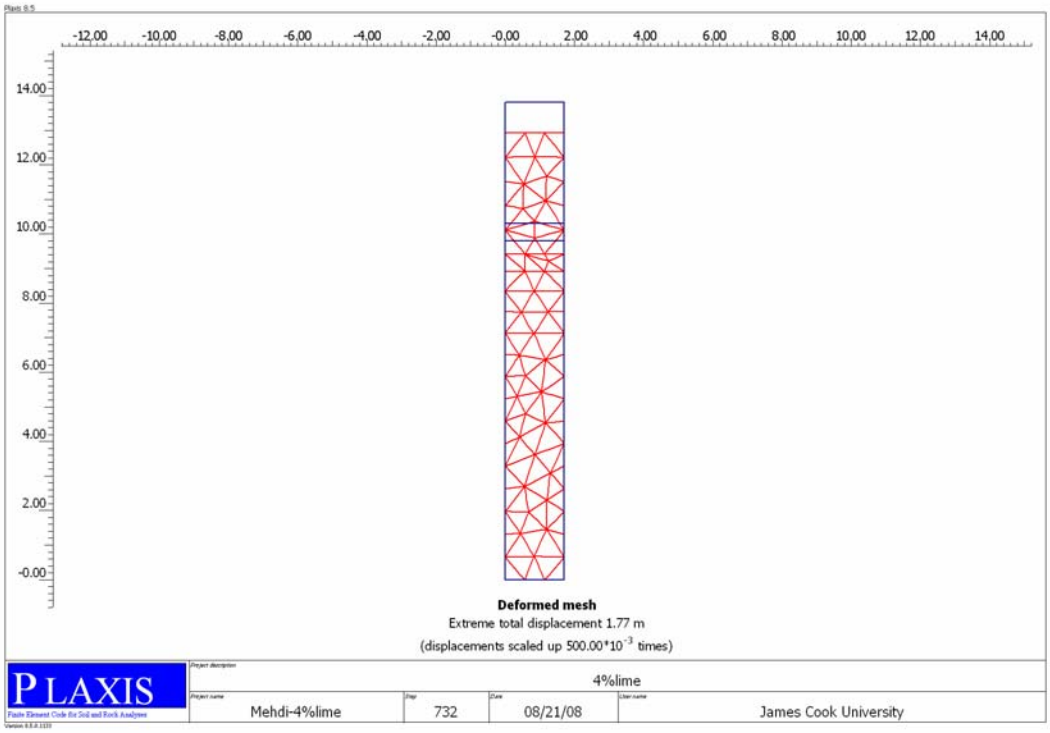

Figure 7.8 Deformed mesh of unit cell with 4% lime

As mentioned earlier, the empirical equation of $k_v = c_v \times m_v \times \gamma_w$ was employed here to estimate the values of the permeability used in the three dredged mud models. It is important to note that sometimes the accuracy of this equation in estimation the permeability may appear to be questionable. Olson (1985) discussed and examined the various graphical methods available in the literature and concluded that different methods estimate different values of c_v for the same data. The author suggested that the only logical way of evaluating c_v is to determine experimentally the coefficient of permeability, k, and the coefficient of volume compressibility, m_v, and substitute them into the equation.

In this study whereas, the Casagrande's graphical method was assumed as a reliable tool to produce the sound and reliable coefficient of consolidation and the permeability was

estimated thereof. To evaluate the accuracy of this assumption, an attempt was made to predict the settlement behavior of axisymmetric unit-cell drain by means of the analytical solution using the coefficient of consolidation instead of coefficient of permeability. It was envisaged that for the same dimensions of unit-cell model, the analytical solution by using c_v should result in the same consolidation behavior like what observed in modeling by means of Plaxis.

In chapter 5, the total consolidation of the ground due to both vertical and radial flow in vicinity of the ideal vertical drain was proposed as:

$$\overline{U}_{tot} = 1 - (1 - \overline{U}_z)(1 - \overline{U}_r)$$

where: $\overline{U}_z = \frac{2}{l}\sqrt{\frac{c_v t}{\pi}}$, and $\overline{U}_r = 1 - \exp\left(-\frac{8c_h t}{F_n D_e^{\,2}}\right)$

The input parameters used in the equations were similar to those employed in the finite element modeling. The values of the vertical coefficient of consolidation, c_v, for the material containing 0, 2, and 4% lime were considered as 0.32, 1.06, and 3.0 respectively, where $c_h = 1.2c_v$. The Microsoft spreadsheet, Excel, was then employed to calculate the settlement until more than 95% of consolidation in the three models was achieved. The settlement vs time curves of the three conceptual dredged mud layers are shown in Figure 7.9. This figure suggests that in all three cases, the ultimate ground settlement (> 95%) taken place within the elapsed time of 1095 days. This behavior was similar to that observed in Plaxis. However, it was found that for the early stage of consolidation, the rate of ground settlement in three models predicted by Plaxis, is slightly higher than what obtained by analytical approach. The observation of figures 7.5 and 7.9 suggest that the dissimilarity in settlement rate gradually decreases and almost becomes disappeared in the final stages of consolidation.

In overall, the general trend in the ground settlement, predicted by the both methods, confirms that the permeability values obtained by the empirical equation appear to be sound and reliable. In addition, It can be said that the fast ground settlement in initial stages of consolidation, predicted by Plaxis is likely attributed to the function of the

permeability change index parameter, $C_k = \frac{\Delta e}{\Delta \log k}$, employed in the calculation process in Plaxis. This parameter defines the variation of permeability with change in void ratio. In fact, for a given decrease in void ratio, large value of C_k imply small decreases in permeability and like versa. In soft soils, the shape of e versus $\log k$ curves in compression range is such that C_k is not constant and gradually decreases with compression (Terzaghi et al. 1996).

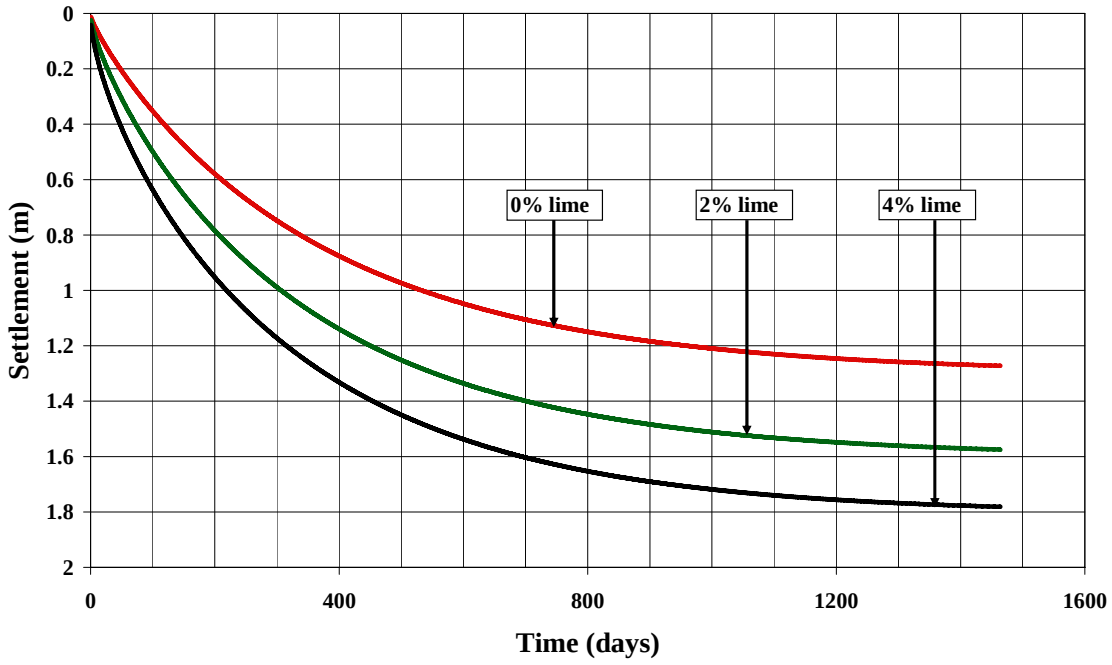

Figure 7.9 Settlement versus time for three unit-cell models (Analytical approach)

7.4.2 Vertical drain spacing

The assessment of the effect of % lime on the influence zone of the vertical drain was extensively conducted by the two analytical and finite element modeling. It was found that with increasing % lime from 0 to 4 percent, the influence drain zone of the vertical drain increases from 1.2 to 3.4 m respectively. This section aims to highlight the effect of this alteration on the vertical drain spacing in the conceptual reclamation site.

As discussed in chapter 5, for the square pattern of the drains installation, the following relationship is proposed:

$$S = \frac{D_e}{1.13}$$

where S is the distance between drains in the square pattern of installation.

According to the above relationship and based on the data in Table 7.2, the distance of 1.1, 1.8, and 3m is considered for the installation of vertical drains in the conceptual reclaimed layers containing 0, 2, and 4% lime respectively.

It can be said that for any reclamation site with a given area, A, the required number of vertical drains, n, in a square pattern is given by:

$$n = \frac{A}{S \times S}$$

For the purpose of this study, if an area of the containment pond in the reclamation site is 10000 m^2, the estimated number of vertical drains to be installed at the distances of 1.1, 1.8, and 3m are 8264, 3086, and 1111 respectively. Hence, the number of vertical drains can be shown by: $1n$, $0.37n$, and $0.13n$ where n is equal to 8264. This means that for any given area, the estimated number of vertical drains is n, $0.37n$, and $0.13n$ for the dredged mud layers treated with 0, and 4% lime respectively. This reduction trend in the required number of the vertical drains is schematically presented for three sites in Figure 7.10 for the purpose of comparison.

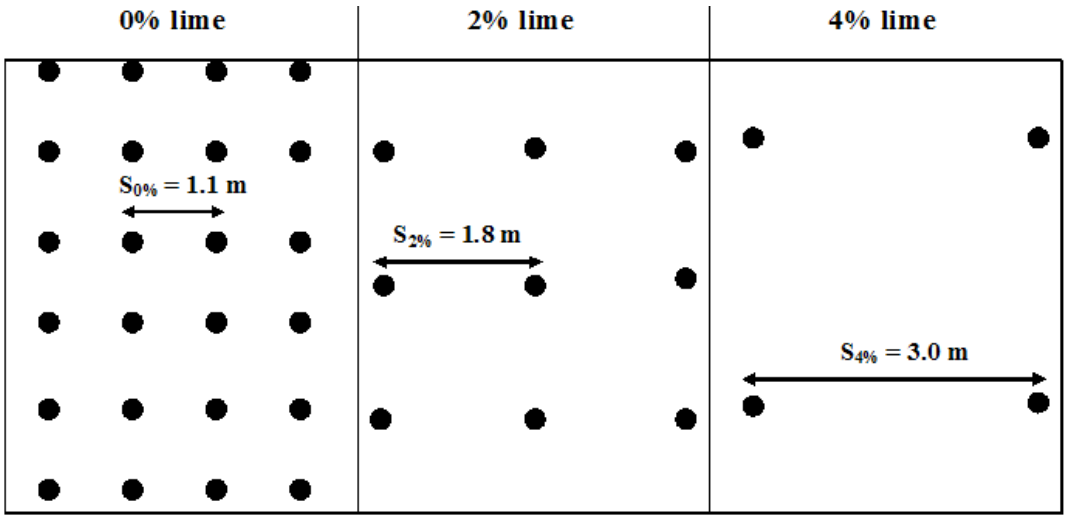

Figure 7.10 The approximate number of the vertical drains in three conceptual sites treated with varying percentages of lime

7.4.3 Full embankment analysis with vertical drains

In this section, the lateral deformation behaviour of the three conceptual models during the construction of embankment was analysed in full scale embankment model. The aim of this study was to assess the effects of % lime together with the rate of construction of embankment on the lateral displacement profile. The finite element mesh was based on 15-node elements. The drain element available in the Plaxis was used by the author to present the vertical drains within the mass of the dredged layer. The drain spacing was adapted based on the findings in section 7.4.1. The shape of embankment was assumed to be symmetrical around the centerline, and no lateral movement or force was assumed to cross the centerline. Based on this assumption, only half the embankment was created and the standard fixity option was used to define the boundary condition. For the all three models, the dimension of the geometry (half of the embankment) in horizontal direction was 50 m. The embankment loading in the three models was simulated by applying incremental vertical load to increase constantly within 30 and 90 days respectively. In modeling the lateral deformations, the input parameters of soil properties used from Tables 7.3 and 7.4. Figure 7.11 shows the typical finite element mesh which was used in analysis.

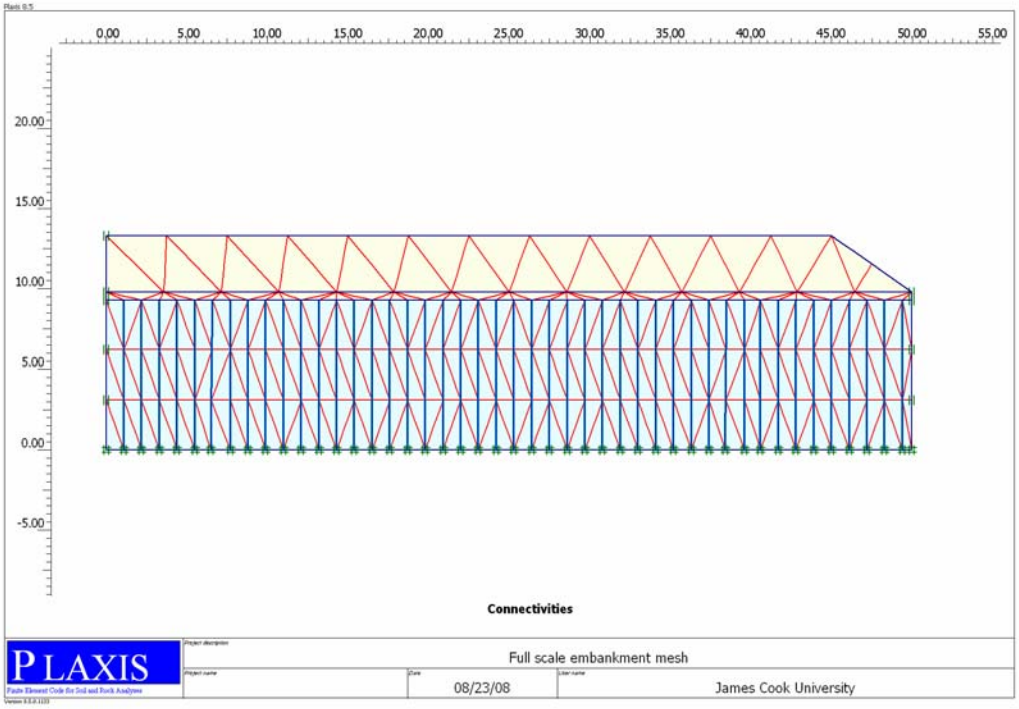

Figure 7.11 Finite element mesh of embankment

Figures 7.12, 7.13, and 7.14, show the general profile of simulated lateral soil deformation beneath the toe of embankment after 30 days, corresponding to the models containing 0, 2, and 4% lime respectively. The observation of these three figures suggests that the lateral displacement is almost independent of the conditions of the models (i.e. void ratio, height of dredged layer) and its extent appeared to be same in the three models. It can be seen that the maximum deformation for the embankment models containing 0, 2, and 4 % is 0.643, 0.516, and 0.560 m respectively. As clearly shown in the all models, the maximum displacement has taken place at relatively shallow depths below the ground surface. The deformation contours show that the magnitude of the lateral settlement gradually decreases with depth and in all three models the influence depth disappears at the middle of the dredged layer.

Figures 7.15, 7.16, and 7.17, show the occurrence of the lateral displacement after 90 days of construction phase corresponding to the models containing 0, 2, and 4% lime.

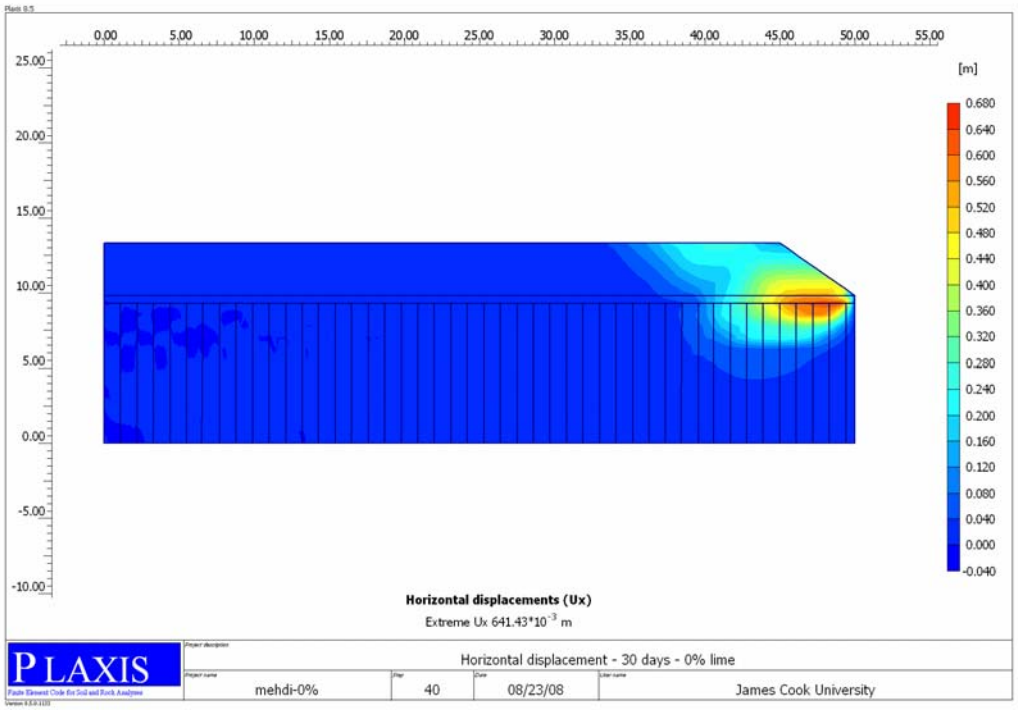

Figure 7.12 Lateral deformation contours at the toe of embankment for the model with 0% lime (30 days construction phase)

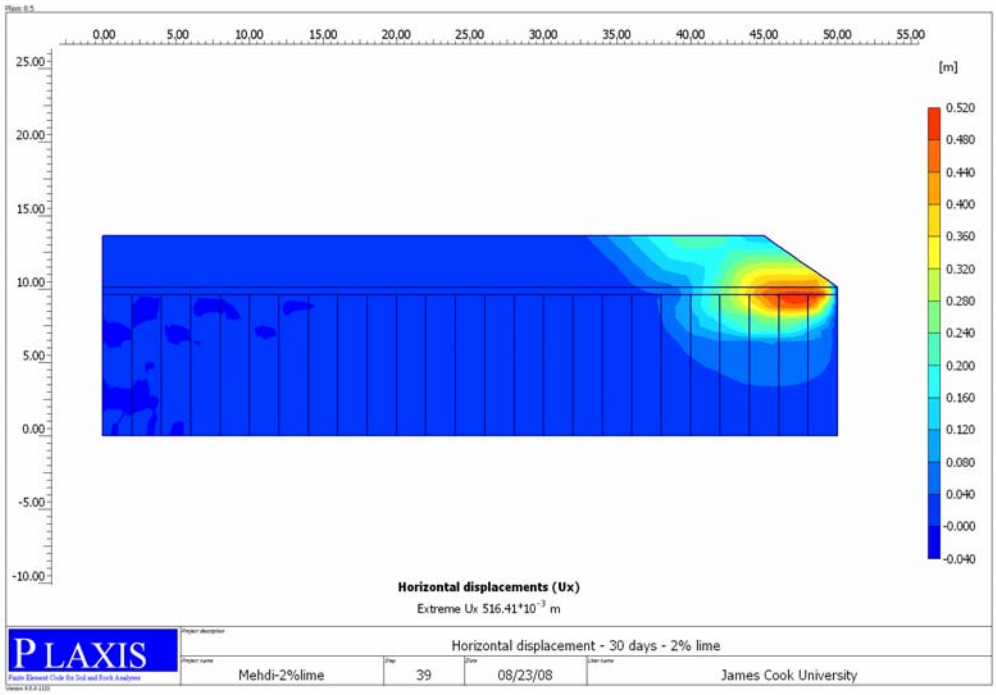

Figure 7.13 Lateral deformation contours at the toe of embankment for the model with 2% lime (30 days construction phase)

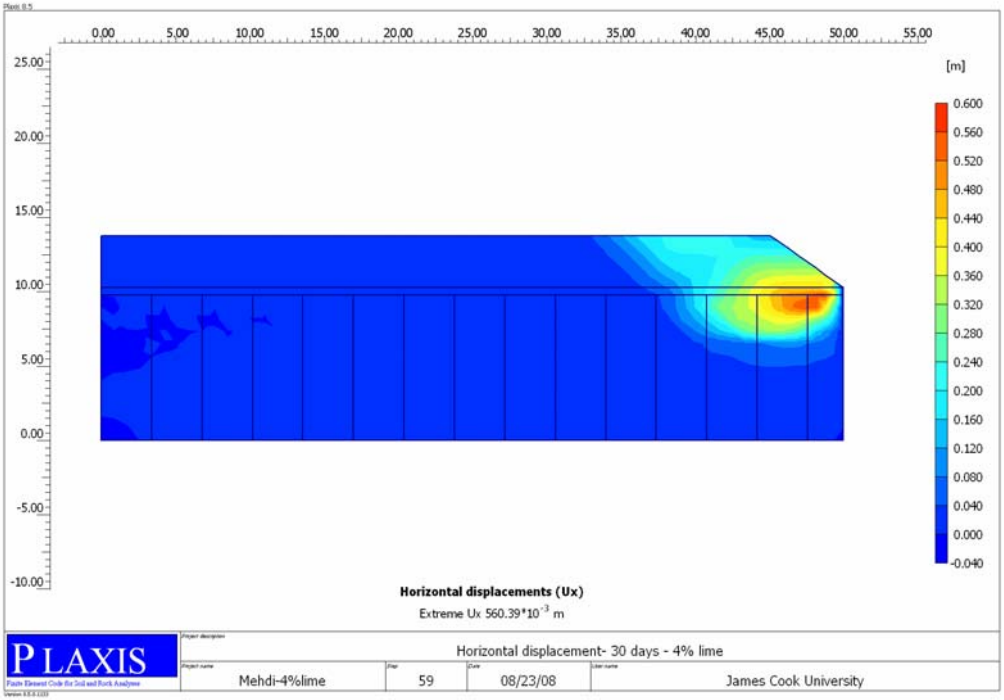

Figure 7.14 Lateral deformation contours at the toe of embankment for the model with 4% lime (30 days construction phase)

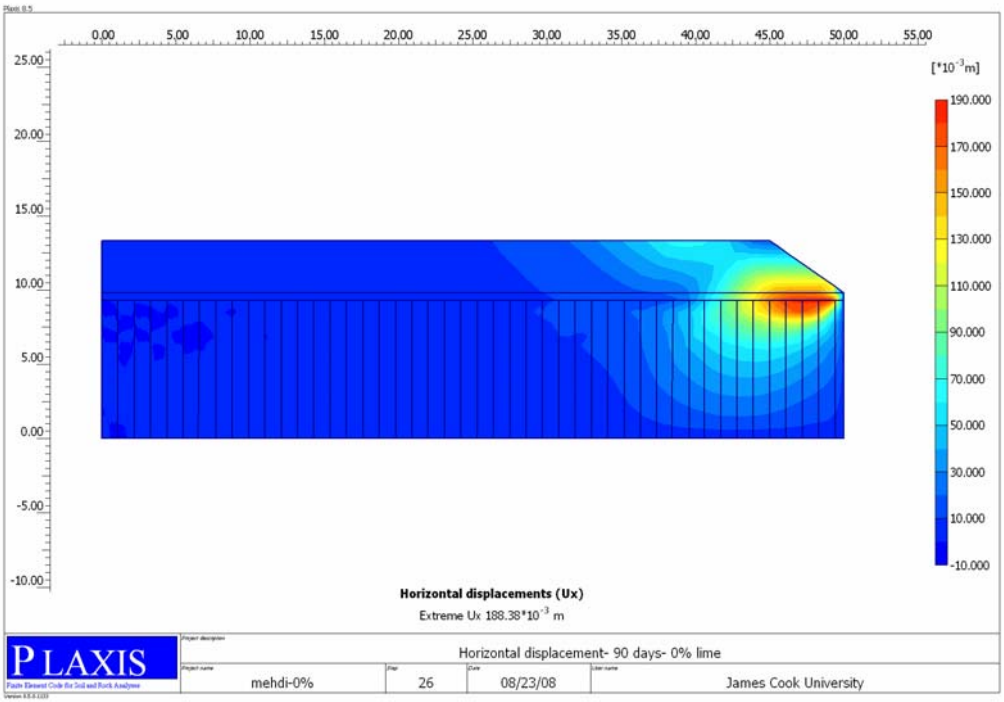

Figure 7.15 Lateral deformation contours at the toe of embankment for the model with 0% lime (90 days construction phase)

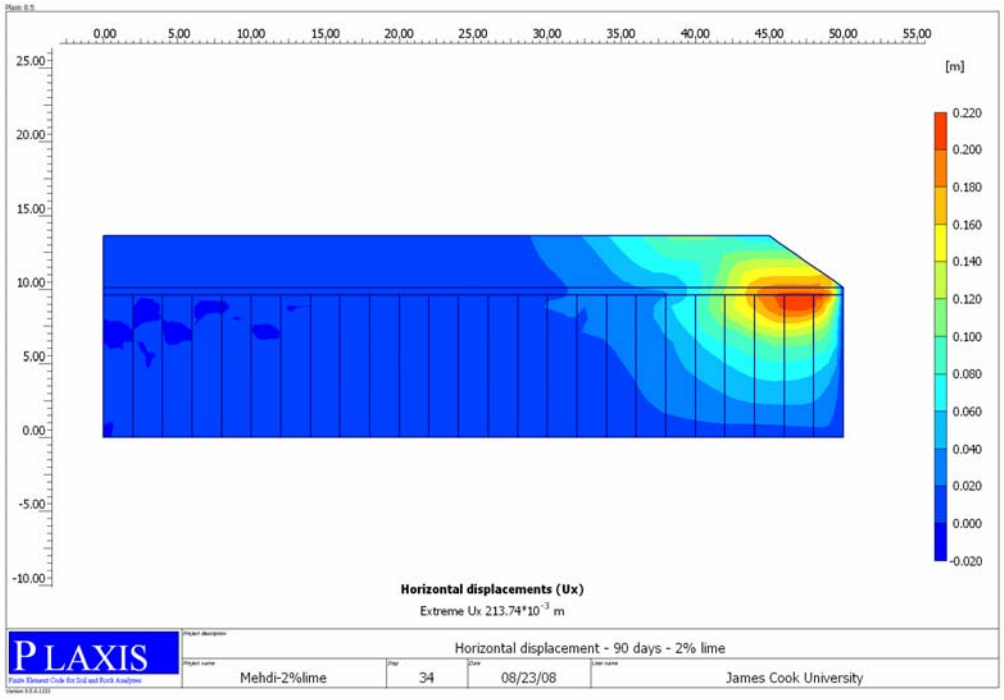

Figure 7.16 Lateral deformation contours at the toe of embankment for the model with 2% lime (90 days construction phase)

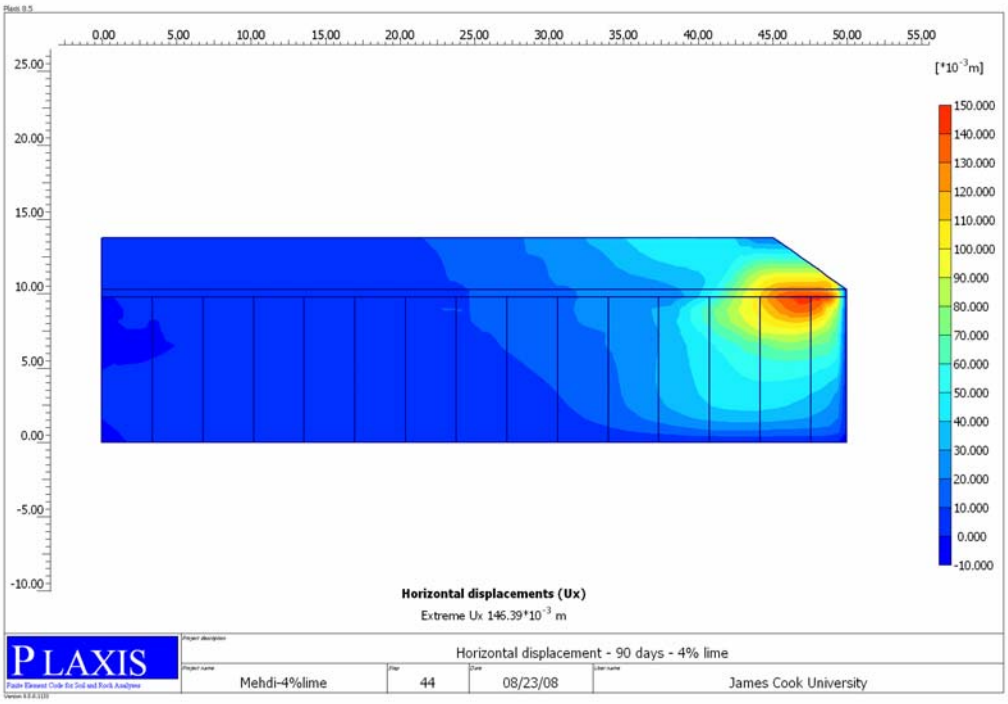

Figure 7.17 Lateral deformation contours at the toe of embankment for the model with 4% lime (90 days construction phase)

It can be seen that with decreasing the construction rate, the significant reduction in the maximum lateral displacement occurs. It is found that at the end of 90 days construction phase, the maximum lateral deformations of 0.188, 0.213, and 0.146 m has taken place in the models containing 0, 2, and 4 % lime respectively. The observation of figures associated with 90 days construction period, suggests that the lateral displacement develops rapidly at the surface (i.e. toe of the embankment) and spread downwards, under the lower rate, towards the bottom of layer (i.e. higher influence depth). Furthermore, with increasing the construction time, more lateral deformation occurs at the distances closer to the centerline. This behavior is likely attributed to the larger degree of pore water pressure dissipation in the recent models that resulting in an increase in effective stress within the soft layer beneath the embankment.

As it is shown, the three conceptual layers employed in the above modeling exercise, exhibited the different properties in terms of void ratio, permeability, and drain spacing.

However, in spite of these differences, their responses to the external load in respect to lateral displacement were almost same. This similarity in behavior may supports the idea that pretreatment of the dredged mud with hydrated lime, has no negative effects on the dredged deposit, in terms of the lateral stress-strain behavior.

7.5 Secondary compression settlement

In this chapter three conceptual models of reclamation sites were proposed. The dredged material of each model was assumed to contain 0, 2 and 4% lime. As discussed, in attempt to create more meaningful models, a few assumptions were considered for the conceptual sites. It was assumed that the surcharge preloading applies a total of 80 kPa effective stress where the surcharge load only accounts for 40 kPa. Since the final design load, placed after the removal of surcharge was considered as 20 kPa, it can be said that the effective surcharge ratio of 0.33 was employed. It was also assumed that rebound after removal of the surcharge was negligible. These assumptions are considered in this section to assess further ground settlement of the models upon EOP in the secondary compression stage.

It was stated in Chapter 5 that the settlement of the ground due to post-construction secondary compression is given by:

$$S = \frac{C_{\alpha}^{'}}{1+e_0} H_0 \log \frac{t}{t_p}$$

where e_0 and H_0 are void ratio and thickness of the layers at EOP before removal of the surcharge as shown at the beginning of this chapter. t_p is the preloading time of 3 years (1095 days), and t is any elapsed time beyond t_p.

The values of post-construction secondary compression index, $C_{\alpha}^{'}$, corresponding to the effective surcharge ratio of 0.33 can be derived from Figure 6.23 in chapter 6.

Figure 7.18 shows the calculated ground settlement of the three conceptual sites due to post-construction secondary compression for the period of 100 years. As shown in Figure

7.18, for the non-treated dredged layer (i.e. 0% lime), a total settlement of 80 mm is anticipated to take place over the period of 100 years. The compression settlement in both layers containing 2% and 4% lime follow the same pattern and overlap at all times. An observation of Figure 6.23 shows that the post-construction secondary compression index corresponding to the effective surcharge ratio of 0.33 for the material containing 2 and 4% lime is 0.008 and 0.006 respectively. The slight difference in the value of the secondary compression index of the two materials is responsible for the same compression settlement behavior. For the non-treated dredged mud however, the post-construction secondary compression index of 0.014 is high enough to bring about significant ground settlement. It also has to be mentioned that the initial void ratio is another factor that accounts for secondary compression settlement. As shown in Table 7.1, at the applied effective stress of 80 kPa, the materials containing 0, 2, and 4% lime, present the void ratio of 1.38, 1.79, and 2.34 respectively. Since the initial thickness is assumed to be constant for the three models, with an increase in the void ratio, the ratio $\frac{H_0}{1+e_0}$ reduces, which obviously lessens in secondary compression settlement.

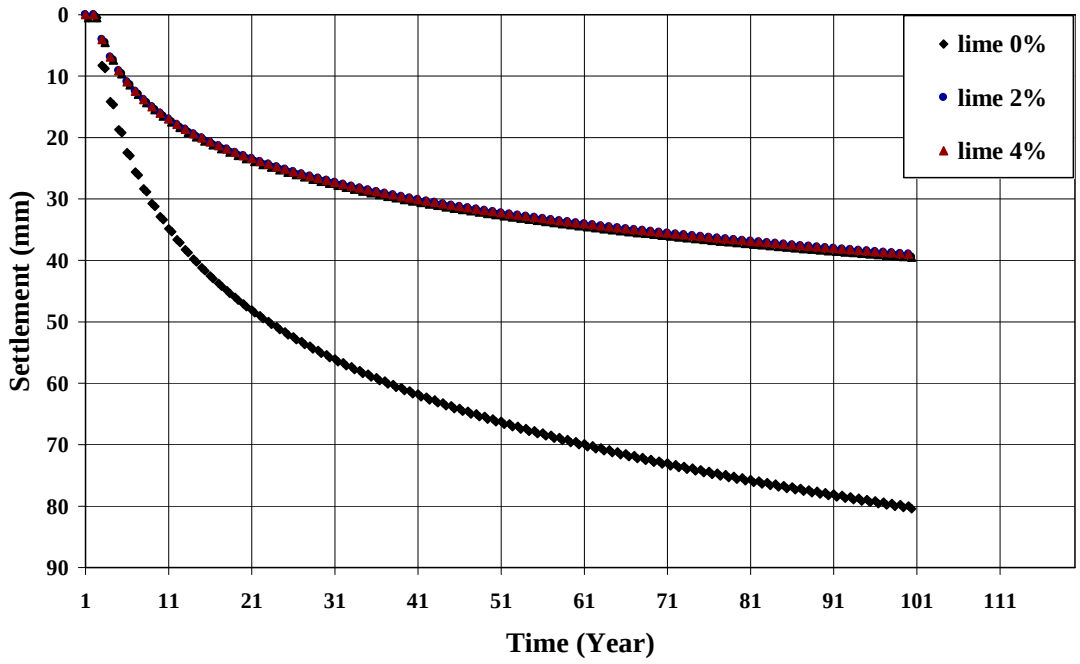

Figure 7.18 Secondary compression settlements of the three sites treated with varying percentages of lime

7.6 Summary and conclusion

This chapter aimed to create a conceptual reclaimed layer in a man-made island by utilizing laboratory consolidation test data. A general process of construction of a man-made island from dredging to ground improvement by means of surcharge preload was discussed. A systematic procedure for the estimation of the ground conditions in terms of void ratio and elevation before and after placement of surcharge preload was proposed. The development of the conceptual sites was based on a few assumptions as fully discussed. The main objectives of modeling the reclamation sites were to evaluate the effect of % lime on the variation of vertical drain spacing, lateral displacement, and secondary compression settlement. Modeling of the consolidation behavior of dredged mud layer and prefabricated vertical drains (PVD) was carried out by the finite element modeling method using Plaxis Version 8 software. As an alternative, the analytical approach was used to validate the Plaxis outputs. The behavior of the vertical drains was analyzed by plane strain theory for the unit-cell models. The analysis of the three unit cell models in the conceptual dredged mud layer containing 0, 2, and 4% lime showed that for a given preloading time, the influence zone of the unit-cell increases as % lime increases. This behavior was further analyzed and interpreted to estimate the required number of vertical drains for any containment pond with an area of A. It was found that for the type of dredged mud used in this study, for any area of a reclaimed land, as % lime increases from 0, to 2, and 4%, the required number of vertical drain decreases from n, to $0.37n$, and $0.13n$ respectively.

As a second objective, the effect of % lime on the development of lateral displacement of the three models during the construction of embankment was evaluated by full scale analysis method using a 2D model. For the same conceptual site, the analysis was carried out twice to assess the rate of construction of embankment on development of the lateral displacement. It was found that the lateral displacement is almost irrespective to the conditions of the models (i.e. void ratio, height of dredged layer) and its extent appeared to be same in the three models. The comparison between analysis of the models at 30 and 90 days suggested that with decreasing the rate of construction of embankment, the

maximum lateral displacement decreases while the influence zone in both vertical and horizontal direction (i.e. from the toe of embankment) increases.

Prediction of the secondary compression settlement of the three conceptual sites was carried out for the project design life of 100 years. It was found that the secondary compression settlement of the non-treated ground was almost twice those with 2 and 4% lime. However, there was no distinct difference in terms of secondary compression settlement for the grounds with 2 and 4% lime.

As a conclusion, it can be said that the pre-treatment of the dredged mud prior to discharging in the containment pond can significantly contribute towards the economy of the project by eliminating the requirement for a high number of vertical drains in order to meet the tight scheduled preloading time. The full scale embankment analysis also showed that the proposed approach in ground improvement is less likely to affect and alter the lateral stress-strain behavior of the dredged mud deposits.

The post-construction secondary compression settlement usually poses a threat to infrastructure facilities constructed on the soft ground. As stated in chapter 5, one way to mitigate this problem is by increasing the surcharging effort to lessen the secondary compression settlement. One solution to increase the surcharging effort is by placing more fill material on top of the soft foundation (i.e. increasing the elevation of the embankment). Such a strategy requires further need for high quality fill materials that are normally obtained from inland. It is certain that this approach contributes a significant cost to the project development. However, a modification of clay particles chemistry with the addition of a slight amount of lime to the dredged mud slurry, for a given surcharge effort, the post-construction secondary compression settlement can be significantly reduced.

Chapter 8

Summary, Conclusions and Recommendations for Future Research

8.1 Summary

Dredged mud may be used as a fill material in the construction of a man-made island. This material mainly consists of silt or clay grains with high moisture content, resulting in low shear strength and poor consolidation behavior. Thus, some kind of treatment is necessary to achieve adequate engineering properties for the soft ground created by utilizing the dredged mud. To improve the engineering behavior of the soft deposit, several improvement techniques are available in geotechnical engineering practice, one of which is surcharge preloading with vertical drain. The consolidation of a soft foundation under preload is the process of decreasing the volume of saturated soil by expelling the pore water. The rate of ground consolidation is governed by the three factors: Compressibility, Permeability, and Length of the drainage paths. Furthermore, after removal of surcharge and under the application of final design load the settlement of the soft ground will continue. The surcharging effort which is defined as an effective surcharge ratio, governs the extent of the post-construction secondary compression settlement.

An attempt was made to provide insight into some factors, aimed to improve efficiency of the surcharge preload technique. A series of laboratory tests was performed to evaluate the effect of clay fabric, altered due to the addition of hydrated lime into slurry, on the primary and secondary consolidation behavior of dredged mud samples.

The experimental program commenced with a field trip to the reclamation site of the Port of Brisbane to gather information about the general dredging operation of the project and perform sampling. The laboratory study was started with a basic study on the properties of the dredged mud including, particle size distribution, Atterberg limits, specific gravity, quantitative assessment of the mineralogy, and scanning electron microscopy. A simple laboratory apparatus, named seepage induced consolidation test, was proposed as a new technique in determination the threshold value of lime in soil, below which the maximum flocculation takes place. The seepage induced consolidation test was performed on the natural and lime treated dredged mud slurry under the condition of 350% and 550% moisture content, to verify the Lime Modification Optimum of the dredged mud. As a second sequence of the laboratory study, a series of the oedometer test was conducted on the natural and lime treated dredged mud. The prime objective of the consolidation tests program was to assess the effect of % lime on the primary consolidation and secondary compression behavior of the dredged mud. The new approach of the rapid loading consolidation test was proposed to precisely evaluate the primary and secondary consolidation behaviour of the dredged mud. To study the anisotropy of the dredged mud, the modified ring for oedometer test was developed to facilitate the consolidation test with the radial flow.

The large industrial size of the conceptual reclamation site was generated by means of the laboratory data. The aims of this simulation were to evaluate the effect of % lime on the influence zone of the prefabricated vertical drain, lateral displacement, and the secondary compression settlement of the soft ground. For the first two objectives, modeling of the consolidation behavior of the dredged layer with installed vertical drains was carried out by the finite element modeling (FEM) method, using Plaxis Version 8. The plane strain unit-cell approach was employed to estimate the effect of % lime of the influence zone of the vertical drain while the full scale embankment analysis used in prediction of lateral displacement behavior of the dredged layer. As a third objective, the secondary compression settlement of the conceptual reclaimed sites was evaluated by analytical solution.

8.2 Conclusion

The conclusions drawn from this thesis are divided into the sections corresponding to the assessment made through the study.

8.2.1 Laboratory study – Phase 1

A series of laboratory studies were undertaken on the dredged mud sample obtained from the reclamation site of the Port of Brisbane in Australia to evaluate both chemical and mechanical properties of the dredged mud. It was found that the index properties and specific gravity of the base sample were drastically affected by the method of preparation. The liquid limit, plastic limit and specific gravity reduce as the samples are dried out for preparation purposes. The extent of these changes increase as higher temperatures is applied during preparation.

One of the main objectives was to introduce a new laboratory technique to determine the threshold value of lime in clay soil, below which only flocculation of particles takes place. This threshold value is termed “Lime Modification Optimum” and was first introduced to the literature by McCallister and Petry (1992). This technique is known as the seepage-induced consolidation test which is primarily devised to study the consolidation behavior of the soft clay. This research however, proposed a different application for this laboratory setup aimed at evaluating the lime modification optimum (LMO) for the clay soil. The experimental data showed that for the type of clay soil used in this study, the maximum flocculation and permeability of amended soil was achieved when 4% of lime is added. To evaluate the accuracy of the data obtained from the seepage-induced consolidation test another laboratory setup known as a sedimentation column was employed to investigate the percentages of lime which contribute towards modification (i.e. flocculation) of the clay particles. The test results obtained from this laboratory arrangement showed that the addition of 4% lime should be considered as a threshold value, below which maximum flocculation takes place in the type of material used in this study. These findings, together with a study of the photographs taken by the

scanning electron microscope suggested that the proposed seepage-induced consolidation test can be used as a reliable and fast laboratory technique to determine the LMO.

It is interesting to note that addition of lime to the dredged mud induced flocculation and caused both the void ratio and permeability to gradually increase with % lime. The higher capacity in holding water as a result of changing the fabric was also observed in the liquid limit of the lime treated dredged mud which showed increase as % lime increased.

The most significant interpretation which can be made from the seepage-induced consolidation test results is that the modification affect of lime on clay particles is independent of the degree of initial moisture content. In the experimental program, two representative lime-treated sub-samples were tested with high moisture content (350% and 550%) in order to evaluate the effect of moisture content on the lime-clay modification reaction. It was found that in the both sub-samples the similar results in terms of void ratio and permeability were achieved, indicating that the mechanism of lime-clay modification is not negatively affected by the degree of moisture content.

8.2.2 Laboratory study – Phase 2

The main objective of the laboratory test program in this section was to evaluate the effect of % lime up to the lime modification optimum, on consolidation parameters of the dredged mud. A set of oedometer tests was conducted in both normally consolidated and artificially overconsolidated stages on both natural and lime treated samples. It was found that the new fabric of sediment under varying percentages of lime affects the consolidation behavior of the lime treated dredged mud to varying extents. The laboratory findings revealed that in both compression and recompression states, the coefficient of consolidation drastically increases. In the compression range, the increase of c_v was observed up to ten fold, with an increase of lime up to 4 percent. The coefficient of consolidation governs the rate of ground settlement. The higher the values of the coefficient of consolidation, the faster the ground reaches its ultimate primary consolidation settlement.

Observation of the test results suggests that in the compression range, the values of the compression index increase when increasing the lime content whereas in the recompression range, the value of the recompression index gradually decreases with increasing % lime. This finding indicates that with increasing % lime, the magnitude of primary consolidation in the NC state increases while in the OC state it decreases.

It is interesting to note that the secondary compression index in both the compression and recompression range decreases with increasing % lime. In the compression range the decreasing of C_α together with an increase of C_c, results in a gradual reduction of C_α / C_c as the amount of lime increases. It is worthwhile stating that the surcharging effort was found to be more effective in a further reduction of the secondary compression index of the natural dredged mud in comparison with lime treated dredged mud.

The empirical correlation between coefficient of consolidation, void ratio and corresponding effective stress was proposed and evaluated in this chapter. It was found that for the type of the dredged mud used in this study, irrespective of the percentages of added lime, the coefficient of consolidation can be obtained by knowing the state of void ratio and effective stress at any instance during consolidation. Even though this equation holds true for all natural and lime treated specimens in the laboratory however, the applicability of the equation in predicting the coefficient of consolidation of the soft ground in the field requires more assessment.

The modified oedometer apparatus with horizontal drainage was developed to determine the horizontal coefficient of consolidation and evaluate the state of anisotropy of the natural and lime treated dredged mud. The anisotropy was defined as a ratio of c_h / c_v. It was found that with increasing the % lime, the horizontal coefficient of consolidation increases in the same manner of vertical coefficient of consolidation, resulting in c_h / c_v ratio almost being in unity. Since the coefficient of volume compressibility is independent to the drainage condition, $k_v = c_v m_v \gamma_w$, and $k_h = c_h m_v \gamma_w$. Therefore, the ratio

of c_h / c_v is similar to the ratio of k_h / k_v. Because $k_h / k_v \approx 1$ is valid for the natural and lime treated specimens, it was concluded that in spite of the change in the fabric (i.e. increase in void ratio at the same effective stress), with increasing % lime, the state of the permeability isotropy remained unchanged.

8.2.3 Modeling of a man-made island

A general process of construction of a man-made island from dredging to ground improvement by means of surcharge preload was discussed. A systematic procedure for the estimation of the ground conditions in terms of void ratio and elevation before and after placement of surcharge preload was proposed. The development of the conceptual sites was based on a few assumptions as fully discussed. The main objectives of modeling the reclamation sites were to evaluate the effect of % lime on the variation of vertical drain spacing, lateral displacement, and secondary compression settlement. Modeling of the consolidation behavior of dredged mud layer and prefabricated vertical drains (PVD) was carried out by the finite element modeling method using Plaxis Version 8 software. As an alternative, the analytical approach was used to validate the accuracy of the Plaxis outputs. The behaviour of the vertical drains was analyzed by plane strain theory for the unit-cell models. The analysis of the three unit cell models in the conceptual dredged mud layer containing 0, 2, and 4% lime showed that for a given preloading time, the influence zone of the unit-cell increases as % lime increases. This behavior was further analyzed and interpreted to estimate the required number of vertical drains for any containment pond.. It was found that for the type of dredged mud used in this study, for any area of a reclaimed land, as % lime increases from 0, to 2, and 4%, the required number of vertical drain decreases from n, to $0.37n$, and $0.13n$ respectively.

As a second objective, the effect of % lime on the development of lateral displacement of the three models during the construction of embankment was evaluated by full scale analysis method using a 2D model. For the same conceptual site, the analysis was carried out twice to assess the rate of construction of embankment on development of the lateral

displacement. It was found that the lateral displacement is almost independent to the conditions of the models (i.e. void ratio, height of dredged layer) and its extent appeared to be same in the three models. The comparison between analysis of the models at 30 and 90 days suggested that with decreasing the rate of construction of embankment, the maximum lateral displacement decreases while the influence zone in both vertical and horizontal direction (i.e. from the toe of embankment) increases.

A prediction of the secondary compression settlement of the three conceptual sites was carried out for the project design life of 100 years. It was found that the secondary compression settlement of the non-treated ground was almost twice those with 2 and 4% lime. However, there was no distinct difference in terms of secondary compression settlement for the grounds with 2 and 4% lime.

8.3 Recommendations for future research

Whilst there have been considerable achievement through this dissertation in understanding the beneficial potential of lime-clay modification in the construction of a man-made, there are one area that deserve further study.

The settling rate of dredged clay is an important factor to consider in land reclamation planning and for the used of the reclaimed land. The settling types of the dredged mud in a containment pond are divided to zone settling and consolidation settling (Imai, 1980). During zone settling, discrete flocs are formed from clay or flocculated particles and settle slowly at a constant rate. In consolidation phase, no discrete flocs present and in comparison to the settling zone, the consolidation rate of the solid- liquid interface is very slow. This type of settlement is known as self-weight consolidation. It has been found that the Terzaghi's classic consolidation theory is not applicable for predicting the settlement rate due to self-weight consolidation. Gibson et al. (1967, 1981) proposed the equation for one-dimensional finite strain consolidation including self-weight for homogeneous layers. In reclamation projects, the design and operation plan must

accurately account for the long-term increase in storage capacity of containment pond resulting from decreases in the height of dredged fill deposited. Since the consolidation process is slow, particularly in the case of fine-grained materials, it is likely that the total settlement will not have taken place before the containment area is required for additional placement of the dredged materials.

As it was shown in chapter 4, the dredged mud specimen treated with varying percentages of lime, exhibit the different self-weight consolidation behaviour. Therefore, it is recommended that further research in the self-weight consolidation behaviour of the lime treated slurry would be valuable.

REFERENCES

Ahnberg, H. (2007) On yeild stresses and the influence of curing stresses on stress paths and strength measured in triaxial testing of stabilized soil. *Canadian Geotechnical Journal*, **44**(1), 54-66.

Anson, R.W.W., and Hawkins, A.B. (1998) The effects of calcium ions in pore water on the residual shear strength of kaolinite and sodium montmorillonite, *Geotechnique* **48**(6), 787–800.

Akagi, T. (1977) Effect of mandrel-driven sand drains on strength, *Proceeding of the 9th International Conference on Soil Mechanic and Foundation Engineering*, Tokyo, **Vol. 1,** 3-6.

Arman, A. and Munfakh, G.A. (1970) Stabilization of Organic Soils with Lime Engineering Research Bulletin, **103**, Louisiana State University,USA.

Asaoka, A. (1978) Observation procedure of settlement prediction. *Soils and Foundations,* **18**(4), 87-101.

Barron, R.A. (1948) Consolidation of fine-grained soils by drain wells, *Trans. ASCE*, 113 (Paper No. 2346), 718-742.

Bell, F. G. (1988) Stabilisation and Treatment of Clay Soils with Lime. Ground Engineering **21**(1), 10-15.

Bennett, R. H., and Hulbert, M. H. (1986) *Clay Microstructure*. International Human Resources Development Corp, Boston.

Bergado, D.T., Anderson, L.R., Miura, N., and Balasubramaniam, A.S. (1996) Soft ground Improvement in lowland and other environments, American Society of Civil Engineeris, USA

Bergado, D.T., Alfaro, M.C., Balasubramaniam, A.S. (1993). Improvement of soft Bangkok clay using vertical drains. *Geotextiles and Geomembranes*, **12,** 615-663.

Bergado, D.T., Asakami, H., Alfaro, M.C., Balasubramaniam, A.S. (1991) Smear effects of vertical drains on soft Bangkok clay. *Journal of Geotechnical engineering, ASCE,* **117**(10), 1509-1530.

Bjerrum, L. (1973) Problems of Soil Mechanics and Construction on Soft Clays, State-of-the-Art Report to Session IV, *Proceedings of the 8th International Conference on Soil Mechanics and Foundation Engineering*, Moscow, **Vol.3**, 111-159.

Boardman, D. I., Glendinning, S., and Rogers, C. D. F. (2001) Developement of stabilisation and solidification in lime-clay mixes. *Geotechnique*, **50**(6) 533-543.

Boynton, R. (1980) *Chemistry and technology of lime and limestone*. New York, John Wiley and Sons Inc.

Brandl, H. (1981). Alteration of soil parameters by stabilisation with lime. *Proceedings of the 10th International Conference on Soil Mechanics and Foundation Engineering Stockholm*, Sweden, pp 587-595

British Standards Institution (1990). Stabilized materials for civil engineering purpose. Methods of test for cement-stabilized and lime-stabilized materials, *BS* 1924: Part 2. London: BSI.

Broms, B., and Boaman, P. (1979) Lime columns- A new foundation method, *Journal od Geotechnical Engineering, ASCE*, **105**, 539-590

Broms, B. and P. Boman (1975) Lime stabilized columns. *5th Asian Regional Conference on Soil Mechanics and Foundation Engineering,* Bangalore, India.

Buensuceso, B. R. (1990) Engineering behavior of lime treated soft bangkok Clay. Asian Institute of Technology. *Ph.D thesis*, Asian Institute of Technology, Bangkok.

Cargill, K. W. (1983) Procedure for prediction of consolidation in soft fine-grained dredged material. Vicksburg,MS., U.S. Army Waterways Experiment Station.

Carrillo, N. (1942) Simple two and three dimensional cases in the theory of consolidation of soils. *Journal of Mathematics and Physics*, **21**(1), 1-5

Cassagrande, A. and Fadum, R.E. (1940) Notes on soil testing for engineering purposes. *Harvard University Graduate School Engineering Publication*, No. 8.

Chai, J.C., Shen, S.L., Miura, N. and Bergado, D.T. (2001) Simple method of modeling PVD improved subsoil, *Journal of Geotechnical Engineering, ASCE*, **127**(11), 965-972.

Chaddock, B.C.J. (1996) The structural performance of stabilised soil in road foundations. *In Lime Estabilisation*, 75-94. London: Thomas Telford.

Chapman, D.L. (1913), A contribution to the theory of electrocapillarity: *Philosophical Magazine*, ser. 6, v.25, 475-481.

Chu, J., Bo, M.W., Choa, V. (2004) Practical considerations for using vertical drains in soil improvement projects. *Geotextiles and Geomembranes,* **22**, 101-117.

Clare, K. E. and Pollard, A.E. (1951) *Magazine of Concrete Research*, No. SP57, London.

Coffey Geosciences (2004) Onshore Reclamation Study Paddocks S2, S3a, and S3b, Port of Brisbane Corporation.

De Wit, P. J. (1995), Liquefaction of cohesive sediments caused by waves. *PhD dissertation*, Delft University of Technology, the Netherlands.

Diamond, S. and Kinter, B. (1965) Mechanisms of Soil Stabilisation, *Highway Research Record* 92 W. National Research Council.

Eades, J. L., and Grim, R. E. (1966) A quick test to determine lime requirements of lime stabilisation. In Bahaviour characteristics of lime-soil mixtures. *Highway Research Record*, **139,** 61-72.

El-Rawi, N. M., and Awad, A. A. A. (1981) Permeability of lime stabilized soils. *Transportation Engineering Journal*, **107**(1), 25-35.

Feng, T.-W. (2002). Effects of small cement content on consolidation behavior of a lacustrine clay. *Geotechnical Testing Journal*, **25**(1), 53-60.

Fossberg, E. (1965) Some Fundamental Engineering Properties of Stabilised Clay. *Proceeding of the 6th International Conference of Soil Mechanics and Foundation Engineering*, Montreal,Canada.

Fox, P. J. (1996) Analysis of hydraulic gradient effects for laboratory hydraulic conductivity testing. *Geotechnical Testing Journal*, **19**(2), 181-190.

FPE Seawall Alliance (2003) Factual Geotechnical Report.

Galvao, T. C. B., A. Elsharief, Gustavo Ferreira Simoes (2004) Effects of lime on permeability and compressibility of two tropical residual soils. *Journal of Environmental Engineering*, **130**(8), 881-885.

Gibson, R.E., England, G.L., and Hussey, M.J.L (1967) The theory of one-dimensional consolidation of saturated clays, I- Finite non linear consolidation of thin homogeneous layers. *Geotechnique*, **Vol. 17**, 261-273.

Gibson, R.E., Schiffman, R.L., and Cargill, K.W. (1981) The theory of one-dimensional consolidation of saturated clays, II- Finite non linear consolidation of thick homogeneous layers. *Canadian Geotechnical Journal*, **Vol.18**, 280-293.

Gouy, J. (1909) Sur la constitution de la charge electrique a la surface d'un electrolyte: Comptes Rendus des Seances de l'Academic des Science, **Vol. 149**, 654-657.

Grim, R.E, (1968) *Clay Mineralogy*, 2nd ed.: New York, McGraw-Hill Book Co.

Groenewold, S. and Dankers, N.M.J.A (2002) Ecoslib,de ecologische rol van slib, Tech. Rept. 519, Alterra, Wageningen.

Hansbo, S. (2005) Experience of consolidation process from test areas with and without vertical drains. *Ground Improvement*, Elsevier, **3,** 3-49.

Hansbo, S. (2004) Band drains, In Moseley, M.P. & Krisch, K. *Ground Improvement*, Taylor and Francis Group, London and New York.

Hansbo, S. (1997) Aspects of vertical drain design: Darcian and non- Darcian flow. *Geotechnique*, **47**(5), 983-992.

Hansbo, S. (1987) Design aspects of vertical drains and lime column installation, *Proceedings of the 9th Southeast Asian Geotechnical Conference*, **Vol. 2,** No.8, 1-12.

Hanbo, S. (1981) Consolidation of fine- grained soils by prefabricated drains, *Proceeding of the* 10th *International Conferences on Soil Mechanics and Foundation Engineering*, Stockholm, **Vol.3,** Paper 12/22 677-682.

Hansbo, S. (1979) Consolidation of clay by band-shaped prefabricated drains. *Ground Engineering*, **12**(5), 16-25.

Hebib, S. and Farrel, E.R (2002) Deep Soil Mixing for Organic Soils. *The Engineers Journal*, 25-29.

Hebib, S. and Farrel, E.R. (2003) Some experience on the stabilisation of Irish peat. *Canadian Geotechnical Journal*, **40**, 107-120.

Hird, C.C., Pyrah, I.C., and Russell, D. (1992) Finite element modeling of vertical drains beneath embankments on soft ground, *Geotechnique*, **42**(3), 499-511.

Holm, G. (1999) Application of dry mix methods for deep soil Stabilizations. *Deep Mix Methods for Deep Soil Stabilization*, Rotterdam.

Holm, G., Bredenberg, H., and Broms, B.B. (1981) Lime columns as foundations for light structures. *Proceedings of the 10th International Conference on SM and FE*, Stockholm, **Vol. 3**, 687-694.

Holt, C.C., Freer-Hewish, R.J. (1998) Use of lime- treated British clays in pavement construction, Part 1: The effect of mellowing on the modification process, *Proceedings of the institution of civil engineers, Transport*, **V129**, 228-239.

Holtz, R.D. & Holm, G. (1973) Excavation and sampling around some drains at Ska-Edeby, Sweden, *Proceeding of the Nordic Geotechnical Meeting*, Trondheim, Norwegian Geotechnical Institute.

Imai, G. (1980) Settling behavior of clay suspension. *Soils and Foundations*, **20**(2), 61-67

Imai, G. (1979) Developement of a new consolidation test procedure using seepage force. *Soils and Foundations*, **19**(3), 45-60.

Imai, G., Yano, K., and Aoki, S. (1984) Applicability of hydraulic consolidation test for very soft clayey soils. *Soils and Foundations*, **24**(2), 29-42.

Indraratna, B., Sathananthan, I., Bamunawita, C., Balasubramaniam, A.S., (2005) Theoretical and numerical perspectives and field observations for the design and performance evaluation of embankments constructed on soft marine clay. In *Ground Improvement*, Elsevier, **3,** 51-89.

Indraratna, B. & Redana, I.W. (1998) Laboratory determination of smear zone due to vertical drain installation. *Journal of Geotechnical Engineering, ASCE*, **125**(1), 96-99.

Indraratna, B, & Redana, I.W. (1997) Plane strain modeling of smear effects associated with vertical drains. *Journal of Geotechnical Engineering, ASCE*, **123**(5), 474-478.

Jamiolkowski, M. & Lancellotta, R. (1981). Consolidation by vertical drains-Uncertainties involved in prediction of settlement rates. Panel Discussion, *Proceeding of the 10th International Conference on Soil Mechanic and Foundation Engineering*, Stockholm, **Vol. 1**, 345-451.

Kezdi, A. (1979) Stabilization with lime. Development in geotechnical engineering, **Vol. 19**, *Elsevier Scientific*: Amsterdam, 163-174

Kinhill (1999) Accelerated Leaching of Fine Dredged Material by Mixing with Green Waste and Explosure to Rain, Port of Brisbane Corporation.

Kitazume, M., and Hyano, K. (2007) Strength properties and variance of cement-treated ground using pneumatic flow mixing method. *Ground Improvement*, **11**(1), 21-26.

Kitazume, M., and Satoh, T. (2003) Development of a pneumatic flow mixing method and its application to Central Japan International Airport construction. *Ground Improvement*, **7**(3), 139-148.

Lau, K.W.K & Cowland, J.W. (2000) Geosynthetically enhanced embankments for the Shenzhen river, adv. *Transport. and Geoenviron. Systems Geosynth*.,Geotechnical Special Publication no. **103,** 140-161.

Kitazume, M., and Satoh, T. (2005) Quality control in Central Japan International Airport construction. *Ground improvement*, **9**(2), 59-66.

Lagaly, G. and Köster, H.M.(1993) Tone und Tonminerale. In: K. Jasmund and G. Lagaly, Editors, *Tonminerale und Tone: Struktur, Eigenschaften, Anwendung und Einsatz in Industrie und Umwelt*, Steinkopff, Darmstadt 490.

Lin et al. (2000) Numerical Modelling of Prefabricated Vertical Drain. *Geotechnical Engineering Journal*, **31**(2), 109-125.

Locat, J., Berube, M. A., and Choquette, M. (1990) Laboratory investigations on the lime stabilization of sensetive clays: Shear strength development. *Canadian Geotechnical Journal*, **27**, 294-304.

Locat, J., Tremblay, H., and Leroueil, S. (1996) Mechanical and hydraulic behaviour of a soft inorganic clay treated with lime. *Canadian Geotechnical Journal*, **33**, 654-669.

Loughnan, F.C. (1969) *Chemical weathering of silicate minerals*. New York, Elsevier.

McBride, M.B. (1994) *Environmental chemistry of soils*. New York, Oxford University Press

McCallister, L.D., and Petry, T.M. (1992a) Leach test on lime- treated clays. *Geotechnical Testing Journal*, **15**, 106-114.

McCallister, L.D. & Petry, T.M. (1992b) Techniques for estimating the longevity of lime-treated expansive clays. *Geotechnical Testing Journal*, **15**(3), 231-237.

Mesri, G., & Ajlouni, A.M. (2007) Engineering properties of fibrous peats. *Journal of Geotechnical and Geoenvironmental Engineering*, **July**, 850-866.

Mesri, G., Ajlouni, M.A., Feng, T.W., and Lo, D.O.K. (2001) Surcharging of soft ground to reduce secondary settlement. *Proceedings of the 3rd International Conference on Soft Soil Engineering*, Hong Kong, 55-65.

Mesri, G., Stark, T.D., Ajlouni, M.S., and Chen, C.S.(1997) Secondary compression of peat with or without surcharging. *Journal of Geotechnical and Geoenvironmental Engineering*, **123**(5), 411-421.

Mesri, G., and Feng, T.W. (1991) Surcharging to reduce secondary settlements. *Proceeding of the International Conference on Geotechnical Engineering for Coastal Development*, Yokohama, 359-364.

Mesri, G., and Castro, A. (1987) $C\alpha/Cc$ concept and K_0 during secondary compression. *Journal of Geotechnical Engineering*, **113**(3), 230-246.

Mesri, G., and Godlewski, P.M. (1977) Time-and stress-compressibility interrralationship. *Journal of the Geotechnical Engineering*, Division **103**(GT5), 417-430.

Mitchell, J. K. (1976), *Fundamentals of Soil Behaviour*, New York, John Wiley and Sons.

Nagaraj, T. S., N. Miura, et al. (1997) Re-examination of classification of soft clay deposits- Needs and methodology. *Indian Geotechnical Conference*, Vododara,India.

Oates, J. A. H. (1998) Lime and Limestone, Chemistry and Technology, Production and Uses. Weinheim, Wiley-VCH Verlag GmbH.

Partheniades, E. (1980). Cohesive sediment transport mechanic and estuarine sedimentation. *Lecture Notes*.

Porbaha, A. (1998) State o f Art in Deep Mixing Technology, Part1: Basic Concepts and Overview. *Ground Improvement* , **Vol. 2**, 81-92.

Pradhan, T.B.S., Imai, G., Murata, T., Kamon, M., and Suwa, S. (1993) Experiment study on the equivalent diameter of a prefabricated band-shaped drain. *Proceedings of the 11th Southeast Asian Geotechnical Conference*, **Vol. 1,** 391-396

Powis, F.(1916) The coagulation of colloidal arsenious sulfide by electrolytes and its relation to the potential difference at the surface of the particles. *Journal of Chemical society,* Transactions, **Vol.109**, 734-744

Rajasekaran, G., and Narasimha Rao, S. (2002) Permeability characteristics of lime treated marine clay. *Ocean Engineering*, **29**, 113-127.

Ranganatham, B.V. (1961) Soil structure and consolidation characteristics of black cotton clay. *Geotechnique* **11**, pp. 333–338.

Rendulic, L. (1936) Relation between void ratio and effective principal stresses for a remoulded silty clay. *Proceedings of the1st International Conference on Soil Mechanics*, Harvard, **Vol. 3,** 48-53.

Rixner, J.J., Kraemer, S.R. and Smith, A.D. (1986) Prefabricated vertical drains, Vol. I, II, and III: Summary of Research Report-Final Report, *Federal Highway Admin*., Report No. FHWA-RD-86/169, Washington, DC, 433pp

Rogers, C. D. F., Glendinning, S., and Roff, T. E. J. (1997). Modification of clay soils for construction expediency, geotechnical engineering. *Proceedings Institution of Civil Engineers, Geotechnical Egineering*, London, 242-249.

Scott, R. F. (1963) *Principles of Soil Mechanics.* Palo-Alto, CA., Addison-Wesley Publishing Co.

Sherwood, P. T. (1993) *Soil stabilisation with cement and lime*. London, HMSO.

Sivakugan, N., Chameau, J.L., Holtz, R.D. (1993) Anisotropy studies on cuboidal shear device. *Journal of geotechnical Engineering, ASCE*, **119**(6), 973-983

Sivapullaiah, P. V., Sridharan, A. et al. (2000) Role of amount and type of clay in the lime stabilization of soil. *Ground Improvement*, **4**(1), 37-45.

Skempton, A. W. H., D.J. (1953). The Post-Glacial Clays of the Thames Estuary at Tibury and Shellhaven. *Soil Mechanics and Foundation Engineering*.

Sparks, D.L. (1995) *Environmental soil chemistry*. London, Academic Press.

Sridharan, A., and Prakash, K. (1999a) Simplified Seepage consolidation test for soft sediments. *Geotechnical Testing Journal*, **22**(3), 235-244.

Sridharan, A., and Prakash, K. (1999b) Influence of clay mineralogy and pore-medium chemistry on clay sediment formation. *Canadian geotechnical Journal*, **36**(5), 961-966.

Stepkowska, E.T., Thorborg, B., Wichman, B. (1995) Stress state-permeability relationships for dredged sludge and their dependence on microstructure. *Geotechnique*, **45**(2), 307-316.

Stern, O. (1924) Zur theori der electrolytischen doppelschicht: Zeitschrift fur Electrochemie, **30**, 508-517.

Taylor, H. F. W. (1997) *Cement Chemistry*. London, Thomas Telford.

Taylor, W. H. and A. Arman (1960) Lime Stabilization Using Pre-Conditioned Soils *Highway Research Board Bulletin*, 262**,** 1-19.

Taylor, D.W. (1942) Research on the Consolidation of Clays. *Massachusetts Institute of Technology, Department of Civil and Sanitary Engineering*, Serial 82.
Terzaghi, K., Perch, R.B., Mesri, G. (1996) Settlement during Secondary Consolidation. *Soil Mechanics in Engineering Practice*. New York, Wiley**,** 108-112.

Terzaghi, K. (1925) Settlement and Consolidation of Clay. *Engineering News-Record,* 874-878.

Terashi, M. (1997) Theme lecture: Deep Mixing Method- Brief State of the Art. Proceeding of 14th ICSMFE, **4**, 2475-2478.

Terashi, M., & Katagiri, M. (2005) Key issues in the application of vertical drains to a sea reclamation by extremely soft clay slurry. In *Ground Improvement, Elsevier*, **3,** 231-246.

Thompson, M.R. (1965) Influence of Soil Properties on Lime-Soil Reactions. *Public Works,* **96**(8).

Thompson, M.R. (1966) Shear Strength and Elastic Properties of Lime-Soil Mixtures. Washington, *National Research Council***,** 1-14.

Townsend, D.C. and Kylm, T.W. (1966) Durability of lime-stabilized soils**.** *Highway Research Board, National Research Council*, Washington DC. Highway Research Record No.**139**, 25-41.

TRB (1987) Lime Stabilisation, Reactions, Properties, Design and Construction. Washington, State-of-the-Art Report5. *Transportation Research Board*. Washington D.C.

Tremblay, H., J. Duchesne, et al. (2002) Influence of the nature of organic compound on fine soil stabilization with cement. *Canadian Geotechnical Journal*, **39**, 535-546.

Tremblay, H., Leroueil, S., Locat, S. (2001) Mechanical improvement and vertical yield stress prediction of clayey soils from eastern Canada treated with lime or cement. *Canadian Geotechnical Journal,* **38**, 567-579.

URS (2001). Geotechnical Investigation-Future Port Expansion,Port of Brisbane.

van Olphen, H. (1962) *An introduction to clay colloid chemistry*. New York, Interscience**,** 92-110.

Wong, P. (2005) Application of analytical method for preloading design of selected case studies. In *Ground Improvement, Elsevier*, **3,** 231-246.

Wood, D.M. (1991) *Soil Behaviour and Critical State Soil Mechanics*. London, Cambridge University Press.

APPENDIX

SUBJECT OF REPORT

Quantitative XRD Analysis

Confidential

ADMINISTRATIVE DOCUMENTATION HAS BEEN REMOVED